AUTOMATED LONGITUDINAL PAYLOAD LIFT-UP USING BRIDGE CRANES

A Thesis
Presented to
The Academic Faculty

By

Yujia Yang

In Partial Fulfillment
of the Requirements for the Degree
Master of Science in
George W. Woodruff School of Mechanical Engineering

Georgia Institute of Technology

May 2017

AUTOMATED LONGITUDINAL PAYLOAD LIFT-UP USING BRIDGE CRANES

Approved by:

Dr. William Singhose, Advisor
George W. Woodruff School of Mechanical Engineering
Georgia Institute of Technology

Dr. Ueda Jun
George W. Woodruff School of Mechanical Engineering
Georgia Institute of Technology

Dr. Aldo A. Ferri
George W. Woodruff School of Mechanical Engineering
Georgia Institute of Technology

Date Approved: March 11, 2017

Rest In Peace, Dad.

ACKNOWLEDGEMENTS

First, I would like to thank my adviser Dr. Singhose for the abundant opportunities and guidance he provided. Without him, I wouldn't have the chance to be where I am now. I would also like to thank my mother for her boundless and endless support through out the years. Lastly, I would like to thank all my labmates for the excellent working environment they built up.

TABLE OF CONTENTS

Acknowledgments v

List of Tables ix

List of Figures x

Summary xii

Chapter 1: Introduction 1

1.1 Motivation 1

1.2 Experimental Setup 2

1.3 Problem Statement 4

1.4 Approach 5

1.4.1 Input Shaping Strategies 7

1.4.2 Payload Stabilization Strategies 8

1.5 Thesis Contribution 9

1.6 Thesis Outline 9

Chapter 2: Automated Payload Alignment 10

2.1 Trolley and Hook Alignment 11

2.2 Payload Orientation Detection 13

2.3 System Model 15
2.3.1 Model Derivation 16
2.3.2 Model Verification 20
2.4 Simplified System Model 22
2.4.1 Simplified Model Derivation 22
2.4.2 Simplified Model Verification 24
2.5 Input-Shaped Payload Alignment 27
2.5.1 Speed Command Limitation 27
2.5.2 Input-Shaper Design 31
2.5.3 Simulation Verification 33
2.5.4 Experimental Verification 34

Chapter 3: Lift-Up Trajectory Development 38

3.1 Model Based Friction Analysis 39
3.1.1 Static Friction Analysis 40
3.1.2 Dynamic Friction Analysis 41
3.2 Trajectory Generation Strategy 45
3.2.1 Velocity Planning 47

Chapter 4: Off-Center Lift-Off Vibration Reduction 50

4.1 Model Reference Control 50
4.1.1 System Model 51
4.1.2 Reference Model 56
4.1.3 Control Law Derivation 56

4.2 State Observer 58

4.2.1 Observer Design 59

4.2.2 Observer Verification 60

4.3 Simulation and Experimental Verification 61

Chapter 5: Conclusion and Future Works 65

5.1 Conclusion 65

5.2 Future Work 66

Appendix A: Nonlinear Side-Swing Model Derivation 69

Appendix B: Simplified Side-Swing Model Derivation 84

Appendix C: Double Pendulum Free-Hanging Model Derivation 89

Appendix D: MRC Control Law Derivation 94

Appendix E: MRC Control Law Derivation 98

Appendix F: Payload Alignment Simulation 102

Appendix G: Lift-up Trajectory Generation 109

Appendix H: MRC + Observer Residual Vibration Reduction 114

References 120

LIST OF TABLES

1 Bridge Crane Setup Parameters 3

2 Parameters Known Prior to Operation 7

3 Variables Used in Chapter 2 10

4 Damping Ratio Experiment Parameters and Results 21

5 Damping Ratio Experiment Parameters and Results 22

6 Variables Used in Chapter 3 38

7 Variables Used in Chapter 4 50

LIST OF FIGURES

1 Aluminum ingot lift-up with bridge crane 1

2 Small-scale bridge crane 3

3 Side view of manual lift-up process 4

4 Top view of realistic payload position versus ideal payload position 5

5 Automated payload lift-up process 6

6 Trolley auto-aligns to the hook, and payload is lifted up for a minor angle. . 11

7 Experimental results of trolley position correction in x-axis with proportional controller. Y-axis results ignored for being identical. 12

8 Payload orientation detection by sampling multiple points on the side swing trajectory, from top view. 13

9 Experimental result of pivot point detection 15

10 Schematic of payload alignment model 16

11 Change in ϕ from induced payload side-swing 21

12 Natural frequency change with respect to trolley y-axis position change,predicted by simulation and calculated from experimental results. 23

13 Schematic diagram of the simple model 25

14 Natural frequency change with respect to trolley y-axis position change predicted by complex and simple model simulations. Red line shows percentage error between the two model. 26

15 Free body diagram of the payload in side-swing. 28

16 Simulated tension and maximum friction during the alignment side-swing with fixed maximum static friction coefficient. 29

17 Friction tolerance change with respect to change in maximum static friction coefficient. 30

18 Input shaping process 32

19 Input-shaped commands and trajectories 33

20 Sensitivity curve of the ZV and ZVD shaper 34

21 Residual vibration of payload alignment using different shapers 36

22 Free body diagram of the payload in circular lift-up 39

23 Sub-regions of the operation space 41

24 Dynamic safety boundary 46

25 Cross-over position 47

26 Lift-up trajectory 48

27 Command velocity change with respect to angle change 49

28 Model reference control 51

29 Free body diagram of the system in double pendulum configuration. 52

30 Simulation result of off-center-lift 55

31 Model reference control with Luenberger observer 59

32 Luenberger observer 60

33 Simulation results of observer 62

34 Simulation of MRC + Observer 63

35 Experimental results of MRC + Observer 64

SUMMARY

Longitudinal payloads are a challenging portion of the payloads being transported in various industries. One way of transporting them is by attaching the payloads vertically to bridge cranes in double-pendulum configurations. The lift-up of a longitudinal payload lying on the ground to the aforementioned configuration is normally done manually. This process has disadvantages consisting of the misalignment between payload and bridge, human operator error, and uncontrollable system oscillation.

In this thesis, the automated lift-up of longitudinal payloads using bridge cranes is proposed. The problems specific to each stage of this process are studied and solutions are developed. A side-swing trajectory is designed based on the detected and desired position of the payload. Input-shaping, a command modification method, is used to optimize this trajectory to lower oscillation. A circular lift-up trajectory is developed based on the dynamic model of the system and velocity commands to achieve the process is obtained through simulation. Observer-based model reference control is used to reduce residual vibration when the payload is lifted off ground. A dynamic model of the crane and payload system is constructed to design a meaningful reference model. Results show that both input shaping and model reference control helped reduce oscillation in the automated payload lift-up process.

CHAPTER 1

INTRODUCTION

1.1 Motivation

Longitudinal payloads are a challenging portion of payloads transported in industries such as ship assembly, building construction, wood cutting, metal processing, etc. In such industries, cranes are often used in lift-up and transportation of these heavy longitudinal payloads. Figure 1 shows a bridge crane lifting an aluminum ingot in a double-pendulum configuration. To safely and effectively transport the payloads, it is necessary to ensure the payload is free of large oscillation. In constrained work-spaces, swinging heavy payloads can pose danger to the environment, including the operators, the machines, and so on. The pulling force induced by the payload oscillation on the crane can also be damaging.

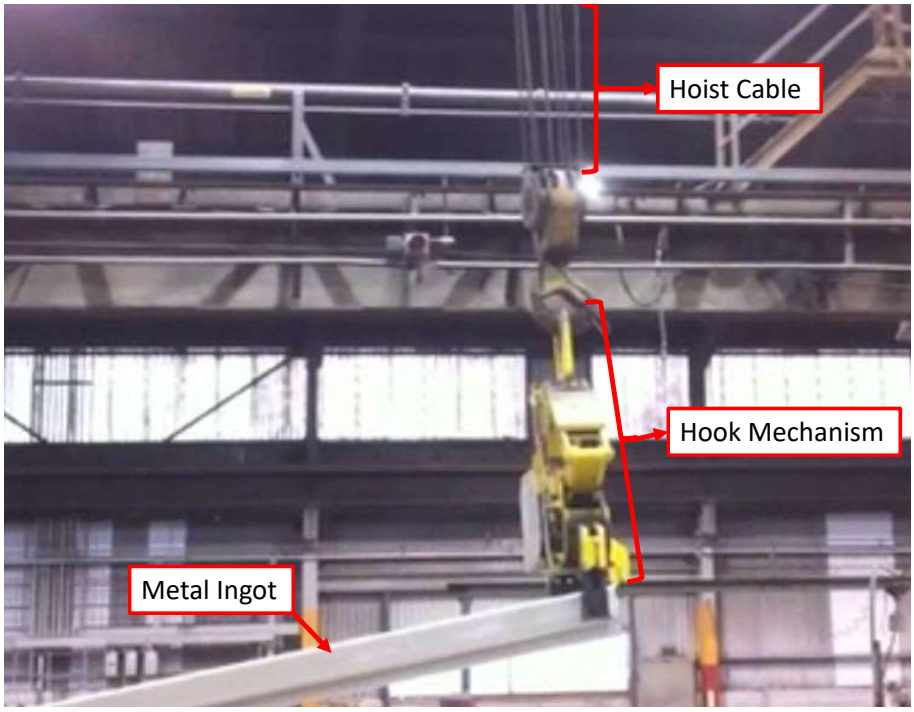

Figure 1: Aluminum ingot lift-up with bridge crane

However, cranes are both under-actuated and under-damped systems. They are under-actuated because the actuators on the crane do not provide direct control over the payload's swing angle. They are under-damped because the cranes give no means to actively damp out the payload oscillation. Waiting for the swing to naturally damp out undermines the operation efficiency.

This thesis presents research on automating the process of longitudinal payload lift-up using bridge cranes, with the goal of achieving a lifted and stabilized longitudinal payload within a short time period so that further transportation can take place in an efficient manner.

1.2 Experimental Setup

The modeling and experiments performed for this thesis utilize the small-scale bridge crane located in the Georgia Tech Manufacturing Institute. Figure 2 shows a labeled picture of the crane. The main body of the crane is a rectangular aluminum frame and two of its top members form a runway. An additional beam that moves along the runway forms the bridge. The trolley moves back and forth along the bridge. The hook, consisting of two pulleys and a metal plate, is connected to, and hoisted by, the trolley using thin steel cable.

The bridge, trolley and hoist are all actuated by motors controlled using Siemens Simotion drives and PLCs. With the motors' built-in encoders, measurements of the position of the trolley and length of the hoist cable are constantly available. A camera is fixed to the trolley with its lens pointing vertically downward so that the sensor can capture relative position of the hook by receiving light reflected by the reflective material attached to top of the hook. A wooden board on the ground functions as a test surface that allows for changes in contact friction. When the payload slips, the distance of slipping can be measured by a scale on the test surface. A rectangular aluminum payload, with a rotational junction at its top, is connected to the hook by a strong magnet.

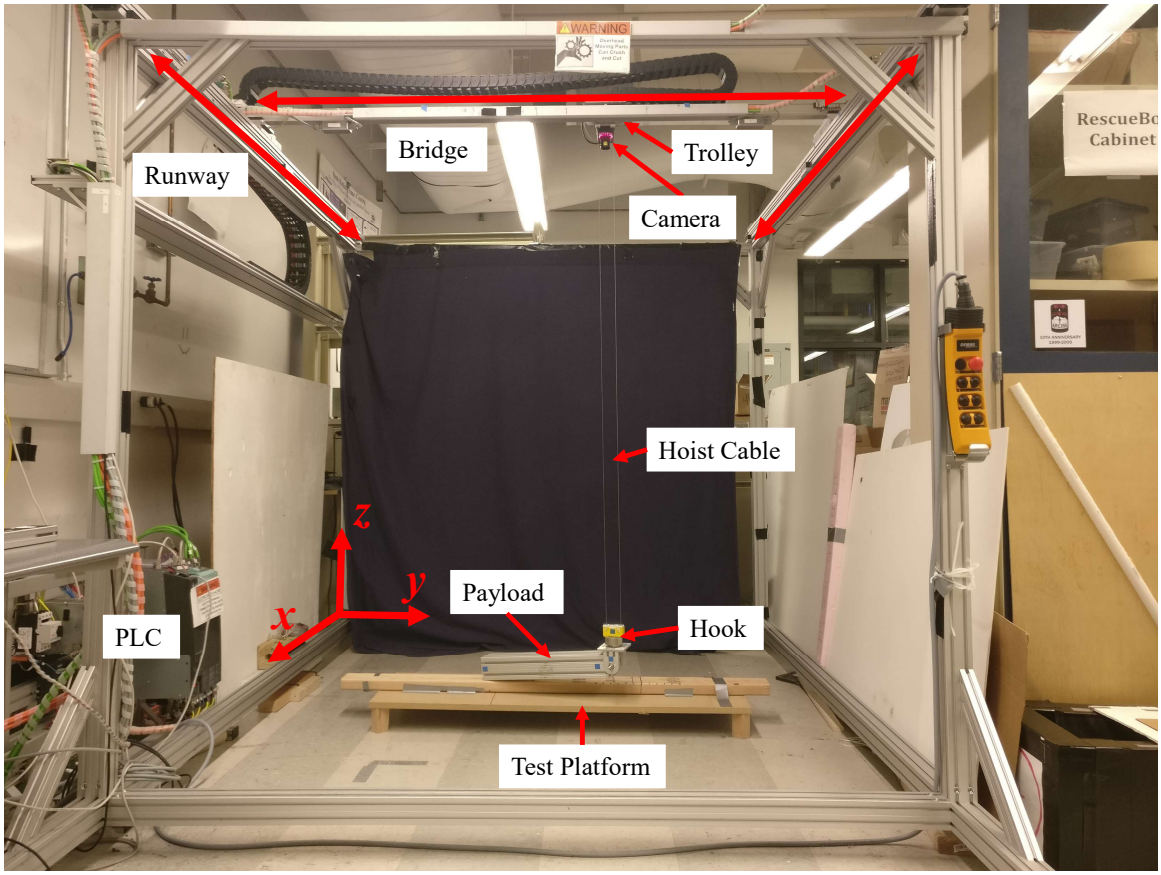

Figure 2: Small-scale bridge crane

Table 1 lists the important physical parameters of the bridge crane setup. The motors are all capable of functioning in velocity control mode. It is the primary actuation mode used throughout this research.

Table 1: Bridge Crane Setup Parameters

Parameter	Value
Hook Mass	0.66 kg
Payload Mass	3.13 kg
Payload Length	0.35 m
Payload Width	0.08 m
Range of Hoist	1.82 m
Maximum Hoist/Trolley/Bridge Acceleration	1 m/s^2
Maximum Hoist/Trolley/Bridge Velocity	0.2 m/s
Laser Sensor Pixel to Angle Ratio	2.85 mm/pixel

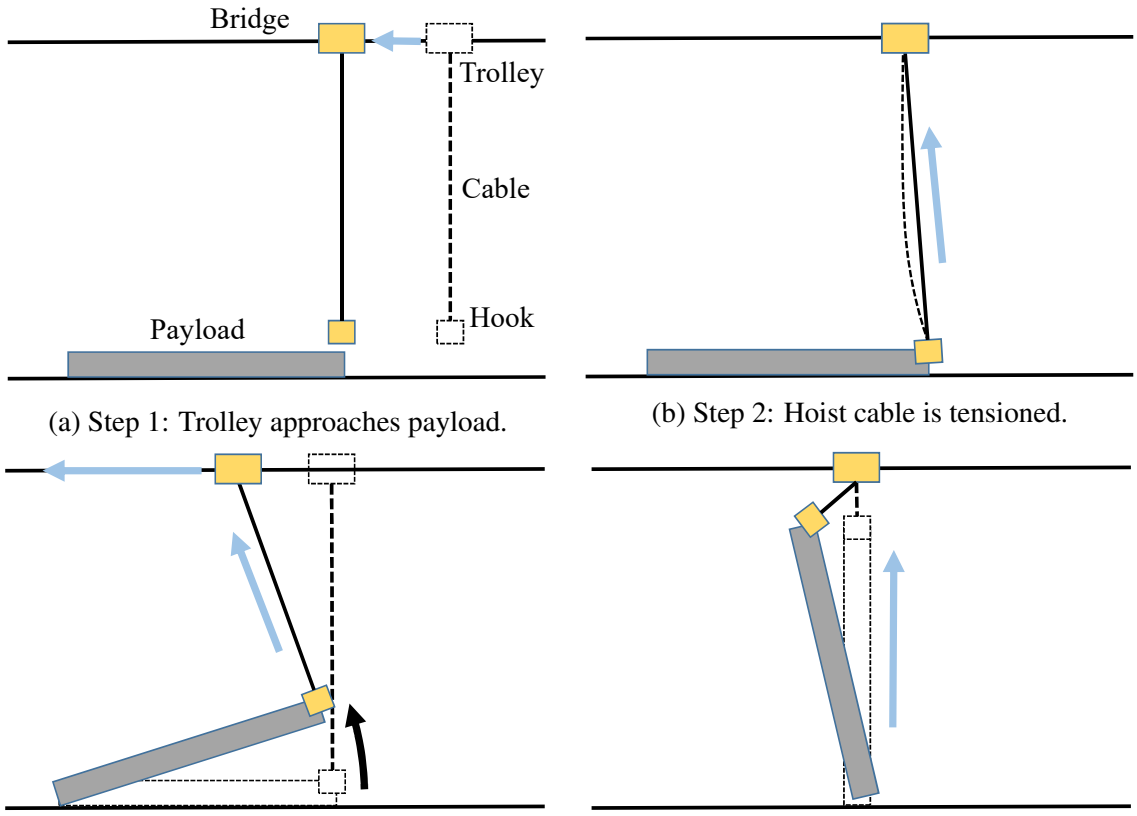

(a) Step 1: Trolley approaches payload.

(b) Step 2: Hoist cable is tensioned.

(c) Step 3: Coordinated circular payload lift-up.

(d) Step 4: Payload directly lifted off ground.

Figure 3: Side view of manual lift-up process

1.3 Problem Statement

Figure 3 illustrates a typical manual lift-up for longitudinal payloads. At first, the operator navigates the trolley to a location above the payload. Secondly, the operator connects the hook to one end of the payload, while adjusting the cable length to ensure the cable is in tension. In the third step, the operator attempts to lift the payload in a circular trajectory by coordinating trolley and cable motions. Finally, the erected payload is lifted off the ground.

To complete step one, the payload needs to be placed in parallel alignment with the bridge. Such an initial condition cannot be guaranteed given that crane trolleys are high above the ground and it is difficult for the operator to determine the trolley/payload alignment. During step one, it is also hard to position the trolley directly over the end of the payload. Figure 4 compares a realistic alignment scenario and the ideal scenario.

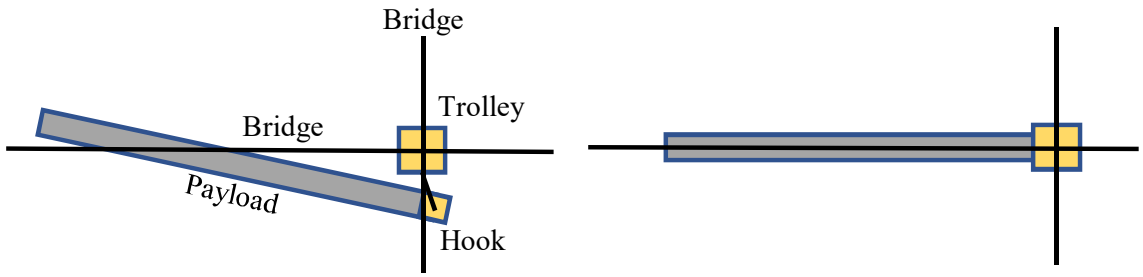

(a) Realistic scenario: Payload unaligned with the bridge's axis.

(b) Ideal scenario: Payload and bridge on same axis.

Figure 4: Top view of realistic payload position versus ideal payload position

In step two, the adjustment of the cable length is based on the operator's observation, which can lead to misjudgment. The circular trajectory in step three is difficult for inexperienced operators to carry out. Sudden accelerations and decelerations result in non-smooth velocity profiles and lead to slipping of the payload at its ground contact point.

In the last step, the accumulated error leads to a phenomenon called off-center-lifting, where the lifting force and the gravitational force of the payload do not share the same vertical axis. Once the payload is lifted off the ground, the resulting torque will pull the payload into side swing and twist. While the side swing is controllable by calculated trolley motion in the x and y-axis, the actuators of the crane have no control over the twist. Waiting for it to naturally damp out is the only option.

Overall, any slipping during the process can be challenging to both the payload and the ground. It also poses a collision danger with people and obstacles. The payload swing and twist after lift-off pose additional dangers.

1.4 Approach

In order to resolve the problems identified above, an automated payload lift-up process is developed. The process is schematically illustrated in Figure 5. This automation process assumes that the geometry of the crane and payload are known. However, the payload's position and orientation relative to the crane is initially unknown. It also assumes that the

position of the trolley and hook relative to the crane reference frame are measurable by adding an encoder and/or laser sensor to the crane.

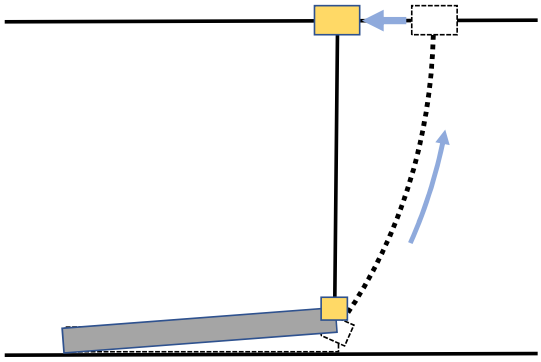

(a) Step 1: Trolley auto-aligned with hook.; Cable auto-tensioned.

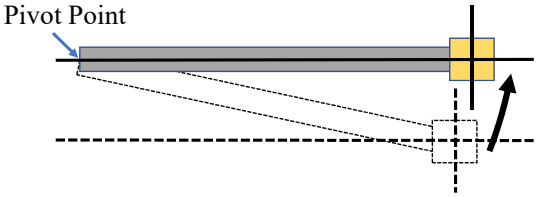

(b) Step 2: Payload auto-aligned with bridge in a side swing.

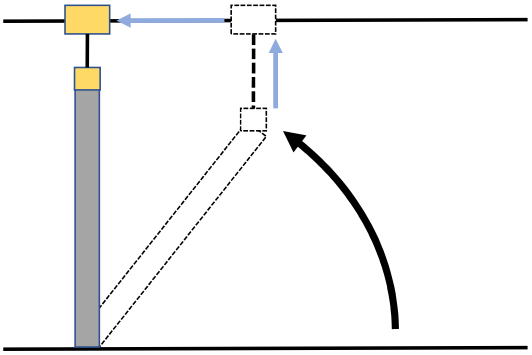

(c) Step 3. Payload lifted up in circular trajectory.

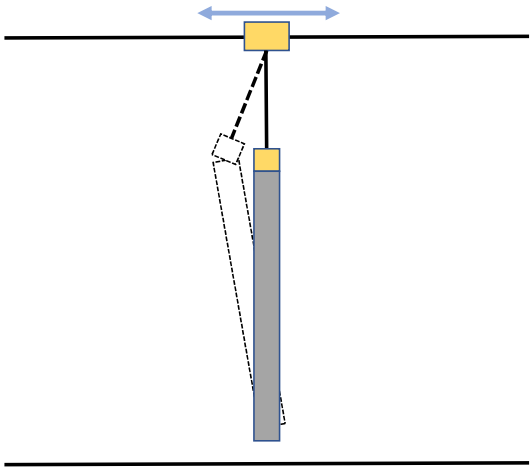

(d) Step 4. Payload lifted off ground.; Vibration suppressed by feedback control.

Figure 5: Automated payload lift-up process

To initiate the operation, the operator connects the hook to one end of the payload, where the hoist cable is not required to be in tension. This is the only time manual input is required during the process. In step one, the trolley is moved to the position directly over the hook through feedback control, during which the cable is hoisted up to a length slightly shorter than the crane height. This action elevates the payload by a small angle and allows it to rotate sideways with respect to its left end, as shown in Figure 5b. In the second step, the trolley follows a specially-shaped trajectory and aligns the payload to the

bridge. Next, the payload is lifted to a vertical orientation. The trolley and cable are moved according to a smoothed trajectory confined by a friction analysis to ensure no slipping. In step four, the near vertical payload is lifted off the ground. While this is still an off-center-lift, the vibration is limited to the vertical plane where the bridge sets, because the payload alignment in step two has eliminated deflection angles in the sideways direction, and thus, reduces the possibility of twisting. Once the payload is lifted into the air, feedback control is employed to reduce any swing that might exist.

Table 2 contains a list all the parameters known prior to the operation. In a realistic situation, such specifications of both the crane and the payload would be approximately known by the operator.

Table 2: Parameters Known Prior to Operation

Variable	Meaning
H	Distance from bridge to ground
L	Length of the payload
W	Width of the payload
m_p	Mass of the payload
m_h	Mass of the hook

1.4.1 Input Shaping Strategies

Previous works have established various techniques to reduce vibration of dynamic systems by optimizing the input command [1]. Starr [2] derived an input-shaper for cranes called a Zero Vibration (ZV) shaper to surpress the payload swing induced in a path controlled robot manipulator system. Smith *et al.* [3] further developed the ZV shaper using an energy method so that it accommodates for nonlinear systems. Singer *et al.* [4] extended the work to include input-shaper's effect on payloads transported by gantry cranes. Singhose *et al.* [5] presented a vector diagram method that provides a shortcut to design multi-impulse shapers that can reliably reduce system vibration.

Singhose *et al.* [6] also investigated the effects of Zero Vibration Derivative (ZVD) and Extra-Insensitive (EI) shapers. They showed that EI shaper is able to suppress vibration over a larger range of frequencies than a ZVD shaper. Han *et al.* [7] explored an input-shaping technique for under-damped systems that only requires the system's outputs without the need of an accurate system model. This provides great freedom when the physical system has unknown dynamics. Chen *et al.* [8] used a energy method to derive a general input-shaper design method for single freedom nonlinear systems. This provides insight for the shaper choice in this thesis as the system studied in step 2 of the process is a nonlinear and has one degree of freedom.

1.4.2 Payload Stabilization Strategies

Model Reference Control (MRC) is a control strategy that forces the plant to act like the chosen reference model and, thus, can be applied to systems with complex dynamics and uncertainties. This property of MRC becomes very powerful when the plants are time-varying [9][10][11] or nonlinear [12][13][14]. While some MRC designs are based on the assumption that suitable reference model is always available [15][16], large variation between reference model and actual plant can cause the effectiveness of MRC to degrade.

To ensure robustness of this control method, multiple studies were conducted [17][18][19]. Sun *et al.* [20] improved robustness of a MRC controlled system by adding model matching feedback and error compensator. Patino *et al.* [21] proposed a model reference adaptive control based on neural network to improve robustness of a first order system. Pedret *et al.* [22] developed a robust MRC structure based on right coprime factorization of the plant. While MRC is advantageous at controlling a plant with unmodeled characteristics, it generally requires all states of the system to be known. Therefore, a state observer may be needed.

1.5 Thesis Contribution

This thesis establishes an automated process for lifting up a longitudinal payload using a bridge crane. The process eliminates most of the manual work and increases operation efficiency and safety. The major contributions are as follows:

1. Numerical modeling of a longitudinal payload swinging sideways.
2. Control of side swing using input shaping.
3. Static and dynamic friction analysis of a payload in a circular lift-up motion.
4. Reduction of swing and twist from off-center lifts using feedback control.

1.6 Thesis Outline

Chapter 2 presents the automated trolley alignment. A dynamic model of the side swing is then derived and used to develop input-shaping strategies. Chapter 3 demonstrates the static and dynamic friction analysis during payload lift-up. Velocity command limitations are then proposed. Chapter 4 models the system as a double pendulum and investigates feedback control strategies to reduce swing and twist. Chapter 5 concludes the work done in this thesis and suggests future work.

CHAPTER 2

AUTOMATED PAYLOAD ALIGNMENT

Table 3 contains all the variables used in this chapter.

Table 3: Variables Used in Chapter 2

Variable	Meaning
x_t	Position of the trolley in the x-axis
y_t	Position of the trolley in the y-axis
z_t	Position of the trolley in the z-axis
H	Distance from the trolley to the ground
x_h	Position of the hook in the x-axis
y_h	Position of the hook in the y-axis
z_h	Position of the hook in the z-axis
l_d	Desired cable length in trolley alignment
γ	Desired elevation angle in trolley alignment
P	Proportional gain of the trolley alignment controller
L	Length of the payload
l	Length of the hoist cable
θ	Elevation angle of the payload in side swing
ϕ	Deflection angle of the payload in side swing
σ	Deflection angle of the trolley from the z-axis
h_1	Height of the payload's COG
h_2	Height of the hook's COG
P_x	Position of the payload's COG in the x-axis
P_y	Position of the payload's COG in the y-axis
y_p	Position of the pivot point in the x-axis
z_p	Position of the pivot point in the z-axis
v_b	Bridge velocity
v_t	Trolley velocity
T	Tension in the hoist cable
f	Static friction force at the pivot point
N	Normal force at the pivot point
μ_{max}	Maximum static friction coefficient

At the beginning of the automated payload lift-up process, the operator connects the payload to the hook while leaving the hoist cable slightly slack. This is done to ensure that

the payload is completely lying on the ground and that the payload can be easily attached to the hook.

2.1 Trolley and Hook Alignment

After the hook is attached, the trolley is moved to align with the same vertical axis as the hook, the cable is hoisted to be in tension, and the payload is lifted to a minor elevation degree γ, as presented in Figure 6.

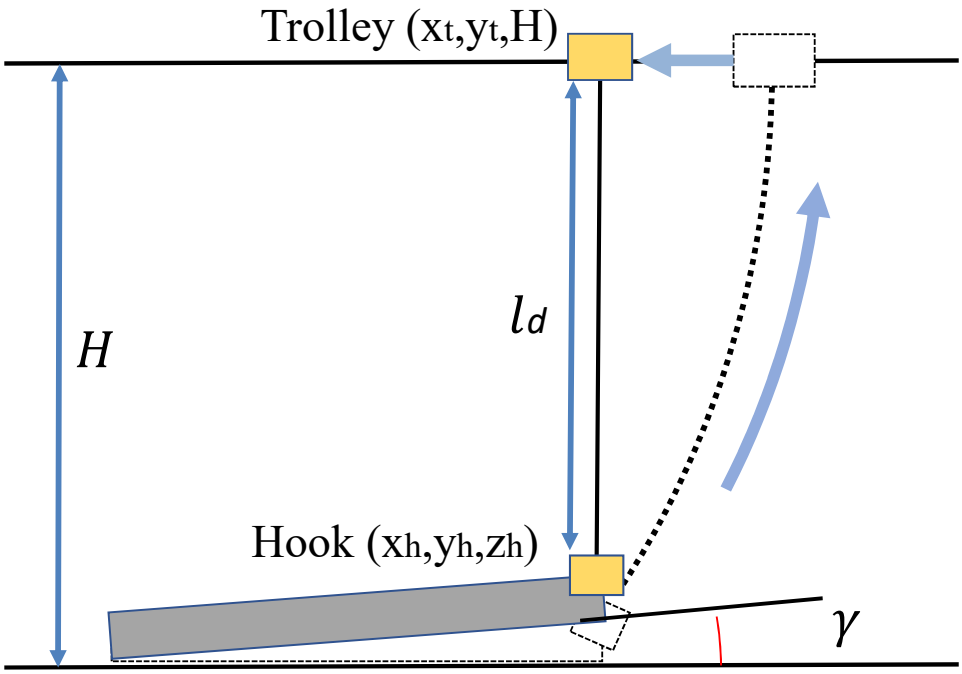

Figure 6: Trolley auto-aligns to the hook, and payload is lifted up for a minor angle.

Feedback control is implemented to achieve this maneuver. Because the motors are in velocity control mode and have identical settings, the trolley's motion in both x-axis and y-axis share the same transfer function:

$$\frac{X(s)}{U(s)} = \frac{1}{s} \tag{1}$$

where *X(s)* represents trolley displacement and *U(s)* represents velocity input. Because the

system is a type 1 system, a proportional controller is sufficient to drive the trolley to the desired position without steady-state error. The trolley's position relative to the hook is x_t and y_t. The reference command to the system is $x_{t,d} = 0$ and $y_{t,d} = 0$.

Figure 7 presents the change in trolley's distance from the hook's position in the x-axis with an initial position of 73 pixels[1]. Three trials, using controllers with proportional gains of 1, 2 and 3 respectively, are shown in the figure. As the proportional gain increases, rise time of the system decreases. There is no overshoot in any of the trials.

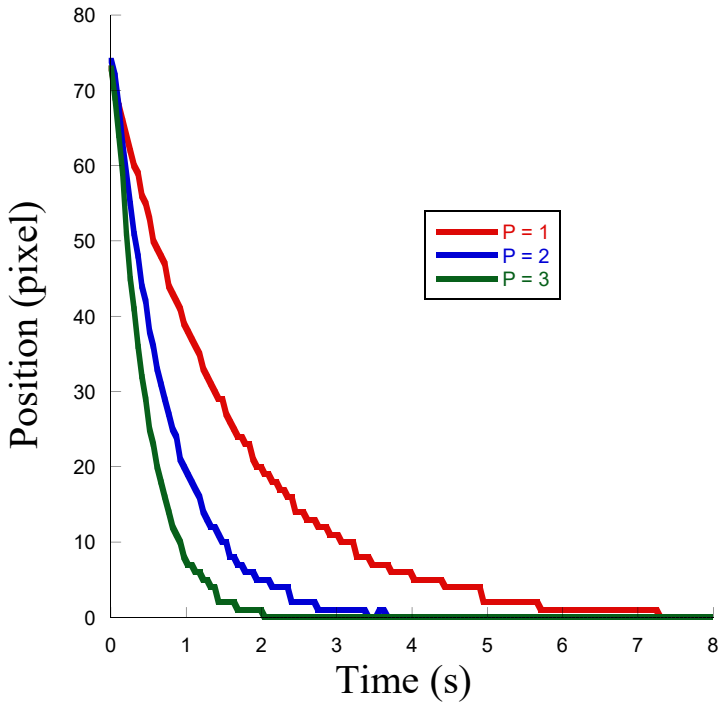

Figure 7: Experimental results of trolley position correction in x-axis with proportional controller. Y-axis results ignored for being identical.

While the trolley moves towards the hook's position, the cable is hoisted up. Hoist speed of the cable is calculated by differentiating the geometric constraint that relates position of the trolley and the hook:

$$\dot{z_h} = \frac{x_t \dot{x_t} + y_t \dot{y_t}}{\sqrt{H^2 + x_t^2 + y_t^2}} \tag{2}$$

[1]The units of (pixels) are used because an overhead camera is used to measure the hook position

where $\dot{z}_h$ is the hoist speed, H is the vertical distance from the hook to the bridge, $\dot{x}_t$ and $\dot{y}_t$ are the trolley's speed in the x-axis and y-axis, respectively. Once the trolley arrives at its desired position, the cable is hoisted up more so that the payload is lifted at a small angle, no larger than 5 degrees. The final cable length is:

$$l_d = H - L\sin(\gamma) \tag{3}$$

where l_d is the desired cable length, L is length of the payload and γ is the elevation angle of the payload from the ground. This slight elevation allows the payload to swing sideways.

2.2 Payload Orientation Detection

If we know the position of the trolley, the hook, and the payload end that collocates with the hook, then the position of the other end of the payload, as well as the deflection angle of the payload relative to the crane frame need to be determined. To do so, the trolley is slowly moved along the x-axis for a short distance to pull the payload into a small side swing. The trajectory of the swing is then recorded. By assuming no slipping occurs at the pivot point, the position of the pivot point is calculated based on the geometrical relationships shown in Figure 8.

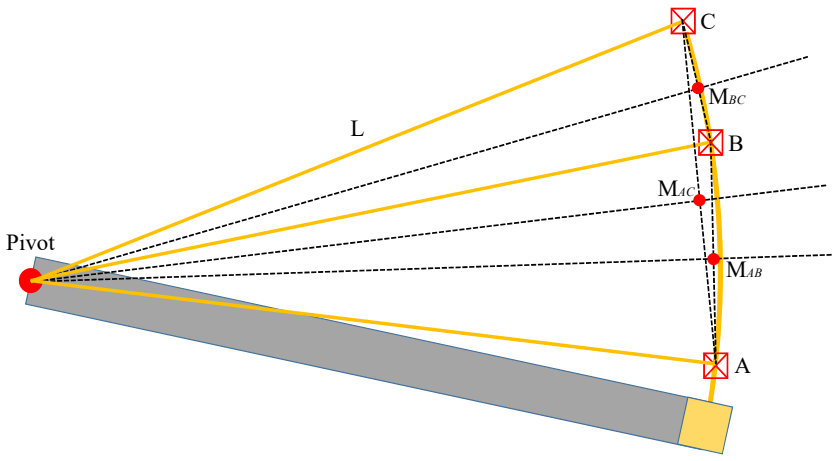

Figure 8: Payload orientation detection by sampling multiple points on the side swing trajectory, from top view.

First, the middle point of any two points on the trajectory is calculated using:

$$M_x = \frac{A_x + B_x}{2} \quad \text{and} \quad M_y = \frac{A_y + B_y}{2} \tag{4}$$

where A_x, A_y specify the position of point A, B_x, B_y specify position of point B, and M_x, M_y represent the position of the midpoint M. Then, the position of the pivot is calculated as:

$$P_x = M_x + L\frac{|A_y - B_y|}{\sqrt{(A_x - B_x)^2 + (A_x - B_x)^2}}, \quad P_y = M_x - L\frac{\text{sign}((A_x - B_x)(A_y - B_y))\,|A_x - B_x|}{\sqrt{(A_x - B_x)^2 + (A_x - B_x)^2}}$$

or

$$P_x = M_x - L\frac{|A_y - B_y|}{\sqrt{(A_x - B_x)^2 + (A_x - B_x)^2}}, \quad P_y = M_x + L\frac{\text{sign}((A_x - B_x)(A_y - B_y))\,|A_x - B_x|}{\sqrt{(A_x - B_x)^2 + (A_x - B_x)^2}} \tag{5}$$

where P_x, P_y represent the position of the pivot point P. There exist two possible solutions because two points on a circle are not sufficient for determining the circle's center. For this reason, three points on the trajectory are selected to perform the calculation in three pairs. By comparing the distances between the six possible centers, three of them can be determined as the correct solution. These are averaged to obtain the estimated pivot point. Figure 9 presents an experimental result of such pivot point calculations. The estimated pivot point is only 0.62 cm away from the actual pivot point.

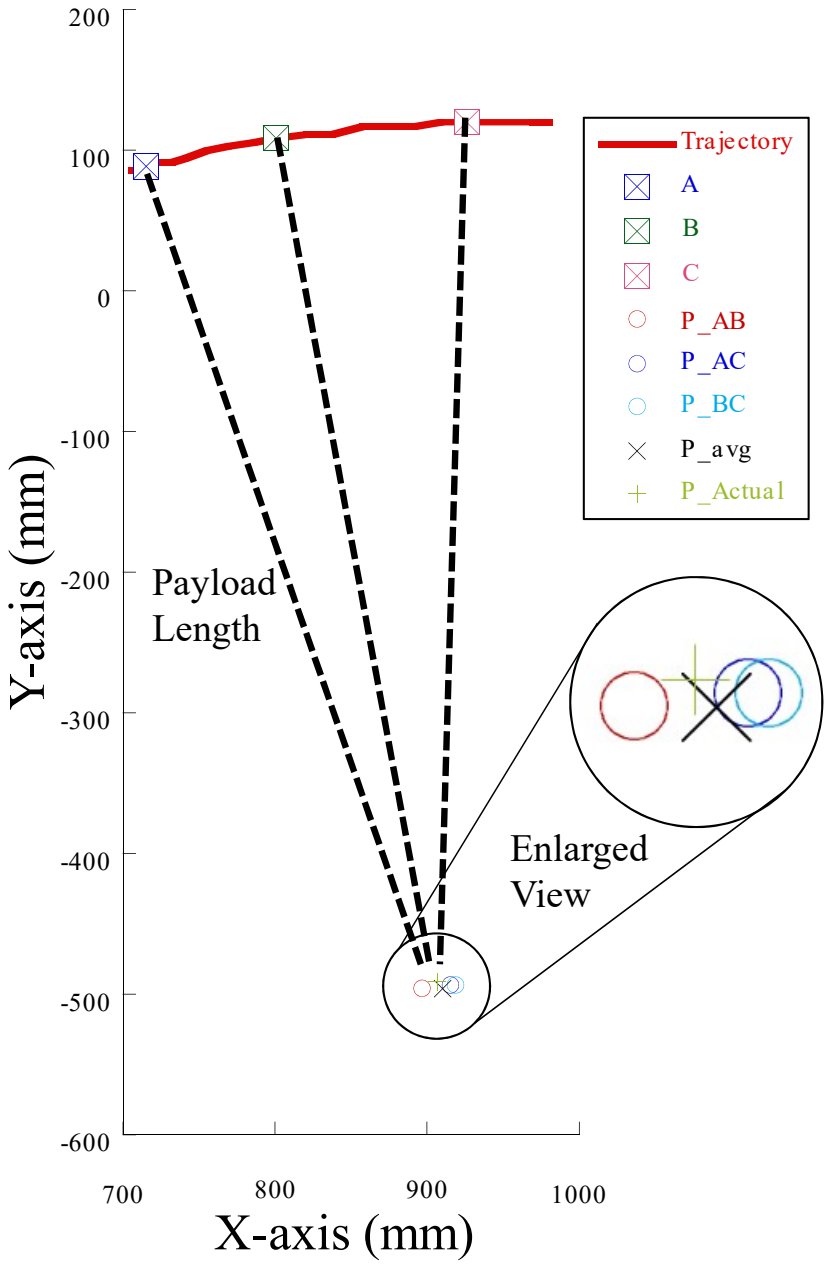

Figure 9: Experimental result of pivot point detection

2.3 System Model

To align the payload and bridge, the payload moved through an input-shaped side swing motion with respect to the pivot point. Because input-shaping utilizes the natural frequency of the dynamic system, a numerical model is created to describe the system. Figure 10 presents the schematic diagram of the system model. A spherical coordinate system located

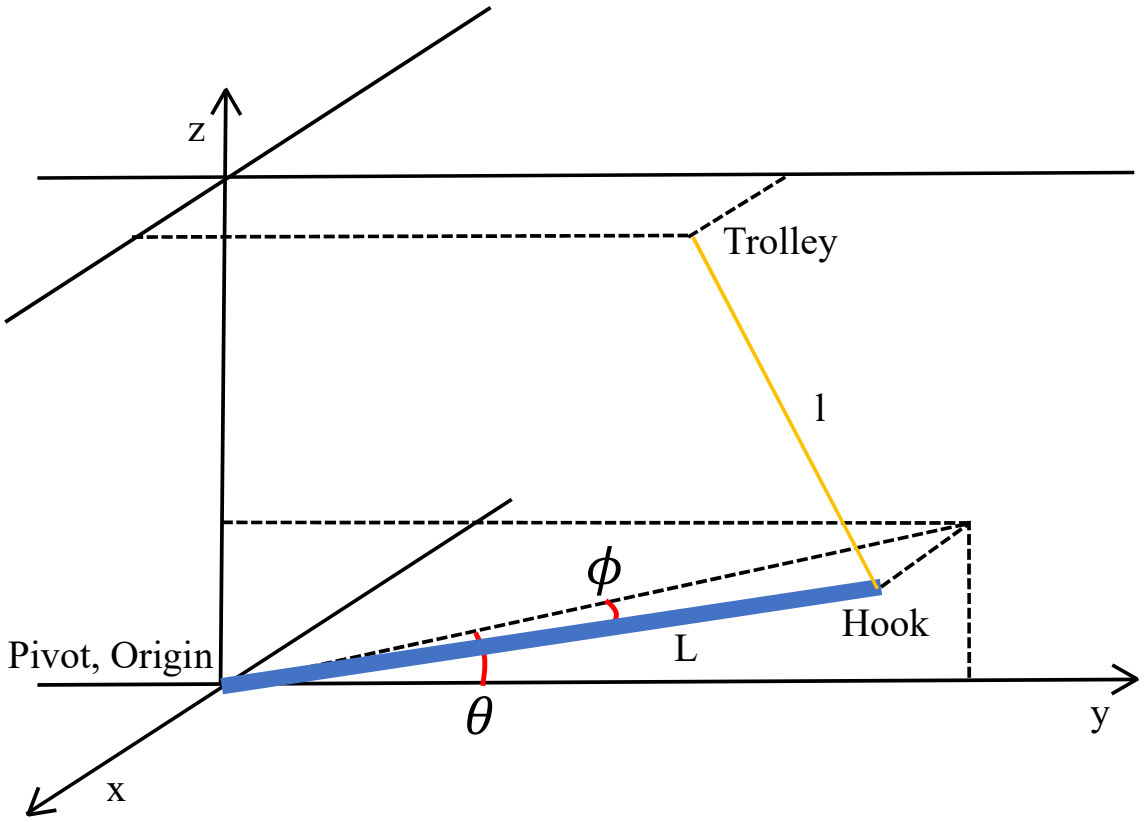

Figure 10: Schematic of payload alignment model

at the pivot point is used to describe position and orientation of the payload, where θ is the elevation angle of the payload from ground and ϕ is the payload's deflection angle from the vertical yz-plane. The payload length, cable length, and crane height are denoted as *L*, *l*, and *H* respectively.

2.3.1 Model Derivation

To obtain the natural frequency of the system, the equation of motion is needed. The constrained form of the Lagrange Equation is employed to achieve this goal. Based on the assumption that the cable is always in tension and has constant length, a constraint equation characterizing the system's position constraints is:

$$l^2 = (H - Lcos(\phi)sin(\theta))^2 + (x_t - Lsin(\phi))^2 + (y_t - Lcos(\phi)cos(\theta))^2 \qquad (6)$$

where x_t, y_t represents position of the trolley, and are assumed to be constant. The velocity constraint equation is obtained by differentiating the position constraint:

$$\begin{bmatrix} \mathrm{a} \end{bmatrix} \dot{\vec{q}} + \begin{bmatrix} \mathrm{b} \end{bmatrix} = \begin{bmatrix} 0 \end{bmatrix}$$

$$\begin{bmatrix} \mathrm{a} \end{bmatrix} = \begin{bmatrix} -2L\cos(\phi)(H\cos(\theta) - y_t\sin(\theta)) \\ 2L\sin(\phi)(H\sin(\theta) + y_t\cos(\theta)) - 2Lx_t\cos(\phi) \end{bmatrix}^{\mathrm{T}}, \dot{\vec{q}} = \begin{bmatrix} \dot{\theta} \\ \dot{\phi} \end{bmatrix} \quad \text{and} \quad \begin{bmatrix} \mathrm{b} \end{bmatrix} = \begin{bmatrix} 0 \\ 0 \end{bmatrix} \tag{7}$$

Next, the velocity constraint equation is differentiated to obtain the acceleration constraint:

$$\begin{bmatrix} \mathrm{a} \end{bmatrix} \ddot{\vec{q}} + \begin{bmatrix} \dot{\mathrm{a}} \end{bmatrix} \dot{\vec{q}} + \begin{bmatrix} \dot{\mathrm{b}} \end{bmatrix} = \begin{bmatrix} 0 \end{bmatrix}$$

$$\begin{bmatrix} \dot{\mathrm{a}} \end{bmatrix}$$

$$= \begin{bmatrix} 2L(\dot{\theta}\cos(\phi)(H\sin(\theta) + y_t\cos(\theta)) + \dot{\phi}\sin(\phi)(H\cos(\theta) - y_t\sin(\theta))) \\ 2L(\dot{\phi}(H\sin(\theta)\cos(\phi) + x_t\sin(\phi) + y_t\cos(\theta)\cos(\phi)) + \dot{\theta}\sin(\phi)(H\cos(\theta) - y_t\sin(\theta))) \end{bmatrix}^{\mathrm{T}},$$

$$\ddot{\vec{q}} = \begin{bmatrix} \ddot{\theta} \\ \ddot{\phi} \end{bmatrix} \quad \text{and} \quad \begin{bmatrix} \dot{\mathrm{b}} \end{bmatrix} = \begin{bmatrix} 0 \\ 0 \end{bmatrix} \tag{8}$$

After attaining all the constraints, the Newton-Euler formulation is applied to derive the kinetic and potential energy equations:

$$T = \frac{1}{2}L^2 m_h \left(\cos^4(\theta)\dot{\phi}^2 + \dot{\theta}^2\right) + \frac{1}{6}L^2 m_p \left(\cos^4(\theta)\dot{\phi}^2 + \dot{\theta}^2\right) \tag{9}$$

$$V = gL\left(m_h + \frac{m_p}{2}\right)\cos(\phi)\sin(\theta) \tag{10}$$

where the payload is treated as a beam with uniformly distributed mass m_p, and the hook is a point mass m_h. The kinetic energy of the payload and the hook both consist of the rotational

energy in the θ and ϕ directions. The Lagrangian is then calculated and simplified:

$$\begin{aligned} L &= T - V \\ L &= gL\left(m_h + \frac{m_p}{2}\right)\cos(\phi)\sin(\theta) \end{aligned} \tag{11}$$

By applying the constrained Lagrange equation, two Lagrange equations are obtained:

$$\frac{\mathrm{d}}{\mathrm{d}t}\frac{\partial L}{\partial \dot{q_j}} - \frac{\partial L}{\partial q_j} = {Q_j}^{(a)} + \sum_{i=1}^{j} a_{ij}\lambda_i \qquad j = 1, 2$$

$$\frac{1}{6}L\left(3g\cos(\theta)(2m_h + m_p)\cos(\phi) + 2L(3m_h + m_p)\left(2\sin(\theta)\cos^3(\theta)\dot{\phi}^2 + \ddot{\theta}\right)\right) = 0 \tag{12}$$

$$-\frac{1}{2}gL\sin(\theta)(2m_h + m_p)\sin(\phi) + \frac{1}{3}L^2\cos^3(\theta)(3m_h + m_p)(\cos(\theta)\ddot{\phi} - 4\dot{\theta}\dot{\phi}\sin(\theta)) + c\dot{\phi} = 0 \tag{13}$$

where c is a virtual damping term used to characterize energy dissipation of the system. This approximation used due to the difficulty in accurately modeling friction at the pivot point and capturing minor energy loss in the mechanical parts. The augmented system of matrices is:

$$\begin{bmatrix} [\mathrm{M}] & -[\mathrm{a}]^T \\ -[\mathrm{a}] & 0 \end{bmatrix} \begin{bmatrix} \ddot{\vec{q}} \\ \vec{\lambda} \end{bmatrix} = \begin{bmatrix} [\mathrm{F}(\vec{q}, \dot{\vec{q}})] \\ [\dot{\mathrm{a}}]\dot{\vec{q}} + [\dot{\mathrm{b}}] \end{bmatrix}$$

$$\Big[\mathrm{M}\Big] = \begin{bmatrix} \frac{1}{3}L^2(3m_h + m_p) & 0 \\ 0 & \frac{1}{3}L^2(3m_h + m_p)\cos^4(\theta) \end{bmatrix}$$

$$\Big[\mathrm{F}\Big] = \begin{bmatrix} -\frac{1}{6}L\cos(\theta)\left(4L(3m_h + m_p)\cos^2(\theta)\sin(\theta)\dot{\phi}^2 + 3g(2m_h + m_p)\cos(\phi)\right) \\ \frac{1}{3}\dot{\phi}\left(4L^2(3m_h + m_p)\cos^3(\theta)\sin(\theta)\dot{\theta} - 3c\right) + \frac{1}{2}gL(2m_h + m_p)\sin(\theta)\sin(\phi) \end{bmatrix} \tag{14}$$

To obtain equations of motion related to $\ddot{\theta}$ and $\ddot{\phi}$, (14) is transformed to:

$$\begin{bmatrix} [\ddot{\vec{q}}] \\ [\lambda] \end{bmatrix} = \begin{bmatrix} [\mathrm{M}] & -[\mathrm{a}]^T \\ -[\mathrm{a}] & 0 \end{bmatrix}^{-1} \begin{bmatrix} [F(\vec{q}, \dot{\vec{q}})] \\ [\dot{\mathrm{a}}]\dot{\vec{q}} + [\dot{\mathrm{b}}] \end{bmatrix} \tag{15}$$

Next, the equations of motion are organized into matrix form. The exact solution for the natural frequency can be calculated and linearized to estimate the natural frequency:

$$\left[\mathrm{M}\right] \ddot{\vec{q}} + \left[\mathrm{C}\right] \dot{\vec{q}} + \left[\mathrm{K}\right] \vec{q} = 0 \quad \text{and} \quad \omega_n = \sqrt{\frac{\mathrm{K}}{\mathrm{M}}} \tag{16}$$

Despite having the augmented system of matrices, matrix inversion, and matrix multiplication of (15) require calculations that cannot be done in closed form. This is because in attempt to fully describe the dynamic system, trigonometrical functions are multiplied together and high power terms, such as those in (12), are created. Beyond this, deriving natural frequency by taking square root of K/M adds extra complexity to the problem.

Even though the above process does not generate an analytical solution for natural frequency, (15) can still be used to generate a mathematical simulation, where the matrices on the right side of the equation are numerically determined before inversion and multiplication at each iteration. With small enough step size and an experimentally determined damping coefficient, the simulation result can closely resemble the behavior of the actual system. The natural frequency can then be obtained by examining the simulation results.

2.3.2 Model Verification

Since the side-swing motion of the payload demonstrates characteristics similar to that of a simple harmonic motion, its damping coefficient can be calculated:

$$\begin{aligned} c &= \zeta c_{critical} \\ c &= \zeta 2m\omega_n \\ c &= \zeta 2m\omega_d/\sqrt{1-\zeta^2} \end{aligned} \tag{17}$$

where ζ is the damping ratio of the system, ω_d is the damped frequency, and m is the mass term from the **M** matrix that corresponds to the side swing angle ϕ.

To determine damping coefficient of the actual setup, an experiment was performed. The payload was released from a fixed angle and the change in ϕ was recorded. The logarithmic decrements method is applied to the experimental data to calculate the damping ratio:

$$\zeta = \frac{\delta}{\sqrt{(2\pi k)^2 + \delta^2)}} \quad \text{and} \quad \delta \doteq \ln(\frac{x_1}{x_2}) \tag{18}$$

where x_1 is amplitude of the first peak, x_2 is amplitude of the second peak, and k is the number of periods separating the two peaks. Three peaks were chosen from the experimental data. Then, three pairs of two peaks were formed to calculate three damping ratios. The three results were averaged to obtain the damping ratio of the system. Figure 11 presents the recorded ϕ angle change over time, where exponential decay of the oscillation amplitude can be clearly observed. Table 4 contains the experiment parameters and damping ratios calculated from the three peaks chosen. Also obtained from the data is the damped frequency. The damping coefficient of the system is then determined with the damping ratio and damped frequency. This damping coefficient can be used in the mathematical simulations.

To verify the effectiveness of the simulation, the natural frequency calculated from simulated results is compared to those obtained from experiments under identical system con-

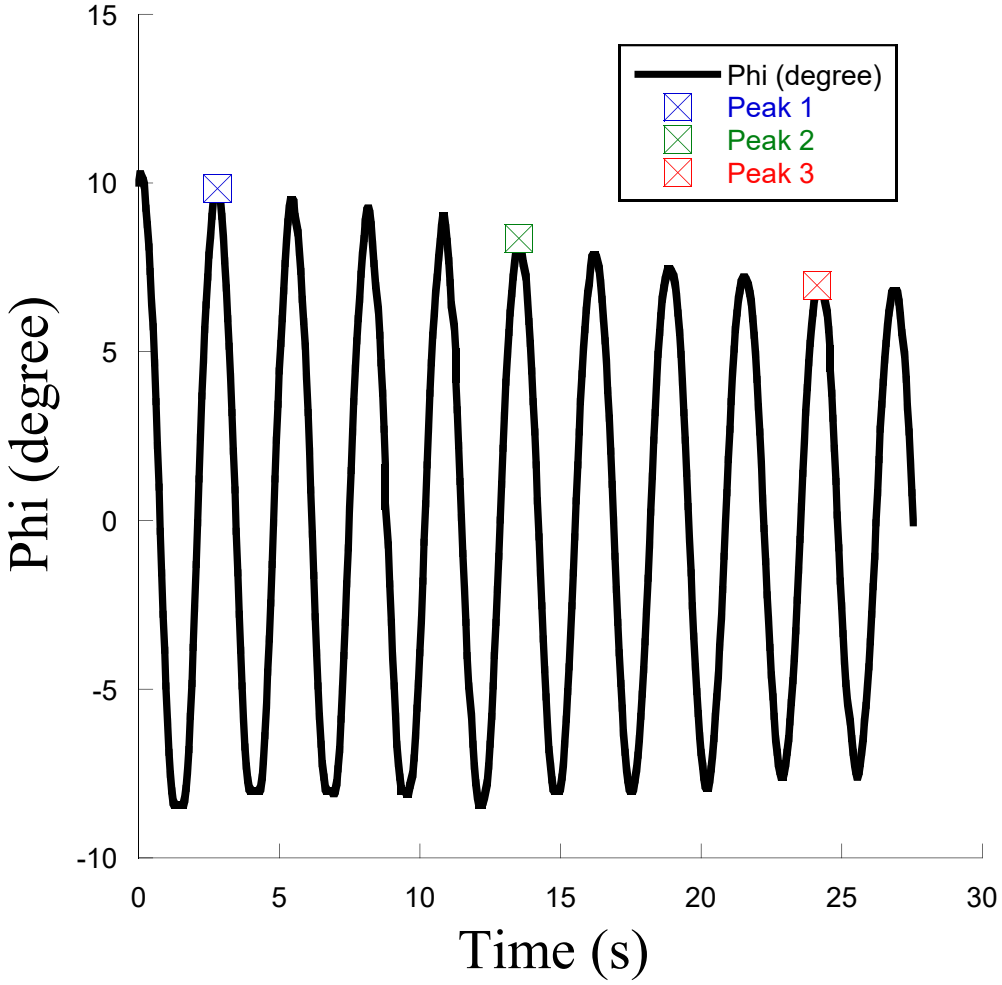

Figure 11: Change in ϕ from induced payload side-swing

-

Table 4: Damping Ratio Experiment Parameters and Results

Parameter	Value
θ_i	1.4 degree
ϕ_i	10 degree
t_x	0 m
t_y	0.58 m
Contact Surface	Aluminum Edge vs. Aluminum Surface
Results	**Value**
ζ_{12}	0.0065
ζ_{13}	0.0068
ζ_{23}	0.0072
ζ_{avg}	0.0068

Table 5: Damping Ratio Experiment Parameters and Results

Parameter	Value
θ_i	2 degree
ϕ_i	15 degree
t_x	0 m
Contact Surface	Aluminum Edge vs. Aluminum Surface
Results	Natural frequency & Error
t_y = 0.505 m	2.185 rad/s & 3.91%
t_y = 0.555 m	2.371 rad/s & 6.30%
t_y = 0.61 m	2.545 rad/s & 3.31%
t_y = 0.66 m	2.832 rad/s & 2.62%
t_y = 0.72 m	2.959 rad/s & 2.74%

figurations. Figure 12 presents the change in natural frequency as t_y, the distance between the hook and trolley along the payload's longitudinal axis, changes while other parameters are kept constant. As can be seen, the natural frequency of the system increases as the trolley moves from the left side to the right side of the hooks position. Table 5 documents the experiment configuration and results. The experimental result demonstrated the same trend of growing natural frequency, as suggested by the simulation. Also, the natural frequencies predicted by the simulation has errors ranging from 2.62% to 6.30%. Therefore, the simulation can be considered a reliable way of predicting the system's motion. The cause of the errors can be the relatively low resolution of the camera. It can also be caused by the unmodeled motion within mechanical parts of the crane and payload.

2.4 Simplified System Model

2.4.1 Simplified Model Derivation

Despite the fact that simulation can give accurate estimations of natural frequency, its time-consuming nature limits its use to analysis before and after operations. Figure 13 is a simpler model for real-time frequency calculations during operation. It ignores the the small elevation angle of the payload. Kinetic energy of this system only consists of the

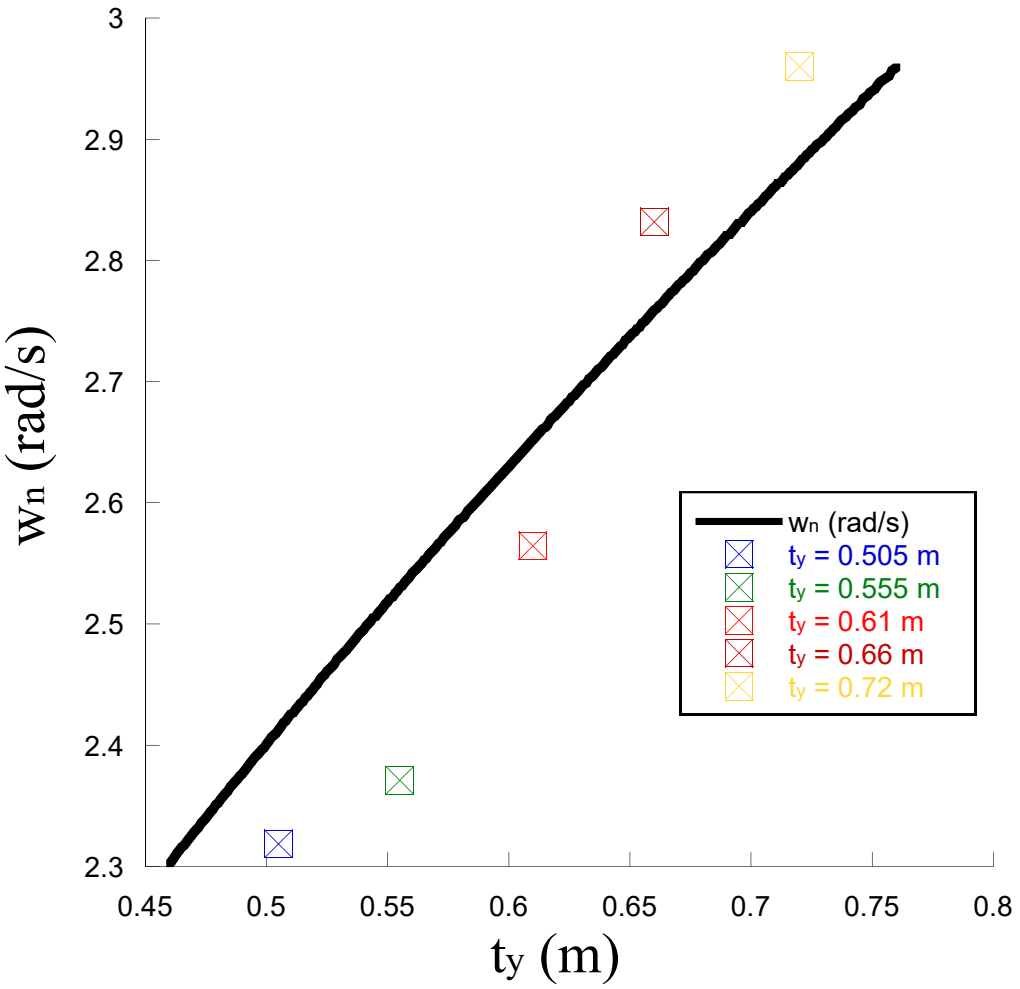

Figure 12: Natural frequency change with respect to trolley y-axis position change,predicted by simulation and calculated from experimental results.

payload's side swing motion and that of the hook's pendulum motion. To calculate potential energy of the payload, it is treated as a point mass, whose height above ground is always half that of the hook. The energy equations of the system are revised as:

$$T = \frac{1}{2}m_h l^2(\frac{\dot{\theta}}{\cos(\sigma)})^2 + \frac{1}{6}m_p l^2(\frac{\dot{\theta}}{\cos(\sigma)})^2 \tag{19}$$

$$V = (m_h + \frac{1}{2}m_p)gl\cos(\sigma)(1 - \cos(\frac{\theta}{\cos(\sigma)}) \tag{20}$$

$$L = \frac{1}{6}l\cos(\sigma)\left(3g(2m_h + m_p)(\cos(\theta\sec(\sigma)) - 1) + l(\dot{\theta})^2(3m_h + m_p)\sec^3(\sigma)\right) \tag{21}$$

The Lagrange equation is then applied to the energy equations to obtain the equation of motion:

$$l^2(m_h + \frac{1}{3}m_p)\frac{1}{\cos^2(\sigma)}\ddot{\theta} + c\dot{\theta} + lg(m_h + \frac{1}{2}m_p)\sin(\frac{\theta}{\cos(\sigma)}) = 0 \tag{22}$$

where c is the damping ratio determined previously. It is then linearized by assuming $\sin(\theta/\cos(\sigma)) = \theta/\cos(\sigma)$. Finally, the expression of natural frequency is:

$$w_n = \sqrt{\frac{g(m_h + \frac{1}{2}m_p)\cos(\sigma)}{l(m_h + \frac{1}{3}m_p)}} \tag{23}$$

2.4.2 Simplified Model Verification

Figure 14 presents a comparison between the natural frequency calculated from the complex model and the simplified model. The simulation parameters are identical to that in Table 5. As can be observed, both models are able to characterize the parabolic shape of natural frequency change with respect to the trolley's position change in the y-axis. However, the simplified model fails to indicate the continued growth of the natural frequency as σ becomes negative. As the trolley approaches the hook's position from the left side, the error decreases. As the trolley moves further away to the right side, the error increases.

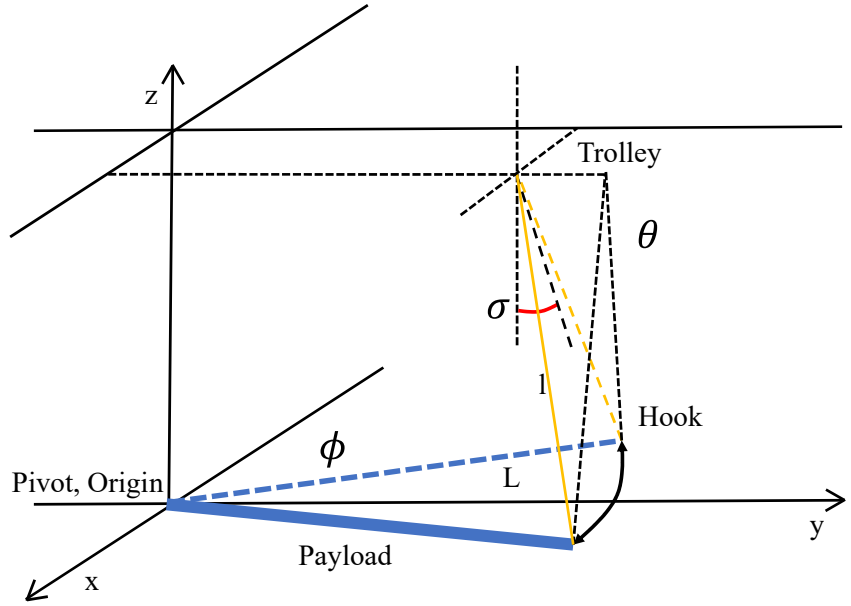

(a) Kinetic energy model for the simplified system

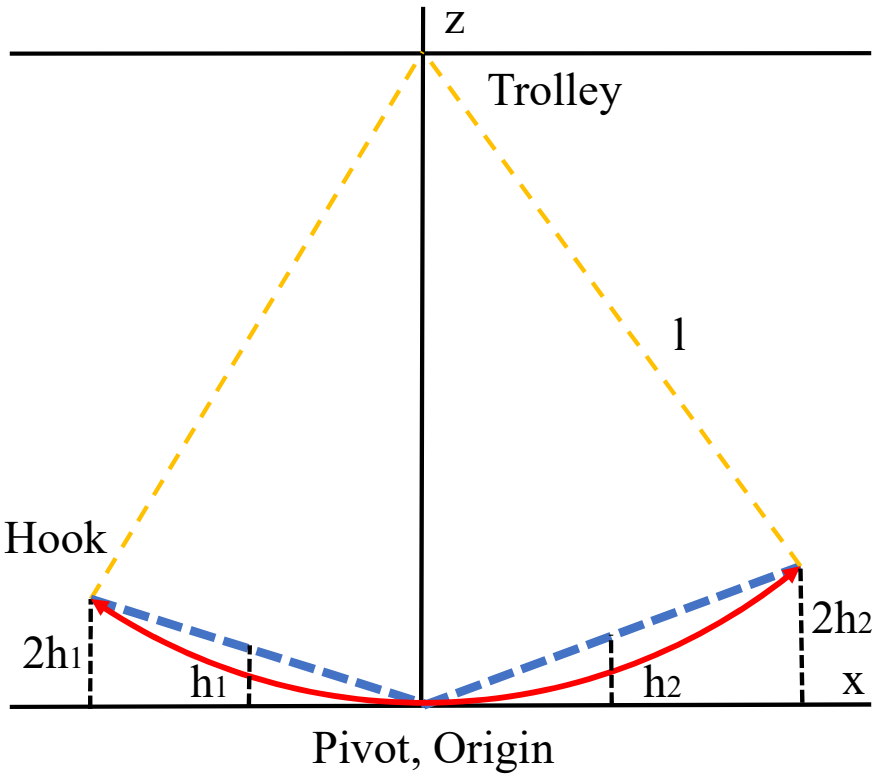

(b) Potential energy model for the simplified system

Figure 13: Schematic diagram of the simple model

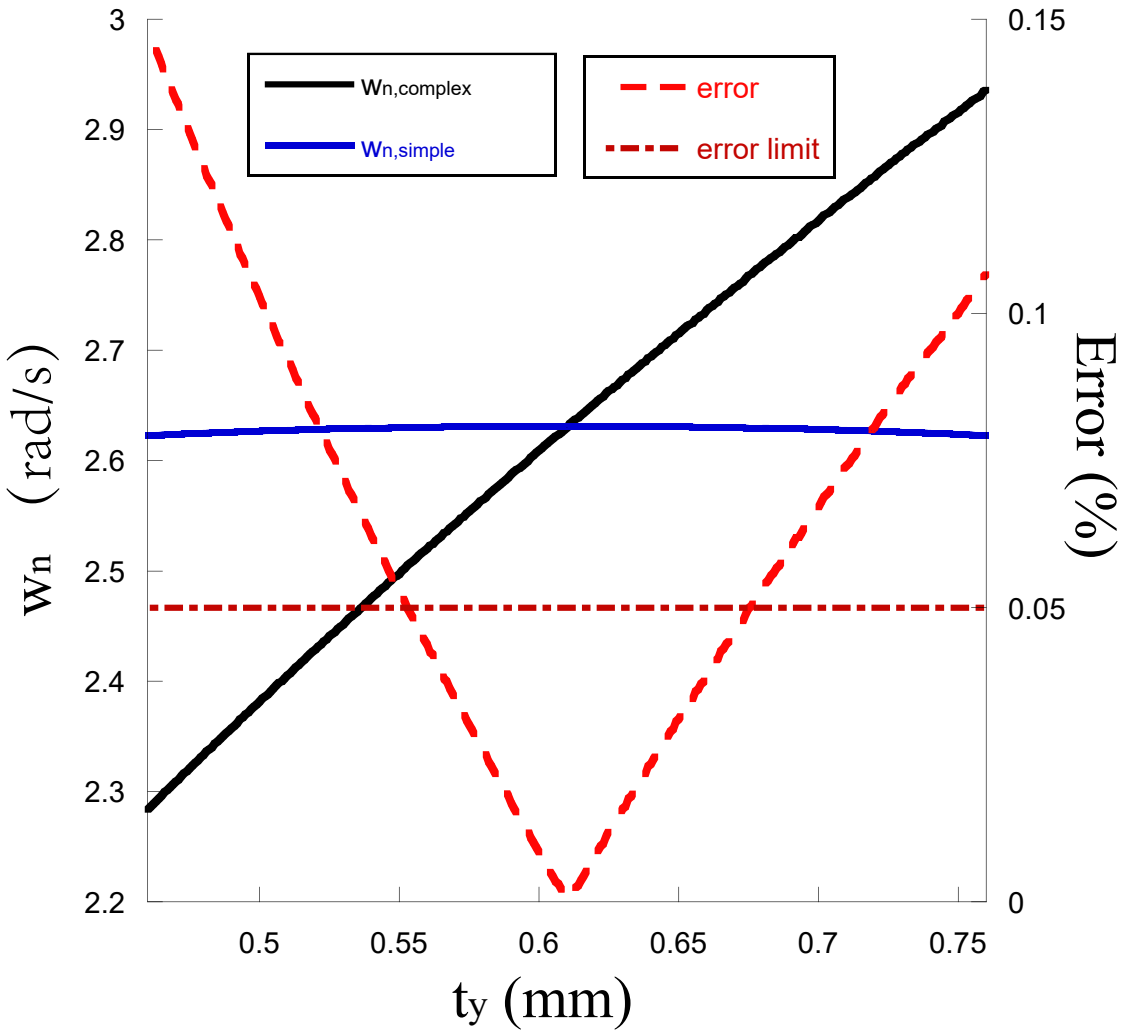

Figure 14: Natural frequency change with respect to trolley y-axis position change predicted by complex and simple model simulations. Red line shows percentage error between the two model.

Also, no error occurs when the trolley is directly over the hook position. The region within which the error of the simplified model is less than 5% is defined as the effective region. For a θ angle of 2 degrees, the simplified model can effectively estimate the natural frequency as long as σ is within 1.73 degrees to -1.95 degrees. This is acceptable because the error produced by trolley and hook alignment is contained in this range, as indicated by Figure 7.

2.5 Input-Shaped Payload Alignment

After obtaining the natural frequency and damping ratio of the system, input shaping can be applied. Input shaping is a technique used to minimize oscillation by modifying input commands, at the cost of slightly longer operation time.

2.5.1 Speed Command Limitation

The command to be modified in the payload alignment process is a velocity command that moves the payload in a circular trajectory from a deflected position to a position that is parallel to, and vertically under, the bridge. Because position of the hook and pivot point are known from hook alignment and payload orientation detection respectively, the desired rotation can be calculated:

$$\lambda = \arctan(\frac{h_x - P_x}{h_y - P_y}) \tag{24}$$

where λ is deflection angle of the payload with respect to the bridge. The speed command corresponding to this angular speed is then determined as:

$$v_b = L\dot{\lambda}\cos(\lambda) \tag{25}$$

$$v_t = -L\dot{\lambda}\sin(\lambda) \tag{26}$$

where v_b is speed of the bridge motion and v_t is the trolley motion. Because the motors are limited to a speed of 0.2 m/s, $\dot{\lambda}$ is limited to 20 degree/s to ensure the velocity command can be fully executed, assuming the biggest deflection angle that can be encountered is 20 degrees.

A vital assumption made for the alignment process is that the pivot point, which is the middle point of the payload's edge in contact with the ground, is fixed. Furthermore, the static frictional force incurred by the ground is assumed to be a point force and only applies to the pivot point. The speed of the angular velocity command should be chosen

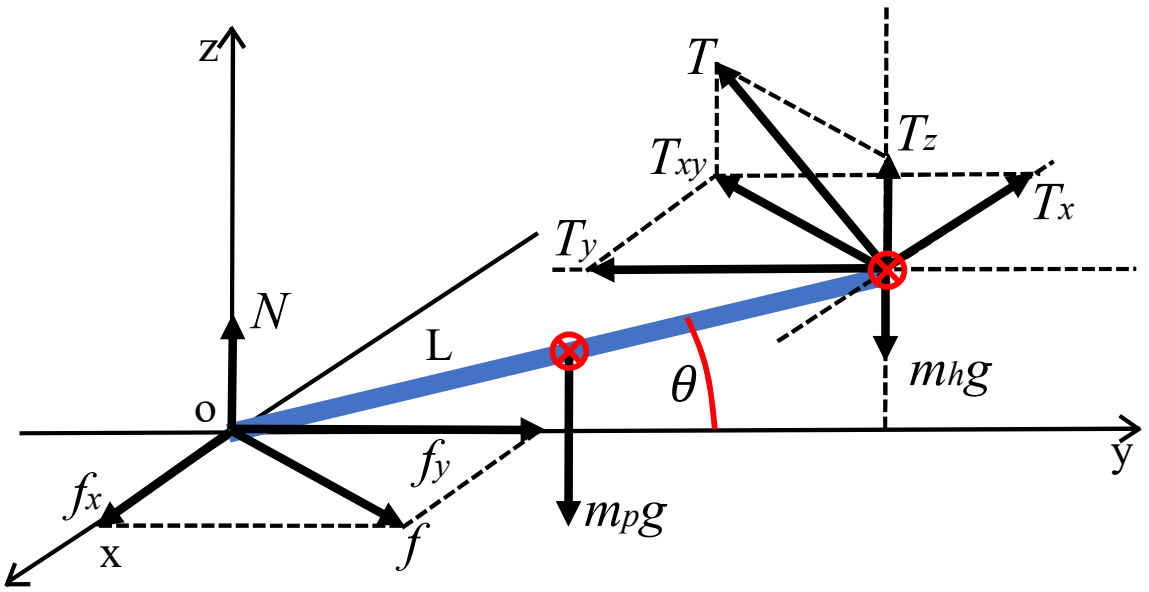

Figure 15: Free body diagram of the payload in side-swing.

to satisfy these assumptions. Figure 15 is free body diagram of a payload being pulled to the side. The coordinate system is shown at the pivot point. The y-axis is constantly aligned with the payload. N, f and T represent the normal force, the static friction force, and the tension, respectively. By applying Newton's second law, the following force and momentum relationships are obtained:

$$\sum F_x = f_x - T_x = 0 \tag{27}$$

$$\sum F_y = f_y - T_y = 0 \tag{28}$$

$$\sum F_z = N + T_z - (m_p + m_h)g = 0 \tag{29}$$

$$\sum M_x = T_z L\cos(\theta) - (\frac{1}{2}m_p + m_h)gL\cos(\theta) = I_{p+h} * \dot{\theta} \tag{30}$$

$$\sum M_y = T_x L = I_{p+h} * \dot{\phi} \tag{31}$$

where ϕ and θ refer to same angles labeled previously in Figure 10. To preserve the as-

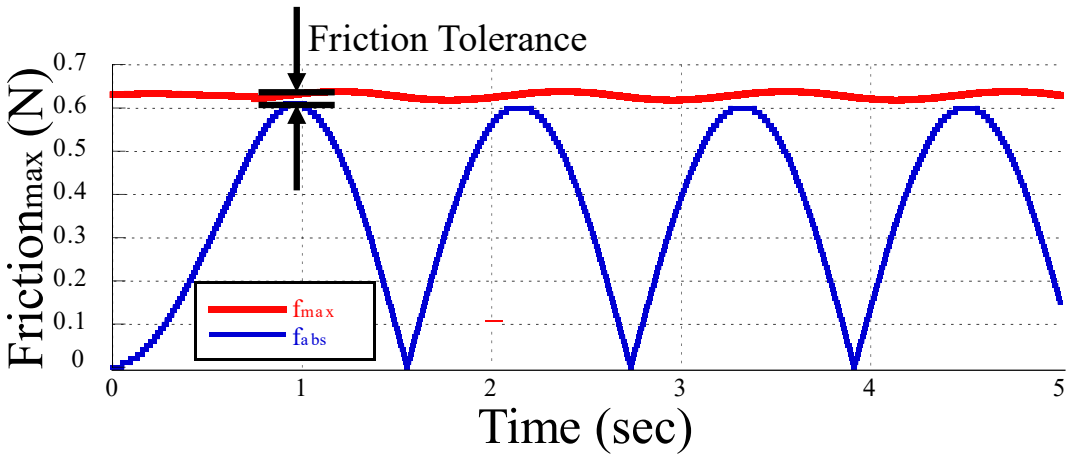

Figure 16: Simulated tension and maximum friction during the alignment side-swing with fixed maximum static friction coefficient.

sumption of a fixed pivot point, the following must be true:

$$|f| < f_{max} \tag{32}$$

$$\text{and} \quad f_{max} = \mu_{max} N$$

$$f = T_{xy}$$

where f_{max} is the maximum static friction force and μ_{max} is the maximum static friction coefficient that can be experimentally determined. The equations that provide the friction coefficient will be discussed in the next chapter. However, the scope of this thesis does not include specific experimental methods of measuring the friction coefficient.

From the simulation, the position, velocity and acceleration of the hook, trolley, and angles is obtained. This allows us to apply and solve equations (26) to (30) in order to check if the assumption of a fixed pivot point stays true. Figure 16 presents the change in tension and maximum static friction with respect to time for a simulation trial where μ_{max} is 0.2 and angular velocity is 20 degree/s. The first peak of the tension is located right after the velocity command ends. The difference between this peak and the corresponding friction is defined as friction tolerance.

By running simulations for a range of command velocities and μ_{max}, a velocity bound-

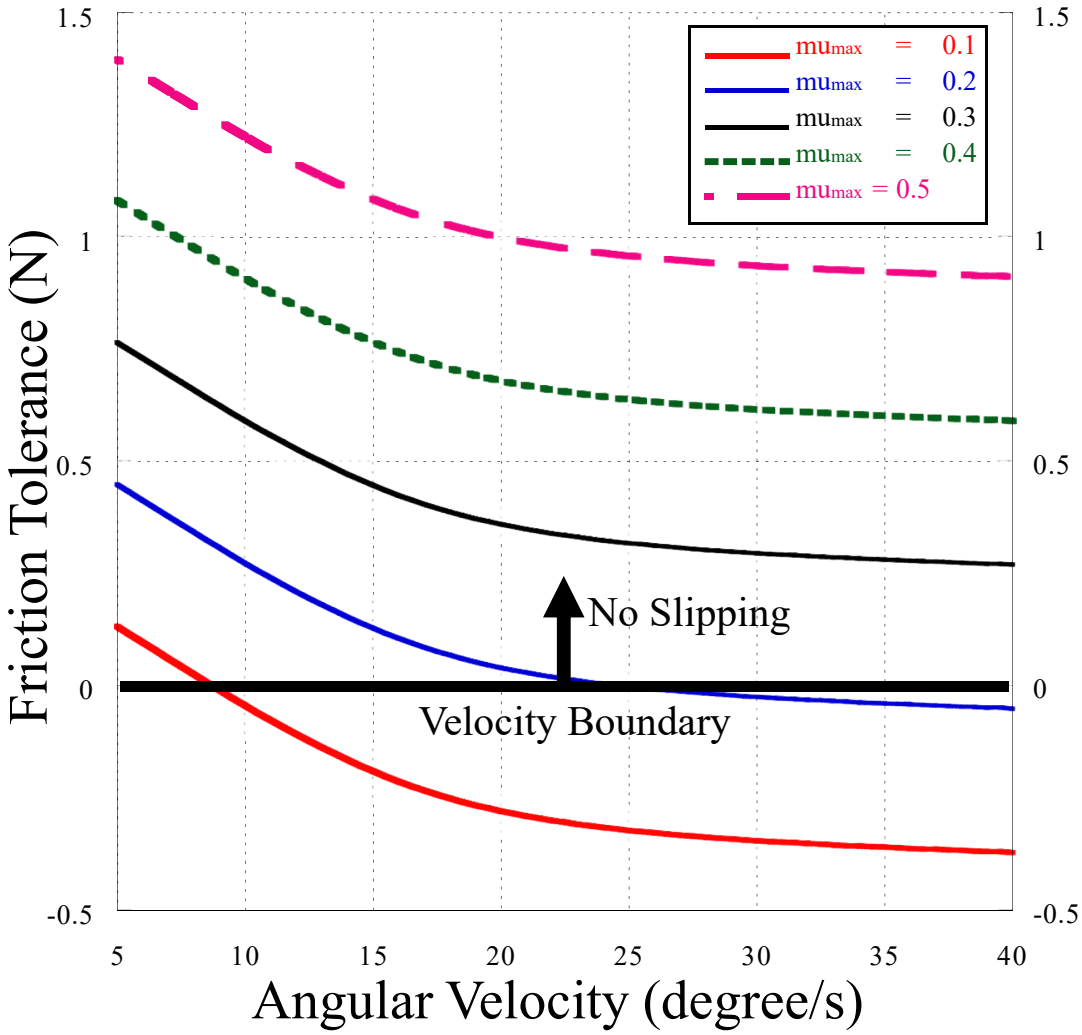

Figure 17: Friction tolerance change with respect to change in maximum static friction coefficient.

ary under which no slipping happens can be derived. Figure 17 presents the change in friction tolerance with angular velocity for different friction conditions. As demonstrated, the friction tolerance is smaller when angular velocity increases and when the maximum friction coefficient decreases. To prevent slipping when using an angular velocity of 20 degree/s, a friction coefficient of 0.5 is required.

Because the speed limitation analysis is simulation based, it must be completed before the lift-up operation. The method can be used to calculate and tabulate speed limitations for the material frequently transported in a specific workspace so that the limitation is readily

available.

2.5.2 Input-Shaper Design

Input shaping is implemented by convolving the reference command with an impulse pattern that has time delays. The impulse patterns are called input shapers. The dynamic system's responses induced by the convolved command can cancel each other in the way of destructive interference and the command can be executed with minimum residual vibration. Input shaping is an advantageous control method because it does not need the current state of the system, which saves the cost of sensors and computation. Furthermore, the input command can be generated by simply knowing the plant dynamics before the operation.

A generic process of input shaping is presented in Figure 18. At first, the reference command is convolved with an input-shaper consisting of two impulses. The resultant command consequently becomes the addition of two smaller step commands with a delay δt. As a result, most of the vibration caused by the first step input, except for the first peak, is canceled by the vibration caused by the second step input. This is in fact a Zero Vibration (ZV) shaper, which has the transfer function of:

$$\mathbb{G}(s) = A_1 + A_2 e^{-t_2 s} \tag{33}$$

where A_1, A_2 are the amplitude of the first impulse and second impulse respectively, and t_2 is the time delay between the two impulses. The value of these three parameters are designed relative to the vibration system's natural frequency and damping ratio using:

$$\begin{bmatrix} A_1 & A_2 \\ 0 & t_1 \end{bmatrix} = \begin{bmatrix} \frac{1}{1+K} & \frac{K}{1+K} \\ 0 & \frac{\pi}{\omega_d} \end{bmatrix} \quad \text{where} \quad K = \exp(-\frac{\zeta\pi}{\sqrt{1-\zeta^2}}) \tag{34}$$

As has been proven by Figure 14, the system's natural frequency estimated by a sim-

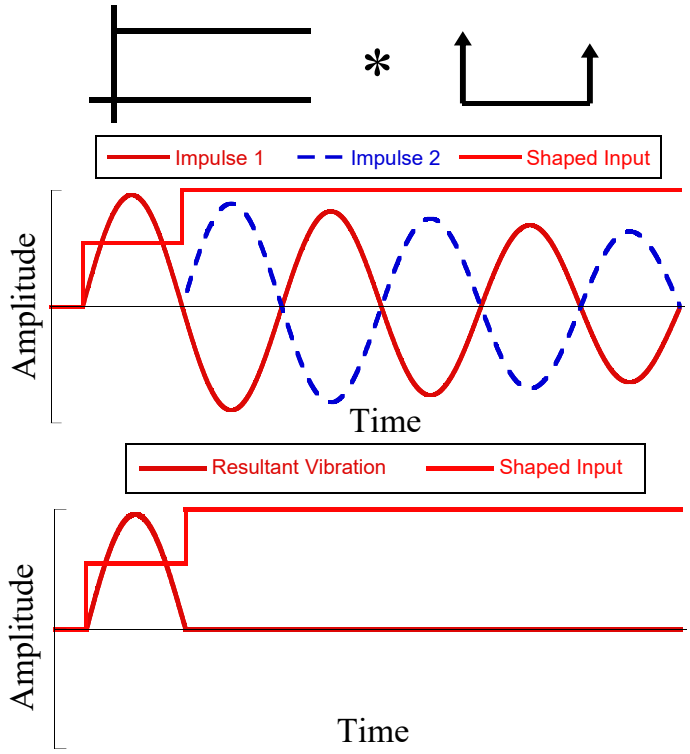

Figure 18: Input shaping process

plified model is not perfect. The ZV shaper, being the most simplistic shaper, lacks the robustness to such modeling errors. A robust shaper called the ZVD shaper can be designed to cope with the model uncertainty. It is a shaper with three impulses:

$$\begin{bmatrix} A_1 & A_2 & A_3 \\ 0 & t_1 & t_2 \end{bmatrix} = \begin{bmatrix} \frac{1}{K^2+2K+1} & \frac{2K}{K^2+2K+1} & \frac{K^2}{K^2+2K+1} \\ 0 & \frac{\pi}{\omega_d} & \frac{2\pi}{\omega_d} \end{bmatrix} \tag{35}$$

Figure 19 presents the comparison between unshaped, ZV-shaped, and ZVD-shaped velocity commands. It also presents the angular position change of the payload. As demonstrated by Figure 19a, the command modified by the ZVD shaper takes the longest operation time and the command shaped by the ZV shaper is faster. However, trajectories of the shaped commands are smoother than that of the unshaped command. This characteristic can also be observed in the velocity command comparisons. The shaped commands, while using more time, are smoother than the unshaped command. This is especially apparent in

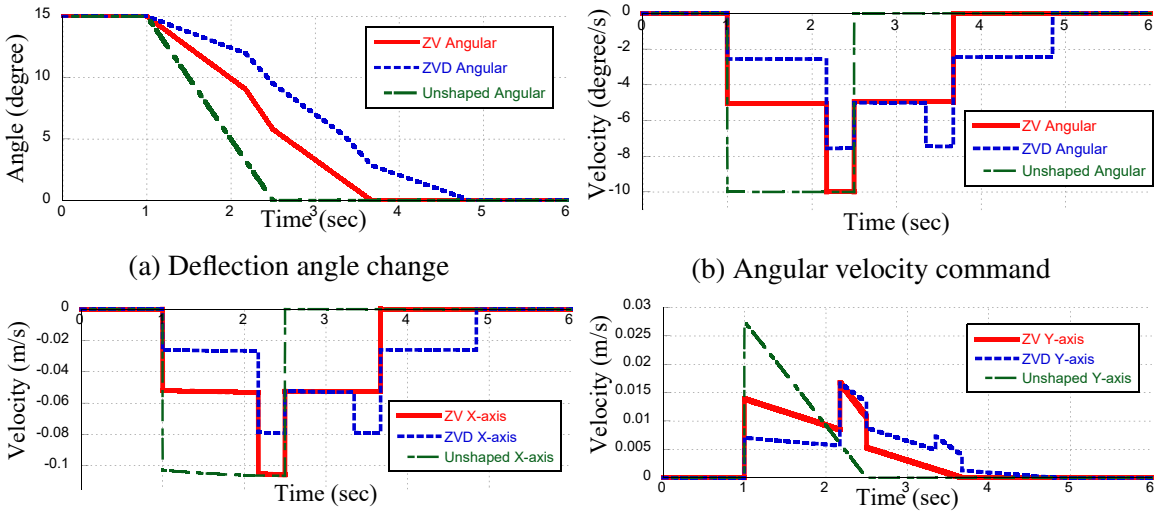

(a) Deflection angle change

(b) Angular velocity command

(c) Velocity command in x-axis

(d) Velocity command in y-axs

Figure 19: Input-shaped commands and trajectories

Figure 19d.

2.5.3 Simulation Verification

To verify effectiveness of the input shaper designs and examine their differences, the simulation from the last section is modified by dismissing the assumption in Equation 14 that y_t and y_t are constant. The resulting new velocity and acceleration constraint equations can then help account for the motion of the trolley. The simulation starts with an initial condition of 15 degrees of deflection angle, 2 degrees of elevation angle and a trolley position directly on top of the hook. Figure 20 presents sensitivity curve of the ZV and ZVD shapers for this particular system. The residual vibration is normalized by dividing it by the vibration amplitude of the unshaped response. The normalized error is obtained by benchmarking against the simulated natural frequency. It can be clearly observed that the ZVD shaper is much more robust to modeling error, compared to the ZV shaper. It is also noticed that the sensitivity curve follows the same trend as the modeling error presented in Figure 14, which proves the validity of this simulation. For both sensitivity curves, the change of residual vibration with respect to the normalized error from negative spectrum

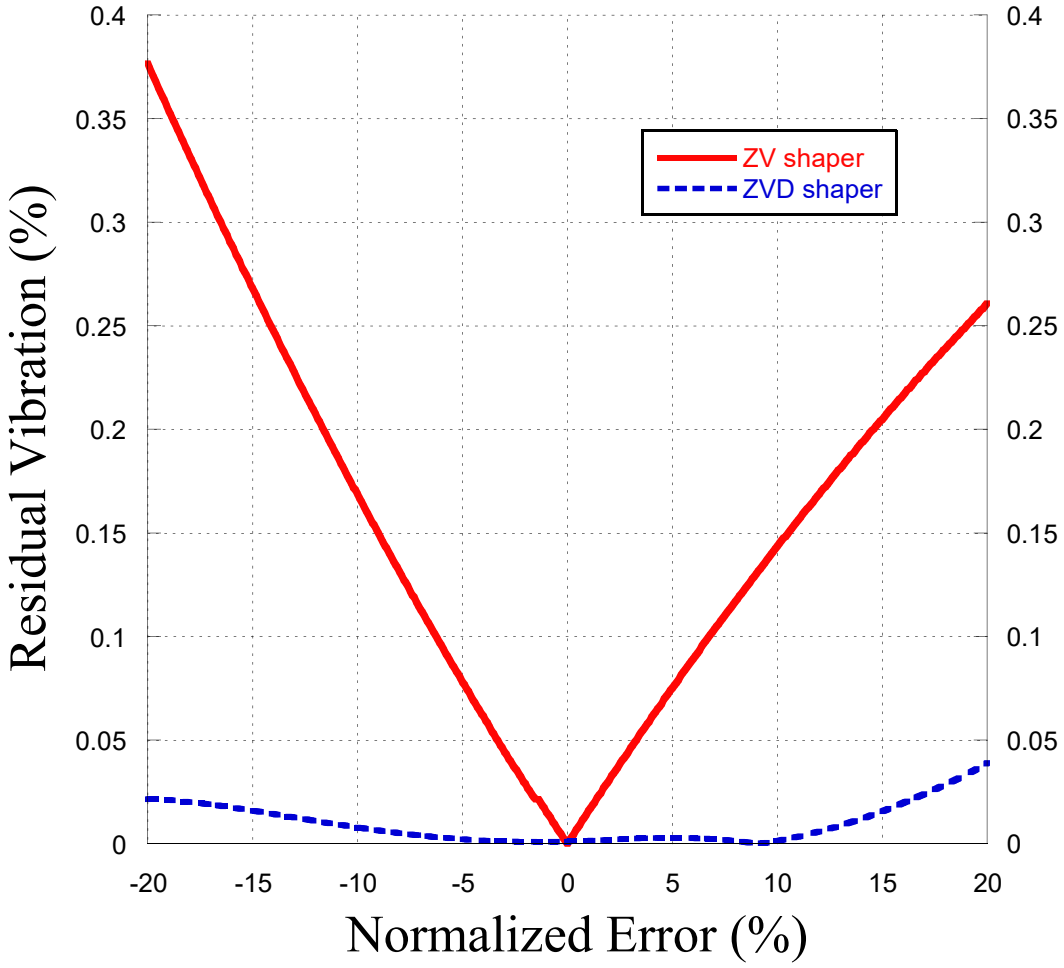

Figure 20: Sensitivity curve of the ZV and ZVD shaper

to positive spectrum is asymmetrical. This is caused by non-linearity in the model. When considering the physical meaning of the error, a negative error indicates the trolley is closer to the pivot point, while a positive error indicates the trolley is further away from the pivot point.

2.5.4 Experimental Verification

Experiments were conducted to validate the predictions from simulation. The payload was placed at 15 degrees of deflection angle with respect to the bridge's axis. Then, the trolley was aligned to the hook's position. Velocity commands were given to the motors in x and

y-aixs in a coordinated manner to reproduce the input-shaped angular velocity command so that the payload was aligned with the bridge. To introduce modeling error, t_y is either increased or decreased, and the trolley is no longer aligned to the hook's position. The velocity commands are also modified to account for the initial trolley position change.

Figure 21 presents the results of the input-shaped payload alignment experiment. The selected data is recorded right at the moment the velocity command becomes zero to only capture the hook's residual vibration in the x-axis. Figure 21a presents the comparison between residual vibration from unshaped command, ZV, and ZVD shaped commands. As can be clearly observed, the unshaped command induces deflection as large as 29 cm, while the deflections caused by input shaped commands are less than 1 cm. This proves that input shaping provides significant advantages over unmodified commands.

Figure 21b compares residual vibrations caused by ZV shaped commands. The natural frequency on which the shapers are designed is referred to as the base frequency. When using ZV shapers on a system with 85% of the base frequency, the initial amplitude of deflection is increased slightly from 1 cm to 2 cm. When using ZV shapers on a system with 115% of the base frequency, the initial amplitude of deflection is increased significantly to 9 cm. Both positive and negative errors result in increased deflection. However, the ZV shaper is much less sensitive to a negative error than to a positive one, which is not predicted by the sensitivity curve from simulation.

Figure 21c compares residual vibrations caused by ZVD shaped commands. When using a ZVD shaper on a system with 85% of the base frequency, the amplitude of residual vibration is negligible, as it is not measurable to the camera. When using a ZVD shaper on a system with 115% of the base frequency, the initial amplitude of deflection is increased from 0 cm to 3 cm. The comparison between performance of the ZV and ZVD shaper shows that the ZVD shaper is much more robust to modeling errors than the ZV shaper, as predicted by the sensitivity curve. Both shapers share a general trend of being more sensitive to positive modeling error than to a negative one.

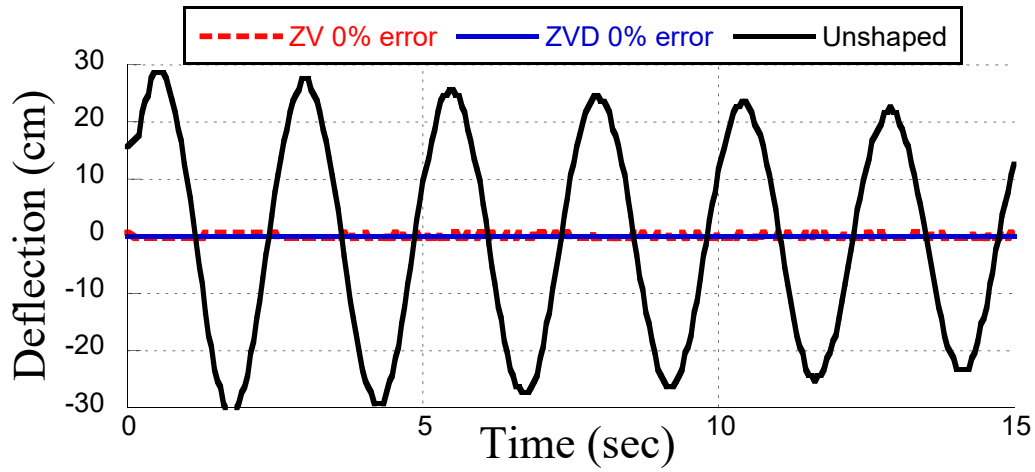

(a) Shaped and unshaped command

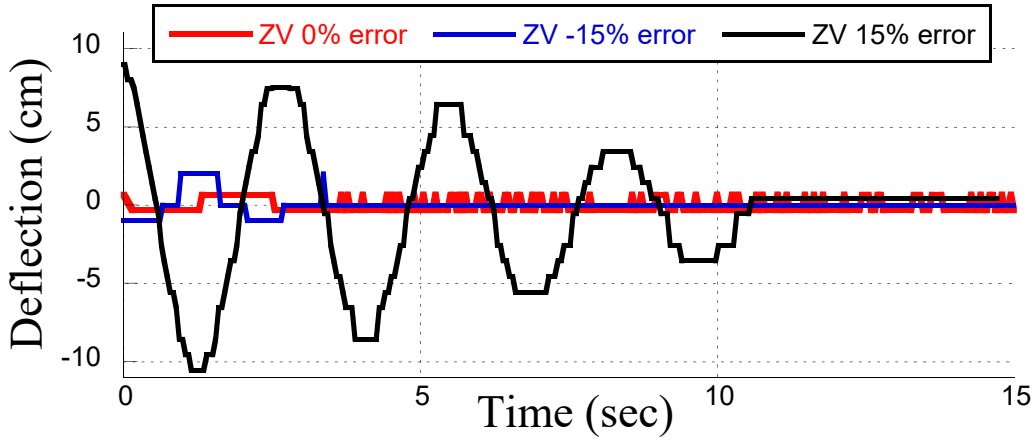

(b) ZV shaped command

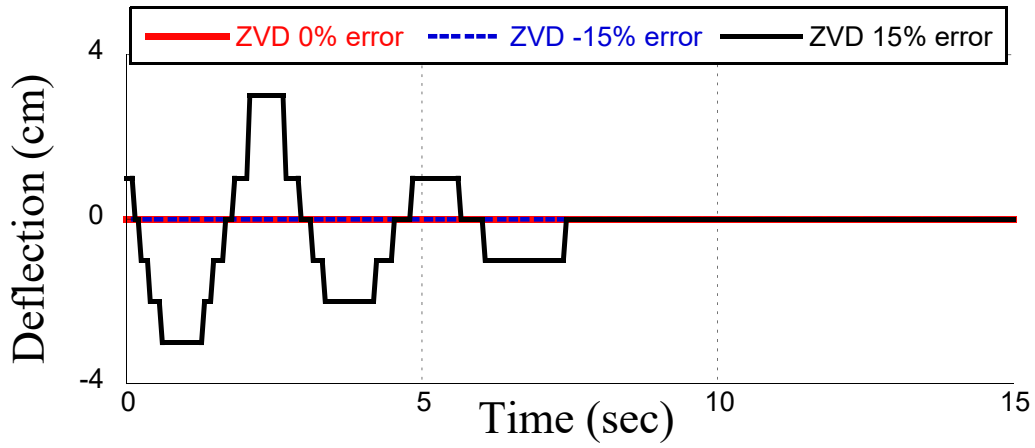

(c) ZVD shaped command

Figure 21: Residual vibration of payload alignment using different shapers

When considering the physical system, a positive error in natural frequency means that the trolley is moved away from the hook position and toward the pivot position. At this position, the trolley is less capable of pulling the payload when it travels in the trajectory of constant angular speed. Thus, after trolley motion ends, the payload is further away from the equilibrium position compared to when the trolley starts from right on top of the hook. This bigger initial swing angle then results in bigger residual vibration.

Additionally, it was discovered that when the deflection angle is small, the movement along the y-axis is negligible. The cost of ignoring motion in the y direction is that the system will end up with a natural frequency differing from that used for the shaper. However, it is well within the tolerable range of the shapers under small angle assumptions. This makes the command easier to implement. Furthermore, by designing more complicated input shapers, the payload orientation detection process can be integrated into the payload alignment process, as the first step input from the command provides enough swing in the system for the pivot point to be detected. As soon as position of the pivot point is available, swing trajectory and natural frequency of the system can be calculated. The shaper can, then, be modified to calculate a new input command.

CHAPTER 3

LIFT-UP TRAJECTORY DEVELOPMENT

Table 6 contains all the variables used in this chapter.

Table 6: Variables Used in Chapter 3

Variable	Meaning
y_t	Position of the trolley in the y-axis
z_t	Position of the trolley in the z-axis
L	Length of the payload
W	Width of the payload
l	Length of the hoist cable
m_p	Mass of the payload
m_h	Mass of the hook
θ	Elevation angle of the payload in side swing
ϕ	Deflection angle of the hoist cable from the Z-axis
y_p	Position of the pivot point in the x-axis
z_p	Position of the pivot point in the z-axis
T	Tension in the hoist cable
f	Static friction force at the pivot point
N	Normal force at the pivot point
mu_{max}	Maximum static friction coefficient

With the alignment process eliminating the payload's deviation in the x-axis, the payload is prepared to be lifted to a near vertical configuration in a circular trajectory motion constrained to the y-z-plane. The lift-up process should satisfy two conditions. First, no slipping should happen at the pivot point, where the payload and ground touch. Second, at the end of the lift-up, oscillation in the system should be limited to a low level, so that the incoming off-center lift-up has a more relaxed condition to start with. While meeting the necessary conditions, the trajectory should be executed in an efficient manner to save time.

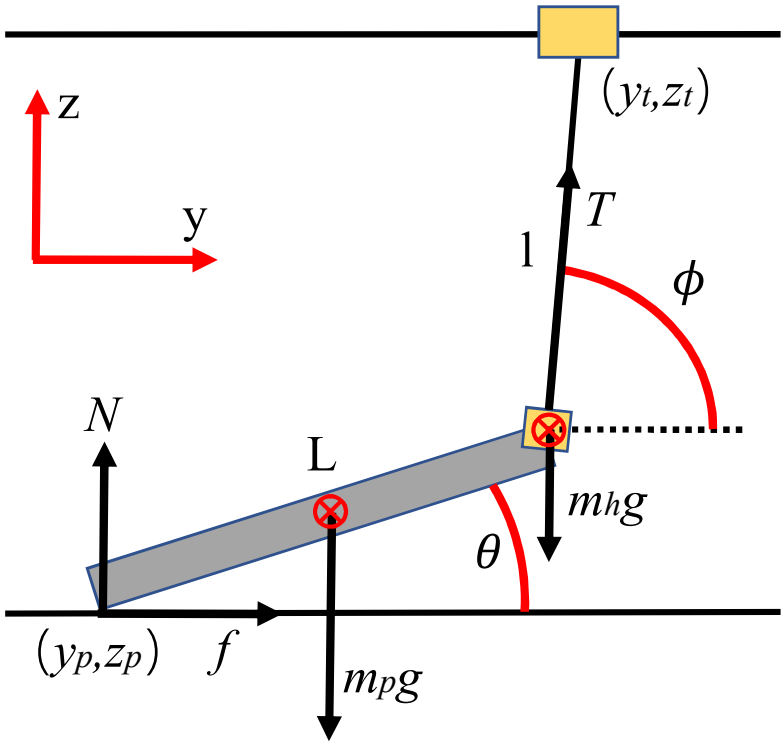

Figure 22: Free body diagram of the payload in circular lift-up

3.1 Model Based Friction Analysis

Figure 22 presents the free body diagram of the payload and the hook as a system. To guarantee that no slipping happens during the lift-up, the following conditions must be met:

$$|f| < f_{max} \tag{36}$$

$$\text{and} \quad f_{max} = \mu_{max} N$$

Furthermore, for the lift-up process to make physical sense, the following must be true:

$$N > 0$$

$$T > 0$$

$$\phi \geqslant \theta$$

The above must be true because the payload has to be in contact with the ground and the ground cannot pull on the payload for obvious reasons. Tension in the cable can neither be zero nor be negative because the hoist cable cannot slack off or push on the payload. Also, a configuration where ϕ is smaller than θ is physically impossible.

3.1.1 Static Friction Analysis

When the velocity command is slow enough, the payload can be considered to be pseudo-static in every infinitesimally short time interval. By balancing the forces and momentum acting on the payload, it can be obtained that:

$$\sum F_y = f + T\cos(\phi) = 0 \tag{37}$$

$$\sum F_z = N + T\sin(\phi) - (m_p + m_h)g = 0 \tag{38}$$

$$\sum M_x = TL\sin(\phi - \theta) - (\frac{1}{2}m_p + m_h)gL\cos(\theta) = 0 \tag{39}$$

Next, T, N and f in relation to angle θ and ϕ are obtained by solving the above equations:

$$T = \frac{(\frac{1}{2}m_p + m_h)g\cos(\theta)}{\sin(\phi - \theta)} \tag{40}$$

$$N = (m_p + m_h)g - \frac{(\frac{1}{2}m_p + m_h)g\cos(\theta)\sin(\phi)}{\sin(\phi - \theta)} \tag{41}$$

$$f = -\frac{(\frac{1}{2}m_p + m_h)g\cos(\theta)\cos(\phi)}{\sin(\phi - \theta)} \tag{42}$$

During the payload lift-up, the change in θ and ϕ can range from 0 to 90 degrees and 0 to 180 degrees, respectively. The space formed by all possible θ and ϕ combinations represents the operation space consisting of all geometrically possible payload and trolley positions. However, only part of the space can satisfy all the requirements listed previously. Figure 23 presents the operable region, non-slip region and static safety region consecutively.

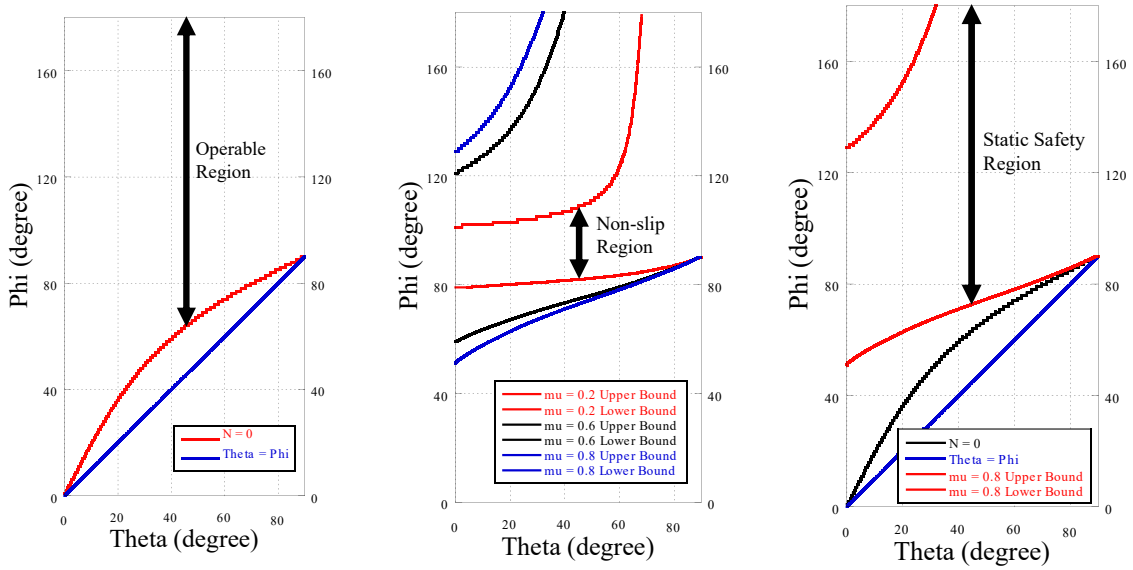

(a) Operable region (b) Non-slip region (c) Static safety region

Figure 23: Sub-regions of the operation space

The operable region is where T, N are greater than zero and θ is greater than ϕ. In other words, all of the configurations inside this region are physically possible. The boundaries are obtained by equating the constraint equations to zero.

The non-slip region is where no slipping happens at the pivot point. As presented, an increasing static friction coefficient expands the non-slip region, which matches the real-world expectation. The upper and lower boundaries are obtained by equating absolute value of f over N to the maximum static friction coefficient.

By overlapping the operable region with the non-slip region, a static safety region is constructed. When the trolley velocity is slow enough, this region guarantees that no slipping happens and the system is physically plausible. An additional observation is that the lower bound of the non-slip region is always above the boundary where N equals zero. This is true because a non-zero normal force is the prerequisite for friction to exist.

3.1.2 Dynamic Friction Analysis

Although cranes often operate at low velocity, higher velocity commands can increase efficiency. This leads to the necessity of analyzing dynamic states of the payload model.

It is done by adding acceleration terms to the existing force and momentum equations. When considering the payload and the hook as a combined slender rod, the position of the system's center of gravity with respect to the pivot point can be expressed as:

$$R_G = \frac{1}{2}L\frac{m_p + 2m_h}{m_p + m_h}(\cos(\theta)\hat{j} + \sin(\theta)\hat{k}) \tag{43}$$

where $\hat{j}$ and $\hat{k}$ correspond to the y-axis and the z-axis, respectively. Next, the acceleration of the rod is derived by differentiating the positional vector twice:

$$a_G = \frac{1}{2}L\frac{m_p + 2m_h}{m_p + m_h}\left((-\ddot{\theta}\sin(\theta) - \dot{\theta}^2\cos(\theta))\hat{j} + (\ddot{\theta}\cos(\theta) - \dot{\theta}^2\sin(\theta))\hat{k}\right) \tag{44}$$

With the above information, the dynamic equations can be obtained by modifying the static equations derived previously:

$$\sum F_y = f + T\cos(\phi) = -\frac{1}{2}L(m_p + 2m_h)(\ddot{\theta}\sin(\theta) - \dot{\theta}^2\cos(\theta)) \tag{45}$$

$$\sum F_z = N + T\sin(\phi) - (m_p + m_h)g = \frac{1}{2}L(m_p + 2m_h)(\ddot{\theta}\cos(\theta) - \dot{\theta}^2\sin(\theta)) \tag{46}$$

$$\sum M_x = TL\sin(\phi - \theta) - (\frac{1}{2}m_p + m_h)gL\cos(\theta) = I_{p,h}\ddot{\theta} \tag{47}$$

where $I_{p,h}$ is the rotational moment of inertia of the payload and the hook combined, and takes the form:

$$I_{p,h} = (\frac{1}{3}m_p + m_h)L^2 \tag{48}$$

By solving the force and momentum equations, it is found that:

$$T = \frac{\left((\frac{1}{2}m_p + m_h)g\cos(\theta) + I_{p,h}\ddot{\theta}\right)}{\sin(\phi - \theta)} \tag{49}$$

$$N = (m_p + n_h)g - \frac{\left((\frac{1}{2}m_p + m_h)g\cos(\theta) + I_{p,h}\ddot{\theta}\right)}{\sin(\phi - \theta)}\sin(\theta) + \frac{1}{2}L\frac{m_p + 2m_h}{m_p + m_h}(\ddot{\theta}\cos(\theta) - \dot{\theta}^2\sin(\theta)) \tag{50}$$

$$f = -\frac{\left((\frac{1}{2}m_p + m_h)g\cos(\theta) + I_{p,h}\ddot{\theta}\right)}{\sin(\phi - \theta)}\cos(\phi) - \frac{1}{2}L\frac{m_p + 2m_h}{m_p + m_h}(\ddot{\theta}\sin(\theta) - \dot{\theta}^2\cos(\theta)) \tag{51}$$

The above equations shows that *T*, *N* and *f* are all determined by ϕ, θ, $\dot{\theta}$ and $\ddot{\theta}$. Expressions for the payload's angular velocity and acceleration are obtained by solving the kinematics problem constrained by the geometry of the system:

$$y_t = L\cos(\theta) + l\cos(\phi) \tag{52}$$

$$z_t = L\sin(\theta) + l\sin(\phi) \tag{53}$$

Notice that all motors in the bridge crane are able to operate under velocity control mode and their accelerations are considered to be fast enough so that the acceleration time can be ignored in modeling. Also, the height of the crane bridge is constant. Using these information, time derivative of the geometrical constraints is simplified:

$$L\cos(\theta)\dot{\theta} + l\cos(\phi)\dot{\phi} + \dot{l}\sin(\phi) = 0 \tag{54}$$

$$-L\sin(\theta)\dot{\theta} - l\sin(\phi)\dot{\phi} + \dot{l}\sin(\phi) = \dot{y_t} \tag{55}$$

The velocity constraint equations are then obtained by solving previous equations:

$$\dot{\theta} = -\frac{\dot{l} - \dot{y_t}\cos(\phi)}{L\sin(\phi - \theta)} \tag{56}$$

$$\dot{\phi} = \frac{\dot{l}\cos(\phi - \theta) - \dot{y_t}\cos(\theta)}{l\sin(\phi - \theta)} \tag{57}$$

Angular velocity of the rod is differentiated to get angular acceleration:

$$\ddot{\theta} = \frac{\cot(\phi - \theta)(\dot{l} - \cos(\theta)\dot{y_t})(\dot{\phi} - \dot{\theta}) - \dot{y_t}\sin(\theta)\dot{\theta}}{L^2\sin(\phi - \theta)} \tag{58}$$

By substituting $\dot{\phi}$, $\dot{\theta}$ and $\ddot{\theta}$ into the expressions for *T*, *N* and *f*, it is found that all of the forces are dependent on ϕ, θ, $\dot{l}$ and $\dot{y_t}$. By keeping $\dot{l}$ constant, a 3-D boundary surface showing the limit of $\dot{y_t}$ can be obtained. By keeping $\dot{y_t}$ constant, a 3-D boundary surface showing the limit of $\dot{l}$ can be obtained. The 3-D space under the boundary surface consists of all the angle and velocity combinations that satisfy the requirement of positive tension, positive normal force, and a static friction smaller than the limit.

Figure 24 presents the boundary surfaces under various parameter combinations. The views of the 3-D surfaces are limited to the θ-ϕ plane for clarity. In the figures, brightness of the surface represents change in either $\dot{l}$ or $\dot{y_t}$, with the brightest color corresponding to 0.2 m/s (highest velocity achievable by the crane) and the darkest color corresponding to 0 m/s.

As can be seen, when μ_{max} is fixed, increment in $\dot{y_t}$ leads to a smaller safety region for $\dot{l}$ and increment in $\dot{l}$ leads to a smaller safety region for $\dot{y_t}$. The general trend is that increasing μ_{max} gives significantly more safety region for both fixed $\dot{l}$ and $\dot{y_t}$. This general trend is analogous to the static safety region. When designing lift-up trajectory, the trade off between $\dot{l}$ and $\dot{y_t}$ must be considered. Furthermore, it should be noticed that the tolerance for velocity command is very low at the region around θ = 90 degrees and ϕ = 90 degrees. Since geometrical configuration of the erected payload lies in this region, extra attention

should be directed to the velocity command design at the end of the lift-up process.

3.2 Trajectory Generation Strategy

The trajectory generation strategy proposed in this section is twofold. First, the trajectory is designed based on the system's geometry. Secondly, dynamic analysis is done to determine the velocity at which the trajectory is executed.

The start point of the trajectory is (θ_i, ϕ_i) where θ_i is the small elevation angle created by the payload alignment process and ϕ_i is 90 degrees. The end point of the trajectory is (θ_f, ϕ_f) and, ideally, both angles should be 0 degree. However, this is only true when the payload can be considered a slender beam. For the aluminum block used in this research, its width must be considered. As shown in Figure 25, when θ increases, the center of gravity of the payload and hook combined will finally pass through the vertical axis where the pivot point is located. When the center of gravity moves into left side of the axis, the payload will suddenly accelerate in a tip-over-like motion. Consequently, the payload may slip. To stop the payload before the cross-over happens, ϕ_f is kept at 0 degree and θ_f is recalculated:

$$\theta_f = 90 - \arctan(\frac{L(m_p + 2m_h)}{W(m_p + m_h)}) \tag{59}$$

where *W* is width of the aluminum block. Another benefit of this endpoint selection is that it is further away from the boundary of the dynamic safety region, meaning that the payload is less likely to slip at higher velocity.

The safety region graphs are utilized for planning the trajectory, as presented in Figure 26. Figure 26a shows that any connection between the initial point and the end point can be a trajectory, like the blue, green and red lines presented. The red line is the efficient trajectory proposed by this thesis, and is designed in consideration of three factors. First, the length of a trajectory is used to define efficiency of the trajectory. A straight line con-

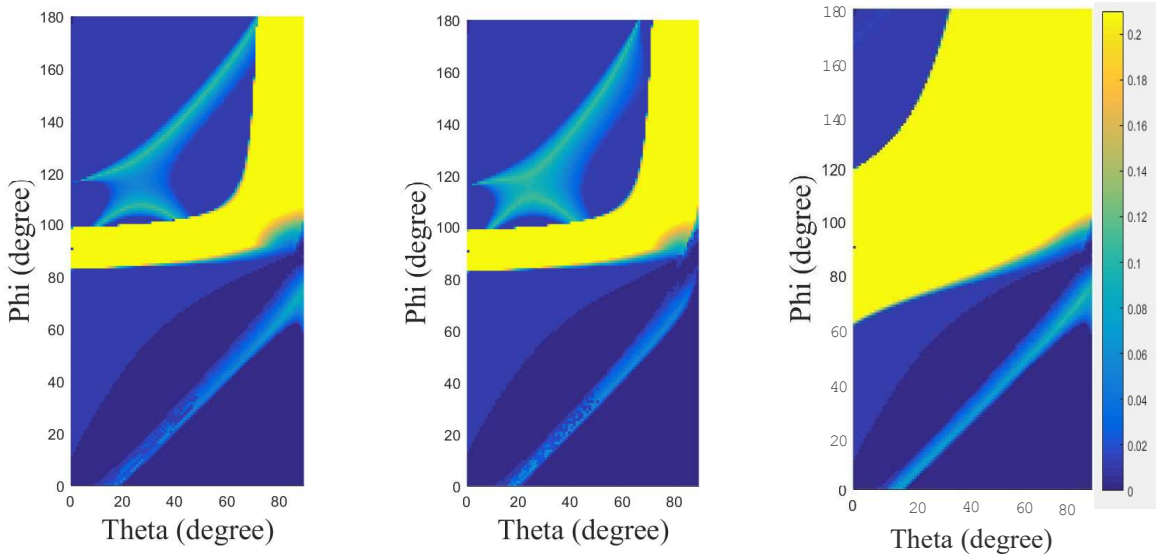

(a) μ_{max}=0.2, $\dot{y}_t$=0.1 m/s, $\dot{l}$ = variable

(b) μ_{max}=0.2, $\dot{y}_t$=0.2 m/s, $\dot{l}$ = variable

(c) μ_{max}=0.8, $\dot{y}_t$=0.1 m/s, $\dot{l}$ = variable

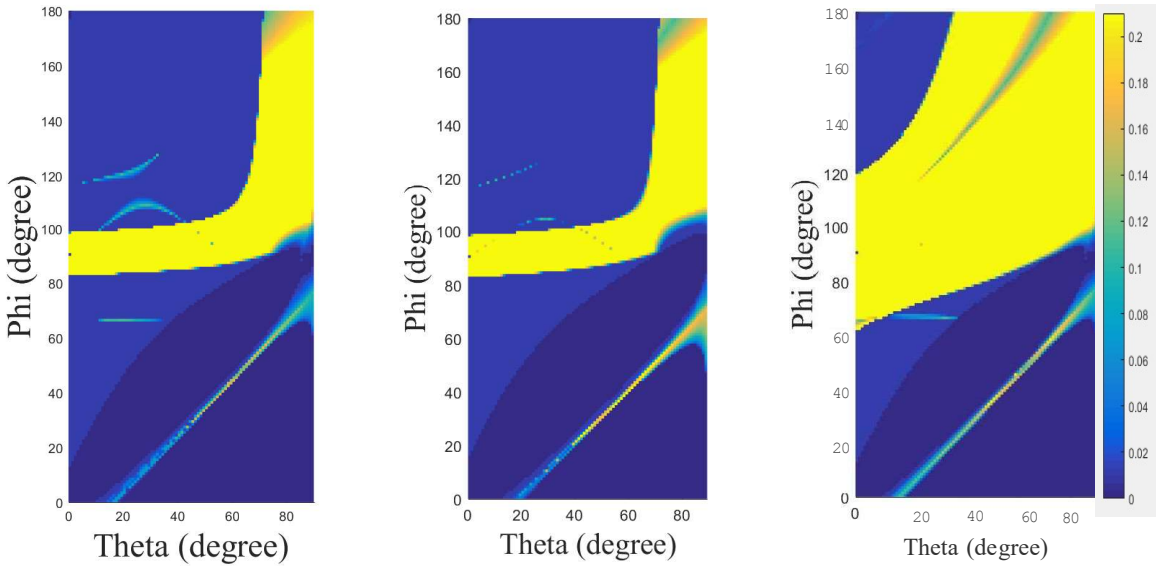

(d) μ_{max}=0.2, $\dot{y}_t$=variable, $\dot{l}$=0.1 m/s

(e) μ_{max}=0.2, $\dot{y}_t$=variable, $\dot{l}$=0.2 m/s

(f) μ_{max}=0.8, $\dot{y}_t$=variable, $\dot{l}$=0.1 m/s

Figure 24: Dynamic safety boundary

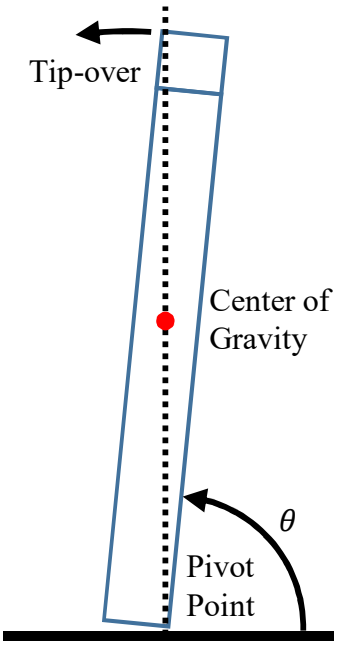

Figure 25: Cross-over position

necting the start and endpoint is most efficient, but is less likely achievable. Second, the shortest distance between any point on the trajectory to the safety boundary is defined as the safety factor. By segmenting the trajectory into equal length increments, safety factors can be calculated. They are then summed and averaged to obtain the average safety factor, whose value is determined based on the desired safety level specific to the application. The third factor to be considered is the above-mentioned dangerous region where both θ and ϕ equals 90 degrees, as can be observed from Figure 26b. To cope with this, the trajectory is designed to approach the endpoint in a direction parallel to the gradient of change in the velocity limit. Visually speaking, it is the gradient of the change in color.

3.2.1 Velocity Planning

Notice the proposed trajectory only indicates the geometrical trajectory. The corresponding hoist and trolley velocities at which the trajectory is executed are yet to be determined. To finish the trajectory in minimum time, the velocity must be maximized. The criteria for maximized velocity is defined as following: At any point on the trajectory, the $\dot{l}$ and $\dot{y_t}$

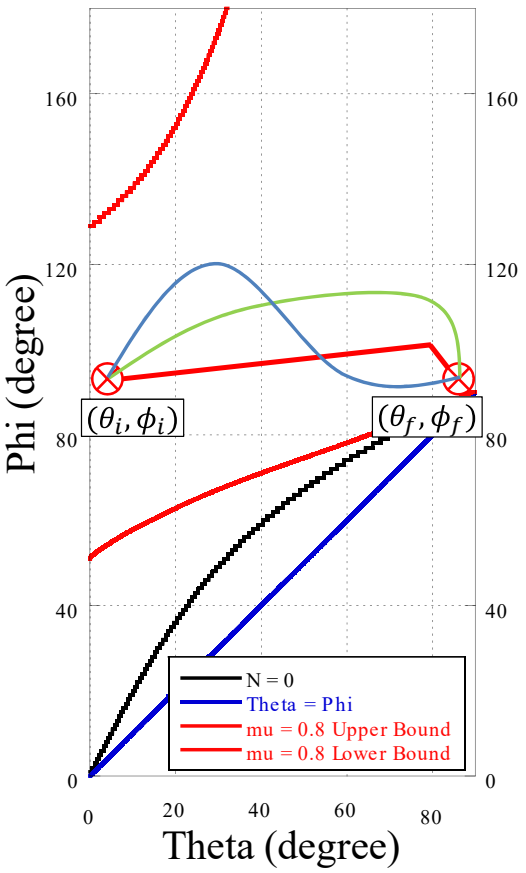

(a) Static safety region, μ_{max}=0.8

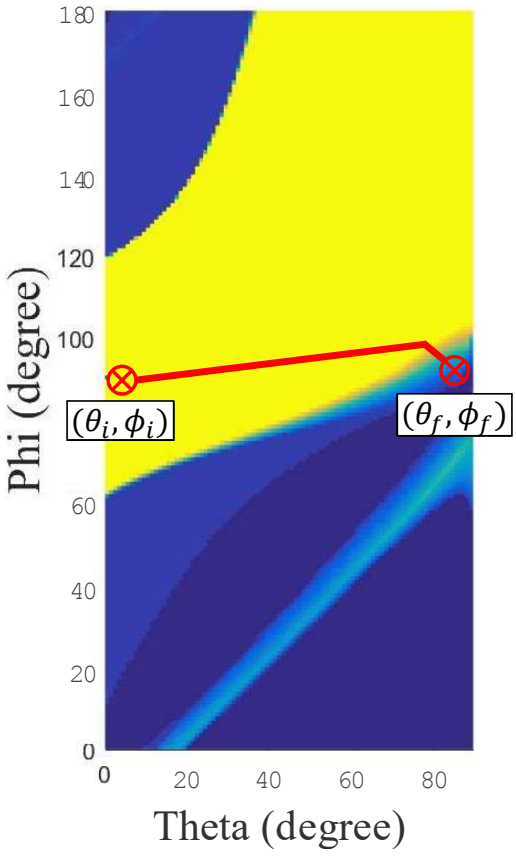

(b) Dynamic safety region, μ_{max}=0.8, $\dot{y}_t$=0.1 m/s, $\dot{l}$ = variable

Figure 26: Lift-up trajectory

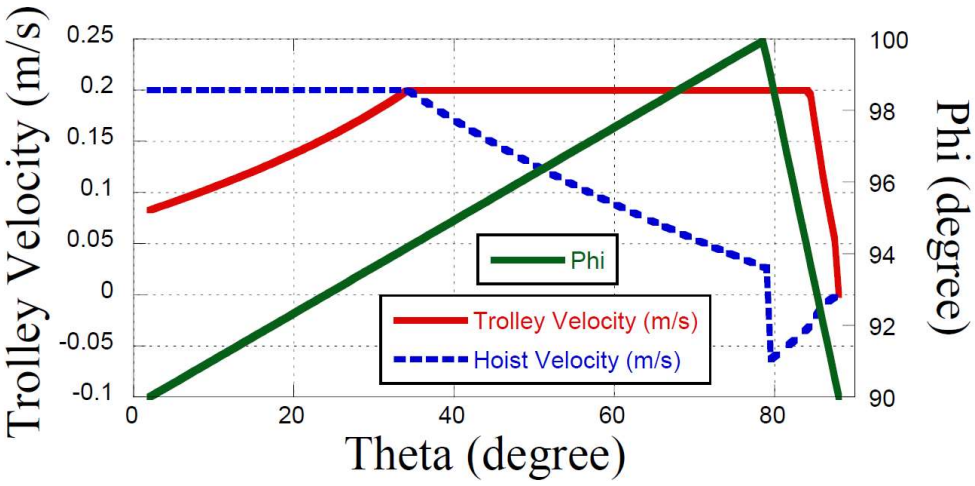

Figure 27: Command velocity change with respect to angle change

combination should result in greatest $\dot{\theta}$ while meeting all the requirements of the dynamic safety region. The relationship between $\dot{l}$ and $\dot{y}_t$ can be characterized by:

$$\frac{\dot{\phi}}{\dot{\theta}} = C = \frac{\dot{l}\cos(\phi - \theta) - \dot{y}_t \cos(\theta)}{\dot{l} + \dot{y}_t \cos(\theta)} \tag{60}$$

where C is slope of the trajectory in the $\theta - \phi$ plane.

Simulation is done using a trajectory characterized by three points: (2,90),(80,100) and (88,90). The maximum friction coefficient chosen is 0.5. Figure 27 presents the change in $\dot{l}$ and $\dot{y}_t$ with respect to the changes in θ and ϕ. As can be seen, to maximize efficiency, either the hoist or the trolley has to run at full speed, except for the last portion where the trajectory approaches the endpoint.

CHAPTER 4

OFF-CENTER LIFT-OFF VIBRATION REDUCTION

Table 7 contains all the variables used in this chapter.

Table 7: Variables Used in Chapter 4

Variable	Meaning
x_t	Position of the trolley in the x-axis
y_t	Position of the trolley in the y-axis
y_h	Position of the hook in the y-axis
z_h	Position of the hook in the z-axis
L	Length of the payload
l	Length of the hoist cable
l_m	Length of the hoist cable in the reference model
θ	Elevation angle of the payload in side swing
ϕ	Deflection angle of the payload in side swing
y_p	Position of the pivot point in the x-axis
z_p	Position of the pivot point in the z-axis
c	Damping coefficient of the system
c_m	Damping coefficient of the reference model

After being lifted up in a circular trajectory, the payload is now resting in a near vertical position constrained to the vertical y-z-plane. Lifting the payload off ground from this position inevitably results in an off-center lift. Without any active vibration reduction method, the induced two-mode vibration will take a long time to naturally damp out.

4.1 Model Reference Control

To reduce the said vibration, model reference control (MRC) is implemented. Figure 28 presents the block diagram of MRC, where *v* is the input command, *u* is the control input, x_d is the state of the reference model and *x* is the state of the plant. The reference command in MRC is the state of the reference command, which is not necessarily constant, and is

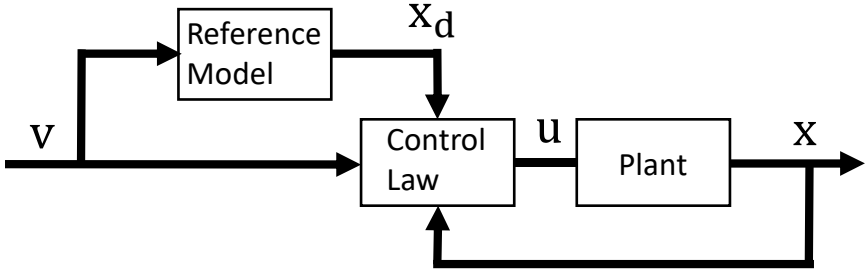

Figure 28: Model reference control

dependent on the input command. The control law is designed to drive the state of the plant to that of the reference model.

MRC is chosen for two major reasons. First, MRC allows for the repetitive usage of the same reference model when the payloads in the industry have various dimensions. Secondly, MRC is less sensitive to modeling error and unmodeled dynamics such as the connection mechanism between the payload and the hook. Additionally, MRC is proven to successfully suppress vibration in transnational motion of payloads carried by cranes in double pendulum configurations. This means the control algorithm used in the lift-up process can be directly used in payload transportation.

4.1.1 System Model

In order to pick a reasonable reference model, as well as to enable mathematical simulation, the dynamic system consisting of the crane, the hook and the payload is modeled. Figure 29 is the free body diagram of the system, where l is the length of the hoist cable, L is the length of the payload, y_t is the distance from the origin to the trolley along the bridge, ϕ, θ are the hoist cable's and the payload's deflection angle from the vertical axis, respectively; m_h,m_p are the center of gravity of the hook and payload, respectively; (y_h,z_h),(y_p,z_p) are the center of gravity of the hook and payload, respectively.

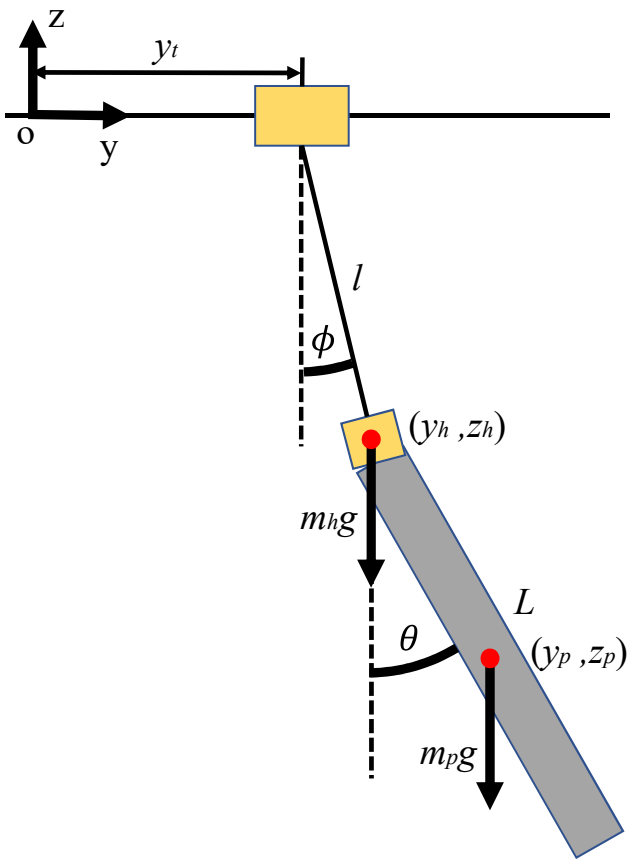

Figure 29: Free body diagram of the system in double pendulum configuration.

Model Derivation

The center of gravity of the hook and the payload are expressed in terms of the known variables:

$$y_h = y_t + l\sin(\phi) \tag{61}$$

$$z_h = -l\cos(\phi) \tag{62}$$

$$y_p = y_t + \frac{1}{2}L\sin(\theta) + l\sin(\phi) \tag{63}$$

$$z_p = -\frac{1}{2}L\cos(\theta) - l\cos(\phi) \tag{64}$$

The Lagrangian of the system is formulated:

$$T = \frac{1}{2}m_h(\dot{y_h})^2 + \frac{1}{2}m_h(\dot{z_h})^2 + \frac{1}{2}m_p(\dot{y_p})^2 + \frac{1}{2}m_p(\dot{z_p})^2 + \frac{1}{2}I_p\dot{\theta}^2 \quad \text{where} \quad I_p = \frac{1}{12}m_pL^2 \tag{65}$$

$$V = m_hgz_h + m_pgz_p \tag{66}$$

$$L = T - V = -gm_p\left(-l\cos(\phi) - \frac{1}{2}L\cos(\theta)\right) + glm_h\cos(\phi) + \frac{1}{6}\Big(3l^2(m_h+m_p)\dot{\phi}^2 + 3\dot{y_t}(2l(m_h+m_p)\dot{\phi}\cos(\phi) + Lm_p\dot{\theta}\cos(\theta)) + 3lLm_p\dot{\theta}\dot{\phi}\cos(\theta-\phi) + L^2m_p\dot{\theta}^2 + 3(m_h+m_p)\dot{y_t}^2\Big) \tag{67}$$

where I_p is the moment of inertia of the payload with respect to its center of gravity. Next, the equations of motion are obtained by applying the Lagrange equation:

$$c\dot{\theta} + \frac{1}{2}gLm_p\sin(\theta) + \frac{1}{6}\Big(-3lLm_p\dot{\phi}(\dot{\theta}-\dot{\phi})\sin(\theta-\phi) + 3lLm_p\ddot{\phi}\cos(\theta-\phi) + 2L^2m_p\ddot{\theta} - 3Lm_p\dot{\theta}\sin(\theta)\dot{y_t} + 3Lm_p\cos(\theta)\ddot{y_t}\Big) = 0 \tag{68}$$

$$c\dot{\phi} + gl(m_h+m_p)\sin(\phi) + \frac{1}{6}\Big(6l^2(m_h+m_p)\ddot{\phi} - 3lLm_p\dot{\theta}(\dot{\theta}-\dot{\phi})\sin(\theta-\phi) + 3lLm_p\ddot{\theta}\cos(\theta-\phi) - 6l(m_h+m_p)\dot{y_t}\dot{\phi}\sin(\phi) + 6l(m_h+m_p)\ddot{y_t}\cos(\phi)\Big) = 0 \tag{69}$$

where the damping coefficient between the hoist cable and trolley, and that between the hook and the payload are both assumed to be the same constant, c. The experimental method for determining the damping coefficient is not within the scope of this research. Finally, θ and ϕ are found by solving the two equations of motion:

$$\ddot{\theta} = -\frac{3(2c\dot{\theta} + g\theta L m_p + l L m_p(\theta-\phi)\dot{\phi}(\dot{\phi}-\dot{\theta}) - \theta L m_p \dot{\theta}\dot{y}_t)}{2L^2 m_p} \tag{70}$$

$$\begin{aligned}\ddot{\phi} =&(\dot{\phi}(-8c + 4lLm_p(\phi-\theta)\dot{\theta} + 8l\phi(m_h+m_p)\dot{y}_t) - gl\phi(8m_h+5m_p) \\ &+ 3lm_p(g\sin(2\theta-\phi) + \ddot{y}_t)\cos(2\theta-\phi)))/\left(2l^2(4m_h+m_p)\right)\end{aligned} \tag{71}$$

The system is then linearized under the assumption that θ and ϕ are small angles, and described in state space form:

$$\left[\dot{\mathrm{x}}\right] = \left[\mathrm{A}\right]\vec{x} + \left[\mathrm{B}\right]\vec{u}$$

$$\left[\mathrm{A}\right] = \begin{bmatrix} 0 & 1 & 0 & 0 & 0 & 0 \\ -\frac{6g(m_h+m_p)}{L(4m_h+m_p)} & -\frac{12c(m_h+m_p)}{L^2 m_p(4m_h+m_p)} & \frac{6g(m_h+m_p)}{L(4m_h+m_p)} & \frac{6c}{4lLm_h+lLm_p} & 0 & 0 \\ 0 & 0 & 0 & 1 & 0 & 0 \\ \frac{3gm_p}{4lm_h+lm_p} & \frac{6c}{4lLm_h+lLm_p} & -\frac{4g(m_h+m_p)}{l(4m_h+m_p)} & -\frac{4c}{l^2 m_p(4m_h+m_p)} & 0 & 0 \\ 0 & 0 & 0 & 0 & 0 & 1 \\ 0 & 0 & 0 & 0 & 0 & 0 \end{bmatrix} \tag{72}$$

$$\left[\mathrm{B}\right] = \begin{bmatrix} 0 & 0 & 0 & -\frac{1}{l} & 0 & 1 \end{bmatrix}^{\mathrm{T}} \qquad \vec{x} = \begin{bmatrix} \theta & \dot{\theta} & \phi & \dot{\phi} & y_t & \dot{y}_t \end{bmatrix}^{\mathrm{T}}$$

Simulation and Model Verification

Simulation is done in MATLAB using both the nonlinear and linearized angular acceleration expressions. The simulation models the system from the moment the payload is lifted off the ground, when *l* is fixed at 1 m and the initial amplitude of the residual vibration are θ_i and ϕ_i. A damping coefficient of 0.01 is chosen.

Figure 30 presents the simulation results when the system parameters are set to match

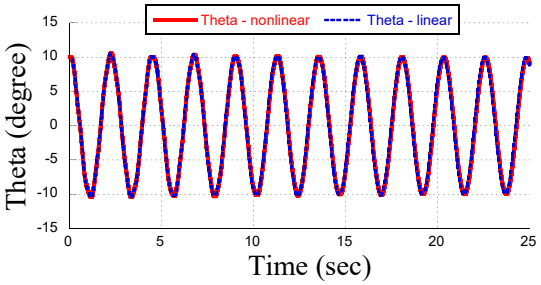

(a) Change in θ when θ_i=10 degrees, ϕ_i=10 degrees

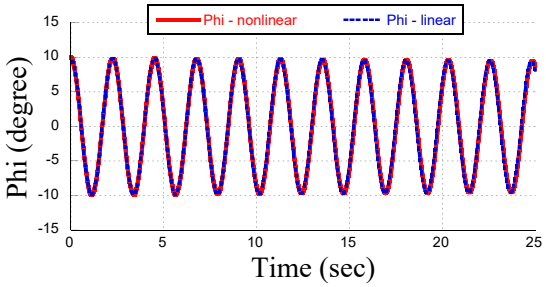

(b) Change in ϕ when θ_i=10 degrees, ϕ_i=10 degrees

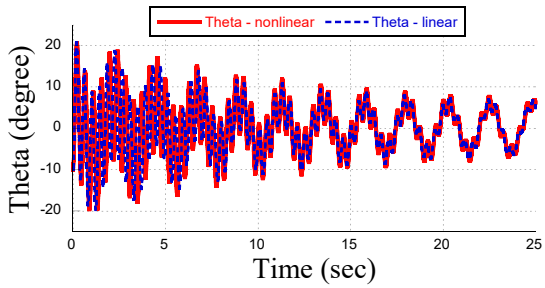

(c) Change in θ when θ_i=-10 degrees, ϕ_i=10 degrees

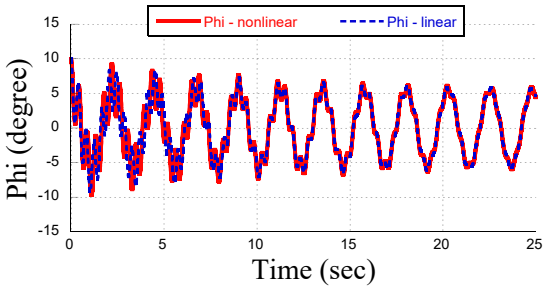

(d) Change in ϕ when θ_i=-10 degrees, ϕ_i=10 degrees

Figure 30: Simulation result of off-center-lift

the actual parameter of the crane and the payload. In all four figures, the system behavior predicted by the linearized model closely follows that predicted by the nonlinear model, when the maximum initial angle is as large as 10 degrees. When the initial angles, θ_i and ϕ_i, are both 10 degrees, the simulation result demonstrates a single mode harmonic motion, where θ and ϕ are in phase and share the same frequency. This result matches expectation from a real world system. When the initial angles, θ_i and ϕ_i, are both 10 degrees but opposite in sign, three observations can be made. First, both of the angles follow the same general harmonic motion. This is because both angles are measured with respect to the vertical axis and the payload's deflection angle is based on the hook's deflection angle. Secondly, even though both angles describe two mode vibrations, θ demonstrates motion of much higher frequency. This is because the payload's length is shorter than the cable's length, and can be estimated as a single pendulum with higher frequency. Lastly, both of the deflection angles decrease much faster than in the previous case. The reason for this is that the high frequency mode in both angles causes energy to dissipate faster. These three

observations, again, match with the expectation from a real world system.

To conclude, the nonlinear model is sufficient in modeling the actual plant, and simulations based on the nonlinear model are considered reliable predictors of the system's physical behavior. Furthermore, the linearized model predicts similar results compared to the nonlinear model. Hence, it is safe to base the reference model on the linearized model.

4.1.2 Reference Model

In MRC, the reference model is selected based on the desired performance of the feedback system. For the crane and payload system studied in this research, the reference model can be selected to be as simple as a single pendulum with high damping coefficient. However, this does not guarantee stability of the system, as it only corresponds to the ϕ angle. Furthermore, even when stability is achieved through tuning, it still requires more control effort to drive the plant's state to that of the single pendulum's state due to the significant difference in models. To obtain stability of the feedback system, the reference model is chosen to share the same form as the linearized model of the actual plant, with the reference model having different, but fixed, physical parameters. The goal of reducing residual vibration is then achieved by forcing the plant to act like a double pendulum whose damping coefficient,c_m, is significantly higher than that of the actual plant.

4.1.3 Control Law Derivation

The plant and the reference model can be represented state space forms:

$$\dot{x} = \mathrm{A}x + \mathrm{B}u \tag{73}$$

$$\dot{x}_d = \mathrm{A}_m x_d + \mathrm{B}_m v \tag{74}$$

Since the goal is to drive $\dot{x}$ to $\dot{x}_d$, the error, and its rate of change can be calculated:

$$e = x_d - x \tag{75}$$

$$\begin{aligned} \dot{e} &= \dot{x}_d - \dot{x} \\ &= \mathrm{A}_m x_d + \mathrm{B}_m v - \mathrm{A}x - \mathrm{B}u \\ &= \mathrm{A}_m(x+e) + \mathrm{B}_m v - \mathrm{A}x - \mathrm{B}u \end{aligned} \tag{76}$$

A control law that guarantees stability of the feedback system is derived by applying Lyapunov's First Theorem. At first, an error function is defined:

$$V(e) = e^{\mathrm{T}}\mathrm{P}e \quad \text{and} \quad -\mathrm{Q} = {\mathrm{A}_m}^{\mathrm{T}}\mathrm{P} + \mathrm{P}\mathrm{A}_m \tag{77}$$

where both Q and P are positive definite real symmetric matrices. For simplicity, Q is chosen to be the identity matrix and will be used for the incoming simulation and experiments. Then, P is calculated accordingly by substituting in the A matrix.

In order to have $V(e)$ become zero, the rate at which the error function changes should be constantly negative, except for when the error is already zero. The time derivative of the error function is:

$$\begin{aligned} \dot{V}(e) &= \dot{e}^{\mathrm{T}}\mathrm{P}e + e^{\mathrm{T}}\mathrm{P}\dot{e} \\ &= (\mathrm{A}_m(x+e) + \mathrm{B}_m v - \mathrm{A}x - \mathrm{B}u)^{\mathrm{T}}\mathrm{P}e \\ &\quad + e^{\mathrm{T}}\mathrm{P}(\mathrm{A}_m(x+e) + \mathrm{B}_m v - \mathrm{A}x - \mathrm{B}u) \\ &= \underbrace{e^{\mathrm{T}}({\mathrm{A}_m}^{\mathrm{T}}\mathrm{P} + \mathrm{P}\mathrm{A}_m)e}_{\text{equals} -e^{\mathrm{T}}\mathrm{Q}e \quad \text{which is negative}} + 2\mathrm{M} \leq 0 \\ &\quad \text{where} \quad \mathrm{M} = e^{\mathrm{T}}\mathrm{P}(\mathrm{A}_m x + \mathrm{B}_m v - \mathrm{A}x - \mathrm{B}u) \end{aligned} \tag{78}$$

As shown by the above equation, to guarantee a negative rate of change of the error function, **M** must be negative. To further secure a negative rate of change in the error, this

criteria is modified as the following:

$$\mathrm{M} = e^{\mathrm{T}}\mathrm{P}(\mathrm{A}_m x + \mathrm{B}_m v - \mathrm{A}x - \mathrm{B}u) = -({e_1}^2 + ... + {e_6}^2) \tag{79}$$

When assuming the only difference between the reference model and the plant is the damping coefficient, the control law for calculating u can be derived by substituting the state space matrices of the plant and the reference model into the above equation:

$$e^{\mathrm{T}}\mathrm{P}\left(\begin{bmatrix} 0 & 0 & 0 & 0 & 0 & 0 \\ 0 & -\frac{12(c_m-c)(m_h+m_p)}{L^2 m_p(4m_h+m_p)} & 0 & \frac{6(c_m-c)}{4lLm_h+lLm_p} & 0 & 0 \\ 0 & 0 & 0 & 0 & 0 & 0 \\ 0 & \frac{6(c_m-c)}{4lLm_h+lLm_p} & 0 & -\frac{4(c_m-c)}{l^2(4m_h+m_p)} & 0 & 0 \\ 0 & 0 & 0 & 0 & 0 & 1 \\ 0 & 0 & 0 & 0 & 0 & 0 \end{bmatrix} \begin{bmatrix} x_1 \\ x_2 \\ x_3 \\ x_4 \\ x_5 \\ x_6 \end{bmatrix} + \begin{bmatrix} 0 \\ 0 \\ 0 \\ -\frac{1}{l} \\ 0 \\ 0 \end{bmatrix} (v-u) \right) + ({e_1}^2 + ... + {e_6}^2) = 0$$

4.2 State Observer

The reference model is chosen based on the assumption that all states of the actual system are constantly known. While ϕ is measured by the camera at all time, no sensor is deployed to measure θ. To resolve the lack of information on the plant state, a Luenberger observer is implemented in conjunction with the MRC. Figure 31 presents the modified block diagram

of the control strategy. Here, the control law takes in the estimated states of the system, $\overline{x}$, from the observer, instead of the actual states, x.

4.2.1 Observer Design

As presented in Figure 32, the Luenberger observer consists of a predictor and a corrector. The predictor is a copy of the linearized model of the actual plant and predicts states of the system based on the current estimated states and the current control input. The corrector modifies the predicted states by comparing the measured states with the estimated states. When the observer gain, L, is properly designed, the estimated states will converge to the actual states of the system.

The observer gain is determined by pole-placement. The prerequisite for applying an observer whose gain is picked by pole-placement is that the system is completely observable. Therefore, the following condition must be true:

$$\text{rank}(\Omega) = n$$

$$\Omega = [\text{C} \quad \text{CA} \cdots \text{CA}^{n-1}]^{\text{T}}$$

$$\text{C} = \begin{bmatrix} 0 & 0 & 1 & 0 & 0 & 0 \\ 0 & 0 & 0 & 0 & 1 & 0 \\ 0 & 0 & 0 & 0 & 0 & 1 \end{bmatrix}$$

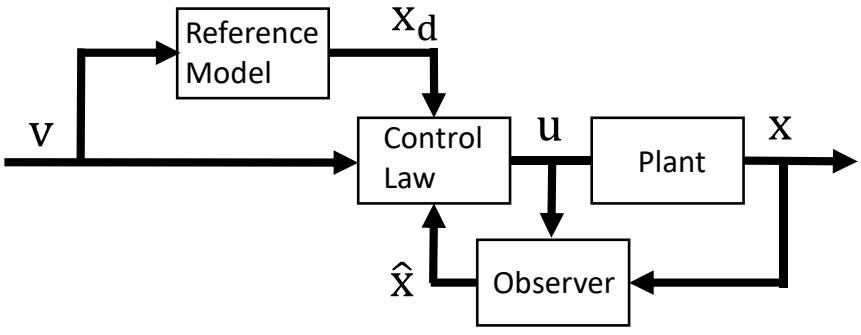

Figure 31: Model reference control with Luenberger observer

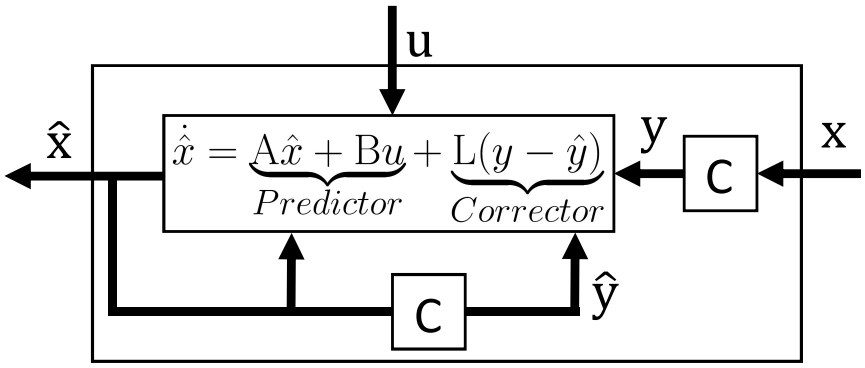

Figure 32: Luenberger observer

where n is the number of states of the system, the first row of C is the phi measurement from the laser sensor, the second and third row of C are the trolley speed and acceleration, respectively, measured by the embedded encoder. For the crane and payload system studied, rank$(\Omega) = 6$, indicating the system is completely observable.

In pole placement, L is chosen so that the eigenvalues of the matrix A $-$ LC equal the selected poles. Given that there are six states, six negative real poles of values (-5, -10, -15, -20, -25, -30) are selected. L is calculated using the MATLAB function *pole()*:

$$\mathrm{L} = \begin{bmatrix} 725 & -7833 & 90 & 2728 & 0 & 0 \\ 0 & 0 & 0 & 0 & 10 & 0 \\ 0 & 0 & 0 & 0 & 1 & 5 \end{bmatrix}^{\mathrm{T}}$$

4.2.2 Observer Verification

Simulation is done in MATLAB using the control schematic presented. The plant model employees parameters and assumptions identical to those used in the system modeling simulation. The three measured states, ϕ, y_t, and $\dot{y_t}$, are forwarded to the aforementioned Luenberger observer after going through a quantizer and a transport delay module consecutively. The quantizer discretizes the linear output from the plant into time intervals of 0.01 sec to emulate the output of the camera. The transport delay is configured to postpone the sensor readings for 0.01 sec for the same purpose.

The comparison between the actual and observed θ and ϕ under different simulation settings and initial conditions is presented in Figure 33. As shown in Figure 33a and 33b, the observer has near perfect tracking over ϕ, since the sensor reading of this angle is constantly given. θ is also closely estimated with the estimation error decreasing as time passes. Then, white noise with signal-to-noise ratio under 40 dB is added to the ϕ measurement. It can be seen from Figure 33c and 33d that both observed θ and ϕ fluctuate at high frequency about the real values. Next, the magnitude of the proposed six poles are reduced by half, meaning that they are shifted rightward, closer to the imaginary axis. As a result, much smoother observed angles are presented in Figure 33e and 33f. However, the rate at which the observed value converges with the real value becomes slower. This can be explained by considering the observer as having characteristics similar to that of a high-pass filter. The larger the poles, the more amplified the high frequency portion of the white noise is. In the last case, θ_i and ϕ_i are chosen as 10 degrees, the poles are no longer halved, and white noise is removed. Figure 33g shows that the observed θ fluctuates around the real value, which can be explained the same way as the previous case: the high frequency component of the sinusoidal wave is amplified.

The simulation suggests that the designed Luenberger observer can reliably predict the vibration angle even when sensor is missing. It also suggested a relationship between poles of the observer and the observed result. The parameters of the observer are tuned when implemented on the hardware.

4.3 Simulation and Experimental Verification

Now that the observer design is verified, simulation of the whole MRC is performed to provide insight on how the controller performs. Again, the simulation parameters stay the same. v, the reference input, is set to zero, because acceleration command besides the control effort is unwanted for reducing residual vibration. Figure 34 presents the change in ϕ under different model settings. Change in θ is neglected since a stabilized ϕ naturally

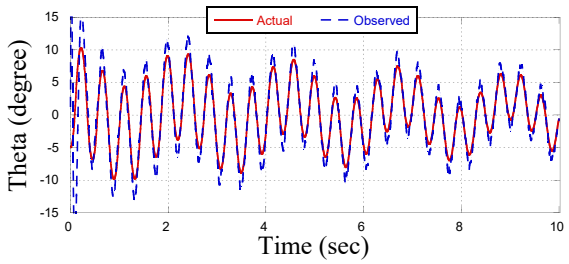

(a) θ_i=-5 degrees, ϕ_i=10 degrees

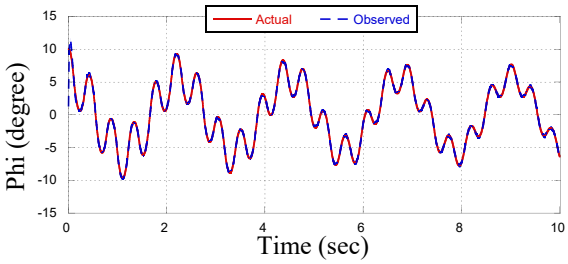

(b) θ_i=-5 degrees, ϕ_i=10 degrees

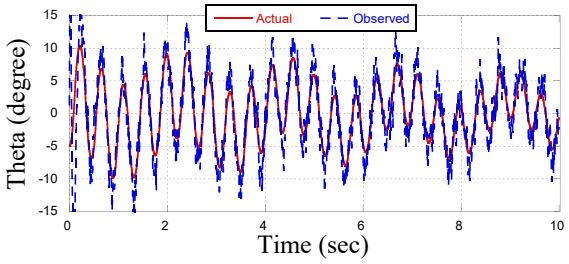

(c) θ_i=-5 degrees, ϕ_i=10 degrees, white noise

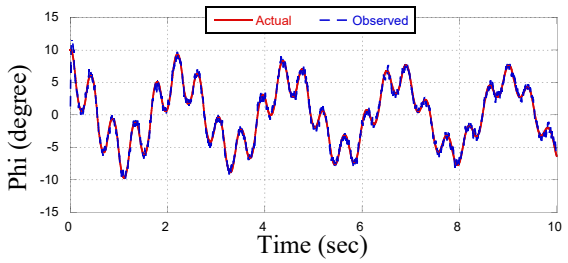

(d) θ_i=-5 degrees, ϕ_i=10 degrees, white noise

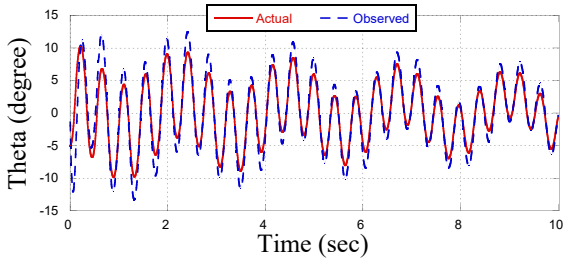

(e) θ_i=-5 degrees, ϕ_i=10 degrees, white noise, smaller poles

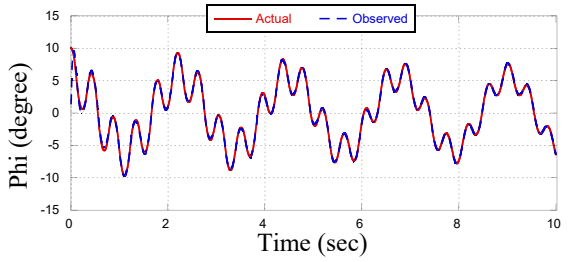

(f) θ_i=-5 degrees, ϕ_i=10 degrees, white noise, smaller poles

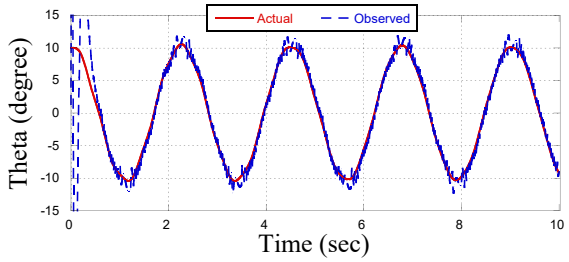

(g) θ_i=10 degrees, ϕ_i=10 degrees

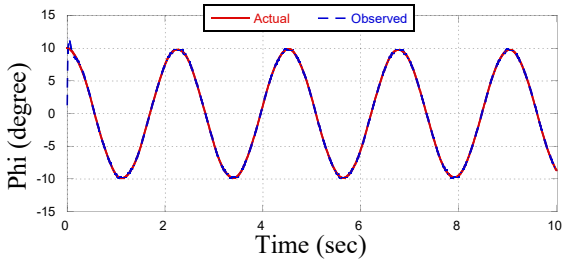

(h) θ_i=10 degrees, ϕ_i=10 degrees

Figure 33: Simulation results of observer

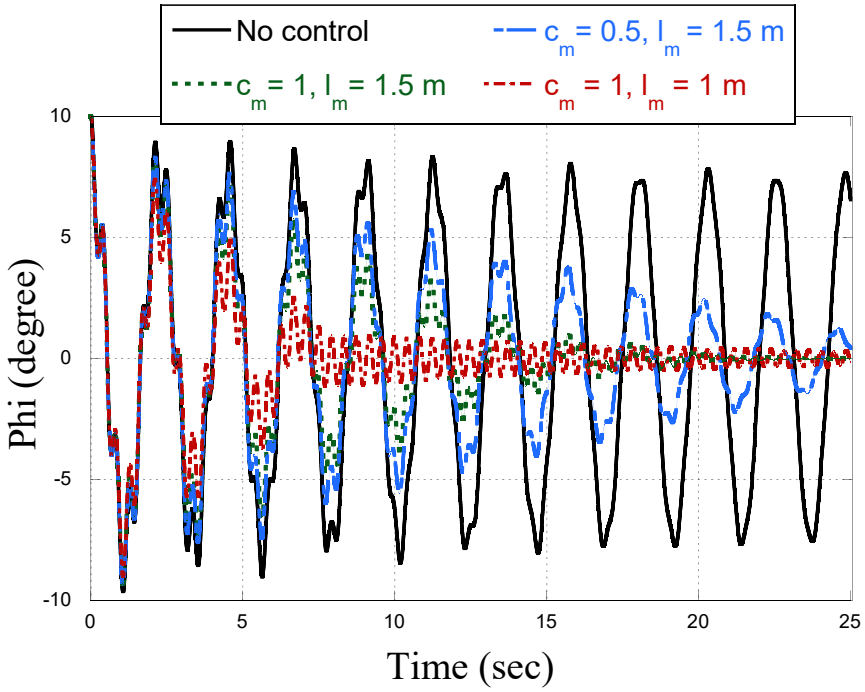

Figure 34: Simulation of MRC + Observer

indicates the stabilization of the system. The payload is released from an initial position of θ_i=0 degree and ϕ_i=10 degrees, where the hoist cable is 1.5 m long. Under this initial condition, a two mode vibration is induced. When no control input is given, the vibration takes a long time to damp out. When c_m is set to 1 and l_m is set to the actual length, the vibration is smoothly damped out and stability is reached at 15 sec. When c_m is reduced to 0.5, the vibration reduction rate becomes much slower, confirming with the expectation of an underdamped system. When c_m is kept at 1 and l_m is set to 1 m, the vibration is reduced rapidly in the 1 sec to 7 sec time interval. However, it takes longer time for the vibration to completely settle down after the 7 sec point when compared to the first case, where l_m equals the actual hoist cable length. The explanation for this case is that MRC forces the actual plant to emulate a model with higher frequency, which leads to faster energy dissipation. However, the large modeling error makes it difficult for the small vibrations to be settled down.

After realizing the effect of different parameter settings on the control performance,

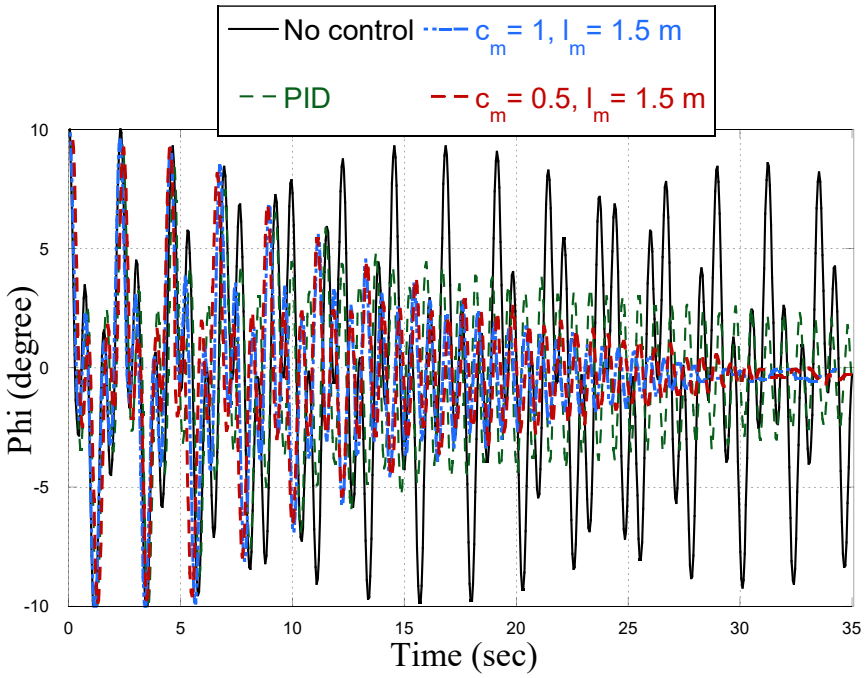

Figure 35: Experimental results of MRC + Observer

MRC is implemented on the bridge crane and the L matrix of the observer is tuned to achieve good performance. Figure 35 compares the recorded change in ϕ when the payload is released from a initial position of θ_i= 0 degree and ϕ_i=10 degrees. When a properly tuned PID controller that aims at reducing only ϕ is used, the settling time is reduced, but the result is not optimal. When c_m is set to 1 and l_m is set to match the actual hoist cable length, the settling time is successfully reduced to 29 seconds. When c_m is reduced to 0.5, the settling time is extended by 3 seconds. The little performance change between different model damping coefficients is likely caused by saturation of the motor. Even though the performance of MRC on the actual system did not match the performance predicted by the simulation, it still significantly reduced the residual vibration compared to the case when no controller is used.

In conclusion, MRC is successfully deployed on the bridge crane and demonstrated significant vibration reduction ability when one of the deflection angles of the payload is not measured.

CHAPTER 5
CONCLUSION AND FUTURE WORKS

5.1 Conclusion

Longitudinal payloads account for a large portion of the payloads being transported in various industries. One way of transporting them is by attaching the payload vertically to bridge cranes in a double-pendulum configuration. The lift-up of a longitudinal payload lying on the ground to the aforementioned configuration is normally done manually. This process has disadvantages including the misalignment between payload and bridge, human operator error and uncontrollable system oscillation. In this thesis, the automated lift-up of longitudinal payloads using bridge cranes was proposed. The problems specific to each stage of this process were studied and solutions were given.

Chapter II discussed the necessary steps to compensate for the misalignment between the payload and the crane bridge. At first, feedback control was designed to navigate the trolley to the position of the hook. Then, the method of detecting orientation of the payload by induced side swing was developed. Knowing the current position and desired position of the payload, a input-shaped side-swing trajectory was proposed for correcting the angular misalignment. A dynamic model was constructed to calculate the system natural frequency necessary for applying input-shaping. A simplified model was also built to speed up the natural frequency calculation. Later, both ZV and ZVD shapers were tested in simulation, implemented on the actual system and demonstrated phenomenal vibration reduction capability.

After successfully regulating the payload to the vertical plane parallel to the bridge, the payload was ready to be lifted up in a circular trajectory. The development of trajectory was discussed in Chapter III. Both a static model and a dynamic model were built to study the

frictional constraints the trajectory needed to follow geometrically. The dynamic model was also used to study the relationship between hoist speed command and trolley speed command.

In the end, Chapter IV demonstrated the use of observer-based model reference control in reducing the payload vibration when it was lifted off the ground. The original plant was numerically modeled so that a reference model could be build. The control schematic was then modified to include a state observer whose performance was decided by pole-placement. After verifying effectiveness of the MRC, it was applied to the system and effectively reduced residual vibration of the double pendulum configuration.

5.2 Future Work

In the beginning of the lift-up process, the operator needs to manually connect the hook to the payload. Machine vision could be applied to further automate this process. Coming with that is a new mechanical design of the hook that can grasp the payload automatically.

Chapter II discussed the possibility of blending the side-swing of payload orientation detection into the input-shaped command pastern during payload alignment. A shaper pattern that can optimally achieve this goal is yet to be developed. Also, computation speed of the PLC should be taken into consideration.

In Chapter IV, the observer showed vulnerability in dealing with white noise. First, white noise may not be the most proper choice to model sensor inaccuracy. More study could be done to improve the simulation. The observer could also be replace by a Kalman filter to better deal with sensor noise. In addition, the MRC design could be tested on translational motion of the payload and be incorporated with input-shaping.

Another area that could be worked on is the application of current knowledge to the lay-down of longitudinal payloads, where the trajectory generation methodology and payload alignment can be both used with minor modification. One specific case where payload alignment is extremely useful is when block payloads are stacked one on another. It is

beneficial to keep the payload pile neat for the sake of saving work-space and further transportation.

Appendices

APPENDIX A

NONLINEAR SIDE-SWING MODEL DERIVATION

```
d (l Cos[λ] Cos[ψ] + L Cos[θ] Cos[ϕ] - yt) /. {dL → 0, dl → 0, dyt → 0} // FullSimplify
```

```
-L (Cos[ϕ] Dt[θ] Sin[θ] + Cos[θ] Dt[ϕ] Sin[ϕ]) - l (Cos[ψ] Dt[λ] Sin[λ] + Cos[λ] Dt[ψ] Sin[ψ])
```

```
FullSimplify[d (l Sin[ψ] + L Sin[ϕ] - xt) /. {d L → 0, d l → 0, d xt → 0}]
```

```
L Cos[ϕ] Dt[ϕ] + l Cos[ψ] Dt[ψ]
```

```
FullSimplify[d (l Sin[λ] Cos[ψ] + L Sin[θ] Cos[ϕ] - zt) /. {d L → 0, d l → 0, d zt → 0}]
```

```
L Cos[θ] Cos[ϕ] Dt[θ] + l Cos[λ] Cos[ψ] Dt[λ] - L Dt[ϕ] Sin[θ] Sin[ϕ] - l Dt[ψ] Sin[λ] Sin[ψ]
```

```
Dt[-Dt[xt] - L (Cos[ϕ] Dt[θ] Sin[θ] + Cos[θ] Dt[ϕ] Sin[ϕ]) - l (Cos[ψ] Dt[λ] Sin[λ] + Cos[λ] Dt[ψ] Sin[ψ])] /. {Dt[L] → 0, Dt[l] → 0} // FullSimplify
```

$$-l\cos(\psi)\left(\cos(\lambda)\left((d\lambda)^2+(d\psi)^2\right)+d(d\lambda)\sin(\lambda)\right)+l\sin(\psi)\left(2\,d\lambda\sin(\lambda)\,d\psi-\cos(\lambda)\,d(d\psi)\right)-L\cos(\phi)\left(\cos(\theta)\left((d\theta)^2+(d\phi)^2\right)+d(d\theta)\sin(\theta)\right)+L\sin(\phi)\left(2\,d\theta\sin(\theta)\,d\phi-\cos(\theta)\,d(d\phi)\right)-d(d\,\mathrm{xt})$$

```
Dt[-Dt[yt] + L Cos[ϕ] Dt[ϕ] + l Cos[ψ] Dt[ψ]] /. {Dt[L] → 0, Dt[l] → 0} // FullSimplify
```

$$-l\,(d\psi)^2\sin(\psi)+l\,d(d\psi)\cos(\psi)-L\,(d\phi)^2\sin(\phi)+L\,d(d\phi)\cos(\phi)-d(d\,\mathrm{yt})$$

```
Dt[L Cos[θ] Cos[ϕ] Dt[θ] + l Cos[λ] Cos[ψ] Dt[λ] - L Dt[ϕ] Sin[θ] Sin[ϕ] - l Dt[ψ] Sin[λ] Sin[ψ]] /. {Dt[L] → 0, Dt[l] → 0} // FullSimplify
```

$$-l\sin(\lambda)\left(\cos(\psi)\left((d\lambda)^2+(d\psi)^2\right)+d(d\psi)\sin(\psi)\right)+l\cos(\lambda)\left(d(d\lambda)\cos(\psi)-2\,d\lambda\,d\psi\sin(\psi)\right)-L\sin(\theta)\left(\cos(\phi)\left((d\theta)^2+(d\phi)^2\right)+d(d\phi)\sin(\phi)\right)+L\cos(\theta)\left(d(d\theta)\cos(\phi)-2\,d\theta\,d\phi\sin(\phi)\right)$$

```
a = {{-L * Cos[ϕ] * Sin[θ], -L * Cos[θ] * Sin[ϕ], -l * Cos[ψ] * Sin[λ], -l * Cos[λ] * Sin[ψ]}, {0, L * Cos[ϕ], 0, l Cos[ψ]}, {L Cos[θ] Cos[ϕ] , -L Sin[θ] Sin[ϕ], l Cos[λ] Cos[ψ], -l Sin[λ] Sin[ψ]}}
```

$$\begin{pmatrix} -L\cos(\phi)\sin(\theta) & -L\cos(\theta)\sin(\phi) & -l\cos(\psi)\sin(\lambda) & -l\cos(\lambda)\sin(\psi) \\ 0 & L\cos(\phi) & 0 & l\cos(\psi) \\ L\cos(\theta)\cos(\phi) & -L\sin(\theta)\sin(\phi) & l\cos(\lambda)\cos(\psi) & -l\sin(\lambda)\sin(\psi) \end{pmatrix}$$

```
adt = Dt[a] /. {Dt[L] → 0, Dt[l] → 0, Dt[θ] → OverDot[θ], Dt[ϕ] → OverDot[ϕ], Dt[λ] → OverDot[λ], Dt[ψ] → OverDot[ψ]} // FullSimplify
```

```
{{L Dt[ϕ] Sin[θ] Sin[ϕ] - L Cos[θ] Cos[ϕ] Dt[θ], L Dt[θ] Sin[θ] Sin[ϕ] - L Cos[θ] Cos[ϕ] Dt[ϕ], l Dt[ψ] Sin[λ] Sin[ψ] - l Cos[λ] Cos[ψ] Dt[λ], l Dt[λ] Sin[λ] Sin[ψ] - l Cos[λ] Cos[ψ] Dt[ψ]},
  {0, -L Dt[ϕ] Sin[ϕ], 0, -l Dt[ψ] Sin[ψ]}, {-L (Cos[ϕ] Dt[θ] Sin[θ] + Cos[θ] Dt[ϕ] Sin[ϕ]), -L (Cos[ϕ] Dt[ϕ] Sin[θ] + Cos[θ] Dt[θ] Sin[ϕ]), -l (Cos[ψ] Dt[λ] Sin[λ] + Cos[λ] Dt[ψ] Sin[ψ]),
   -l (Cos[ψ] Dt[ψ] Sin[λ] + Cos[λ] Dt[λ] Sin[ψ])}} /. {Dt[θ] → OverDot[θ], Dt[ϕ] → OverDot[ϕ], Dt[λ] → OverDot[λ], Dt[ψ] → OverDot[ψ]}
```

$$\begin{pmatrix} L\,\dot{\phi}\sin(\theta)\sin(\phi)-L\cos(\theta)\cos(\phi)\,\dot{\theta} & L\,\dot{\theta}\sin(\theta)\sin(\phi)-L\cos(\theta)\cos(\phi)\,\dot{\phi} & l\,\dot{\psi}\sin(\lambda)\sin(\psi)-l\cos(\lambda)\cos(\psi)\,\dot{\lambda} & l\,\dot{\lambda}\sin(\lambda)\sin(\psi)-l\cos(\lambda)\cos(\psi)\,\dot{\psi} \\ 0 & -L\,\dot{\phi}\sin(\phi) & 0 & -l\,\dot{\psi}\sin(\psi) \\ -L\left(\cos(\phi)\,\dot{\theta}\sin(\theta)+\cos(\theta)\,\dot{\phi}\sin(\phi)\right) & -L\left(\cos(\phi)\,\dot{\phi}\sin(\theta)+\cos(\theta)\,\dot{\theta}\sin(\phi)\right) & -l\left(\cos(\psi)\,\dot{\lambda}\sin(\lambda)+\cos(\lambda)\,\dot{\psi}\sin(\psi)\right) & -l\left(\cos(\psi)\,\dot{\psi}\sin(\lambda)+\cos(\lambda)\,\dot{\lambda}\sin(\psi)\right) \end{pmatrix}$$

```
b = {{Dt[xt]}, {Dt[yt]}, {Dt[zt]}} /. {Dt[zt] → 0}
```

```
{{Dt[xt]}, {Dt[yt]}, {0}}
```

```
bdt = Dt[b]|
```

```
{{Dt[Dt[xt]]}, {Dt[Dt[yt]]}, {0}}
```

```
T = 1 / 2 (mh (L Cos[θ])^2) (Dt[ϕ] Cos[θ])^2  + 1 / 2 (1 / 3 mp (L Cos[θ])^2) (Dt[ϕ] Cos[θ])^2 + 1 / 2 (mh L^2) Dt[θ]^2 + 1 / 2 × 1 / 3 mp L^2 Dt[θ]^2
```

$$\frac{1}{2} L^2\, mh\, Dt[\theta]^2 + \frac{1}{6} L^2\, mp\, Dt[\theta]^2 + \frac{1}{2} L^2\, mh\, Cos[\theta]^4\, Dt[\phi]^2 + \frac{1}{6} L^2\, mp\, Cos[\theta]^4\, Dt[\phi]^2$$

```
V = (mh + 1 / 2 mp) L g Cos[ϕ] Sin[θ]
```

$$g\, L \left(mh + \frac{mp}{2}\right) Cos[\phi]\, Sin[\theta]$$

```
La = T - V // FullSimplify
```

$$\frac{1}{6} L \left(L\, (3\, mh + mp)\, \left(Dt[\theta]^2 + Cos[\theta]^4\, Dt[\phi]^2\right) - 3\, g\, (2\, mh + mp)\, Cos[\phi]\, Sin[\theta]\right)$$

```
D[La, θ] /. {D[Dt[θ]] → 0}
```

$$-g\, L \left(mh + \frac{mp}{2}\right) Cos[\theta]\, Cos[\phi] + k\, \phi^2\, Cos[\theta]\, Sin[\theta] - \frac{2}{3} L^2\, (3\, mh + mp)\, Cos[\theta]^3\, Dt[\phi]^2\, Sin[\theta]$$

```
Dt[D[La, Dt[θ]]] /. {Dt[L] → 0, Dt[l] → 0, Dt[mp] → 0, Dt[mh] → 0} // FullSimplify
```

$$\frac{1}{3} L^2\, (3\, mh + mp)\, Dt[Dt[\theta]]$$

```
D[La, ϕ] /. {D[Dt[ϕ]] → 0}
```

$$-k\, \phi\, Cos[\theta]^2 + g\, L \left(mh + \frac{mp}{2}\right) Sin[\theta]\, Sin[\phi]$$

```
Dt[D[La, Dt[ϕ]]] /. {Dt[L] → 0, Dt[l] → 0, Dt[mp] → 0, Dt[mh] → 0, Dt[k] → 0} // FullSimplify
```

$$\frac{1}{3} L^2\, (3\, mh + mp)\, Cos[\theta]^3\, (Cos[\theta]\, Dt[Dt[\phi]] - 4\, Dt[\theta]\, Dt[\phi]\, Sin[\theta])$$

```
D[La, λ]
```

```
0
```

```
Dt[D[La, Dt[λ]]] /. {Dt[L] → 0, Dt[l] → 0, Dt[mp] → 0, Dt[mh] → 0} // FullSimplify
```

```
0
```

```
Dt[D[La, Dt[ψ]]] /. {Dt[L] → 0, Dt[l] → 0, Dt[mp] → 0, Dt[mh] → 0} // FullSimplify
```

```
0
```

```
M = {{1 / 3 L^2 (3 mh + mp), 0, 0, 0}, {0, 1 / 3 L^2 (3 mh + mp) Cos[θ]^4, 0, 0}, {0, 0, 0, 0}, {0, 0, 0, 0}}
```

$$\left\{\left\{\frac{1}{3} L^2 (3\,\text{mh} + \text{mp}),\ 0,\ 0,\ 0\right\},\ \left\{0,\ \frac{1}{3} L^2 (3\,\text{mh} + \text{mp}) \cos[\theta]^4,\ 0,\ 0\right\},\ \{0, 0, 0, 0\},\ \{0, 0, 0, 0\}\right\}$$

```
AAA = Transpose[Join[M, -a]] // MatrixForm
```

$$\begin{pmatrix} \frac{1}{3} L^2 (3\,\text{mh} + \text{mp}) & 0 & 0 & 0 & L \cos[\phi] \sin[\theta] & 0 & -L \cos[\theta] \cos[\phi] \\ 0 & \frac{1}{3} L^2 (3\,\text{mh} + \text{mp}) \cos[\theta]^4 & 0 & 0 & L \cos[\theta] \sin[\phi] & -L \cos[\phi] & L \sin[\theta] \sin[\phi] \\ 0 & 0 & 0 & 0 & l \cos[\psi] \sin[\lambda] & 0 & -l \cos[\lambda] \cos[\psi] \\ 0 & 0 & 0 & 0 & l \cos[\lambda] \sin[\psi] & -l \cos[\psi] & l \sin[\lambda] \sin[\psi] \end{pmatrix}$$

```
AA = Transpose[Join[Transpose[-a], {{0, 0, 0}, {0, 0, 0}, {0, 0, 0}}]] // MatrixForm
```

$$\begin{pmatrix} L \cos[\phi] \sin[\theta] & L \cos[\theta] \sin[\phi] & l \cos[\psi] \sin[\lambda] & l \cos[\lambda] \sin[\psi] & 0 & 0 & 0 \\ 0 & -L \cos[\phi] & 0 & -l \cos[\psi] & 0 & 0 & 0 \\ -L \cos[\theta] \cos[\phi] & L \sin[\theta] \sin[\phi] & -l \cos[\lambda] \cos[\psi] & l \sin[\lambda] \sin[\psi] & 0 & 0 & 0 \end{pmatrix}$$

```
A = {{(1 / 3) * L^2 * (3 * mh + mp), 0, 0, 0, L * Sin[θ] * Cos[ϕ], 0,
  (-L) * Cos[θ] * Cos[ϕ]}, {0, (1 / 3) * L^2 * Cos[θ]^4 * (3 * mh + mp), 0, 0,
  L * Cos[θ] * Sin[ϕ], (-L) * Cos[ϕ], L * Sin[θ] * Sin[ϕ]},
 {0, 0, 0, 0, l * Sin[λ] * Cos[ψ], 0, (-l) * Cos[λ] * Cos[ψ]},
 {0, 0, 0, 0, l * Cos[λ] * Sin[ψ], (-l) * Cos[ψ], l * Sin[λ] * Sin[ψ]}, {L * Cos[ϕ] * Sin[θ], L * Cos[θ] * Sin[ϕ], l * Cos[ψ] * Sin[λ], l * Cos[λ] * Sin[ψ], 0, 0, 0},
 {0, (-L) * Cos[ϕ], 0, (-l) * Cos[ψ], 0, 0, 0}, {(-L) * Cos[θ] * Cos[ϕ], L * Sin[θ] * Sin[ϕ],
  (-l) * Cos[λ] * Cos[ψ], l * Sin[λ] * Sin[ψ], 0, 0, 0}}
```

$$\begin{pmatrix} \frac{1}{3} L^2 (3\,\text{mh} + \text{mp}) & 0 & 0 & 0 & L \cos(\phi) \sin(\theta) & 0 & -L \cos(\theta) \cos(\phi) \\ 0 & \frac{1}{3} L^2 (3\,\text{mh} + \text{mp}) \cos^4(\theta) & 0 & 0 & L \cos(\theta) \sin(\phi) & -L \cos(\phi) & L \sin(\theta) \sin(\phi) \\ 0 & 0 & 0 & 0 & l \cos(\psi) \sin(\lambda) & 0 & -l \cos(\lambda) \cos(\psi) \\ 0 & 0 & 0 & 0 & l \cos(\lambda) \sin(\psi) & -l \cos(\psi) & l \sin(\lambda) \sin(\psi) \\ L \cos(\phi) \sin(\theta) & L \cos(\theta) \sin(\phi) & l \cos(\psi) \sin(\lambda) & l \cos(\lambda) \sin(\psi) & 0 & 0 & 0 \\ 0 & -L \cos(\phi) & 0 & -l \cos(\psi) & 0 & 0 & 0 \\ -L \cos(\theta) \cos(\phi) & L \sin(\theta) \sin(\phi) & -l \cos(\lambda) \cos(\psi) & l \sin(\lambda) \sin(\psi) & 0 & 0 & 0 \end{pmatrix}$$

```
F = {{-g L (mh + 1 / 2 mp) Cos[θ] Cos[ϕ] + k ϕ^2 Cos[θ] Sin[θ] - 2 / 3 L^2 (3 mh + mp) Cos[θ]^3 Dt[ϕ]^2 Sin[θ]}, {4 / 3 L^2 (3 mh + mp) Cos[θ]^3 Sin[θ] Dt[θ] Dt[ϕ] - k ϕ Cos[θ]^2 + g L (mh + 1 / 2 mp) Sin[θ] Sin[ϕ]},
  {0}, {0}}
```

$$\begin{pmatrix} -\frac{1}{3}\times 2\,L^2\,(3\,\mathrm{mh}+\mathrm{mp})\,(d\phi)^2\sin(\theta)\cos^3(\theta)+\left(\mathrm{mh}+\frac{\mathrm{mp}}{2}\right)(-g)\,L\cos(\phi)\cos(\theta)+k\,\phi^2\sin(\theta)\cos(\theta) \\ \frac{4}{3}\,L^2\,(3\,\mathrm{mh}+\mathrm{mp})\,d\theta\,d\phi\sin(\theta)\cos^3(\theta)-k\,\phi\cos^2(\theta)+\left(\mathrm{mh}+\frac{\mathrm{mp}}{2}\right)g\,L\sin(\theta)\sin(\phi) \\ 0 \\ 0 \end{pmatrix}$$

```
q = Transpose[{{θ, ϕ, λ, ψ}}]
```

```
{{θ}, {ϕ}, {λ}, {ψ}}
```

```
qdt = Dt[q]
```

```
{{Dt[θ]}, {Dt[ϕ]}, {Dt[λ]}, {Dt[ψ]}}
```

```
bdt = Dt[b]
```

```
{{Dt[Dt[xt]]}, {Dt[Dt[yt]]}, {0}}
```

```
BB = adt.qdt // FullSimplify
```

```
{{-L Cos[θ] Cos[ϕ] (Dt[θ]^2 + Dt[ϕ]^2) - l Cos[λ] Cos[ψ] (Dt[λ]^2 + Dt[ψ]^2) + 2 L Dt[θ] Dt[ϕ] Sin[θ] Sin[ϕ] + 2 l Dt[λ] Dt[ψ] Sin[λ] Sin[ψ]},
 {-L Dt[ϕ]^2 Sin[ϕ] - l Dt[ψ]^2 Sin[ψ]}, {-L Cos[ϕ] (Dt[θ]^2 + Dt[ϕ]^2) Sin[θ] - l Cos[ψ] (Dt[λ]^2 + Dt[ψ]^2) Sin[λ] - 2 L Cos[θ] Dt[θ] Dt[ϕ] Sin[ϕ] - 2 l Cos[λ] Dt[λ] Dt[ψ] Sin[ψ]}}
```

```
B = Join[{{0}, {0}, {0}, {0}}, BB]
```

```
{{0}, {0}, {0}, {0}, {-L Cos[θ] Cos[ϕ] (Dt[θ]^2 + Dt[ϕ]^2) - l Cos[λ] Cos[ψ] (Dt[λ]^2 + Dt[ψ]^2) + 2 L Dt[θ] Dt[ϕ] Sin[θ] Sin[ϕ] + 2 l Dt[λ] Dt[ψ] Sin[λ] Sin[ψ]},
 {-L Dt[ϕ]^2 Sin[ϕ] - l Dt[ψ]^2 Sin[ψ]}, {-L Cos[ϕ] (Dt[θ]^2 + Dt[ϕ]^2) Sin[θ] - l Cos[ψ] (Dt[λ]^2 + Dt[ψ]^2) Sin[λ] - 2 L Cos[θ] Dt[θ] Dt[ϕ] Sin[ϕ] - 2 l Cos[λ] Dt[λ] Dt[ψ] Sin[ψ]}}
```

```
qddt = Dt[qdt]
```

```
{{Dt[Dt[θ]]}, {Dt[Dt[ϕ]]}, {Dt[Dt[λ]]}, {Dt[Dt[ψ]]}}
```

```
G = Join[qddt, {{r1}, {r2}, {r3}}]
```

$$\begin{pmatrix} d(d\theta) \\ d(d\phi) \\ d(d\lambda) \\ d(d\psi) \\ \mathrm{r1} \\ \mathrm{r2} \\ \mathrm{r3} \end{pmatrix}$$

```
As = A /. {Sin[θ] → θ, Cos[θ] → 1, Sin[ϕ] → ϕ, Cos[ϕ] → 1, Sin[ψ] → ψ, Cos[ψ] → 1}
```

$$\begin{pmatrix} \frac{1}{3} L^2 (3\,mh + mp) & 0 & 0 & 0 & L\,\theta & 0 & -L \\ 0 & \frac{1}{3} L^2 (3\,mh + mp) & 0 & 0 & L\,\phi & -L & L\,\theta\,\phi \\ 0 & 0 & 0 & 0 & l \sin(\lambda) & 0 & -l \cos(\lambda) \\ 0 & 0 & 0 & 0 & l\,\psi \cos(\lambda) & -l & l\,\psi \sin(\lambda) \\ L\,\theta & L\,\phi & l \sin(\lambda) & l\,\psi \cos(\lambda) & 0 & 0 & 0 \\ 0 & -L & 0 & -l & 0 & 0 & 0 \\ -L & L\,\theta\,\phi & -l \cos(\lambda) & l\,\psi \sin(\lambda) & 0 & 0 & 0 \end{pmatrix}$$

```
Bs = B /. {Sin[θ] → θ, Cos[θ] → 1, Sin[ϕ] → ϕ, Cos[ϕ] → 1, Sin[ψ] → ψ}
```

$$\begin{pmatrix} 0 \\ 0 \\ 0 \\ 0 \\ 2\,L\,\theta\,\phi\,d\theta\,d\phi - L\,((d\theta)^2 + (d\phi)^2) - l \cos(\lambda) \cos(\psi)\,((d\lambda)^2 + (d\psi)^2) + 2\,l\,\psi\,d\lambda\,d\psi \sin(\lambda) \\ -L\,\phi\,(d\phi)^2 - l\,\psi\,(d\psi)^2 \\ -2\,L\,\phi\,d\theta\,d\phi - L\,\theta\,((d\theta)^2 + (d\phi)^2) - 2\,l\,\psi \cos(\lambda)\,d\lambda\,d\psi - l \cos(\psi)\,((d\lambda)^2 + (d\psi)^2) \sin(\lambda) \end{pmatrix}$$

```
Solve[{As[[1]].G == Bs[[1]], As[[2]].G == Bs[[2]], As[[3]].G == Bs[[3]], As[[4]].G == Bs[[4]], As[[5]].G == Bs[[5]], As[[6]].G == Bs[[6]], As[[7]].G == Bs[[7]]},
 {Dt[Dt[θ]], Dt[Dt[ϕ]], Dt[Dt[λ]], Dt[Dt[ψ]], r1, r2, r3}]
```


$$\{\{d(d\theta) \to$$

$$-\left(\left((\theta - \lambda)\left(L\,(d\theta)^2 + L\,\theta\,\lambda\,(d\theta)^2 - 2\,L\,\theta\,\phi\,d\phi\,d\theta + 2\,L\,\lambda\,\phi\,d\phi\,d\theta + l \cos(\lambda) \cos(\psi)\,(d\lambda)^2 + L\,(d\phi)^2 + L\,\theta\,\lambda\,(d\phi)^2 + L\,\lambda^2\,\phi\,\psi\,(d\phi)^2 + L\,\phi\,\psi\,(d\phi)^2 + l\,\lambda^2\,\psi^2\,(d\psi)^2 + l\,\psi^2\,(d\psi)^2 + l \cos(\lambda) \cos(\psi)\,(d\psi)^2 + 2\,l\,\lambda\,\psi \cos(\lambda)\,d\lambda\,d\psi + l\,\lambda \cos(\psi)\,(d\lambda)^2 \sin(\lambda) + l\,\lambda \cos(\psi)\,(d\psi)^2 \sin(\lambda) - 2\,l\,\psi\,d\lambda\,d\psi \sin(\lambda)\right)\right) \Big/ \left(L\left(\psi^2\,\lambda^4 - 2\,\theta\,\phi\,\psi\,\lambda^3 + \theta^2\,\phi^2\,\lambda^2 + 2\,\psi^2\,\lambda^2 - 2\,\phi\,\psi\,\lambda^2 + \lambda^2 + 2\,\theta\,\phi^2\,\lambda - 2\,\theta\,\lambda - 2\,\theta\,\phi\,\psi\,\lambda + \theta^2 + \phi^2 + \psi^2 - 2\,\phi\,\psi\right)\right)\right),$$

$$d(d\phi) \to \left(\left(-\psi\,\lambda^2 + \theta\,\phi\,\lambda + \phi - \psi\right)\left(-L\,(d\theta)^2 - L\,\theta\,\lambda\,(d\theta)^2 + 2\,L\,\theta\,\phi\,d\phi\,d\theta - 2\,L\,\lambda\,\phi\,d\phi\,d\theta - l \cos(\lambda) \cos(\psi)\,(d\lambda)^2 - L\,(d\phi)^2 - L\,\theta\,\lambda\,(d\phi)^2 - L\,\lambda^2\,\phi\,\psi\,(d\phi)^2 - L\,\phi\,\psi\,(d\phi)^2 - l\,\lambda^2\,\psi^2\,(d\psi)^2 - l\,\psi^2\,(d\psi)^2 - l \cos(\lambda) \cos(\psi)\,(d\psi)^2 - 2\,l\,\lambda\,\psi \cos(\lambda)\,d\lambda\,d\psi - l\,\lambda \cos(\psi)\,(d\lambda)^2 \sin(\lambda) - l\,\lambda \cos(\psi)\,(d\psi)^2 \sin(\lambda) + 2\,l\,\psi\,d\lambda\,d\psi \sin(\lambda)\right)\right) \Big/ \left(L\left(\psi^2\,\lambda^4 - 2\,\theta\,\phi\,\psi\,\lambda^3 + \theta^2\,\phi^2\,\lambda^2 + 2\,\psi^2\,\lambda^2 - 2\,\phi\,\psi\,\lambda^2 + \lambda^2 + 2\,\theta\,\phi^2\,\lambda - 2\,\theta\,\lambda - 2\,\theta\,\phi\,\psi\,\lambda + \theta^2 + \phi^2 + \psi^2 - 2\,\phi\,\psi\right)\right),$$

$$d(d\lambda) \to -\left(\left(-L\,(d\theta)^2\,\theta^3 - L\,(d\phi)^2\,\theta^3 - 2\,L\,\lambda\,\phi^3\,d\theta\,d\phi\,\theta^3 + L\,\lambda\,(d\theta)^2\,\theta^2 + L\,\lambda\,\phi\,\psi\,(d\theta)^2\,\theta^2 + l\,\lambda\,\phi^2 \cos(\lambda) \cos(\psi)\,(d\lambda)^2\,\theta^2 + L\,\lambda\,(d\phi)^2\,\theta^2 + L\,\lambda\,\phi^3\,\psi\,(d\phi)^2\,\theta^2 + l\,\lambda\,\phi^2\,\psi^2\,(d\psi)^2\,\theta^2 - l\,\lambda\,\psi^2\,(d\psi)^2\,\theta^2 + l\,\lambda\,\phi^2 \cos(\lambda) \cos(\psi)\,(d\psi)^2\,\theta^2 - 2\,L\,\phi^3\,d\theta\,d\phi\,\theta^2 + 4\,L\,\lambda^2\,\phi^2\,\psi\,d\theta\,d\phi\,\theta^2 + 2\,L\,\phi^2\,\psi\,d\theta\,d\phi\,\theta^2 - 2\,l\,\psi \cos(\lambda)\,d\lambda\,d\psi\,\theta^2 - l \cos(\psi)\,(d\lambda)^2 \sin(\lambda)\,\theta^2 - l \cos(\psi)\,(d\psi)^2 \sin(\lambda)\,\theta^2 - 2\,l\,\lambda\,\phi^2\,\psi\,d\lambda\,d\psi \sin(\lambda)\,\theta^2 - L\,\lambda^2\,\psi^2\,(d\theta)^2\,\theta - L\,\psi^2\,(d\theta)^2\,\theta - L\,(d\theta)^2\,\theta - L\,\lambda^2\,\phi\,\psi\,(d\theta)^2\,\theta + L\,\phi\,\psi\,(d\theta)^2\,\theta + l\,\phi^2 \cos(\lambda) \cos(\psi)\,(d\lambda)^2\,\theta - l \cos(\lambda) \cos(\psi)\,(d\lambda)^2\,\theta - 2\,l\,\lambda^2\,\phi\,\psi \cos(\lambda) \cos(\psi)\,(d\lambda)^2\,\theta - l\,\phi\,\psi \cos(\lambda) \cos(\psi)\,(d\lambda)^2\,\theta - L\,\lambda^2\,\psi^2\,(d\phi)^2\,\theta - L\,\lambda^2\,\phi^2\,\psi^2\,(d\phi)^2\,\theta - L\,\phi^2\,\psi^2\,(d\phi)^2\,\theta - L\,\psi^2\,(d\phi)^2\,\theta - L\,(d\phi)^2\,\theta - L\,\lambda^2\,\phi^3\,\psi\,(d\phi)^2\,\theta + L\,\phi^3\,\psi\,(d\phi)^2\,\theta - l\,\lambda^2\,\phi\,\psi^3\,(d\psi)^2\,\theta - l\,\phi\,\psi^3\,(d\psi)^2\,\theta + l\,\lambda^2\,\psi^2\,(d\psi)^2\,\theta - l\,\lambda^2\,\phi^2\,\psi^2\,(d\psi)^2\,\theta + l\,\phi^2\,\psi^2\,(d\psi)^2\,\theta - l\,\psi^2\,(d\psi)^2\,\theta + l\,\phi^2 \cos(\lambda) \cos(\psi)\,(d\psi)^2\,\theta - l \cos(\lambda) \cos(\psi)\,(d\psi)^2\,\theta - 2\,l\,\lambda^2\,\phi\,\psi \cos(\lambda) \cos(\psi)\,(d\psi)^2\,\theta - l\,\phi\,\psi \cos(\lambda) \cos(\psi)\,(d\psi)^2\,\theta - 2\,L\,\lambda\,\phi^3\,d\theta\,d\phi\,\theta - 2\,L\,\lambda^3\,\phi\,\psi^2\,d\theta\,d\phi\,\theta - 2\,L\,\lambda\,\phi\,\psi^2\,d\theta\,d\phi\,\theta + 4\,L\,\lambda\,\phi^2\,\psi\,d\theta\,d\phi\,\theta + 2\,l\,\lambda\,\phi\,\psi^2 \cos(\lambda)\,d\lambda\,d\psi\,\theta - 2\,l\,\lambda\,\phi^2\,\psi \cos(\lambda)\,d\lambda\,d\psi\,\theta + 2\,l\,\lambda\,\psi \cos(\lambda)\,d\lambda\,d\psi\,\theta - l\,\lambda\,\phi^2 \cos(\psi)\,(d\lambda)^2 \sin(\lambda)\,\theta + l\,\lambda \cos(\psi)\,(d\lambda)^2 \sin(\lambda)\,\theta + l\,\lambda\,\phi\,\psi \cos(\psi)\,(d\lambda)^2 \sin(\lambda)\,\theta - l\,\lambda\,\phi^2 \cos(\psi)\,(d\psi)^2 \sin(\lambda)\,\theta + l\,\lambda \cos(\psi)\,(d\psi)^2 \sin(\lambda)\,\theta + l\,\lambda\,\phi\,\psi \cos(\psi)\,(d\psi)^2 \sin(\lambda)\,\theta + 4\,l\,\lambda^2\,\phi\,\psi^2\,d\lambda\,d\psi \sin(\lambda)\,\theta + 2\,l\,\phi\,\psi^2\,d\lambda\,d\psi \sin(\lambda)\,\theta - 2\,l\,\phi^2\,\psi\,d\lambda\,d\psi \sin(\lambda)\,\theta + 2\,l\,\psi\,d\lambda\,d\psi \sin(\lambda)\,\theta + L\,\lambda^3\,\psi^2\,(d\theta)^2 + L\,\lambda\,\psi^2\,(d\theta)^2 + L\,(d\theta)^2 - L\,\lambda\,\phi\,\psi\,(d\theta)^2 + l\,\lambda^3\,\psi^2 \cos(\lambda) \cos(\psi)\,(d\lambda)^2 + l\,\lambda\,\psi^2 \cos(\lambda) \cos(\psi)\,(d\lambda)^2 + l\,\lambda \cos(\lambda) \cos(\psi)\,(d\lambda)^2 - l\,\lambda\,\phi\,\psi \cos(\lambda) \cos(\psi)\,(d\lambda)^2 + L\,\lambda^3\,\psi^2\,(d\phi)^2 + L\,\lambda^3\,\phi^2\,\psi^2\,(d\phi)^2 + L\,\lambda\,\phi^2\,\psi^2\,(d\phi)^2 + L\,\lambda\,\psi^2\,(d\phi)^2 + L\,(d\phi)^2 - L\,\lambda\,\phi^3\,\psi\,(d\phi)^2 + l\,\lambda^3\,\phi\,\psi^3\,(d\psi)^2 + l\,\lambda\,\phi\,\psi^3\,(d\psi)^2 - l\,\lambda\,\phi^2\,\psi^2\,(d\psi)^2 + l\,\lambda\,\psi^2\,(d\psi)^2 + l\,\lambda^3\,\psi^2 \cos(\lambda) \cos(\psi)\,(d\psi)^2 + l\,\lambda\,\psi^2 \cos(\lambda) \cos(\psi)\,(d\psi)^2 + l\,\lambda \cos(\lambda) \cos(\psi)\,(d\psi)^2 - l\,\lambda\,\phi\,\psi \cos(\lambda) \cos(\psi)\,(d\psi)^2 - 2\,L\,\phi^3\,d\theta\,d\phi - 2\,L\,\lambda^2\,\phi^3\,\psi\,d\theta\,d\phi - 2\,L\,\phi\,\psi^2\,d\theta\,d\phi + 4\,L\,\phi^2\,\psi\,d\theta\,d\phi + 2\,l\,\phi\,\psi\,d\lambda\,d\psi - 2\,l\,\lambda^2\,\psi^2 \cos(\psi)\,(d\lambda)^2 \sin(\lambda) - l\,\lambda^2\,\psi^2 \cos(\psi)\,(d\lambda)^2 \sin(\lambda) - l\,\psi^2 \cos(\psi)\,(d\lambda)^2 \sin(\lambda) + l\,\lambda^2\,\phi\,\psi \cos(\psi)\,(d\lambda)^2 \sin(\lambda) + 2\,l\,\phi\,\psi \cos(\psi)\,(d\lambda)^2 \sin(\lambda) - l\,\phi^2 \cos(\psi)\,(d\psi)^2 \sin(\lambda) - l\,\lambda^2\,\psi^2 \cos(\psi)\,(d\psi)^2 \sin(\lambda) - l\,\psi^2 \cos(\psi)\,(d\psi)^2 \sin(\lambda) + l\,\lambda^2\,\phi\,\psi \cos(\psi)\,(d\psi)^2 \sin(\lambda) + 2\,l\,\phi\,\psi \cos(\psi)\,(d\psi)^2 \sin(\lambda) - 2\,l\,\lambda^3\,\psi^3\,d\lambda\,d\psi \sin(\lambda) - 2\,l\,\lambda\,\psi^3\,d\lambda\,d\psi \sin(\lambda) + 2\,l\,\lambda\,\phi\,\psi^2\,d\lambda\,d\psi \sin(\lambda) - 2\,l\,\lambda\,\psi\,d\lambda\,d\psi \sin(\lambda)\right) \Big/ \left(l\left(\psi^2\,\lambda^4 - 2\,\theta\,\phi\,\psi\,\lambda^3 + \theta^2\,\phi^2\,\lambda^2 + 2\,\psi^2\,\lambda^2 - 2\,\phi\,\psi\,\lambda^2 + \lambda^2 + 2\,\theta\,\phi^2\,\lambda - 2\,\theta\,\lambda - 2\,\theta\,\phi\,\psi\,\lambda + \theta^2 + \phi^2 + \psi^2 - 2\,\phi\,\psi\right)\right)\right),$$

$$d(d\psi) \to -\left(\left(L\,\theta\,\psi\,(d\theta)^2\,\lambda^3 + L\,\theta\,\phi^2\,\psi\,(d\phi)^2\,\lambda^3 + L\,\theta\,\psi\,(d\phi)^2\,\lambda^3 + l\,\theta\,\phi\,\psi^2\,(d\psi)^2\,\lambda^3 + 2\,L\,\phi\,\psi\,d\theta\,d\phi\,\lambda^3 + 2\,l\,\psi^2 \cos(\lambda)\,d\lambda\,d\psi\,\lambda^3 + l\,\psi \cos(\psi)\,(d\lambda)^2 \sin(\lambda)\,\lambda^3 + l\,\psi \cos(\psi)\,(d\psi)^2 \sin(\lambda)\,\lambda^3 - L\,\theta^2\,\phi\,(d\theta)^2\,\lambda^2 + L\,\psi\,(d\theta)^2\,\lambda^2 + l\,\psi \cos(\lambda) \cos(\psi)\,(d\lambda)^2\,\lambda^2 -\right.$$

$$L\theta^2\phi^3(d\phi)^2\lambda^2 - L\theta^2\phi(d\phi)^2\lambda^2 - L\phi(d\phi)^2\lambda^2 + L\phi^2\psi(d\phi)^2\lambda^2 + L\psi(d\phi)^2\lambda^2 + l\phi\psi^2(d\psi)^2\lambda^2 - l\theta^2\phi^2\psi(d\psi)^2\lambda^2 - l\psi(d\psi)^2\lambda^2 + l\psi\cos(\lambda)\cos(\psi)(d\psi)^2\lambda^2 - 2L\theta\phi^2 d\theta d\phi\lambda^2 - 2L\theta\phi\psi d\theta d\phi\lambda^2 - 2l\theta\phi\psi\cos(\lambda) d\lambda d\psi\lambda^2 - l\theta\phi\cos(\psi)(d\lambda)^2\sin(\lambda)\lambda^2 - l\theta\phi\cos(\psi)(d\psi)^2\sin(\lambda)\lambda^2 - 2l\psi^2 d\lambda d\psi\sin(\lambda)\lambda^2 - 2L\theta\phi(d\theta)^2\lambda + L\theta\psi(d\theta)^2\lambda - l\theta\phi\cos(\lambda)\cos(\psi)(d\lambda)^2\lambda - 2L\theta\phi^3(d\phi)^2\lambda + L\theta\phi^2\psi(d\phi)^2\lambda + L\theta\psi(d\phi)^2\lambda + l\theta\phi\psi^2(d\psi)^2\lambda - 2l\theta\phi^2\psi(d\psi)^2\lambda + 2l\theta\psi(d\psi)^2\lambda - l\theta\phi\cos(\lambda)\cos(\psi)(d\psi)^2\lambda + 2L\theta^2\phi^2 d\theta d\phi\lambda - 2L\phi^2 d\theta d\phi\lambda + 2L\phi\psi d\theta d\phi\lambda + 2l\psi^2\cos(\lambda) d\lambda d\psi\lambda - 2l\phi\psi\cos(\lambda) d\lambda d\psi\lambda - l\phi\cos(\psi)(d\lambda)^2\sin(\lambda)\lambda + l\psi\cos(\psi)(d\lambda)^2\sin(\lambda)\lambda - l\phi\cos(\psi)(d\psi)^2\sin(\lambda)\lambda + l\psi\cos(\psi)(d\psi)^2\sin(\lambda)\lambda + 2l\theta\phi\psi d\lambda d\psi\sin(\lambda)\lambda - L\phi(d\theta)^2 + L\psi(d\theta)^2 - l\phi\cos(\lambda)\cos(\psi)(d\lambda)^2 + l\psi\cos(\lambda)\cos(\psi)(d\lambda)^2 - L\phi^3(d\phi)^2 - L\theta^2\phi(d\phi)^2 - L\phi(d\phi)^2 + L\phi^2\psi(d\phi)^2 + L\psi(d\phi)^2 + l\phi\psi^2(d\psi)^2 - l\theta^2\psi(d\psi)^2 - l\phi^2\psi(d\psi)^2 - l\phi\cos(\lambda)\cos(\psi)(d\psi)^2 + l\psi\cos(\lambda)\cos(\psi)(d\psi)^2 + 2L\theta\phi^2 d\theta d\phi - 2L\theta\phi\psi d\theta d\phi - 2l\psi^2 d\lambda d\psi\sin(\lambda) + 2l\phi\psi d\lambda d\psi\sin(\lambda)\Big)\Big/\Big(l\left(\psi^2\lambda^4 - 2\theta\phi\psi\lambda^3 + \theta^2\phi^2\lambda^2 + 2\psi^2\lambda^2 - 2\phi\psi\lambda^2 + \lambda^2 + 2\theta\phi^2\lambda - 2\theta\lambda - 2\theta\phi\psi\lambda + \theta^2 + \phi^2 + \psi^2 - 2\phi\psi\right)\Big)\Big),$$

$$\text{r1} \to \Big((3\,\text{mh} + \text{mp})\left(L(d\theta)^2 + L\theta\lambda(d\theta)^2 - 2L\theta\phi d\phi d\theta + 2L\lambda\phi d\phi d\theta + l\cos(\lambda)\cos(\psi)(d\lambda)^2 + L(d\phi)^2 + L\theta\lambda(d\phi)^2 + L\lambda^2\phi\psi(d\phi)^2 + L\phi\psi(d\phi)^2 + l\lambda^2\psi^2(d\psi)^2 + l\psi^2(d\psi)^2 + l\cos(\lambda)\cos(\psi)(d\psi)^2 + 2l\lambda\psi\cos(\lambda) d\lambda d\psi + l\lambda\cos(\psi)(d\lambda)^2\sin(\lambda) + l\lambda\cos(\psi)(d\psi)^2\sin(\lambda) - 2l\psi d\lambda d\psi\sin(\lambda)\right)\Big)\Big/\Big(3\left(\psi^2\lambda^4 - 2\theta\phi\psi\lambda^3 + \theta^2\phi^2\lambda^2 + 2\psi^2\lambda^2 - 2\phi\psi\lambda^2 + \lambda^2 + 2\theta\phi^2\lambda - 2\theta\lambda - 2\theta\phi\psi\lambda + \theta^2 + \phi^2 + \psi^2 - 2\phi\psi\right)\Big),$$

$$\text{r2} \to \Big((3\,\text{mh} + \text{mp})\left(\psi\lambda^2 + \psi\right)\left(L(d\theta)^2 + L\theta\lambda(d\theta)^2 - 2L\theta\phi d\phi d\theta + 2L\lambda\phi d\phi d\theta + l\cos(\lambda)\cos(\psi)(d\lambda)^2 + L(d\phi)^2 + L\theta\lambda(d\phi)^2 + L\lambda^2\phi\psi(d\phi)^2 + L\phi\psi(d\phi)^2 + l\lambda^2\psi^2(d\psi)^2 + l\psi^2(d\psi)^2 + l\cos(\lambda)\cos(\psi)(d\psi)^2 + 2l\lambda\psi\cos(\lambda) d\lambda d\psi + l\lambda\cos(\psi)(d\lambda)^2\sin(\lambda) + l\lambda\cos(\psi)(d\psi)^2\sin(\lambda) - 2l\psi d\lambda d\psi\sin(\lambda)\right)\Big)\Big/\Big(3\left(\psi^2\lambda^4 - 2\theta\phi\psi\lambda^3 + \theta^2\phi^2\lambda^2 + 2\psi^2\lambda^2 - 2\phi\psi\lambda^2 + \lambda^2 + 2\theta\phi^2\lambda - 2\theta\lambda - 2\theta\phi\psi\lambda + \theta^2 + \phi^2 + \psi^2 - 2\phi\psi\right)\Big),$$

$$\text{r3} \to \Big((3\,\text{mh} + \text{mp})\lambda\left(L(d\theta)^2 + L\theta\lambda(d\theta)^2 - 2L\theta\phi d\phi d\theta + 2L\lambda\phi d\phi d\theta + l\cos(\lambda)\cos(\psi)(d\lambda)^2 + L(d\phi)^2 + L\theta\lambda(d\phi)^2 + L\lambda^2\phi\psi(d\phi)^2 + L\phi\psi(d\phi)^2 + l\lambda^2\psi^2(d\psi)^2 + l\psi^2(d\psi)^2 + l\cos(\lambda)\cos(\psi)(d\psi)^2 + 2l\lambda\psi\cos(\lambda) d\lambda d\psi + l\lambda\cos(\psi)(d\lambda)^2\sin(\lambda) + l\lambda\cos(\psi)(d\psi)^2\sin(\lambda) - 2l\psi d\lambda d\psi\sin(\lambda)\right)\Big)\Big/\Big(3\left(\psi^2\lambda^4 - 2\theta\phi\psi\lambda^3 + \theta^2\phi^2\lambda^2 + 2\psi^2\lambda^2 - 2\phi\psi\lambda^2 + \lambda^2 + 2\theta\phi^2\lambda - 2\theta\lambda - 2\theta\phi\psi\lambda + \theta^2 + \phi^2 + \psi^2 - 2\phi\psi\right)\Big)\Big\}$$

thetaddt =

```
-(((θ - λ) (L Dt[θ]^2 + L θ λ Dt[θ]^2 + 1 Cos[λ] Cos[ψ] Dt[λ]^2 - 2 L θ ϕ Dt[θ] Dt[ϕ] + 2 L λ ϕ Dt[θ] Dt[ϕ] + L Dt[ϕ]^2 + L θ λ Dt[ϕ]^2 + L ϕ ψ Dt[ϕ]^2 + L λ^2 ϕ ψ Dt[ϕ]^2 + 2 1 λ ψ Cos[λ] Dt[λ] Dt[ψ] +
      1 ψ^2 Dt[ψ]^2 + 1 λ^2 ψ^2 Dt[ψ]^2 + 1 Cos[λ] Cos[ψ] Dt[ψ]^2 + 1 λ Cos[ψ] Dt[λ]^2 Sin[λ] - 2 1 ψ Dt[λ] Dt[ψ] Sin[λ] + 1 λ Cos[ψ] Dt[ψ]^2 Sin[λ])) /
   (L (θ^2 - 2 θ λ + λ^2 + ϕ^2 + 2 θ λ ϕ^2 + θ^2 λ^2 ϕ^2 - 2 ϕ ψ - 2 θ λ ϕ ψ - 2 λ^2 ϕ ψ - 2 θ λ^3 ϕ ψ + ψ^2 + 2 λ^2 ψ^2 + λ^4 ψ^2))) /. {Dt[θ] → 0, Dt[Dt[θ]] → 0}
```

$$-\Big(\big((\theta-\lambda)\left(\lambda^2 l\psi^2(d\psi)^2 - 2l\psi d\lambda\sin(\lambda) d\psi + l(d\lambda)^2\cos(\lambda)\cos(\psi) + 2\lambda l\psi d\lambda\cos(\lambda) d\psi + l\cos(\lambda)(d\psi)^2\cos(\psi) + \lambda l(d\lambda)^2\sin(\lambda)\cos(\psi) + \lambda l\sin(\lambda)(d\psi)^2\cos(\psi) + l\psi^2(d\psi)^2 + \theta\lambda L(d\phi)^2 + \lambda^2 L\psi\phi(d\phi)^2 + L\psi\phi(d\phi)^2 + L(d\phi)^2\right)\big)\Big/$$
$$\left(L\left(\theta^2\lambda^2\phi^2 + \theta^2 - 2\theta\lambda^3\psi\phi + 2\theta\lambda\phi^2 - 2\theta\lambda\psi\phi - 2\theta\lambda + \lambda^4\psi^2 + 2\lambda^2\psi^2 - 2\lambda^2\psi\phi + \lambda^2 + \psi^2 + \phi^2 - 2\psi\phi\right)\right)$$

phiddt =

```
((ϕ + θ λ ϕ - ψ - λ^2 ψ) (-L Dt[θ]^2 - L θ λ Dt[θ]^2 - 1 Cos[λ] Cos[ψ] Dt[λ]^2 + 2 L θ ϕ Dt[θ] Dt[ϕ] - 2 L λ ϕ Dt[θ] Dt[ϕ] - L Dt[ϕ]^2 - L θ λ Dt[ϕ]^2 - L ϕ ψ Dt[ϕ]^2 - L λ^2 ϕ ψ Dt[ϕ]^2 - 2 1 λ ψ Cos[λ] Dt[λ] Dt[ψ] -
      1 ψ^2 Dt[ψ]^2 - 1 λ^2 ψ^2 Dt[ψ]^2 - 1 Cos[λ] Cos[ψ] Dt[ψ]^2 - 1 λ Cos[ψ] Dt[λ]^2 Sin[λ] + 2 1 ψ Dt[λ] Dt[ψ] Sin[λ] - 1 λ Cos[ψ] Dt[ψ]^2 Sin[λ])) /
   (L (θ^2 - 2 θ λ + λ^2 + ϕ^2 + 2 θ λ ϕ^2 + θ^2 λ^2 ϕ^2 - 2 ϕ ψ - 2 θ λ ϕ ψ - 2 λ^2 ϕ ψ - 2 θ λ^3 ϕ ψ + ψ^2 + 2 λ^2 ψ^2 + λ^4 ψ^2))
```

```
((ϕ + θ λ ϕ - ψ - λ^2 ψ) (-L Dt[θ]^2 - L θ λ Dt[θ]^2 - 1 Cos[λ] Cos[ψ] Dt[λ]^2 + 2 L θ ϕ Dt[θ] Dt[ϕ] - 2 L λ ϕ Dt[θ] Dt[ϕ] - L Dt[ϕ]^2 - L θ λ Dt[ϕ]^2 - L ϕ ψ Dt[ϕ]^2 -
      L λ^2 ϕ ψ Dt[ϕ]^2 - 2 1 λ ψ Cos[λ] Dt[λ] Dt[ψ] - 1 ψ^2 Dt[ψ]^2 - 1 λ^2 ψ^2 Dt[ψ]^2 - 1 Cos[λ] Cos[ψ] Dt[ψ]^2 - 1 λ Cos[ψ] Dt[λ]^2 Sin[λ] + 2 1 ψ Dt[λ] Dt[ψ] Sin[λ] - 1 λ Cos[ψ] Dt[ψ]^2 Sin[λ])) /
   (L (θ^2 - 2 θ λ + λ^2 + ϕ^2 + 2 θ λ ϕ^2 + θ^2 λ^2 ϕ^2 - 2 ϕ ψ - 2 θ λ ϕ ψ - 2 λ^2 ϕ ψ - 2 θ λ^3 ϕ ψ + ψ^2 + 2 λ^2 ψ^2 + λ^4 ψ^2))
```

numdaddt =

```
-(((-L θ Dt[θ]^2 - L θ^3 Dt[θ]^2 + L λ Dt[θ]^2 + L θ^2 λ Dt[θ]^2 + L θ ϕ ψ Dt[θ]^2 - L λ ϕ ψ Dt[θ]^2 + L θ^2 λ ϕ ψ Dt[θ]^2 - L θ λ^2 ϕ ψ Dt[θ]^2 - L θ ψ^2 Dt[θ]^2 + L λ ψ^2 Dt[θ]^2 - L θ λ^2 ψ^2 Dt[θ]^2 + L λ^3 ψ^2 Dt[θ]^2 -
      1 θ Cos[λ] Cos[ψ] Dt[λ]^2 + 1 λ Cos[λ] Cos[ψ] Dt[λ]^2 + 1 θ ϕ^2 Cos[λ] Cos[ψ] Dt[λ]^2 + 1 θ^2 λ ϕ^2 Cos[λ] Cos[ψ] Dt[λ]^2 - 1 θ ϕ ψ Cos[λ] Cos[ψ] Dt[λ]^2 - 1 λ ϕ ψ Cos[λ] Cos[ψ] Dt[λ]^2 -
      2 1 θ λ^2 ϕ ψ Cos[λ] Cos[ψ] Dt[λ]^2 + 1 λ ψ^2 Cos[λ] Cos[ψ] Dt[λ]^2 + 1 λ^3 ψ^2 Cos[λ] Cos[ψ] Dt[λ]^2 - 2 L ϕ^3 Dt[θ] Dt[ϕ] - 2 L θ^2 ϕ^3 Dt[θ] Dt[ϕ] - 2 L θ λ ϕ^3 Dt[θ] Dt[ϕ] - 2 L θ^3 λ ϕ^3 Dt[θ] Dt[ϕ] +
      4 L ϕ^2 ψ Dt[θ] Dt[ϕ] + 2 L θ^2 ϕ^2 ψ Dt[θ] Dt[ϕ] + 4 L θ λ ϕ^2 ψ Dt[θ] Dt[ϕ] + 2 L λ^2 ϕ^2 ψ Dt[θ] Dt[ϕ] + 4 L θ^2 λ^2 ϕ^2 ψ Dt[θ] Dt[ϕ] - 2 L ϕ ψ^2 Dt[θ] Dt[ϕ] - 2 L θ λ ϕ ψ^2 Dt[θ] Dt[ϕ] - 2 L λ^2 ϕ ψ^2 Dt[θ] Dt[ϕ] -
      2 L θ λ^3 ϕ ψ^2 Dt[θ] Dt[ϕ] - L θ Dt[ϕ]^2 - L θ^3 Dt[ϕ]^2 + L λ Dt[ϕ]^2 + L θ^2 λ Dt[ϕ]^2 + L θ ϕ^3 ψ Dt[ϕ]^2 - L λ ϕ^3 ψ Dt[ϕ]^2 + L θ^2 λ ϕ^3 ψ Dt[ϕ]^2 - L θ λ^2 ϕ^3 ψ Dt[ϕ]^2 - L θ ψ^2 Dt[ϕ]^2 + L λ ψ^2 Dt[ϕ]^2 -
      L θ λ^2 ψ^2 Dt[ϕ]^2 + L λ^3 ψ^2 Dt[ϕ]^2 - L θ ϕ^2 ψ^2 Dt[ϕ]^2 + L λ ϕ^2 ψ^2 Dt[ϕ]^2 - L θ λ^2 ϕ^2 ψ^2 Dt[ϕ]^2 + L λ^3 ϕ^2 ψ^2 Dt[ϕ]^2 - 2 1 θ^2 ψ Cos[λ] Dt[λ] Dt[ψ] + 2 1 θ λ ψ Cos[λ] Dt[λ] Dt[ψ] - 2 1 ϕ^2 ψ Cos[λ] Dt[λ] Dt[ψ] -
      2 1 θ λ ϕ^2 ψ Cos[λ] Dt[λ] Dt[ψ] + 4 1 ϕ ψ^2 Cos[λ] Dt[λ] Dt[ψ] + 2 1 θ λ ϕ ψ^2 Cos[λ] Dt[λ] Dt[ψ] + 2 1 λ^2 ϕ ψ^2 Cos[λ] Dt[λ] Dt[ψ] - 2 1 ψ^3 Cos[λ] Dt[λ] Dt[ψ] - 2 1 λ^2 ψ^3 Cos[λ] Dt[λ] Dt[ψ] -
```

$$1\,\theta\,\psi^2\,\mathrm{Dt}[\psi]^2+1\,\lambda\,\psi^2\,\mathrm{Dt}[\psi]^2-1\,\theta^2\,\lambda\,\psi^2\,\mathrm{Dt}[\psi]^2+1\,\theta\,\lambda^2\,\psi^2\,\mathrm{Dt}[\psi]^2+1\,\theta\,\phi^2\,\psi^2\,\mathrm{Dt}[\psi]^2-1\,\lambda\,\phi^2\,\psi^2\,\mathrm{Dt}[\psi]^2+1\,\theta^2\,\lambda\,\phi^2\,\psi^2\,\mathrm{Dt}[\psi]^2-1\,\theta\,\lambda^2\,\phi^2\,\psi^2\,\mathrm{Dt}[\psi]^2-1\,\theta\,\phi\,\psi^3\,\mathrm{Dt}[\psi]^2+1\,\lambda\,\phi\,\psi^3\,\mathrm{Dt}[\psi]^2-1\,\theta\,\lambda^2\,\phi\,\psi^3\,\mathrm{Dt}[\psi]^2+1\,\lambda^3\,\phi\,\psi^3\,\mathrm{Dt}[\psi]^2-1\,\theta\,\mathrm{Cos}[\lambda]\,\mathrm{Cos}[\psi]\,\mathrm{Dt}[\psi]^2+1\,\lambda\,\mathrm{Cos}[\lambda]\,\mathrm{Cos}[\psi]\,\mathrm{Dt}[\psi]^2+1\,\theta\,\phi^2\,\mathrm{Cos}[\lambda]\,\mathrm{Cos}[\psi]\,\mathrm{Dt}[\psi]^2+1\,\theta^2\,\lambda\,\phi^2\,\mathrm{Cos}[\lambda]\,\mathrm{Cos}[\psi]\,\mathrm{Dt}[\psi]^2-1\,\theta\,\phi\,\psi\,\mathrm{Cos}[\lambda]\,\mathrm{Cos}[\psi]\,\mathrm{Dt}[\psi]^2-1\,\lambda\,\phi\,\psi\,\mathrm{Cos}[\lambda]\,\mathrm{Cos}[\psi]\,\mathrm{Dt}[\psi]^2-2\,1\,\theta\,\lambda^2\,\phi\,\psi\,\mathrm{Cos}[\lambda]\,\mathrm{Cos}[\psi]\,\mathrm{Dt}[\psi]^2+1\,\lambda\,\psi^2\,\mathrm{Cos}[\lambda]\,\mathrm{Cos}[\psi]\,\mathrm{Dt}[\psi]^2+1\,\lambda^3\,\psi^2\,\mathrm{Cos}[\lambda]\,\mathrm{Cos}[\psi]\,\mathrm{Dt}[\psi]^2-1\,\theta^2\,\mathrm{Cos}[\psi]\,\mathrm{Dt}[\lambda]^2\,\mathrm{Sin}[\lambda]+1\,\theta\,\lambda\,\mathrm{Cos}[\psi]\,\mathrm{Dt}[\lambda]^2\,\mathrm{Sin}[\lambda]-1\,\phi^2\,\mathrm{Cos}[\psi]\,\mathrm{Dt}[\lambda]^2\,\mathrm{Sin}[\lambda]-1\,\theta\,\lambda\,\phi^2\,\mathrm{Cos}[\psi]\,\mathrm{Dt}[\lambda]^2\,\mathrm{Sin}[\lambda]+2\,1\,\phi\,\psi\,\mathrm{Cos}[\psi]\,\mathrm{Dt}[\lambda]^2\,\mathrm{Sin}[\lambda]+1\,\theta\,\lambda\,\phi\,\psi\,\mathrm{Cos}[\psi]\,\mathrm{Dt}[\lambda]^2\,\mathrm{Sin}[\lambda]+1\,\lambda^2\,\phi\,\psi\,\mathrm{Cos}[\psi]\,\mathrm{Dt}[\lambda]^2\,\mathrm{Sin}[\lambda]-1\,\psi^2\,\mathrm{Cos}[\psi]\,\mathrm{Dt}[\lambda]^2\,\mathrm{Sin}[\lambda]-1\,\lambda^2\,\psi^2\,\mathrm{Cos}[\psi]\,\mathrm{Dt}[\lambda]^2\,\mathrm{Sin}[\lambda]+2\,1\,\theta\,\psi\,\mathrm{Dt}[\lambda]\,\mathrm{Dt}[\psi]\,\mathrm{Sin}[\lambda]-2\,1\,\lambda\,\psi\,\mathrm{Dt}[\lambda]\,\mathrm{Dt}[\psi]\,\mathrm{Sin}[\lambda]-2\,1\,\theta\,\phi^2\,\psi\,\mathrm{Dt}[\lambda]\,\mathrm{Dt}[\psi]\,\mathrm{Sin}[\lambda]-2\,1\,\theta^2\,\lambda\,\phi^2\,\psi\,\mathrm{Dt}[\lambda]\,\mathrm{Dt}[\psi]\,\mathrm{Sin}[\lambda]+2\,1\,\theta\,\phi\,\psi^2\,\mathrm{Dt}[\lambda]\,\mathrm{Dt}[\psi]\,\mathrm{Sin}[\lambda]+2\,1\,\lambda\,\phi\,\psi^2\,\mathrm{Dt}[\lambda]\,\mathrm{Dt}[\psi]\,\mathrm{Sin}[\lambda]+4\,1\,\theta\,\lambda^2\,\phi\,\psi^2\,\mathrm{Dt}[\lambda]\,\mathrm{Dt}[\psi]\,\mathrm{Sin}[\lambda]-2\,1\,\lambda^3\,\psi^3\,\mathrm{Dt}[\lambda]\,\mathrm{Dt}[\psi]\,\mathrm{Sin}[\lambda]-2\,1\,\lambda^3\,\psi^3\,\mathrm{Dt}[\lambda]\,\mathrm{Dt}[\psi]\,\mathrm{Sin}[\lambda]-1\,\theta^2\,\mathrm{Cos}[\psi]\,\mathrm{Dt}[\psi]^2\,\mathrm{Sin}[\lambda]+1\,\theta\,\lambda\,\mathrm{Cos}[\psi]\,\mathrm{Dt}[\psi]^2\,\mathrm{Sin}[\lambda]-1\,\phi^2\,\mathrm{Cos}[\psi]\,\mathrm{Dt}[\psi]^2\,\mathrm{Sin}[\lambda]-1\,\theta\,\lambda\,\phi^2\,\mathrm{Cos}[\psi]\,\mathrm{Dt}[\psi]^2\,\mathrm{Sin}[\lambda]+2\,1\,\phi\,\psi\,\mathrm{Cos}[\psi]\,\mathrm{Dt}[\psi]^2\,\mathrm{Sin}[\lambda]+1\,\theta\,\lambda\,\phi\,\psi\,\mathrm{Cos}[\psi]\,\mathrm{Dt}[\psi]^2\,\mathrm{Sin}[\lambda]+1\,\lambda^2\,\phi\,\psi\,\mathrm{Cos}[\psi]\,\mathrm{Dt}[\psi]^2\,\mathrm{Sin}[\lambda]-1\,\psi^2\,\mathrm{Cos}[\psi]\,\mathrm{Dt}[\psi]^2\,\mathrm{Sin}[\lambda]-1\,\lambda^2\,\psi^2\,\mathrm{Cos}[\psi]\,\mathrm{Dt}[\psi]^2\,\mathrm{Sin}[\lambda]\Big)\Big/\Big(1\,\big(\theta^2-2\,\theta\,\lambda+\lambda^2+\phi^2+2\,\theta\,\lambda\,\phi^2+\theta^2\,\lambda^2\,\phi^2-2\,\phi\,\psi-2\,\theta\,\lambda\,\phi\,\psi-2\,\lambda^2\,\phi\,\psi-2\,\theta\,\lambda^3\,\phi\,\psi+\psi^2+2\,\lambda^2\,\psi^2+\lambda^4\,\psi^2\big)\Big)\Big)$$

psiddt =

$$-\Big(\Big(-\mathrm{L}\,\phi\,\mathrm{Dt}[\theta]^2-2\,\mathrm{L}\,\theta\,\lambda\,\phi\,\mathrm{Dt}[\theta]^2-\mathrm{L}\,\theta^2\,\lambda^2\,\phi\,\mathrm{Dt}[\theta]^2+\mathrm{L}\,\psi\,\mathrm{Dt}[\theta]^2+\mathrm{L}\,\theta\,\lambda\,\psi\,\mathrm{Dt}[\theta]^2+\mathrm{L}\,\lambda^2\,\psi\,\mathrm{Dt}[\theta]^2+\mathrm{L}\,\theta\,\lambda^3\,\psi\,\mathrm{Dt}[\theta]^2-1\,\phi\,\mathrm{Cos}[\lambda]\,\mathrm{Cos}[\psi]\,\mathrm{Dt}[\lambda]^2-1\,\theta\,\lambda\,\phi\,\mathrm{Cos}[\lambda]\,\mathrm{Cos}[\psi]\,\mathrm{Dt}[\lambda]^2+1\,\psi\,\mathrm{Cos}[\lambda]\,\mathrm{Cos}[\psi]\,\mathrm{Dt}[\lambda]^2+1\,\lambda^2\,\psi\,\mathrm{Cos}[\lambda]\,\mathrm{Cos}[\psi]\,\mathrm{Dt}[\lambda]^2+2\,\mathrm{L}\,\theta\,\phi^2\,\mathrm{Dt}[\theta]\,\mathrm{Dt}[\phi]-2\,\mathrm{L}\,\lambda\,\phi^2\,\mathrm{Dt}[\theta]\,\mathrm{Dt}[\phi]+2\,\mathrm{L}\,\theta^2\,\lambda\,\phi^2\,\mathrm{Dt}[\theta]\,\mathrm{Dt}[\phi]-2\,\mathrm{L}\,\theta\,\lambda^2\,\phi^2\,\mathrm{Dt}[\theta]\,\mathrm{Dt}[\phi]-2\,\mathrm{L}\,\theta\,\phi\,\psi\,\mathrm{Dt}[\theta]\,\mathrm{Dt}[\phi]+2\,\mathrm{L}\,\lambda\,\phi\,\psi\,\mathrm{Dt}[\theta]\,\mathrm{Dt}[\phi]-2\,\mathrm{L}\,\theta\,\lambda^2\,\phi\,\psi\,\mathrm{Dt}[\theta]\,\mathrm{Dt}[\phi]+2\,\mathrm{L}\,\lambda^3\,\phi\,\psi\,\mathrm{Dt}[\theta]\,\mathrm{Dt}[\phi]-\mathrm{L}\,\phi\,\mathrm{Dt}[\phi]^2-\mathrm{L}\,\theta^2\,\phi\,\mathrm{Dt}[\phi]^2-\mathrm{L}\,\lambda^2\,\phi\,\mathrm{Dt}[\phi]^2-\mathrm{L}\,\theta^2\,\lambda^2\,\phi\,\mathrm{Dt}[\phi]^2-\mathrm{L}\,\phi^3\,\mathrm{Dt}[\phi]^2-2\,\mathrm{L}\,\theta\,\lambda\,\phi^3\,\mathrm{Dt}[\phi]^2-\mathrm{L}\,\theta^2\,\lambda^2\,\phi^3\,\mathrm{Dt}[\phi]^2+\mathrm{L}\,\psi\,\mathrm{Dt}[\phi]^2+\mathrm{L}\,\theta\,\lambda\,\psi\,\mathrm{Dt}[\phi]^2+\mathrm{L}\,\lambda^2\,\psi\,\mathrm{Dt}[\phi]^2+\mathrm{L}\,\theta\,\lambda^3\,\psi\,\mathrm{Dt}[\phi]^2+\mathrm{L}\,\phi^2\,\psi\,\mathrm{Dt}[\phi]^2+\mathrm{L}\,\theta\,\lambda\,\phi^2\,\psi\,\mathrm{Dt}[\phi]^2+\mathrm{L}\,\lambda^2\,\phi^2\,\psi\,\mathrm{Dt}[\phi]^2+\mathrm{L}\,\theta\,\lambda^3\,\phi^2\,\psi\,\mathrm{Dt}[\phi]^2-2\,1\,\lambda\,\phi\,\psi\,\mathrm{Cos}[\lambda]\,\mathrm{Dt}[\lambda]\,\mathrm{Dt}[\psi]-2\,1\,\theta\,\lambda^2\,\phi\,\psi\,\mathrm{Cos}[\lambda]\,\mathrm{Dt}[\lambda]\,\mathrm{Dt}[\psi]+2\,1\,\lambda\,\psi^2\,\mathrm{Cos}[\lambda]\,\mathrm{Dt}[\lambda]\,\mathrm{Dt}[\psi]+2\,1\,\lambda^3\,\psi^2\,\mathrm{Cos}[\lambda]\,\mathrm{Dt}[\lambda]\,\mathrm{Dt}[\psi]-1\,\theta^2\,\psi\,\mathrm{Dt}[\psi]^2+2\,1\,\theta\,\lambda\,\psi\,\mathrm{Dt}[\psi]^2-1\,\lambda^2\,\psi\,\mathrm{Dt}[\psi]^2-1\,\phi^2\,\psi\,\mathrm{Dt}[\psi]^2-2\,1\,\theta\,\lambda\,\phi^2\,\psi\,\mathrm{Dt}[\psi]^2-1\,\theta^2\,\lambda^2\,\phi^2\,\psi\,\mathrm{Dt}[\psi]^2+1\,\phi\,\psi^2\,\mathrm{Dt}[\psi]^2+1\,\theta\,\lambda\,\phi\,\psi^2\,\mathrm{Dt}[\psi]^2+1\,\lambda^2\,\phi\,\psi^2\,\mathrm{Dt}[\psi]^2+1\,\theta\,\lambda^3\,\phi\,\psi^2\,\mathrm{Dt}[\psi]^2-1\,\phi\,\mathrm{Cos}[\lambda]\,\mathrm{Cos}[\psi]\,\mathrm{Dt}[\psi]^2-1\,\theta\,\lambda\,\phi\,\mathrm{Cos}[\lambda]\,\mathrm{Cos}[\psi]\,\mathrm{Dt}[\psi]^2+1\,\psi\,\mathrm{Cos}[\lambda]\,\mathrm{Cos}[\psi]\,\mathrm{Dt}[\psi]^2+1\,\lambda^2\,\psi\,\mathrm{Cos}[\lambda]\,\mathrm{Cos}[\psi]\,\mathrm{Dt}[\psi]^2-1\,\lambda\,\phi\,\mathrm{Cos}[\psi]\,\mathrm{Dt}[\lambda]^2\,\mathrm{Sin}[\lambda]-1\,\theta\,\lambda^2\,\phi\,\mathrm{Cos}[\psi]\,\mathrm{Dt}[\lambda]^2\,\mathrm{Sin}[\lambda]+1\,\lambda\,\psi\,\mathrm{Cos}[\psi]\,\mathrm{Dt}[\lambda]^2\,\mathrm{Sin}[\lambda]+1\,\lambda^3\,\psi\,\mathrm{Cos}[\psi]\,\mathrm{Dt}[\lambda]^2\,\mathrm{Sin}[\lambda]+2\,1\,\phi\,\psi\,\mathrm{Dt}[\lambda]\,\mathrm{Dt}[\psi]\,\mathrm{Sin}[\lambda]+2\,1\,\theta\,\lambda\,\phi\,\psi\,\mathrm{Dt}[\lambda]\,\mathrm{Dt}[\psi]\,\mathrm{Sin}[\lambda]-2\,1\,\psi^2\,\mathrm{Dt}[\lambda]\,\mathrm{Dt}[\psi]\,\mathrm{Sin}[\lambda]-2\,1\,\lambda^2\,\psi^2\,\mathrm{Dt}[\lambda]\,\mathrm{Dt}[\psi]\,\mathrm{Sin}[\lambda]-1\,\lambda\,\phi\,\mathrm{Cos}[\psi]\,\mathrm{Dt}[\psi]^2\,\mathrm{Sin}[\lambda]-1\,\theta\,\lambda^2\,\phi\,\mathrm{Cos}[\psi]\,\mathrm{Dt}[\psi]^2\,\mathrm{Sin}[\lambda]+1\,\lambda\,\psi\,\mathrm{Cos}[\psi]\,\mathrm{Dt}[\psi]^2\,\mathrm{Sin}[\lambda]+1\,\lambda^3\,\psi\,\mathrm{Cos}[\psi]\,\mathrm{Dt}[\psi]^2\,\mathrm{Sin}[\lambda]\Big)\Big/\Big(1\,\big(\theta^2-2\,\theta\,\lambda+\lambda^2+\phi^2+2\,\theta\,\lambda\,\phi^2+\theta^2\,\lambda^2\,\phi^2-2\,\phi\,\psi-2\,\theta\,\lambda\,\phi\,\psi-2\,\lambda^2\,\phi\,\psi-2\,\theta\,\lambda^3\,\phi\,\psi+\psi^2+2\,\lambda^2\,\psi^2+\lambda^4\,\psi^2\big)\Big)\Big)$$

Inverse[As]

$$\Big\{\Big\{\Big(-1^4\,\mathrm{L}^2\,\phi^2-2\,1^4\,\mathrm{L}^2\,\theta\,\lambda\,\phi^2-1^4\,\mathrm{L}^2\,\theta^2\,\lambda^2\,\phi^2+2\,1^4\,\mathrm{L}^2\,\phi\,\psi+2\,1^4\,\mathrm{L}^2\,\theta\,\lambda\,\phi\,\psi+2\,1^4\,\mathrm{L}^2\,\lambda^2\,\phi\,\psi+2\,1^4\,\mathrm{L}^2\,\theta\,\lambda^3\,\phi\,\psi-1^4\,\mathrm{L}^2\,\psi^2-2\,1^4\,\mathrm{L}^2\,\lambda^2\,\psi^2-1^4\,\mathrm{L}^2\,\lambda^4\,\psi^2\Big)\Big/$$
$$\Big(-1^4\,\mathrm{L}^4\,\mathrm{mh}\,\theta^2-\frac{1}{3}\,1^4\,\mathrm{L}^4\,\mathrm{mp}\,\theta^2+2\,1^4\,\mathrm{L}^4\,\mathrm{mh}\,\theta\,\lambda+\frac{2}{3}\,1^4\,\mathrm{L}^4\,\mathrm{mp}\,\theta\,\lambda-1^4\,\mathrm{L}^4\,\mathrm{mh}\,\lambda^2-\frac{1}{3}\,1^4\,\mathrm{L}^4\,\mathrm{mp}\,\lambda^2-1^4\,\mathrm{L}^4\,\mathrm{mh}\,\phi^2-\frac{1}{3}\,1^4\,\mathrm{L}^4\,\mathrm{mp}\,\phi^2-2\,1^4\,\mathrm{L}^4\,\mathrm{mh}\,\theta\,\lambda\,\phi^2-\frac{2}{3}\,1^4\,\mathrm{L}^4\,\mathrm{mp}\,\theta\,\lambda\,\phi^2-1^4\,\mathrm{L}^4\,\mathrm{mh}\,\theta^2\,\lambda^2\,\phi^2-\frac{1}{3}\,1^4\,\mathrm{L}^4\,\mathrm{mp}\,\theta^2\,\lambda^2\,\phi^2+2\,1^4\,\mathrm{L}^4\,\mathrm{mh}\,\phi\,\psi+\frac{2}{3}\,1^4\,\mathrm{L}^4\,\mathrm{mp}\,\phi\,\psi+2\,1^4\,\mathrm{L}^4\,\mathrm{mh}\,\theta\,\lambda\,\phi\,\psi+\frac{2}{3}\,1^4\,\mathrm{L}^4\,\mathrm{mp}\,\theta\,\lambda\,\phi\,\psi+2\,1^4\,\mathrm{L}^4\,\mathrm{mh}\,\lambda^2\,\phi\,\psi+\frac{2}{3}\,1^4\,\mathrm{L}^4\,\mathrm{mp}\,\lambda^2\,\phi\,\psi+2\,1^4\,\mathrm{L}^4\,\mathrm{mh}\,\theta\,\lambda^3\,\phi\,\psi+\frac{2}{3}\,1^4\,\mathrm{L}^4\,\mathrm{mp}\,\theta\,\lambda^3\,\phi\,\psi-1^4\,\mathrm{L}^4\,\mathrm{mh}\,\psi^2-\frac{1}{3}\,1^4\,\mathrm{L}^4\,\mathrm{mp}\,\psi^2-2\,1^4\,\mathrm{L}^4\,\mathrm{mh}\,\lambda^2\,\psi^2-\frac{2}{3}\,1^4\,\mathrm{L}^4\,\mathrm{mp}\,\lambda^2\,\psi^2-1^4\,\mathrm{L}^4\,\mathrm{mh}\,\lambda^4\,\psi^2-\frac{1}{3}\,1^4\,\mathrm{L}^4\,\mathrm{mp}\,\lambda^4\,\psi^2\Big),$$
$$\Big(1^4\,\mathrm{L}^2\,\theta\,\phi-1^4\,\mathrm{L}^2\,\lambda\,\phi+1^4\,\mathrm{L}^2\,\theta^2\,\lambda\,\phi-1^4\,\mathrm{L}^2\,\theta\,\lambda^2\,\phi-1^4\,\mathrm{L}^2\,\theta\,\psi+1^4\,\mathrm{L}^2\,\lambda\,\psi-1^4\,\mathrm{L}^2\,\theta\,\lambda^2\,\psi+1^4\,\mathrm{L}^2\,\lambda^3\,\psi\Big)\Big/\Big(-1^4\,\mathrm{L}^4\,\mathrm{mh}\,\theta^2-\frac{1}{3}\,1^4\,\mathrm{L}^4\,\mathrm{mp}\,\theta^2+2\,1^4\,\mathrm{L}^4\,\mathrm{mh}\,\theta\,\lambda+\frac{2}{3}\,1^4\,\mathrm{L}^4\,\mathrm{mp}\,\theta\,\lambda-1^4\,\mathrm{L}^4\,\mathrm{mh}\,\lambda^2-\frac{1}{3}\,1^4\,\mathrm{L}^4\,\mathrm{mp}\,\lambda^2-$$
$$1^4\,\mathrm{L}^4\,\mathrm{mh}\,\phi^2-\frac{1}{3}\,1^4\,\mathrm{L}^4\,\mathrm{mp}\,\phi^2-2\,1^4\,\mathrm{L}^4\,\mathrm{mh}\,\theta\,\lambda\,\phi^2-\frac{2}{3}\,1^4\,\mathrm{L}^4\,\mathrm{mp}\,\theta\,\lambda\,\phi^2-1^4\,\mathrm{L}^4\,\mathrm{mh}\,\theta^2\,\lambda^2\,\phi^2-\frac{1}{3}\,1^4\,\mathrm{L}^4\,\mathrm{mp}\,\theta^2\,\lambda^2\,\phi^2+2\,1^4\,\mathrm{L}^4\,\mathrm{mh}\,\phi\,\psi+\frac{2}{3}\,1^4\,\mathrm{L}^4\,\mathrm{mp}\,\phi\,\psi+2\,1^4\,\mathrm{L}^4\,\mathrm{mh}\,\theta\,\lambda\,\phi\,\psi+\frac{2}{3}\,1^4\,\mathrm{L}^4\,\mathrm{mp}\,\theta\,\lambda\,\phi\,\psi+$$
$$2\,1^4\,\mathrm{L}^4\,\mathrm{mh}\,\lambda^2\,\phi\,\psi+\frac{2}{3}\,1^4\,\mathrm{L}^4\,\mathrm{mp}\,\lambda^2\,\phi\,\psi+2\,1^4\,\mathrm{L}^4\,\mathrm{mh}\,\theta\,\lambda^3\,\phi\,\psi+\frac{2}{3}\,1^4\,\mathrm{L}^4\,\mathrm{mp}\,\theta\,\lambda^3\,\phi\,\psi-1^4\,\mathrm{L}^4\,\mathrm{mh}\,\psi^2-\frac{1}{3}\,1^4\,\mathrm{L}^4\,\mathrm{mp}\,\psi^2-2\,1^4\,\mathrm{L}^4\,\mathrm{mh}\,\lambda^2\,\psi^2-\frac{2}{3}\,1^4\,\mathrm{L}^4\,\mathrm{mp}\,\lambda^2\,\psi^2-1^4\,\mathrm{L}^4\,\mathrm{mh}\,\lambda^4\,\psi^2-\frac{1}{3}\,1^4\,\mathrm{L}^4\,\mathrm{mp}\,\lambda^4\,\psi^2\Big),$$
$$\Big(1^3\,\mathrm{L}^3\,\phi^2+1^3\,\mathrm{L}^3\,\theta^2\,\phi^2+1^3\,\mathrm{L}^3\,\theta\,\lambda\,\phi^2+1^3\,\mathrm{L}^3\,\theta^3\,\lambda\,\phi^2-2\,1^3\,\mathrm{L}^3\,\phi\,\psi-1^3\,\mathrm{L}^3\,\theta^2\,\phi\,\psi-2\,1^3\,\mathrm{L}^3\,\theta\,\lambda\,\phi\,\psi-1^3\,\mathrm{L}^3\,\lambda^2\,\phi\,\psi-2\,1^3\,\mathrm{L}^3\,\theta^2\,\lambda^2\,\phi\,\psi+1^3\,\mathrm{L}^3\,\psi^2+1^3\,\mathrm{L}^3\,\theta\,\lambda\,\psi^2+1^3\,\mathrm{L}^3\,\lambda^2\,\psi^2+1^3\,\mathrm{L}^3\,\theta\,\lambda^3\,\psi^2\Big)\Big/$$
$$\Big(-1^4\,\mathrm{L}^4\,\mathrm{mh}\,\theta^2-\frac{1}{3}\,1^4\,\mathrm{L}^4\,\mathrm{mp}\,\theta^2+2\,1^4\,\mathrm{L}^4\,\mathrm{mh}\,\theta\,\lambda+\frac{2}{3}\,1^4\,\mathrm{L}^4\,\mathrm{mp}\,\theta\,\lambda-1^4\,\mathrm{L}^4\,\mathrm{mh}\,\lambda^2-\frac{1}{3}\,1^4\,\mathrm{L}^4\,\mathrm{mp}\,\lambda^2-1^4\,\mathrm{L}^4\,\mathrm{mh}\,\phi^2-\frac{1}{3}\,1^4\,\mathrm{L}^4\,\mathrm{mp}\,\phi^2-2\,1^4\,\mathrm{L}^4\,\mathrm{mh}\,\theta\,\lambda\,\phi^2-\frac{2}{3}\,1^4\,\mathrm{L}^4\,\mathrm{mp}\,\theta\,\lambda\,\phi^2-1^4\,\mathrm{L}^4\,\mathrm{mh}\,\theta^2\,\lambda^2\,\phi^2-\frac{1}{3}\,1^4\,\mathrm{L}^4\,\mathrm{mp}\,\theta^2\,\lambda^2\,\phi^2+2\,1^4\,\mathrm{L}^4\,\mathrm{mh}\,\phi\,\psi+\frac{2}{3}\,1^4\,\mathrm{L}^4\,\mathrm{mp}\,\phi\,\psi+2\,1^4\,\mathrm{L}^4\,\mathrm{mh}\,\theta\,\lambda\,\phi\,\psi+\frac{2}{3}\,1^4\,\mathrm{L}^4\,\mathrm{mp}\,\theta\,\lambda\,\phi\,\psi+2\,1^4\,\mathrm{L}^4\,\mathrm{mh}\,\lambda^2\,\phi\,\psi+\frac{2}{3}\,1^4\,\mathrm{L}^4\,\mathrm{mp}\,\lambda^2\,\phi\,\psi+2\,1^4\,\mathrm{L}^4\,\mathrm{mh}\,\theta\,\lambda^3\,\phi\,\psi+\frac{2}{3}\,1^4\,\mathrm{L}^4\,\mathrm{mp}\,\theta\,\lambda^3\,\phi\,\psi-1^4\,\mathrm{L}^4\,\mathrm{mh}\,\psi^2-\frac{1}{3}\,1^4\,\mathrm{L}^4\,\mathrm{mp}\,\psi^2-2\,1^4\,\mathrm{L}^4\,\mathrm{mh}\,\lambda^2\,\psi^2-\frac{2}{3}\,1^4\,\mathrm{L}^4\,\mathrm{mp}\,\lambda^2\,\psi^2-1^4\,\mathrm{L}^4\,\mathrm{mh}\,\lambda^4\,\psi^2-\frac{1}{3}\,1^4\,\mathrm{L}^4\,\mathrm{mp}\,\lambda^4\,\psi^2\Big),$$

$$\left(-1^3\,L^3\,\theta\,\phi+1^3\,L^3\,\lambda\,\phi-1^3\,L^3\,\theta^2\,\lambda\,\phi+1^3\,L^3\,\theta\,\lambda^2\,\phi+1^3\,L^3\,\theta\,\psi-1^3\,L^3\,\lambda\,\psi+1^3\,L^3\,\theta\,\lambda^2\,\psi-1^3\,L^3\,\lambda^3\,\psi\right)\Big/\left(-1^4\,L^4\,mh\,\theta^2-\frac{1}{3}\,1^4\,L^4\,mp\,\theta^2+2\,1^4\,L^4\,mh\,\theta\,\lambda+\frac{2}{3}\,1^4\,L^4\,mp\,\theta\,\lambda-1^4\,L^4\,mh\,\lambda^2-\frac{1}{3}\,1^4\,L^4\,mp\,\lambda^2-1^4\,L^4\,mh\,\phi^2-\right.$$
$$\frac{1}{3}\,1^4\,L^4\,mp\,\phi^2-2\,1^4\,L^4\,mh\,\theta\,\lambda\,\phi^2-\frac{2}{3}\,1^4\,L^4\,mp\,\theta\,\lambda\,\phi^2-1^4\,L^4\,mh\,\theta^2\,\lambda^2\,\phi^2-\frac{1}{3}\,1^4\,L^4\,mp\,\theta^2\,\lambda^2\,\phi^2+2\,1^4\,L^4\,mh\,\phi\,\psi+\frac{2}{3}\,1^4\,L^4\,mp\,\phi\,\psi+2\,1^4\,L^4\,mh\,\theta\,\lambda\,\phi\,\psi+\frac{2}{3}\,1^4\,L^4\,mp\,\theta\,\lambda\,\phi\,\psi+2\,1^4\,L^4\,mh\,\lambda^2\,\phi\,\psi+\frac{2}{3}\,1^4\,L^4\,mp\,\lambda^2\,\phi\,\psi+$$
$$\left.2\,1^4\,L^4\,mh\,\theta\,\lambda^3\,\phi\,\psi+\frac{2}{3}\,1^4\,L^4\,mp\,\theta\,\lambda^3\,\phi\,\psi-1^4\,L^4\,mh\,\psi^2-\frac{1}{3}\,1^4\,L^4\,mp\,\psi^2-2\,1^4\,L^4\,mh\,\lambda^2\,\psi^2-\frac{2}{3}\,1^4\,L^4\,mp\,\lambda^2\,\psi^2-1^4\,L^4\,mh\,\lambda^4\,\psi^2-\frac{1}{3}\,1^4\,L^4\,mp\,\lambda^4\,\psi^2\right),\ \left(-1^4\,L^3\,mh\,\theta-\frac{1}{3}\,1^4\,L^3\,mp\,\theta+1^4\,L^3\,mh\,\lambda+\frac{1}{3}\,1^4\,L^3\,mp\,\lambda\right)\Big/$$
$$\left(-1^4\,L^4\,mh\,\theta^2-\frac{1}{3}\,1^4\,L^4\,mp\,\theta^2+2\,1^4\,L^4\,mh\,\theta\,\lambda+\frac{2}{3}\,1^4\,L^4\,mp\,\theta\,\lambda-1^4\,L^4\,mh\,\lambda^2-\frac{1}{3}\,1^4\,L^4\,mp\,\lambda^2-1^4\,L^4\,mh\,\phi^2-\frac{1}{3}\,1^4\,L^4\,mp\,\phi^2-2\,1^4\,L^4\,mh\,\theta\,\lambda\,\phi^2-\frac{2}{3}\,1^4\,L^4\,mp\,\theta\,\lambda\,\phi^2-1^4\,L^4\,mh\,\theta^2\,\lambda^2\,\phi^2-\frac{1}{3}\,1^4\,L^4\,mp\,\theta^2\,\lambda^2\,\phi^2+2\,1^4\,L^4\,mh\,\phi\,\psi+\right.$$
$$\left.\frac{2}{3}\,1^4\,L^4\,mp\,\phi\,\psi+2\,1^4\,L^4\,mh\,\theta\,\lambda\,\phi\,\psi+\frac{2}{3}\,1^4\,L^4\,mp\,\theta\,\lambda\,\phi\,\psi+2\,1^4\,L^4\,mh\,\lambda^2\,\phi\,\psi+\frac{2}{3}\,1^4\,L^4\,mp\,\lambda^2\,\phi\,\psi+2\,1^4\,L^4\,mh\,\theta\,\lambda^3\,\phi\,\psi+\frac{2}{3}\,1^4\,L^4\,mp\,\theta\,\lambda^3\,\phi\,\psi-1^4\,L^4\,mh\,\psi^2-\frac{1}{3}\,1^4\,L^4\,mp\,\psi^2-2\,1^4\,L^4\,mh\,\lambda^2\,\psi^2-\frac{2}{3}\,1^4\,L^4\,mp\,\lambda^2\,\psi^2-1^4\,L^4\,mh\,\lambda^4\,\psi^2-\frac{1}{3}\,1^4\,L^4\,mp\,\lambda^4\,\psi^2\right),$$
$$-\left(\left(1\left(\frac{1}{3}\,1\,L^3\,(3\,mh+mp)\,\theta\left(1^2\,\psi+1^2\,\lambda^2\,\psi\right)-\frac{1}{3}\,1\,L^3\,(3\,mh+mp)\,\lambda\left(1^2\,\psi+1^2\,\lambda^2\,\psi\right)\right)\right)\Big/\left(-1^4\,L^4\,mh\,\theta^2-\frac{1}{3}\,1^4\,L^4\,mp\,\theta^2+2\,1^4\,L^4\,mh\,\theta\,\lambda+\frac{2}{3}\,1^4\,L^4\,mp\,\theta\,\lambda-1^4\,L^4\,mh\,\lambda^2-\frac{1}{3}\,1^4\,L^4\,mp\,\lambda^2-1^4\,L^4\,mh\,\phi^2-\frac{1}{3}\,1^4\,L^4\,mp\,\phi^2-\right.$$
$$2\,1^4\,L^4\,mh\,\theta\,\lambda\,\phi^2-\frac{2}{3}\,1^4\,L^4\,mp\,\theta\,\lambda\,\phi^2-1^4\,L^4\,mh\,\theta^2\,\lambda^2\,\phi^2-\frac{1}{3}\,1^4\,L^4\,mp\,\theta^2\,\lambda^2\,\phi^2+2\,1^4\,L^4\,mh\,\phi\,\psi+\frac{2}{3}\,1^4\,L^4\,mp\,\phi\,\psi+2\,1^4\,L^4\,mh\,\theta\,\lambda\,\phi\,\psi+\frac{2}{3}\,1^4\,L^4\,mp\,\theta\,\lambda\,\phi\,\psi+2\,1^4\,L^4\,mh\,\lambda^2\,\phi\,\psi+\frac{2}{3}\,1^4\,L^4\,mp\,\lambda^2\,\phi\,\psi+$$
$$\left.2\,1^4\,L^4\,mh\,\theta\,\lambda^3\,\phi\,\psi+\frac{2}{3}\,1^4\,L^4\,mp\,\theta\,\lambda^3\,\phi\,\psi-1^4\,L^4\,mh\,\psi^2-\frac{1}{3}\,1^4\,L^4\,mp\,\psi^2-2\,1^4\,L^4\,mh\,\lambda^2\,\psi^2-\frac{2}{3}\,1^4\,L^4\,mp\,\lambda^2\,\psi^2-1^4\,L^4\,mh\,\lambda^4\,\psi^2-\frac{1}{3}\,1^4\,L^4\,mp\,\lambda^4\,\psi^2\right)\Big),\ \left(-1^4\,L^3\,mh\,\theta\,\lambda-\frac{1}{3}\,1^4\,L^3\,mp\,\theta\,\lambda+1^4\,L^3\,mh\,\lambda^2+\frac{1}{3}\,1^4\,L^3\,mp\,\lambda^2\right)\Big/$$
$$\left(-1^4\,L^4\,mh\,\theta^2-\frac{1}{3}\,1^4\,L^4\,mp\,\theta^2+2\,1^4\,L^4\,mh\,\theta\,\lambda+\frac{2}{3}\,1^4\,L^4\,mp\,\theta\,\lambda-1^4\,L^4\,mh\,\lambda^2-\frac{1}{3}\,1^4\,L^4\,mp\,\lambda^2-1^4\,L^4\,mh\,\phi^2-\frac{1}{3}\,1^4\,L^4\,mp\,\phi^2-2\,1^4\,L^4\,mh\,\theta\,\lambda\,\phi^2-\frac{2}{3}\,1^4\,L^4\,mp\,\theta\,\lambda\,\phi^2-1^4\,L^4\,mh\,\theta^2\,\lambda^2\,\phi^2-\frac{1}{3}\,1^4\,L^4\,mp\,\theta^2\,\lambda^2\,\phi^2+2\,1^4\,L^4\,mh\,\phi\,\psi+\right.$$
$$\left.\frac{2}{3}\,1^4\,L^4\,mp\,\phi\,\psi+2\,1^4\,L^4\,mh\,\theta\,\lambda\,\phi\,\psi+\frac{2}{3}\,1^4\,L^4\,mp\,\theta\,\lambda\,\phi\,\psi+2\,1^4\,L^4\,mh\,\lambda^2\,\phi\,\psi+\frac{2}{3}\,1^4\,L^4\,mp\,\lambda^2\,\phi\,\psi+2\,1^4\,L^4\,mh\,\theta\,\lambda^3\,\phi\,\psi+\frac{2}{3}\,1^4\,L^4\,mp\,\theta\,\lambda^3\,\phi\,\psi-1^4\,L^4\,mh\,\psi^2-\frac{1}{3}\,1^4\,L^4\,mp\,\psi^2-2\,1^4\,L^4\,mh\,\lambda^2\,\psi^2-\frac{2}{3}\,1^4\,L^4\,mp\,\lambda^2\,\psi^2-1^4\,L^4\,mh\,\lambda^4\,\psi^2-\frac{1}{3}\,1^4\,L^4\,mp\,\lambda^4\,\psi^2\right)\Big\},$$
$$\left\{\left(1^4\,L^2\,\theta\,\phi-1^4\,L^2\,\lambda\,\phi+1^4\,L^2\,\theta^2\,\lambda\,\phi-1^4\,L^2\,\theta\,\lambda^2\,\phi-1^4\,L^2\,\theta\,\psi+1^4\,L^2\,\lambda\,\psi-1^4\,L^2\,\theta\,\lambda^2\,\psi+1^4\,L^2\,\lambda^3\,\psi\right)\Big/\left(-1^4\,L^4\,mh\,\theta^2-\frac{1}{3}\,1^4\,L^4\,mp\,\theta^2+2\,1^4\,L^4\,mh\,\theta\,\lambda+\frac{2}{3}\,1^4\,L^4\,mp\,\theta\,\lambda-1^4\,L^4\,mh\,\lambda^2-\frac{1}{3}\,1^4\,L^4\,mp\,\lambda^2-1^4\,L^4\,mh\,\phi^2-\right.$$
$$\frac{1}{3}\,1^4\,L^4\,mp\,\phi^2-2\,1^4\,L^4\,mh\,\theta\,\lambda\,\phi^2-\frac{2}{3}\,1^4\,L^4\,mp\,\theta\,\lambda\,\phi^2-1^4\,L^4\,mh\,\theta^2\,\lambda^2\,\phi^2-\frac{1}{3}\,1^4\,L^4\,mp\,\theta^2\,\lambda^2\,\phi^2+2\,1^4\,L^4\,mh\,\phi\,\psi+\frac{2}{3}\,1^4\,L^4\,mp\,\phi\,\psi+2\,1^4\,L^4\,mh\,\theta\,\lambda\,\phi\,\psi+\frac{2}{3}\,1^4\,L^4\,mp\,\theta\,\lambda\,\phi\,\psi+2\,1^4\,L^4\,mh\,\lambda^2\,\phi\,\psi+$$
$$\left.\frac{2}{3}\,1^4\,L^4\,mp\,\lambda^2\,\phi\,\psi+2\,1^4\,L^4\,mh\,\theta\,\lambda^3\,\phi\,\psi+\frac{2}{3}\,1^4\,L^4\,mp\,\theta\,\lambda^3\,\phi\,\psi-1^4\,L^4\,mh\,\psi^2-\frac{1}{3}\,1^4\,L^4\,mp\,\psi^2-2\,1^4\,L^4\,mh\,\lambda^2\,\psi^2-\frac{2}{3}\,1^4\,L^4\,mp\,\lambda^2\,\psi^2-1^4\,L^4\,mh\,\lambda^4\,\psi^2-\frac{1}{3}\,1^4\,L^4\,mp\,\lambda^4\,\psi^2\right),\ \left(-1^4\,L^2\,\theta^2+2\,1^4\,L^2\,\theta\,\lambda-1^4\,L^2\,\lambda^2\right)\Big/$$
$$\left(-1^4\,L^4\,mh\,\theta^2-\frac{1}{3}\,1^4\,L^4\,mp\,\theta^2+2\,1^4\,L^4\,mh\,\theta\,\lambda+\frac{2}{3}\,1^4\,L^4\,mp\,\theta\,\lambda-1^4\,L^4\,mh\,\lambda^2-\frac{1}{3}\,1^4\,L^4\,mp\,\lambda^2-1^4\,L^4\,mh\,\phi^2-\frac{1}{3}\,1^4\,L^4\,mp\,\phi^2-2\,1^4\,L^4\,mh\,\theta\,\lambda\,\phi^2-\frac{2}{3}\,1^4\,L^4\,mp\,\theta\,\lambda\,\phi^2-1^4\,L^4\,mh\,\theta^2\,\lambda^2\,\phi^2-\frac{1}{3}\,1^4\,L^4\,mp\,\theta^2\,\lambda^2\,\phi^2+2\,1^4\,L^4\,mh\,\phi\,\psi+\right.$$
$$\left.\frac{2}{3}\,1^4\,L^4\,mp\,\phi\,\psi+2\,1^4\,L^4\,mh\,\theta\,\lambda\,\phi\,\psi+\frac{2}{3}\,1^4\,L^4\,mp\,\theta\,\lambda\,\phi\,\psi+2\,1^4\,L^4\,mh\,\lambda^2\,\phi\,\psi+\frac{2}{3}\,1^4\,L^4\,mp\,\lambda^2\,\phi\,\psi+2\,1^4\,L^4\,mh\,\theta\,\lambda^3\,\phi\,\psi+\frac{2}{3}\,1^4\,L^4\,mp\,\theta\,\lambda^3\,\phi\,\psi-1^4\,L^4\,mh\,\psi^2-\frac{1}{3}\,1^4\,L^4\,mp\,\psi^2-2\,1^4\,L^4\,mh\,\lambda^2\,\psi^2-\frac{2}{3}\,1^4\,L^4\,mp\,\lambda^2\,\psi^2-1^4\,L^4\,mh\,\lambda^4\,\psi^2-\frac{1}{3}\,1^4\,L^4\,mp\,\lambda^4\,\psi^2\right),$$
$$\left(-1^3\,L^3\,\theta\,\phi-1^3\,L^3\,\theta^3\,\phi+1^3\,L^3\,\lambda\,\phi+1^3\,L^3\,\theta^2\,\lambda\,\phi+1^3\,L^3\,\theta\,\psi-1^3\,L^3\,\lambda\,\psi+1^3\,L^3\,\theta^2\,\lambda\,\psi-1^3\,L^3\,\theta\,\lambda^2\,\psi\right)\Big/\left(-1^4\,L^4\,mh\,\theta^2-\frac{1}{3}\,1^4\,L^4\,mp\,\theta^2+2\,1^4\,L^4\,mh\,\theta\,\lambda+\frac{2}{3}\,1^4\,L^4\,mp\,\theta\,\lambda-1^4\,L^4\,mh\,\lambda^2-\frac{1}{3}\,1^4\,L^4\,mp\,\lambda^2-\right.$$
$$1^4\,L^4\,mh\,\phi^2-\frac{1}{3}\,1^4\,L^4\,mp\,\phi^2-2\,1^4\,L^4\,mh\,\theta\,\lambda\,\phi^2-\frac{2}{3}\,1^4\,L^4\,mp\,\theta\,\lambda\,\phi^2-1^4\,L^4\,mh\,\theta^2\,\lambda^2\,\phi^2-\frac{1}{3}\,1^4\,L^4\,mp\,\theta^2\,\lambda^2\,\phi^2+2\,1^4\,L^4\,mh\,\phi\,\psi+\frac{2}{3}\,1^4\,L^4\,mp\,\phi\,\psi+2\,1^4\,L^4\,mh\,\theta\,\lambda\,\phi\,\psi+\frac{2}{3}\,1^4\,L^4\,mp\,\theta\,\lambda\,\phi\,\psi+$$
$$\left.2\,1^4\,L^4\,mh\,\lambda^2\,\phi\,\psi+\frac{2}{3}\,1^4\,L^4\,mp\,\lambda^2\,\phi\,\psi+2\,1^4\,L^4\,mh\,\theta\,\lambda^3\,\phi\,\psi+\frac{2}{3}\,1^4\,L^4\,mp\,\theta\,\lambda^3\,\phi\,\psi-1^4\,L^4\,mh\,\psi^2-\frac{1}{3}\,1^4\,L^4\,mp\,\psi^2-2\,1^4\,L^4\,mh\,\lambda^2\,\psi^2-\frac{2}{3}\,1^4\,L^4\,mp\,\lambda^2\,\psi^2-1^4\,L^4\,mh\,\lambda^4\,\psi^2-\frac{1}{3}\,1^4\,L^4\,mp\,\lambda^4\,\psi^2\right),$$
$$\left(1^3\,L^3\,\theta^2-2\,1^3\,L^3\,\theta\,\lambda+1^3\,L^3\,\lambda^2\right)\Big/\left(-1^4\,L^4\,mh\,\theta^2-\frac{1}{3}\,1^4\,L^4\,mp\,\theta^2+2\,1^4\,L^4\,mh\,\theta\,\lambda+\frac{2}{3}\,1^4\,L^4\,mp\,\theta\,\lambda-1^4\,L^4\,mh\,\lambda^2-\frac{1}{3}\,1^4\,L^4\,mp\,\lambda^2-1^4\,L^4\,mh\,\phi^2-\frac{1}{3}\,1^4\,L^4\,mp\,\phi^2-2\,1^4\,L^4\,mh\,\theta\,\lambda\,\phi^2-\frac{2}{3}\,1^4\,L^4\,mp\,\theta\,\lambda\,\phi^2-\right.$$
$$1^4\,L^4\,mh\,\theta^2\,\lambda^2\,\phi^2-\frac{1}{3}\,1^4\,L^4\,mp\,\theta^2\,\lambda^2\,\phi^2+2\,1^4\,L^4\,mh\,\phi\,\psi+\frac{2}{3}\,1^4\,L^4\,mp\,\phi\,\psi+2\,1^4\,L^4\,mh\,\theta\,\lambda\,\phi\,\psi+\frac{2}{3}\,1^4\,L^4\,mp\,\theta\,\lambda\,\phi\,\psi+2\,1^4\,L^4\,mh\,\lambda^2\,\phi\,\psi+\frac{2}{3}\,1^4\,L^4\,mp\,\lambda^2\,\phi\,\psi+2\,1^4\,L^4\,mh\,\theta\,\lambda^3\,\phi\,\psi+$$
$$\left.\frac{2}{3}\,1^4\,L^4\,mp\,\theta\,\lambda^3\,\phi\,\psi-1^4\,L^4\,mh\,\psi^2-\frac{1}{3}\,1^4\,L^4\,mp\,\psi^2-2\,1^4\,L^4\,mh\,\lambda^2\,\psi^2-\frac{2}{3}\,1^4\,L^4\,mp\,\lambda^2\,\psi^2-1^4\,L^4\,mh\,\lambda^4\,\psi^2-\frac{1}{3}\,1^4\,L^4\,mp\,\lambda^4\,\psi^2\right),\ \left(1^2\,L^2\,(3\,mh+mp)\left(-1^2\,L\,\phi-1^2\,L\,\theta\,\lambda\,\phi+1^2\,L\,\psi+1^2\,L\,\lambda^2\,\psi\right)\right)\Big/$$
$$\left(3\left(-1^4\,L^4\,mh\,\theta^2-\frac{1}{3}\,1^4\,L^4\,mp\,\theta^2+2\,1^4\,L^4\,mh\,\theta\,\lambda+\frac{2}{3}\,1^4\,L^4\,mp\,\theta\,\lambda-1^4\,L^4\,mh\,\lambda^2-\frac{1}{3}\,1^4\,L^4\,mp\,\lambda^2-1^4\,L^4\,mh\,\phi^2-\frac{1}{3}\,1^4\,L^4\,mp\,\phi^2-2\,1^4\,L^4\,mh\,\theta\,\lambda\,\phi^2-\frac{2}{3}\,1^4\,L^4\,mp\,\theta\,\lambda\,\phi^2-1^4\,L^4\,mh\,\theta^2\,\lambda^2\,\phi^2-\frac{1}{3}\,1^4\,L^4\,mp\,\theta^2\,\lambda^2\,\phi^2+2\,1^4\,L^4\,mh\,\phi\,\psi+\frac{2}{3}\,1^4\,L^4\,mp\,\phi\,\psi+\right.\right.$$

$$2\,l^4\,L^4\,mh\,\theta\,\lambda\,\phi\,\psi+\frac{2}{3}\,l^4\,L^4\,mp\,\theta\,\lambda\,\phi\,\psi+2\,l^4\,L^4\,mh\,\lambda^2\,\phi\,\psi+\frac{2}{3}\,l^4\,L^4\,mp\,\lambda^2\,\phi\,\psi+2\,l^4\,L^4\,mh\,\theta\,\lambda^3\,\phi\,\psi+\frac{2}{3}\,l^4\,L^4\,mp\,\theta\,\lambda^3\,\phi\,\psi-l^4\,L^4\,mh\,\psi^2-\frac{1}{3}\,l^4\,L^4\,mp\,\psi^2-2\,l^4\,L^4\,mh\,\lambda^2\,\psi^2-\frac{2}{3}\,l^4\,L^4\,mp\,\lambda^2\,\psi^2-l^4\,L^4\,mh\,\lambda^4\,\psi^2-\frac{1}{3}\,l^4\,L^4\,mp\,\lambda^4\,\psi^2\Big)\Big)\Big\},$$

$$\Big\{\Big(l^3\,L^3\,\phi^2+l^3\,L^3\,\theta^2\,\phi^2+l^3\,L^3\,\theta\,\lambda\,\phi^2+l^3\,L^3\,\theta^3\,\lambda\,\phi^2-2\,l^3\,L^3\,\phi\,\psi-l^3\,L^3\,\theta^2\,\phi\,\psi-2\,l^3\,L^3\,\theta\,\lambda\,\phi\,\psi-l^3\,L^3\,\lambda^2\,\phi\,\psi-2\,l^3\,L^3\,\theta^2\,\lambda^2\,\phi\,\psi+l^3\,L^3\,\psi^2+l^3\,L^3\,\theta\,\lambda\,\psi^2+l^3\,L^3\,\lambda^2\,\psi^2+l^3\,L^3\,\theta\,\lambda^3\,\psi^2\Big)\Big/$$
$$\Big(-l^4\,L^4\,mh\,\theta^2-\frac{1}{3}\,l^4\,L^4\,mp\,\theta^2+2\,l^4\,L^4\,mh\,\theta\,\lambda+\frac{2}{3}\,l^4\,L^4\,mp\,\theta\,\lambda-l^4\,L^4\,mh\,\lambda^2-\frac{1}{3}\,l^4\,L^4\,mp\,\lambda^2-l^4\,L^4\,mh\,\phi^2-\frac{1}{3}\,l^4\,L^4\,mp\,\phi^2-2\,l^4\,L^4\,mh\,\theta\,\lambda\,\phi^2-\frac{2}{3}\,l^4\,L^4\,mp\,\theta\,\lambda\,\phi^2-l^4\,L^4\,mh\,\theta^2\,\lambda^2\,\phi^2-\frac{1}{3}\,l^4\,L^4\,mp\,\theta^2\,\lambda^2\,\phi^2+2\,l^4\,L^4\,mh\,\phi\,\psi+\frac{2}{3}\,l^4\,L^4\,mp\,\phi\,\psi+$$
$$2\,l^4\,L^4\,mh\,\theta\,\lambda\,\phi\,\psi+\frac{2}{3}\,l^4\,L^4\,mp\,\theta\,\lambda\,\phi\,\psi+2\,l^4\,L^4\,mh\,\lambda^2\,\phi\,\psi+\frac{2}{3}\,l^4\,L^4\,mp\,\lambda^2\,\phi\,\psi+2\,l^4\,L^4\,mh\,\theta\,\lambda^3\,\phi\,\psi+\frac{2}{3}\,l^4\,L^4\,mp\,\theta\,\lambda^3\,\phi\,\psi-l^4\,L^4\,mh\,\psi^2-\frac{1}{3}\,l^4\,L^4\,mp\,\psi^2-2\,l^4\,L^4\,mh\,\lambda^2\,\psi^2-\frac{2}{3}\,l^4\,L^4\,mp\,\lambda^2\,\psi^2-l^4\,L^4\,mh\,\lambda^4\,\psi^2-\frac{1}{3}\,l^4\,L^4\,mp\,\lambda^4\,\psi^2\Big),$$

$$\Big(-l^3\,L^3\,\theta\,\phi-l^3\,L^3\,\theta^3\,\phi+l^3\,L^3\,\lambda\,\phi+l^3\,L^3\,\theta^2\,\lambda\,\phi+l^3\,L^3\,\theta\,\psi-l^3\,L^3\,\lambda\,\psi+l^3\,L^3\,\theta^2\,\lambda\,\psi-l^3\,L^3\,\theta\,\lambda^2\,\psi\Big)\Big/\Big(-l^4\,L^4\,mh\,\theta^2-\frac{1}{3}\,l^4\,L^4\,mp\,\theta^2+2\,l^4\,L^4\,mh\,\theta\,\lambda+\frac{2}{3}\,l^4\,L^4\,mp\,\theta\,\lambda-l^4\,L^4\,mh\,\lambda^2-\frac{1}{3}\,l^4\,L^4\,mp\,\lambda^2-$$
$$l^4\,L^4\,mh\,\phi^2-\frac{1}{3}\,l^4\,L^4\,mp\,\phi^2-2\,l^4\,L^4\,mh\,\theta\,\lambda\,\phi^2-\frac{2}{3}\,l^4\,L^4\,mp\,\theta\,\lambda\,\phi^2-l^4\,L^4\,mh\,\theta^2\,\lambda^2\,\phi^2-\frac{1}{3}\,l^4\,L^4\,mp\,\theta^2\,\lambda^2\,\phi^2+2\,l^4\,L^4\,mh\,\phi\,\psi+\frac{2}{3}\,l^4\,L^4\,mp\,\phi\,\psi+2\,l^4\,L^4\,mh\,\theta\,\lambda\,\phi\,\psi+\frac{2}{3}\,l^4\,L^4\,mp\,\theta\,\lambda\,\phi\,\psi+$$
$$2\,l^4\,L^4\,mh\,\lambda^2\,\phi\,\psi+\frac{2}{3}\,l^4\,L^4\,mp\,\lambda^2\,\phi\,\psi+2\,l^4\,L^4\,mh\,\theta\,\lambda^3\,\phi\,\psi+\frac{2}{3}\,l^4\,L^4\,mp\,\theta\,\lambda^3\,\phi\,\psi-l^4\,L^4\,mh\,\psi^2-\frac{1}{3}\,l^4\,L^4\,mp\,\psi^2-2\,l^4\,L^4\,mh\,\lambda^2\,\psi^2-\frac{2}{3}\,l^4\,L^4\,mp\,\lambda^2\,\psi^2-l^4\,L^4\,mh\,\lambda^4\,\psi^2-\frac{1}{3}\,l^4\,L^4\,mp\,\lambda^4\,\psi^2\Big),$$

$$\Big(-l^2\,L^4\,\phi^2-2\,l^2\,L^4\,\theta^2\,\phi^2-l^2\,L^4\,\theta^4\,\phi^2+2\,l^2\,L^4\,\phi\,\psi+2\,l^2\,L^4\,\theta^2\,\phi\,\psi+2\,l^2\,L^4\,\theta\,\lambda\,\phi\,\psi+2\,l^2\,L^4\,\theta^3\,\lambda\,\phi\,\psi-l^2\,L^4\,\psi^2-2\,l^2\,L^4\,\theta\,\lambda\,\psi^2-l^2\,L^4\,\theta^2\,\lambda^2\,\psi^2\Big)\Big/$$
$$\Big(-l^4\,L^4\,mh\,\theta^2-\frac{1}{3}\,l^4\,L^4\,mp\,\theta^2+2\,l^4\,L^4\,mh\,\theta\,\lambda+\frac{2}{3}\,l^4\,L^4\,mp\,\theta\,\lambda-l^4\,L^4\,mh\,\lambda^2-\frac{1}{3}\,l^4\,L^4\,mp\,\lambda^2-l^4\,L^4\,mh\,\phi^2-\frac{1}{3}\,l^4\,L^4\,mp\,\phi^2-2\,l^4\,L^4\,mh\,\theta\,\lambda\,\phi^2-\frac{2}{3}\,l^4\,L^4\,mp\,\theta\,\lambda\,\phi^2-l^4\,L^4\,mh\,\theta^2\,\lambda^2\,\phi^2-\frac{1}{3}\,l^4\,L^4\,mp\,\theta^2\,\lambda^2\,\phi^2+2\,l^4\,L^4\,mh\,\phi\,\psi+\frac{2}{3}\,l^4\,L^4\,mp\,\phi\,\psi+$$
$$2\,l^4\,L^4\,mh\,\theta\,\lambda\,\phi\,\psi+\frac{2}{3}\,l^4\,L^4\,mp\,\theta\,\lambda\,\phi\,\psi+2\,l^4\,L^4\,mh\,\lambda^2\,\phi\,\psi+\frac{2}{3}\,l^4\,L^4\,mp\,\lambda^2\,\phi\,\psi+2\,l^4\,L^4\,mh\,\theta\,\lambda^3\,\phi\,\psi+\frac{2}{3}\,l^4\,L^4\,mp\,\theta\,\lambda^3\,\phi\,\psi-l^4\,L^4\,mh\,\psi^2-\frac{1}{3}\,l^4\,L^4\,mp\,\psi^2-2\,l^4\,L^4\,mh\,\lambda^2\,\psi^2-\frac{2}{3}\,l^4\,L^4\,mp\,\lambda^2\,\psi^2-l^4\,L^4\,mh\,\lambda^4\,\psi^2-\frac{1}{3}\,l^4\,L^4\,mp\,\lambda^4\,\psi^2\Big),$$

$$\Big(l^2\,L^4\,\theta\,\phi+l^2\,L^4\,\theta^3\,\phi-l^2\,L^4\,\lambda\,\phi-l^2\,L^4\,\theta^2\,\lambda\,\phi-l^2\,L^4\,\theta\,\psi+l^2\,L^4\,\lambda\,\psi-l^2\,L^4\,\theta^2\,\lambda\,\psi+l^2\,L^4\,\theta\,\lambda^2\,\psi\Big)\Big/\Big(-l^4\,L^4\,mh\,\theta^2-\frac{1}{3}\,l^4\,L^4\,mp\,\theta^2+2\,l^4\,L^4\,mh\,\theta\,\lambda+\frac{2}{3}\,l^4\,L^4\,mp\,\theta\,\lambda-l^4\,L^4\,mh\,\lambda^2-\frac{1}{3}\,l^4\,L^4\,mp\,\lambda^2-$$
$$l^4\,L^4\,mh\,\phi^2-\frac{1}{3}\,l^4\,L^4\,mp\,\phi^2-2\,l^4\,L^4\,mh\,\theta\,\lambda\,\phi^2-\frac{2}{3}\,l^4\,L^4\,mp\,\theta\,\lambda\,\phi^2-l^4\,L^4\,mh\,\theta^2\,\lambda^2\,\phi^2-\frac{1}{3}\,l^4\,L^4\,mp\,\theta^2\,\lambda^2\,\phi^2+2\,l^4\,L^4\,mh\,\phi\,\psi+\frac{2}{3}\,l^4\,L^4\,mp\,\phi\,\psi+2\,l^4\,L^4\,mh\,\theta\,\lambda\,\phi\,\psi+\frac{2}{3}\,l^4\,L^4\,mp\,\theta\,\lambda\,\phi\,\psi+$$
$$2\,l^4\,L^4\,mh\,\lambda^2\,\phi\,\psi+\frac{2}{3}\,l^4\,L^4\,mp\,\lambda^2\,\phi\,\psi+2\,l^4\,L^4\,mh\,\theta\,\lambda^3\,\phi\,\psi+\frac{2}{3}\,l^4\,L^4\,mp\,\theta\,\lambda^3\,\phi\,\psi-l^4\,L^4\,mh\,\psi^2-\frac{1}{3}\,l^4\,L^4\,mp\,\psi^2-2\,l^4\,L^4\,mh\,\lambda^2\,\psi^2-\frac{2}{3}\,l^4\,L^4\,mp\,\lambda^2\,\psi^2-l^4\,L^4\,mh\,\lambda^4\,\psi^2-\frac{1}{3}\,l^4\,L^4\,mp\,\lambda^4\,\psi^2\Big),$$

$$\Big(-\frac{1}{3}\,l\,L^3\,(3\,mh+mp)\,\lambda\,\psi\,\big(-l^2\,L\,\phi-l^2\,L\,\theta\,\lambda\,\phi+l^2\,L\,\psi+l^2\,L\,\lambda^2\,\psi\big)-l\,\Big(\frac{1}{3}\,L^3\,(3\,mh+mp)\,\big(-l^2\,L\,\theta+l^2\,L\,\lambda\big)-\frac{1}{3}\,L^3\,(3\,mh+mp)\,\theta\,\phi\,\big(-l^2\,L\,\phi-l^2\,L\,\theta\,\lambda\,\phi+l^2\,L\,\psi+l^2\,L\,\lambda^2\,\psi\big)\Big)\Big)\Big/$$
$$\Big(-l^4\,L^4\,mh\,\theta^2-\frac{1}{3}\,l^4\,L^4\,mp\,\theta^2+2\,l^4\,L^4\,mh\,\theta\,\lambda+\frac{2}{3}\,l^4\,L^4\,mp\,\theta\,\lambda-l^4\,L^4\,mh\,\lambda^2-\frac{1}{3}\,l^4\,L^4\,mp\,\lambda^2-l^4\,L^4\,mh\,\phi^2-\frac{1}{3}\,l^4\,L^4\,mp\,\phi^2-2\,l^4\,L^4\,mh\,\theta\,\lambda\,\phi^2-\frac{2}{3}\,l^4\,L^4\,mp\,\theta\,\lambda\,\phi^2-l^4\,L^4\,mh\,\theta^2\,\lambda^2\,\phi^2-\frac{1}{3}\,l^4\,L^4\,mp\,\theta^2\,\lambda^2\,\phi^2+2\,l^4\,L^4\,mh\,\phi\,\psi+\frac{2}{3}\,l^4\,L^4\,mp\,\phi\,\psi+$$
$$2\,l^4\,L^4\,mh\,\theta\,\lambda\,\phi\,\psi+\frac{2}{3}\,l^4\,L^4\,mp\,\theta\,\lambda\,\phi\,\psi+2\,l^4\,L^4\,mh\,\lambda^2\,\phi\,\psi+\frac{2}{3}\,l^4\,L^4\,mp\,\lambda^2\,\phi\,\psi+2\,l^4\,L^4\,mh\,\theta\,\lambda^3\,\phi\,\psi+\frac{2}{3}\,l^4\,L^4\,mp\,\theta\,\lambda^3\,\phi\,\psi-l^4\,L^4\,mh\,\psi^2-\frac{1}{3}\,l^4\,L^4\,mp\,\psi^2-2\,l^4\,L^4\,mh\,\lambda^2\,\psi^2-\frac{2}{3}\,l^4\,L^4\,mp\,\lambda^2\,\psi^2-l^4\,L^4\,mh\,\lambda^4\,\psi^2-\frac{1}{3}\,l^4\,L^4\,mp\,\lambda^4\,\psi^2\Big),$$

$$\Big(-L\,\Big(\frac{1}{3}\,l^2\,L^2\,(3\,mh+mp)\,\psi\,\big(-1\,L\,\theta\,\phi\,\psi+1\,L\,\lambda\,\phi\,\psi\big)+\frac{1}{3}\,l^2\,L^2\,(3\,mh+mp)\,\lambda^2\,\psi\,\big(-1\,L\,\theta\,\phi\,\psi+1\,L\,\lambda\,\phi\,\psi\big)\Big)-$$
$$1\,\Big(-1\,\Big(\frac{1}{3}\,L^3\,(3\,mh+mp)\,\theta\,(1\,L\,\psi+1\,L\,\theta\,\lambda\,\psi)+\frac{1}{3}\,L^3\,(3\,mh+mp)\,\phi\,\big(-1\,L\,\theta\,\phi\,\psi+1\,L\,\lambda\,\phi\,\psi\big)\Big)-1\,\lambda\,\Big(-\frac{1}{3}\,L^3\,(3\,mh+mp)\,(1\,L\,\psi+1\,L\,\theta\,\lambda\,\psi)+\frac{1}{3}\,L^3\,(3\,mh+mp)\,\theta\,\phi\,\big(-1\,L\,\theta\,\phi\,\psi+1\,L\,\lambda\,\phi\,\psi\big)\Big)\Big)\Big)\Big/$$
$$\Big(-l^4\,L^4\,mh\,\theta^2-\frac{1}{3}\,l^4\,L^4\,mp\,\theta^2+2\,l^4\,L^4\,mh\,\theta\,\lambda+\frac{2}{3}\,l^4\,L^4\,mp\,\theta\,\lambda-l^4\,L^4\,mh\,\lambda^2-\frac{1}{3}\,l^4\,L^4\,mp\,\lambda^2-l^4\,L^4\,mh\,\phi^2-\frac{1}{3}\,l^4\,L^4\,mp\,\phi^2-2\,l^4\,L^4\,mh\,\theta\,\lambda\,\phi^2-\frac{2}{3}\,l^4\,L^4\,mp\,\theta\,\lambda\,\phi^2-l^4\,L^4\,mh\,\theta^2\,\lambda^2\,\phi^2-\frac{1}{3}\,l^4\,L^4\,mp\,\theta^2\,\lambda^2\,\phi^2+2\,l^4\,L^4\,mh\,\phi\,\psi+$$
$$\frac{2}{3}\,l^4\,L^4\,mp\,\phi\,\psi+2\,l^4\,L^4\,mh\,\theta\,\lambda\,\phi\,\psi+\frac{2}{3}\,l^4\,L^4\,mp\,\theta\,\lambda\,\phi\,\psi+2\,l^4\,L^4\,mh\,\lambda^2\,\phi\,\psi+\frac{2}{3}\,l^4\,L^4\,mp\,\lambda^2\,\phi\,\psi+2\,l^4\,L^4\,mh\,\theta\,\lambda^3\,\phi\,\psi+\frac{2}{3}\,l^4\,L^4\,mp\,\theta\,\lambda^3\,\phi\,\psi-l^4\,L^4\,mh\,\psi^2-\frac{1}{3}\,l^4\,L^4\,mp\,\psi^2-2\,l^4\,L^4\,mh\,\lambda^2\,\psi^2-\frac{2}{3}\,l^4\,L^4\,mp\,\lambda^2\,\psi^2-l^4\,L^4\,mh\,\lambda^4\,\psi^2-\frac{1}{3}\,l^4\,L^4\,mp\,\lambda^4\,\psi^2\Big),$$

$$\Big(\frac{1}{3}\,l\,L^3\,(3\,mh+mp)\,\psi\,\big(-l^2\,L\,\phi-l^2\,L\,\theta\,\lambda\,\phi+l^2\,L\,\psi+l^2\,L\,\lambda^2\,\psi\big)+1\,\Big(-\frac{1}{3}\,L^3\,(3\,mh+mp)\,\theta\,\big(-l^2\,L\,\theta+l^2\,L\,\lambda\big)-\frac{1}{3}\,L^3\,(3\,mh+mp)\,\phi\,\big(-l^2\,L\,\phi-l^2\,L\,\theta\,\lambda\,\phi+l^2\,L\,\psi+l^2\,L\,\lambda^2\,\psi\big)\Big)\Big)\Big/$$
$$\Big(-l^4\,L^4\,mh\,\theta^2-\frac{1}{3}\,l^4\,L^4\,mp\,\theta^2+2\,l^4\,L^4\,mh\,\theta\,\lambda+\frac{2}{3}\,l^4\,L^4\,mp\,\theta\,\lambda-l^4\,L^4\,mh\,\lambda^2-\frac{1}{3}\,l^4\,L^4\,mp\,\lambda^2-l^4\,L^4\,mh\,\phi^2-\frac{1}{3}\,l^4\,L^4\,mp\,\phi^2-2\,l^4\,L^4\,mh\,\theta\,\lambda\,\phi^2-\frac{2}{3}\,l^4\,L^4\,mp\,\theta\,\lambda\,\phi^2-l^4\,L^4\,mh\,\theta^2\,\lambda^2\,\phi^2-\frac{1}{3}\,l^4\,L^4\,mp\,\theta^2\,\lambda^2\,\phi^2+2\,l^4\,L^4\,mh\,\phi\,\psi+\frac{2}{3}\,l^4\,L^4\,mp\,\phi\,\psi+$$

$$2\,l^4\,L^4\,mh\,\theta\,\lambda\,\phi\,\psi+\frac{2}{3}\,l^4\,L^4\,mp\,\theta\,\lambda\,\phi\,\psi+2\,l^4\,L^4\,mh\,\lambda^2\,\phi\,\psi+\frac{2}{3}\,l^4\,L^4\,mp\,\lambda^2\,\phi\,\psi+2\,l^4\,L^4\,mh\,\theta\,\lambda^3\,\phi\,\psi+\frac{2}{3}\,l^4\,L^4\,mp\,\theta\,\lambda^3\,\phi\,\psi-l^4\,L^4\,mh\,\psi^2-\frac{1}{3}\,l^4\,L^4\,mp\,\psi^2-2\,l^4\,L^4\,mh\,\lambda^2\,\psi^2-\frac{2}{3}\,l^4\,L^4\,mp\,\lambda^2\,\psi^2-l^4\,L^4\,mh\,\lambda^4\,\psi^2-\frac{1}{3}\,l^4\,L^4\,mp\,\lambda^4\,\psi^2\Big)\Big\},$$

$$\Big\{\Big(-l^3\,L^3\,\theta\,\phi+l^3\,L^3\,\lambda\,\phi-l^3\,L^3\,\theta^2\,\lambda\,\phi+l^3\,L^3\,\theta\,\lambda^2\,\phi+l^3\,L^3\,\theta\,\psi-l^3\,L^3\,\lambda\,\psi+l^3\,L^3\,\theta\,\lambda^2\,\psi-l^3\,L^3\,\lambda^3\,\psi\Big)\Big/\Big(-l^4\,L^4\,mh\,\theta^2-\frac{1}{3}\,l^4\,L^4\,mp\,\theta^2+2\,l^4\,L^4\,mh\,\theta\,\lambda+\frac{2}{3}\,l^4\,L^4\,mp\,\theta\,\lambda-l^4\,L^4\,mh\,\lambda^2-\frac{1}{3}\,l^4\,L^4\,mp\,\lambda^2-$$
$$l^4\,L^4\,mh\,\phi^2-\frac{1}{3}\,l^4\,L^4\,mp\,\phi^2-2\,l^4\,L^4\,mh\,\theta\,\lambda\,\phi^2-\frac{2}{3}\,l^4\,L^4\,mp\,\theta\,\lambda\,\phi^2-l^4\,L^4\,mh\,\theta^2\,\lambda^2\,\phi^2-\frac{1}{3}\,l^4\,L^4\,mp\,\theta^2\,\lambda^2\,\phi^2+2\,l^4\,L^4\,mh\,\phi\,\psi+\frac{2}{3}\,l^4\,L^4\,mp\,\phi\,\psi+2\,l^4\,L^4\,mh\,\theta\,\lambda\,\phi\,\psi+\frac{2}{3}\,l^4\,L^4\,mp\,\theta\,\lambda\,\phi\,\psi+$$
$$2\,l^4\,L^4\,mh\,\lambda^2\,\phi\,\psi+\frac{2}{3}\,l^4\,L^4\,mp\,\lambda^2\,\phi\,\psi+2\,l^4\,L^4\,mh\,\theta\,\lambda^3\,\phi\,\psi+\frac{2}{3}\,l^4\,L^4\,mp\,\theta\,\lambda^3\,\phi\,\psi-l^4\,L^4\,mh\,\psi^2-\frac{1}{3}\,l^4\,L^4\,mp\,\psi^2-2\,l^4\,L^4\,mh\,\lambda^2\,\psi^2-\frac{2}{3}\,l^4\,L^4\,mp\,\lambda^2\,\psi^2-l^4\,L^4\,mh\,\lambda^4\,\psi^2-\frac{1}{3}\,l^4\,L^4\,mp\,\lambda^4\,\psi^2\Big),$$

$$\Big(l^3\,L^3\,\theta^2-2\,l^3\,L^3\,\theta\,\lambda+l^3\,L^3\,\lambda^2\Big)\Big/\Big(-l^4\,L^4\,mh\,\theta^2-\frac{1}{3}\,l^4\,L^4\,mp\,\theta^2+2\,l^4\,L^4\,mh\,\theta\,\lambda+\frac{2}{3}\,l^4\,L^4\,mp\,\theta\,\lambda-l^4\,L^4\,mh\,\lambda^2-\frac{1}{3}\,l^4\,L^4\,mp\,\lambda^2-l^4\,L^4\,mh\,\phi^2-\frac{1}{3}\,l^4\,L^4\,mp\,\phi^2-2\,l^4\,L^4\,mh\,\theta\,\lambda\,\phi^2-\frac{2}{3}\,l^4\,L^4\,mp\,\theta\,\lambda\,\phi^2-$$
$$l^4\,L^4\,mh\,\theta^2\,\lambda^2\,\phi^2-\frac{1}{3}\,l^4\,L^4\,mp\,\theta^2\,\lambda^2\,\phi^2+2\,l^4\,L^4\,mh\,\phi\,\psi+\frac{2}{3}\,l^4\,L^4\,mp\,\phi\,\psi+2\,l^4\,L^4\,mh\,\theta\,\lambda\,\phi\,\psi+\frac{2}{3}\,l^4\,L^4\,mp\,\theta\,\lambda\,\phi\,\psi+2\,l^4\,L^4\,mh\,\lambda^2\,\phi\,\psi+\frac{2}{3}\,l^4\,L^4\,mp\,\lambda^2\,\phi\,\psi+2\,l^4\,L^4\,mh\,\theta\,\lambda^3\,\phi\,\psi+\frac{2}{3}\,l^4\,L^4\,mp\,\theta\,\lambda^3\,\phi\,\psi-$$
$$l^4\,L^4\,mh\,\psi^2-\frac{1}{3}\,l^4\,L^4\,mp\,\psi^2-2\,l^4\,L^4\,mh\,\lambda^2\,\psi^2-\frac{2}{3}\,l^4\,L^4\,mp\,\lambda^2\,\psi^2-l^4\,L^4\,mh\,\lambda^4\,\psi^2-\frac{1}{3}\,l^4\,L^4\,mp\,\lambda^4\,\psi^2\Big),\ \Big(l^2\,L^4\,\theta\,\phi+l^2\,L^4\,\theta^3\,\phi-l^2\,L^4\,\lambda\,\phi-l^2\,L^4\,\theta^2\,\lambda\,\phi-l^2\,L^4\,\theta\,\psi+l^2\,L^4\,\lambda\,\psi-l^2\,L^4\,\theta^2\,\lambda\,\psi+l^2\,L^4\,\theta\,\lambda^2\,\psi\Big)\Big/$$
$$\Big(-l^4\,L^4\,mh\,\theta^2-\frac{1}{3}\,l^4\,L^4\,mp\,\theta^2+2\,l^4\,L^4\,mh\,\theta\,\lambda+\frac{2}{3}\,l^4\,L^4\,mp\,\theta\,\lambda-l^4\,L^4\,mh\,\lambda^2-\frac{1}{3}\,l^4\,L^4\,mp\,\lambda^2-l^4\,L^4\,mh\,\phi^2-\frac{1}{3}\,l^4\,L^4\,mp\,\phi^2-2\,l^4\,L^4\,mh\,\theta\,\lambda\,\phi^2-\frac{2}{3}\,l^4\,L^4\,mp\,\theta\,\lambda\,\phi^2-l^4\,L^4\,mh\,\theta^2\,\lambda^2\,\phi^2-\frac{1}{3}\,l^4\,L^4\,mp\,\theta^2\,\lambda^2\,\phi^2+2\,l^4\,L^4\,mh\,\phi\,\psi+$$
$$\frac{2}{3}\,l^4\,L^4\,mp\,\phi\,\psi+2\,l^4\,L^4\,mh\,\theta\,\lambda\,\phi\,\psi+\frac{2}{3}\,l^4\,L^4\,mp\,\theta\,\lambda\,\phi\,\psi+2\,l^4\,L^4\,mh\,\lambda^2\,\phi\,\psi+\frac{2}{3}\,l^4\,L^4\,mp\,\lambda^2\,\phi\,\psi+2\,l^4\,L^4\,mh\,\theta\,\lambda^3\,\phi\,\psi+\frac{2}{3}\,l^4\,L^4\,mp\,\theta\,\lambda^3\,\phi\,\psi-l^4\,L^4\,mh\,\psi^2-\frac{1}{3}\,l^4\,L^4\,mp\,\psi^2-2\,l^4\,L^4\,mh\,\lambda^2\,\psi^2-\frac{2}{3}\,l^4\,L^4\,mp\,\lambda^2\,\psi^2-l^4\,L^4\,mh\,\lambda^4\,\psi^2-\frac{1}{3}\,l^4\,L^4\,mp\,\lambda^4\,\psi^2\Big),$$

$$\Big(-l^2\,L^4\,\theta^2+2\,l^2\,L^4\,\theta\,\lambda-l^2\,L^4\,\lambda^2\Big)\Big/\Big(-l^4\,L^4\,mh\,\theta^2-\frac{1}{3}\,l^4\,L^4\,mp\,\theta^2+2\,l^4\,L^4\,mh\,\theta\,\lambda+\frac{2}{3}\,l^4\,L^4\,mp\,\theta\,\lambda-l^4\,L^4\,mh\,\lambda^2-\frac{1}{3}\,l^4\,L^4\,mp\,\lambda^2-l^4\,L^4\,mh\,\phi^2-\frac{1}{3}\,l^4\,L^4\,mp\,\phi^2-2\,l^4\,L^4\,mh\,\theta\,\lambda\,\phi^2-\frac{2}{3}\,l^4\,L^4\,mp\,\theta\,\lambda\,\phi^2-$$
$$l^4\,L^4\,mh\,\theta^2\,\lambda^2\,\phi^2-\frac{1}{3}\,l^4\,L^4\,mp\,\theta^2\,\lambda^2\,\phi^2+2\,l^4\,L^4\,mh\,\phi\,\psi+\frac{2}{3}\,l^4\,L^4\,mp\,\phi\,\psi+2\,l^4\,L^4\,mh\,\theta\,\lambda\,\phi\,\psi+\frac{2}{3}\,l^4\,L^4\,mp\,\theta\,\lambda\,\phi\,\psi+2\,l^4\,L^4\,mh\,\lambda^2\,\phi\,\psi+\frac{2}{3}\,l^4\,L^4\,mp\,\lambda^2\,\phi\,\psi+2\,l^4\,L^4\,mh\,\theta\,\lambda^3\,\phi\,\psi+$$
$$\frac{2}{3}\,l^4\,L^4\,mp\,\theta\,\lambda^3\,\phi\,\psi-l^4\,L^4\,mh\,\psi^2-\frac{1}{3}\,l^4\,L^4\,mp\,\psi^2-2\,l^4\,L^4\,mh\,\lambda^2\,\psi^2-\frac{2}{3}\,l^4\,L^4\,mp\,\lambda^2\,\psi^2-l^4\,L^4\,mh\,\lambda^4\,\psi^2-\frac{1}{3}\,l^4\,L^4\,mp\,\lambda^4\,\psi^2\Big),\ -\Big(\big(1\,L^3\ (3\,mh+mp)\ \big(-l^2\,L\,\phi-l^2\,L\,\theta\,\lambda\,\phi+l^2\,L\,\psi+l^2\,L\,\lambda^2\,\psi\big)\big)\Big/$$
$$\Big(3\Big(-l^4\,L^4\,mh\,\theta^2-\frac{1}{3}\,l^4\,L^4\,mp\,\theta^2+2\,l^4\,L^4\,mh\,\theta\,\lambda+\frac{2}{3}\,l^4\,L^4\,mp\,\theta\,\lambda-l^4\,L^4\,mh\,\lambda^2-\frac{1}{3}\,l^4\,L^4\,mp\,\lambda^2-l^4\,L^4\,mh\,\phi^2-\frac{1}{3}\,l^4\,L^4\,mp\,\phi^2-2\,l^4\,L^4\,mh\,\theta\,\lambda\,\phi^2-\frac{2}{3}\,l^4\,L^4\,mp\,\theta\,\lambda\,\phi^2-l^4\,L^4\,mh\,\theta^2\,\lambda^2\,\phi^2-\frac{1}{3}\,l^4\,L^4\,mp\,\theta^2\,\lambda^2\,\phi^2+2\,l^4\,L^4\,mh\,\phi\,\psi+\frac{2}{3}\,l^4\,L^4\,mp\,\phi\,\psi+$$
$$2\,l^4\,L^4\,mh\,\theta\,\lambda\,\phi\,\psi+\frac{2}{3}\,l^4\,L^4\,mp\,\theta\,\lambda\,\phi\,\psi+2\,l^4\,L^4\,mh\,\lambda^2\,\phi\,\psi+\frac{2}{3}\,l^4\,L^4\,mp\,\lambda^2\,\phi\,\psi+2\,l^4\,L^4\,mh\,\theta\,\lambda^3\,\phi\,\psi+\frac{2}{3}\,l^4\,L^4\,mp\,\theta\,\lambda^3\,\phi\,\psi-l^4\,L^4\,mh\,\psi^2-\frac{1}{3}\,l^4\,L^4\,mp\,\psi^2-2\,l^4\,L^4\,mh\,\lambda^2\,\psi^2-\frac{2}{3}\,l^4\,L^4\,mp\,\lambda^2\,\psi^2-l^4\,L^4\,mh\,\lambda^4\,\psi^2-\frac{1}{3}\,l^4\,L^4\,mp\,\lambda^4\,\psi^2\Big)\Big)\Big),$$

$$\Big(1\Big(-1\Big(\frac{1}{3}\,L^3\ (3\,mh+mp)\ \theta\ (-1\,L\,\theta+1\,L\,\lambda)+\frac{1}{3}\,L^3\ (3\,mh+mp)\ \phi\ (-1\,L\,\phi-1\,L\,\theta\,\lambda\,\phi)\Big)-1\,\lambda\Big(-\frac{1}{3}\,L^3\ (3\,mh+mp)\ (-1\,L\,\theta+1\,L\,\lambda)+\frac{1}{3}\,L^3\ (3\,mh+mp)\ \theta\,\phi\ (-1\,L\,\phi-1\,L\,\theta\,\lambda\,\phi)\Big)\Big)+$$
$$L\Big(\frac{1}{3}\,l^2\,L^2\ (3\,mh+mp)\ (-1\,L\,\phi-1\,L\,\theta\,\lambda\,\phi)\ \psi+\frac{1}{3}\,l^2\,L^2\ (3\,mh+mp)\ \lambda^2\ (-1\,L\,\phi-1\,L\,\theta\,\lambda\,\phi)\ \psi\Big)\Big)\Big/\Big(-l^4\,L^4\,mh\,\theta^2-\frac{1}{3}\,l^4\,L^4\,mp\,\theta^2+2\,l^4\,L^4\,mh\,\theta\,\lambda+\frac{2}{3}\,l^4\,L^4\,mp\,\theta\,\lambda-l^4\,L^4\,mh\,\lambda^2-\frac{1}{3}\,l^4\,L^4\,mp\,\lambda^2-l^4\,L^4\,mh\,\phi^2-$$
$$\frac{1}{3}\,l^4\,L^4\,mp\,\phi^2-2\,l^4\,L^4\,mh\,\theta\,\lambda\,\phi^2-\frac{2}{3}\,l^4\,L^4\,mp\,\theta\,\lambda\,\phi^2-l^4\,L^4\,mh\,\theta^2\,\lambda^2\,\phi^2-\frac{1}{3}\,l^4\,L^4\,mp\,\theta^2\,\lambda^2\,\phi^2+2\,l^4\,L^4\,mh\,\phi\,\psi+\frac{2}{3}\,l^4\,L^4\,mp\,\phi\,\psi+2\,l^4\,L^4\,mh\,\theta\,\lambda\,\phi\,\psi+\frac{2}{3}\,l^4\,L^4\,mp\,\theta\,\lambda\,\phi\,\psi+2\,l^4\,L^4\,mh\,\lambda^2\,\phi\,\psi+\frac{2}{3}\,l^4\,L^4\,mp\,\lambda^2\,\phi\,\psi+$$
$$2\,l^4\,L^4\,mh\,\theta\,\lambda^3\,\phi\,\psi+\frac{2}{3}\,l^4\,L^4\,mp\,\theta\,\lambda^3\,\phi\,\psi-l^4\,L^4\,mh\,\psi^2-\frac{1}{3}\,l^4\,L^4\,mp\,\psi^2-2\,l^4\,L^4\,mh\,\lambda^2\,\psi^2-\frac{2}{3}\,l^4\,L^4\,mp\,\lambda^2\,\psi^2-l^4\,L^4\,mh\,\lambda^4\,\psi^2-\frac{1}{3}\,l^4\,L^4\,mp\,\lambda^4\,\psi^2\Big),\ -\Big(\big(1\,L^3\ (3\,mh+mp)\ \lambda\ \big(-l^2\,L\,\phi-l^2\,L\,\theta\,\lambda\,\phi+l^2\,L\,\psi+l^2\,L\,\lambda^2\,\psi\big)\big)\Big/$$
$$\Big(3\Big(-l^4\,L^4\,mh\,\theta^2-\frac{1}{3}\,l^4\,L^4\,mp\,\theta^2+2\,l^4\,L^4\,mh\,\theta\,\lambda+\frac{2}{3}\,l^4\,L^4\,mp\,\theta\,\lambda-l^4\,L^4\,mh\,\lambda^2-\frac{1}{3}\,l^4\,L^4\,mp\,\lambda^2-l^4\,L^4\,mh\,\phi^2-\frac{1}{3}\,l^4\,L^4\,mp\,\phi^2-2\,l^4\,L^4\,mh\,\theta\,\lambda\,\phi^2-\frac{2}{3}\,l^4\,L^4\,mp\,\theta\,\lambda\,\phi^2-l^4\,L^4\,mh\,\theta^2\,\lambda^2\,\phi^2-\frac{1}{3}\,l^4\,L^4\,mp\,\theta^2\,\lambda^2\,\phi^2+2\,l^4\,L^4\,mh\,\phi\,\psi+\frac{2}{3}\,l^4\,L^4\,mp\,\phi\,\psi+$$
$$2\,l^4\,L^4\,mh\,\theta\,\lambda\,\phi\,\psi+\frac{2}{3}\,l^4\,L^4\,mp\,\theta\,\lambda\,\phi\,\psi+2\,l^4\,L^4\,mh\,\lambda^2\,\phi\,\psi+\frac{2}{3}\,l^4\,L^4\,mp\,\lambda^2\,\phi\,\psi+2\,l^4\,L^4\,mh\,\theta\,\lambda^3\,\phi\,\psi+\frac{2}{3}\,l^4\,L^4\,mp\,\theta\,\lambda^3\,\phi\,\psi-l^4\,L^4\,mh\,\psi^2-\frac{1}{3}\,l^4\,L^4\,mp\,\psi^2-2\,l^4\,L^4\,mh\,\lambda^2\,\psi^2-\frac{2}{3}\,l^4\,L^4\,mp\,\lambda^2\,\psi^2-l^4\,L^4\,mh\,\lambda^4\,\psi^2-\frac{1}{3}\,l^4\,L^4\,mp\,\lambda^4\,\psi^2\Big)\Big)\Big)\Big\},$$

$$\Big\{\Big(-l^4\,L^3\,mh\,\theta-\frac{1}{3}\,l^4\,L^3\,mp\,\theta+l^4\,L^3\,mh\,\lambda+\frac{1}{3}\,l^4\,L^3\,mp\,\lambda\Big)\Big/\Big(-l^4\,L^4\,mh\,\theta^2-\frac{1}{3}\,l^4\,L^4\,mp\,\theta^2+2\,l^4\,L^4\,mh\,\theta\,\lambda+\frac{2}{3}\,l^4\,L^4\,mp\,\theta\,\lambda-l^4\,L^4\,mh\,\lambda^2-\frac{1}{3}\,l^4\,L^4\,mp\,\lambda^2-l^4\,L^4\,mh\,\phi^2-\frac{1}{3}\,l^4\,L^4\,mp\,\phi^2-2\,l^4\,L^4\,mh\,\theta\,\lambda\,\phi^2-$$
$$\frac{2}{3}\,l^4\,L^4\,mp\,\theta\,\lambda\,\phi^2-l^4\,L^4\,mh\,\theta^2\,\lambda^2\,\phi^2-\frac{1}{3}\,l^4\,L^4\,mp\,\theta^2\,\lambda^2\,\phi^2+2\,l^4\,L^4\,mh\,\phi\,\psi+\frac{2}{3}\,l^4\,L^4\,mp\,\phi\,\psi+2\,l^4\,L^4\,mh\,\theta\,\lambda\,\phi\,\psi+\frac{2}{3}\,l^4\,L^4\,mp\,\theta\,\lambda\,\phi\,\psi+2\,l^4\,L^4\,mh\,\lambda^2\,\phi\,\psi+\frac{2}{3}\,l^4\,L^4\,mp\,\lambda^2\,\phi\,\psi+2\,l^4\,L^4\,mh\,\theta\,\lambda^3\,\phi\,\psi+$$

$$\frac{2}{3}\,1^4\,L^4\,mp\,\Theta\,\lambda^3\,\phi\,\psi-1^4\,L^4\,mh\,\psi^2-\frac{1}{3}\,1^4\,L^4\,mp\,\psi^2-2\,1^4\,L^4\,mh\,\lambda^2\,\psi^2-\frac{2}{3}\,1^4\,L^4\,mp\,\lambda^2\,\psi^2-1^4\,L^4\,mh\,\lambda^4\,\psi^2-\frac{1}{3}\,1^4\,L^4\,mp\,\lambda^4\,\psi^2\Big),\ \Big(1^2\,L^2\,(3\,mh+mp)\,\Big(-1^2\,L\,\phi-1^2\,L\,\Theta\,\lambda\,\phi+1^2\,L\,\psi+1^2\,L\,\lambda^2\,\psi\Big)\Big)\Big/$$
$$\Big(3\,\Big(-1^4\,L^4\,mh\,\Theta^2-\frac{1}{3}\,1^4\,L^4\,mp\,\Theta^2+2\,1^4\,L^4\,mh\,\Theta\,\lambda+\frac{2}{3}\,1^4\,L^4\,mp\,\Theta\,\lambda-1^4\,L^4\,mh\,\lambda^2-\frac{1}{3}\,1^4\,L^4\,mp\,\lambda^2-1^4\,L^4\,mh\,\phi^2-\frac{1}{3}\,1^4\,L^4\,mp\,\phi^2-2\,1^4\,L^4\,mh\,\Theta\,\lambda\,\phi^2-\frac{2}{3}\,1^4\,L^4\,mp\,\Theta\,\lambda\,\phi^2-1^4\,L^4\,mh\,\Theta^2\,\lambda^2\,\phi^2-\frac{1}{3}\,1^4\,L^4\,mp\,\Theta^2\,\lambda^2\,\phi^2+2\,1^4\,L^4\,mh\,\phi\,\psi+\frac{2}{3}\,1^4\,L^4\,mp\,\phi\,\psi+$$
$$2\,1^4\,L^4\,mh\,\Theta\,\lambda\,\phi\,\psi+\frac{2}{3}\,1^4\,L^4\,mp\,\Theta\,\lambda\,\phi\,\psi+2\,1^4\,L^4\,mh\,\lambda^2\,\phi\,\psi+\frac{2}{3}\,1^4\,L^4\,mp\,\lambda^2\,\phi\,\psi+2\,1^4\,L^4\,mh\,\Theta\,\lambda^3\,\phi\,\psi+\frac{2}{3}\,1^4\,L^4\,mp\,\Theta\,\lambda^3\,\phi\,\psi-1^4\,L^4\,mh\,\psi^2-\frac{1}{3}\,1^4\,L^4\,mp\,\psi^2-2\,1^4\,L^4\,mh\,\lambda^2\,\psi^2-\frac{2}{3}\,1^4\,L^4\,mp\,\lambda^2\,\psi^2-1^4\,L^4\,mh\,\lambda^4\,\psi^2-\frac{1}{3}\,1^4\,L^4\,mp\,\lambda^4\,\psi^2\Big)\Big),$$
$$\Big(1\,\Big(1\,\Big(-\frac{1}{3}\,L^3\,(3\,mh+mp)\,(-1\,L\,\Theta+1\,L\,\lambda)+\frac{1}{3}\,L^3\,(3\,mh+mp)\,\Theta\,\phi\,(-1\,L\,\phi-1\,L\,\Theta\,\lambda\,\phi)\Big)-\frac{1}{3}\,1\,L^3\,(3\,mh+mp)\,\lambda\,(-1\,L\,\phi-1\,L\,\Theta\,\lambda\,\phi)\,\psi\Big)+L\,\Big(\frac{1}{3}\,1\,L^3\,(3\,mh+mp)\,\Theta\,\phi\,\Big(1^2\,\psi+1^2\,\lambda^2\,\psi\Big)-\frac{1}{3}\,1\,L^3\,(3\,mh+mp)\,\lambda\,\psi\,\Big(1^2\,\psi+1^2\,\lambda^2\,\psi\Big)\Big)\Big)\Big/$$
$$\Big(-1^4\,L^4\,mh\,\Theta^2-\frac{1}{3}\,1^4\,L^4\,mp\,\Theta^2+2\,1^4\,L^4\,mh\,\Theta\,\lambda+\frac{2}{3}\,1^4\,L^4\,mp\,\Theta\,\lambda-1^4\,L^4\,mh\,\lambda^2-\frac{1}{3}\,1^4\,L^4\,mp\,\lambda^2-1^4\,L^4\,mh\,\phi^2-\frac{1}{3}\,1^4\,L^4\,mp\,\phi^2-2\,1^4\,L^4\,mh\,\Theta\,\lambda\,\phi^2-\frac{2}{3}\,1^4\,L^4\,mp\,\Theta\,\lambda\,\phi^2-1^4\,L^4\,mh\,\Theta^2\,\lambda^2\,\phi^2-\frac{1}{3}\,1^4\,L^4\,mp\,\Theta^2\,\lambda^2\,\phi^2+2\,1^4\,L^4\,mh\,\phi\,\psi+\frac{2}{3}\,1^4\,L^4\,mp\,\phi\,\psi+$$
$$2\,1^4\,L^4\,mh\,\Theta\,\lambda\,\phi\,\psi+\frac{2}{3}\,1^4\,L^4\,mp\,\Theta\,\lambda\,\phi\,\psi+2\,1^4\,L^4\,mh\,\lambda^2\,\phi\,\psi+\frac{2}{3}\,1^4\,L^4\,mp\,\lambda^2\,\phi\,\psi+2\,1^4\,L^4\,mh\,\Theta\,\lambda^3\,\phi\,\psi+\frac{2}{3}\,1^4\,L^4\,mp\,\Theta\,\lambda^3\,\phi\,\psi-1^4\,L^4\,mh\,\psi^2-\frac{1}{3}\,1^4\,L^4\,mp\,\psi^2-2\,1^4\,L^4\,mh\,\lambda^2\,\psi^2-\frac{2}{3}\,1^4\,L^4\,mp\,\lambda^2\,\psi^2-1^4\,L^4\,mh\,\lambda^4\,\psi^2-\frac{1}{3}\,1^4\,L^4\,mp\,\lambda^4\,\psi^2\Big),$$
$$-\Big(\Big(1\,L^3\,(3\,mh+mp)\,\Big(-1^2\,L\,\phi-1^2\,L\,\Theta\,\lambda\,\phi+1^2\,L\,\psi+1^2\,L\,\lambda^2\,\psi\Big)\Big)\Big/\Big(3\,\Big(-1^4\,L^4\,mh\,\Theta^2-\frac{1}{3}\,1^4\,L^4\,mp\,\Theta^2+2\,1^4\,L^4\,mh\,\Theta\,\lambda+\frac{2}{3}\,1^4\,L^4\,mp\,\Theta\,\lambda-1^4\,L^4\,mh\,\lambda^2-\frac{1}{3}\,1^4\,L^4\,mp\,\lambda^2-1^4\,L^4\,mh\,\phi^2-\frac{1}{3}\,1^4\,L^4\,mp\,\phi^2-$$
$$2\,1^4\,L^4\,mh\,\Theta\,\lambda\,\phi^2-\frac{2}{3}\,1^4\,L^4\,mp\,\Theta\,\lambda\,\phi^2-1^4\,L^4\,mh\,\Theta^2\,\lambda^2\,\phi^2-\frac{1}{3}\,1^4\,L^4\,mp\,\Theta^2\,\lambda^2\,\phi^2+2\,1^4\,L^4\,mh\,\phi\,\psi+\frac{2}{3}\,1^4\,L^4\,mp\,\phi\,\psi+2\,1^4\,L^4\,mh\,\Theta\,\lambda\,\phi\,\psi+\frac{2}{3}\,1^4\,L^4\,mp\,\Theta\,\lambda\,\phi\,\psi+2\,1^4\,L^4\,mh\,\lambda^2\,\phi\,\psi+$$
$$\frac{2}{3}\,1^4\,L^4\,mp\,\lambda^2\,\phi\,\psi+2\,1^4\,L^4\,mh\,\Theta\,\lambda^3\,\phi\,\psi+\frac{2}{3}\,1^4\,L^4\,mp\,\Theta\,\lambda^3\,\phi\,\psi-1^4\,L^4\,mh\,\psi^2-\frac{1}{3}\,1^4\,L^4\,mp\,\psi^2-2\,1^4\,L^4\,mh\,\lambda^2\,\psi^2-\frac{2}{3}\,1^4\,L^4\,mp\,\lambda^2\,\psi^2-1^4\,L^4\,mh\,\lambda^4\,\psi^2-\frac{1}{3}\,1^4\,L^4\,mp\,\lambda^4\,\psi^2\Big)\Big)\Big),\ \Big(1^4\,L^4\,(3\,mh+mp)^2\Big)\Big/$$
$$\Big(9\,\Big(-1^4\,L^4\,mh\,\Theta^2-\frac{1}{3}\,1^4\,L^4\,mp\,\Theta^2+2\,1^4\,L^4\,mh\,\Theta\,\lambda+\frac{2}{3}\,1^4\,L^4\,mp\,\Theta\,\lambda-1^4\,L^4\,mh\,\lambda^2-\frac{1}{3}\,1^4\,L^4\,mp\,\lambda^2-1^4\,L^4\,mh\,\phi^2-\frac{1}{3}\,1^4\,L^4\,mp\,\phi^2-2\,1^4\,L^4\,mh\,\Theta\,\lambda\,\phi^2-\frac{2}{3}\,1^4\,L^4\,mp\,\Theta\,\lambda\,\phi^2-1^4\,L^4\,mh\,\Theta^2\,\lambda^2\,\phi^2-\frac{1}{3}\,1^4\,L^4\,mp\,\Theta^2\,\lambda^2\,\phi^2+2\,1^4\,L^4\,mh\,\phi\,\psi+\frac{2}{3}\,1^4\,L^4\,mp\,\phi\,\psi+$$
$$2\,1^4\,L^4\,mh\,\Theta\,\lambda\,\phi\,\psi+\frac{2}{3}\,1^4\,L^4\,mp\,\Theta\,\lambda\,\phi\,\psi+2\,1^4\,L^4\,mh\,\lambda^2\,\phi\,\psi+\frac{2}{3}\,1^4\,L^4\,mp\,\lambda^2\,\phi\,\psi+2\,1^4\,L^4\,mh\,\Theta\,\lambda^3\,\phi\,\psi+\frac{2}{3}\,1^4\,L^4\,mp\,\Theta\,\lambda^3\,\phi\,\psi-1^4\,L^4\,mh\,\psi^2-\frac{1}{3}\,1^4\,L^4\,mp\,\psi^2-2\,1^4\,L^4\,mh\,\lambda^2\,\psi^2-\frac{2}{3}\,1^4\,L^4\,mp\,\lambda^2\,\psi^2-1^4\,L^4\,mh\,\lambda^4\,\psi^2-\frac{1}{3}\,1^4\,L^4\,mp\,\lambda^4\,\psi^2\Big)\Big),$$
$$\Big(1^2\,L^4\,(3\,mh+mp)^2\,\Big(1^2\,\psi+1^2\,\lambda^2\,\psi\Big)\Big)\Big/\Big(9\,\Big(-1^4\,L^4\,mh\,\Theta^2-\frac{1}{3}\,1^4\,L^4\,mp\,\Theta^2+2\,1^4\,L^4\,mh\,\Theta\,\lambda+\frac{2}{3}\,1^4\,L^4\,mp\,\Theta\,\lambda-1^4\,L^4\,mh\,\lambda^2-\frac{1}{3}\,1^4\,L^4\,mp\,\lambda^2-1^4\,L^4\,mh\,\phi^2-\frac{1}{3}\,1^4\,L^4\,mp\,\phi^2-2\,1^4\,L^4\,mh\,\Theta\,\lambda\,\phi^2-\frac{2}{3}\,1^4\,L^4\,mp\,\Theta\,\lambda\,\phi^2-$$
$$1^4\,L^4\,mh\,\Theta^2\,\lambda^2\,\phi^2-\frac{1}{3}\,1^4\,L^4\,mp\,\Theta^2\,\lambda^2\,\phi^2+2\,1^4\,L^4\,mh\,\phi\,\psi+\frac{2}{3}\,1^4\,L^4\,mp\,\phi\,\psi+2\,1^4\,L^4\,mh\,\Theta\,\lambda\,\phi\,\psi+\frac{2}{3}\,1^4\,L^4\,mp\,\Theta\,\lambda\,\phi\,\psi+2\,1^4\,L^4\,mh\,\lambda^2\,\phi\,\psi+\frac{2}{3}\,1^4\,L^4\,mp\,\lambda^2\,\phi\,\psi+$$
$$2\,1^4\,L^4\,mh\,\Theta\,\lambda^3\,\phi\,\psi+\frac{2}{3}\,1^4\,L^4\,mp\,\Theta\,\lambda^3\,\phi\,\psi-1^4\,L^4\,mh\,\psi^2-\frac{1}{3}\,1^4\,L^4\,mp\,\psi^2-2\,1^4\,L^4\,mh\,\lambda^2\,\psi^2-\frac{2}{3}\,1^4\,L^4\,mp\,\lambda^2\,\psi^2-1^4\,L^4\,mh\,\lambda^4\,\psi^2-\frac{1}{3}\,1^4\,L^4\,mp\,\lambda^4\,\psi^2\Big)\Big),\ \Big(1^4\,L^4\,(3\,mh+mp)^2\,\lambda\Big)\Big/$$
$$\Big(9\,\Big(-1^4\,L^4\,mh\,\Theta^2-\frac{1}{3}\,1^4\,L^4\,mp\,\Theta^2+2\,1^4\,L^4\,mh\,\Theta\,\lambda+\frac{2}{3}\,1^4\,L^4\,mp\,\Theta\,\lambda-1^4\,L^4\,mh\,\lambda^2-\frac{1}{3}\,1^4\,L^4\,mp\,\lambda^2-1^4\,L^4\,mh\,\phi^2-\frac{1}{3}\,1^4\,L^4\,mp\,\phi^2-2\,1^4\,L^4\,mh\,\Theta\,\lambda\,\phi^2-\frac{2}{3}\,1^4\,L^4\,mp\,\Theta\,\lambda\,\phi^2-1^4\,L^4\,mh\,\Theta^2\,\lambda^2\,\phi^2-\frac{1}{3}\,1^4\,L^4\,mp\,\Theta^2\,\lambda^2\,\phi^2+2\,1^4\,L^4\,mh\,\phi\,\psi+\frac{2}{3}\,1^4\,L^4\,mp\,\phi\,\psi+$$
$$2\,1^4\,L^4\,mh\,\Theta\,\lambda\,\phi\,\psi+\frac{2}{3}\,1^4\,L^4\,mp\,\Theta\,\lambda\,\phi\,\psi+2\,1^4\,L^4\,mh\,\lambda^2\,\phi\,\psi+\frac{2}{3}\,1^4\,L^4\,mp\,\lambda^2\,\phi\,\psi+2\,1^4\,L^4\,mh\,\Theta\,\lambda^3\,\phi\,\psi+\frac{2}{3}\,1^4\,L^4\,mp\,\Theta\,\lambda^3\,\phi\,\psi-1^4\,L^4\,mh\,\psi^2-\frac{1}{3}\,1^4\,L^4\,mp\,\psi^2-2\,1^4\,L^4\,mh\,\lambda^2\,\psi^2-\frac{2}{3}\,1^4\,L^4\,mp\,\lambda^2\,\psi^2-1^4\,L^4\,mh\,\lambda^4\,\psi^2-\frac{1}{3}\,1^4\,L^4\,mp\,\lambda^4\,\psi^2\Big)\Big)\Big\},$$
$$-\Big(\Big(1\,\Big(-\frac{1}{3}\,1^2\,L^2\,(3\,mh+mp)\,(-1\,L\,\Theta+1\,L\,\lambda)\,\psi-\frac{1}{3}\,1^2\,L^2\,(3\,mh+mp)\,\lambda^2\,(-1\,L\,\Theta+1\,L\,\lambda)\,\psi\Big)\Big)\Big/\Big(-1^4\,L^4\,mh\,\Theta^2-\frac{1}{3}\,1^4\,L^4\,mp\,\Theta^2+2\,1^4\,L^4\,mh\,\Theta\,\lambda+\frac{2}{3}\,1^4\,L^4\,mp\,\Theta\,\lambda-1^4\,L^4\,mh\,\lambda^2-\frac{1}{3}\,1^4\,L^4\,mp\,\lambda^2-1^4\,L^4\,mh\,\phi^2-$$
$$\frac{1}{3}\,1^4\,L^4\,mp\,\phi^2-2\,1^4\,L^4\,mh\,\Theta\,\lambda\,\phi^2-\frac{2}{3}\,1^4\,L^4\,mp\,\Theta\,\lambda\,\phi^2-1^4\,L^4\,mh\,\Theta^2\,\lambda^2\,\phi^2-\frac{1}{3}\,1^4\,L^4\,mp\,\Theta^2\,\lambda^2\,\phi^2+2\,1^4\,L^4\,mh\,\phi\,\psi+\frac{2}{3}\,1^4\,L^4\,mp\,\phi\,\psi+2\,1^4\,L^4\,mh\,\Theta\,\lambda\,\phi\,\psi+\frac{2}{3}\,1^4\,L^4\,mp\,\Theta\,\lambda\,\phi\,\psi+$$
$$2\,1^4\,L^4\,mh\,\lambda^2\,\phi\,\psi+\frac{2}{3}\,1^4\,L^4\,mp\,\lambda^2\,\phi\,\psi+2\,1^4\,L^4\,mh\,\Theta\,\lambda^3\,\phi\,\psi+\frac{2}{3}\,1^4\,L^4\,mp\,\Theta\,\lambda^3\,\phi\,\psi-1^4\,L^4\,mh\,\psi^2-\frac{1}{3}\,1^4\,L^4\,mp\,\psi^2-2\,1^4\,L^4\,mh\,\lambda^2\,\psi^2-\frac{2}{3}\,1^4\,L^4\,mp\,\lambda^2\,\psi^2-1^4\,L^4\,mh\,\lambda^4\,\psi^2-\frac{1}{3}\,1^4\,L^4\,mp\,\lambda^4\,\psi^2\Big)\Big),$$
$$\Big(-1^4\,L^3\,mh\,\phi\,\psi-\frac{1}{3}\,1^4\,L^3\,mp\,\phi\,\psi-1^4\,L^3\,mh\,\Theta\,\lambda\,\phi\,\psi-\frac{1}{3}\,1^4\,L^3\,mp\,\Theta\,\lambda\,\phi\,\psi-1^4\,L^3\,mh\,\lambda^2\,\phi\,\psi-\frac{1}{3}\,1^4\,L^3\,mp\,\lambda^2\,\phi\,\psi-1^4\,L^3\,mh\,\Theta\,\lambda^3\,\phi\,\psi-\frac{1}{3}\,1^4\,L^3\,mp\,\Theta\,\lambda^3\,\phi\,\psi+1^4\,L^3\,mh\,\psi^2+\frac{1}{3}\,1^4\,L^3\,mp\,\psi^2+2\,1^4\,L^3\,mh\,\lambda^2\,\psi^2+\frac{2}{3}\,1^4\,L^3\,mp\,\lambda^2\,\psi^2+1^4\,L^3\,mh\,\lambda^4\,\psi^2+$$
$$\frac{1}{3}\,1^4\,L^3\,mp\,\lambda^4\,\psi^2\Big)\Big/\Big(-1^4\,L^4\,mh\,\Theta^2-\frac{1}{3}\,1^4\,L^4\,mp\,\Theta^2+2\,1^4\,L^4\,mh\,\Theta\,\lambda+\frac{2}{3}\,1^4\,L^4\,mp\,\Theta\,\lambda-1^4\,L^4\,mh\,\lambda^2-\frac{1}{3}\,1^4\,L^4\,mp\,\lambda^2-1^4\,L^4\,mh\,\phi^2-\frac{1}{3}\,1^4\,L^4\,mp\,\phi^2-2\,1^4\,L^4\,mh\,\Theta\,\lambda\,\phi^2-\frac{2}{3}\,1^4\,L^4\,mp\,\Theta\,\lambda\,\phi^2-1^4\,L^4\,mh\,\Theta^2\,\lambda^2\,\phi^2-\frac{1}{3}\,1^4\,L^4\,mp\,\Theta^2\,\lambda^2\,\phi^2+2\,1^4\,L^4\,mh\,\phi\,\psi+$$
$$\frac{2}{3}\,1^4\,L^4\,mp\,\phi\,\psi+2\,1^4\,L^4\,mh\,\Theta\,\lambda\,\phi\,\psi+\frac{2}{3}\,1^4\,L^4\,mp\,\Theta\,\lambda\,\phi\,\psi+2\,1^4\,L^4\,mh\,\lambda^2\,\phi\,\psi+\frac{2}{3}\,1^4\,L^4\,mp\,\lambda^2\,\phi\,\psi+2\,1^4\,L^4\,mh\,\Theta\,\lambda^3\,\phi\,\psi+\frac{2}{3}\,1^4\,L^4\,mp\,\Theta\,\lambda^3\,\phi\,\psi-1^4\,L^4\,mh\,\psi^2-\frac{1}{3}\,1^4\,L^4\,mp\,\psi^2-2\,1^4\,L^4\,mh\,\lambda^2\,\psi^2-\frac{2}{3}\,1^4\,L^4\,mp\,\lambda^2\,\psi^2-1^4\,L^4\,mh\,\lambda^4\,\psi^2-\frac{1}{3}\,1^4\,L^4\,mp\,\lambda^4\,\psi^2\Big),$$

$$\left(3\left(-1^4\,L^4\,mh\,\Theta^2-\frac{1}{3}\,1^4\,L^4\,mp\,\Theta^2+2\,1^4\,L^4\,mh\,\Theta\,\lambda+\frac{2}{3}\,1^4\,L^4\,mp\,\Theta\,\lambda-1^4\,L^4\,mh\,\lambda^2-\frac{1}{3}\,1^4\,L^4\,mp\,\lambda^2-1^4\,L^4\,mh\,\phi^2-\frac{1}{3}\,1^4\,L^4\,mp\,\phi^2-2\,1^4\,L^4\,mh\,\Theta\,\lambda\,\phi^2-\frac{2}{3}\,1^4\,L^4\,mp\,\Theta\,\lambda\,\phi^2-1^4\,L^4\,mh\,\Theta^2\,\lambda^2\,\phi^2-\frac{1}{3}\,1^4\,L^4\,mp\,\Theta^2\,\lambda^2\,\phi^2+2\,1^4\,L^4\,mh\,\phi\,\psi+\frac{2}{3}\,1^4\,L^4\,mp\,\phi\,\psi+2\,1^4\,L^4\,mh\,\Theta\,\lambda\,\phi\,\psi+\frac{2}{3}\,1^4\,L^4\,mp\,\Theta\,\lambda\,\phi\,\psi+2\,1^4\,L^4\,mh\,\lambda^2\,\phi\,\psi+\frac{2}{3}\,1^4\,L^4\,mp\,\lambda^2\,\phi\,\psi+2\,1^4\,L^4\,mh\,\Theta\,\lambda^3\,\phi\,\psi+\frac{2}{3}\,1^4\,L^4\,mp\,\Theta\,\lambda^3\,\phi\,\psi-1^4\,L^4\,mh\,\psi^2-\frac{1}{3}\,1^4\,L^4\,mp\,\psi^2-2\,1^4\,L^4\,mh\,\lambda^2\,\psi^2-\frac{2}{3}\,1^4\,L^4\,mp\,\lambda^2\,\psi^2-1^4\,L^4\,mh\,\lambda^4\,\psi^2-\frac{1}{3}\,1^4\,L^4\,mp\,\lambda^4\,\psi^2\right)\right),$$

$$\left(1\left(1\left(-\frac{1}{3}\,L^3\,(3\,mh+mp)\,(-1\,L\,\Theta+1\,L\,\lambda)+\frac{1}{3}\,L^3\,(3\,mh+mp)\,\Theta\,\phi\,(-1\,L\,\phi-1\,L\,\Theta\,\lambda\,\phi)\right)-\frac{1}{3}\,1\,L^3\,(3\,mh+mp)\,\lambda\,(-1\,L\,\phi-1\,L\,\Theta\,\lambda\,\phi)\,\psi\right)+L\left(\frac{1}{3}\,1\,L^3\,(3\,mh+mp)\,\Theta\,\phi\,\left(1^2\,\psi+1^2\,\lambda^2\,\psi\right)-\frac{1}{3}\,1\,L^3\,(3\,mh+mp)\,\lambda\,\psi\,\left(1^2\,\psi+1^2\,\lambda^2\,\psi\right)\right)\right)\Big/$$
$$\left(-1^4\,L^4\,mh\,\Theta^2-\frac{1}{3}\,1^4\,L^4\,mp\,\Theta^2+2\,1^4\,L^4\,mh\,\Theta\,\lambda+\frac{2}{3}\,1^4\,L^4\,mp\,\Theta\,\lambda-1^4\,L^4\,mh\,\lambda^2-\frac{1}{3}\,1^4\,L^4\,mp\,\lambda^2-1^4\,L^4\,mh\,\phi^2-\frac{1}{3}\,1^4\,L^4\,mp\,\phi^2-2\,1^4\,L^4\,mh\,\Theta\,\lambda\,\phi^2-\frac{2}{3}\,1^4\,L^4\,mp\,\Theta\,\lambda\,\phi^2-1^4\,L^4\,mh\,\Theta^2\,\lambda^2\,\phi^2-\frac{1}{3}\,1^4\,L^4\,mp\,\Theta^2\,\lambda^2\,\phi^2+2\,1^4\,L^4\,mh\,\phi\,\psi+\frac{2}{3}\,1^4\,L^4\,mp\,\phi\,\psi+2\,1^4\,L^4\,mh\,\Theta\,\lambda\,\phi\,\psi+\frac{2}{3}\,1^4\,L^4\,mp\,\Theta\,\lambda\,\phi\,\psi+2\,1^4\,L^4\,mh\,\lambda^2\,\phi\,\psi+\frac{2}{3}\,1^4\,L^4\,mp\,\lambda^2\,\phi\,\psi+2\,1^4\,L^4\,mh\,\Theta\,\lambda^3\,\phi\,\psi+\frac{2}{3}\,1^4\,L^4\,mp\,\Theta\,\lambda^3\,\phi\,\psi-1^4\,L^4\,mh\,\psi^2-\frac{1}{3}\,1^4\,L^4\,mp\,\psi^2-2\,1^4\,L^4\,mh\,\lambda^2\,\psi^2-\frac{2}{3}\,1^4\,L^4\,mp\,\lambda^2\,\psi^2-1^4\,L^4\,mh\,\lambda^4\,\psi^2-\frac{1}{3}\,1^4\,L^4\,mp\,\lambda^4\,\psi^2\right),$$

$$-\left(\left(1\,L^3\,(3\,mh+mp)\,\left(-1^2\,L\,\phi-1^2\,L\,\Theta\,\lambda\,\phi+1^2\,L\,\psi+1^2\,L\,\lambda^2\,\psi\right)\right)\Big/\left(3\left(-1^4\,L^4\,mh\,\Theta^2-\frac{1}{3}\,1^4\,L^4\,mp\,\Theta^2+2\,1^4\,L^4\,mh\,\Theta\,\lambda+\frac{2}{3}\,1^4\,L^4\,mp\,\Theta\,\lambda-1^4\,L^4\,mh\,\lambda^2-\frac{1}{3}\,1^4\,L^4\,mp\,\lambda^2-1^4\,L^4\,mh\,\phi^2-\frac{1}{3}\,1^4\,L^4\,mp\,\phi^2-\right.\right.\right.$$
$$\left.\left.\left.2\,1^4\,L^4\,mh\,\Theta\,\lambda\,\phi^2-\frac{2}{3}\,1^4\,L^4\,mp\,\Theta\,\lambda\,\phi^2-1^4\,L^4\,mh\,\Theta^2\,\lambda^2\,\phi^2-\frac{1}{3}\,1^4\,L^4\,mp\,\Theta^2\,\lambda^2\,\phi^2+2\,1^4\,L^4\,mh\,\phi\,\psi+\frac{2}{3}\,1^4\,L^4\,mp\,\phi\,\psi+2\,1^4\,L^4\,mh\,\Theta\,\lambda\,\phi\,\psi+\frac{2}{3}\,1^4\,L^4\,mp\,\Theta\,\lambda\,\phi\,\psi+2\,1^4\,L^4\,mh\,\lambda^2\,\phi\,\psi+\right.\right.\right.$$
$$\left.\left.\left.\frac{2}{3}\,1^4\,L^4\,mp\,\lambda^2\,\phi\,\psi+2\,1^4\,L^4\,mh\,\Theta\,\lambda^3\,\phi\,\psi+\frac{2}{3}\,1^4\,L^4\,mp\,\Theta\,\lambda^3\,\phi\,\psi-1^4\,L^4\,mh\,\psi^2-\frac{1}{3}\,1^4\,L^4\,mp\,\psi^2-2\,1^4\,L^4\,mh\,\lambda^2\,\psi^2-\frac{2}{3}\,1^4\,L^4\,mp\,\lambda^2\,\psi^2-1^4\,L^4\,mh\,\lambda^4\,\psi^2-\frac{1}{3}\,1^4\,L^4\,mp\,\lambda^4\,\psi^2\right)\right)\right),\ \left(1^4\,L^4\,(3\,mh+mp)^2\right)\Big/$$
$$\left(9\left(-1^4\,L^4\,mh\,\Theta^2-\frac{1}{3}\,1^4\,L^4\,mp\,\Theta^2+2\,1^4\,L^4\,mh\,\Theta\,\lambda+\frac{2}{3}\,1^4\,L^4\,mp\,\Theta\,\lambda-1^4\,L^4\,mh\,\lambda^2-\frac{1}{3}\,1^4\,L^4\,mp\,\lambda^2-1^4\,L^4\,mh\,\phi^2-\frac{1}{3}\,1^4\,L^4\,mp\,\phi^2-2\,1^4\,L^4\,mh\,\Theta\,\lambda\,\phi^2-\frac{2}{3}\,1^4\,L^4\,mp\,\Theta\,\lambda\,\phi^2-1^4\,L^4\,mh\,\Theta^2\,\lambda^2\,\phi^2-\frac{1}{3}\,1^4\,L^4\,mp\,\Theta^2\,\lambda^2\,\phi^2+2\,1^4\,L^4\,mh\,\phi\,\psi+\frac{2}{3}\,1^4\,L^4\,mp\,\phi\,\psi+\right.\right.$$
$$\left.\left.2\,1^4\,L^4\,mh\,\Theta\,\lambda\,\phi\,\psi+\frac{2}{3}\,1^4\,L^4\,mp\,\Theta\,\lambda\,\phi\,\psi+2\,1^4\,L^4\,mh\,\lambda^2\,\phi\,\psi+\frac{2}{3}\,1^4\,L^4\,mp\,\lambda^2\,\phi\,\psi+2\,1^4\,L^4\,mh\,\Theta\,\lambda^3\,\phi\,\psi+\frac{2}{3}\,1^4\,L^4\,mp\,\Theta\,\lambda^3\,\phi\,\psi-1^4\,L^4\,mh\,\psi^2-\frac{1}{3}\,1^4\,L^4\,mp\,\psi^2-2\,1^4\,L^4\,mh\,\lambda^2\,\psi^2-\frac{2}{3}\,1^4\,L^4\,mp\,\lambda^2\,\psi^2-1^4\,L^4\,mh\,\lambda^4\,\psi^2-\frac{1}{3}\,1^4\,L^4\,mp\,\lambda^4\,\psi^2\right)\right),$$
$$\left(1^2\,L^4\,(3\,mh+mp)^2\,\left(1^2\,\psi+1^2\,\lambda^2\,\psi\right)\right)\Big/\left(9\left(-1^4\,L^4\,mh\,\Theta^2-\frac{1}{3}\,1^4\,L^4\,mp\,\Theta^2+2\,1^4\,L^4\,mh\,\Theta\,\lambda+\frac{2}{3}\,1^4\,L^4\,mp\,\Theta\,\lambda-1^4\,L^4\,mh\,\lambda^2-\frac{1}{3}\,1^4\,L^4\,mp\,\lambda^2-1^4\,L^4\,mh\,\phi^2-\frac{1}{3}\,1^4\,L^4\,mp\,\phi^2-2\,1^4\,L^4\,mh\,\Theta\,\lambda\,\phi^2-\frac{2}{3}\,1^4\,L^4\,mp\,\Theta\,\lambda\,\phi^2-\right.\right.\right.$$
$$\left.\left.\left.1^4\,L^4\,mh\,\Theta^2\,\lambda^2\,\phi^2-\frac{1}{3}\,1^4\,L^4\,mp\,\Theta^2\,\lambda^2\,\phi^2+2\,1^4\,L^4\,mh\,\phi\,\psi+\frac{2}{3}\,1^4\,L^4\,mp\,\phi\,\psi+2\,1^4\,L^4\,mh\,\Theta\,\lambda\,\phi\,\psi+\frac{2}{3}\,1^4\,L^4\,mp\,\Theta\,\lambda\,\phi\,\psi+2\,1^4\,L^4\,mh\,\lambda^2\,\phi\,\psi+\frac{2}{3}\,1^4\,L^4\,mp\,\lambda^2\,\phi\,\psi+\right.\right.\right.$$
$$\left.\left.\left.2\,1^4\,L^4\,mh\,\Theta\,\lambda^3\,\phi\,\psi+\frac{2}{3}\,1^4\,L^4\,mp\,\Theta\,\lambda^3\,\phi\,\psi-1^4\,L^4\,mh\,\psi^2-\frac{1}{3}\,1^4\,L^4\,mp\,\psi^2-2\,1^4\,L^4\,mh\,\lambda^2\,\psi^2-\frac{2}{3}\,1^4\,L^4\,mp\,\lambda^2\,\psi^2-1^4\,L^4\,mh\,\lambda^4\,\psi^2-\frac{1}{3}\,1^4\,L^4\,mp\,\lambda^4\,\psi^2\right)\right),\ \left(1^4\,L^4\,(3\,mh+mp)^2\,\lambda\right)\Big/$$
$$\left(9\left(-1^4\,L^4\,mh\,\Theta^2-\frac{1}{3}\,1^4\,L^4\,mp\,\Theta^2+2\,1^4\,L^4\,mh\,\Theta\,\lambda+\frac{2}{3}\,1^4\,L^4\,mp\,\Theta\,\lambda-1^4\,L^4\,mh\,\lambda^2-\frac{1}{3}\,1^4\,L^4\,mp\,\lambda^2-1^4\,L^4\,mh\,\phi^2-\frac{1}{3}\,1^4\,L^4\,mp\,\phi^2-2\,1^4\,L^4\,mh\,\Theta\,\lambda\,\phi^2-\frac{2}{3}\,1^4\,L^4\,mp\,\Theta\,\lambda\,\phi^2-1^4\,L^4\,mh\,\Theta^2\,\lambda^2\,\phi^2-\frac{1}{3}\,1^4\,L^4\,mp\,\Theta^2\,\lambda^2\,\phi^2+2\,1^4\,L^4\,mh\,\phi\,\psi+\frac{2}{3}\,1^4\,L^4\,mp\,\phi\,\psi+\right.\right.$$
$$\left.\left.2\,1^4\,L^4\,mh\,\Theta\,\lambda\,\phi\,\psi+\frac{2}{3}\,1^4\,L^4\,mp\,\Theta\,\lambda\,\phi\,\psi+2\,1^4\,L^4\,mh\,\lambda^2\,\phi\,\psi+\frac{2}{3}\,1^4\,L^4\,mp\,\lambda^2\,\phi\,\psi+2\,1^4\,L^4\,mh\,\Theta\,\lambda^3\,\phi\,\psi+\frac{2}{3}\,1^4\,L^4\,mp\,\Theta\,\lambda^3\,\phi\,\psi-1^4\,L^4\,mh\,\psi^2-\frac{1}{3}\,1^4\,L^4\,mp\,\psi^2-2\,1^4\,L^4\,mh\,\lambda^2\,\psi^2-\frac{2}{3}\,1^4\,L^4\,mp\,\lambda^2\,\psi^2-1^4\,L^4\,mh\,\lambda^4\,\psi^2-\frac{1}{3}\,1^4\,L^4\,mp\,\lambda^4\,\psi^2\right)\right)\right\},$$

$$-\left(\left(1\left(-\frac{1}{3}\,1^2\,L^2\,(3\,mh+mp)\,(-1\,L\,\Theta+1\,L\,\lambda)\,\psi-\frac{1}{3}\,1^2\,L^2\,(3\,mh+mp)\,\lambda^2\,(-1\,L\,\Theta+1\,L\,\lambda)\,\psi\right)\right)\Big/\left(-1^4\,L^4\,mh\,\Theta^2-\frac{1}{3}\,1^4\,L^4\,mp\,\Theta^2+2\,1^4\,L^4\,mh\,\Theta\,\lambda+\frac{2}{3}\,1^4\,L^4\,mp\,\Theta\,\lambda-1^4\,L^4\,mh\,\lambda^2-\frac{1}{3}\,1^4\,L^4\,mp\,\lambda^2-1^4\,L^4\,mh\,\phi^2-\right.\right.$$
$$\left.\left.\frac{1}{3}\,1^4\,L^4\,mp\,\phi^2-2\,1^4\,L^4\,mh\,\Theta\,\lambda\,\phi^2-\frac{2}{3}\,1^4\,L^4\,mp\,\Theta\,\lambda\,\phi^2-1^4\,L^4\,mh\,\Theta^2\,\lambda^2\,\phi^2-\frac{1}{3}\,1^4\,L^4\,mp\,\Theta^2\,\lambda^2\,\phi^2+2\,1^4\,L^4\,mh\,\phi\,\psi+\frac{2}{3}\,1^4\,L^4\,mp\,\phi\,\psi+2\,1^4\,L^4\,mh\,\Theta\,\lambda\,\phi\,\psi+\frac{2}{3}\,1^4\,L^4\,mp\,\Theta\,\lambda\,\phi\,\psi+\right.\right.$$
$$\left.\left.2\,1^4\,L^4\,mh\,\lambda^2\,\phi\,\psi+\frac{2}{3}\,1^4\,L^4\,mp\,\lambda^2\,\phi\,\psi+2\,1^4\,L^4\,mh\,\Theta\,\lambda^3\,\phi\,\psi+\frac{2}{3}\,1^4\,L^4\,mp\,\Theta\,\lambda^3\,\phi\,\psi-1^4\,L^4\,mh\,\psi^2-\frac{1}{3}\,1^4\,L^4\,mp\,\psi^2-2\,1^4\,L^4\,mh\,\lambda^2\,\psi^2-\frac{2}{3}\,1^4\,L^4\,mp\,\lambda^2\,\psi^2-1^4\,L^4\,mh\,\lambda^4\,\psi^2-\frac{1}{3}\,1^4\,L^4\,mp\,\lambda^4\,\psi^2\right)\right),$$
$$\left(-1^4\,L^3\,mh\,\phi\,\psi-\frac{1}{3}\,1^4\,L^3\,mp\,\phi\,\psi-1^4\,L^3\,mh\,\Theta\,\lambda\,\phi\,\psi-\frac{1}{3}\,1^4\,L^3\,mp\,\Theta\,\lambda\,\phi\,\psi-1^4\,L^3\,mh\,\lambda^2\,\phi\,\psi-\frac{1}{3}\,1^4\,L^3\,mp\,\lambda^2\,\phi\,\psi-1^4\,L^3\,mh\,\Theta\,\lambda^3\,\phi\,\psi-\frac{1}{3}\,1^4\,L^3\,mp\,\Theta\,\lambda^3\,\phi\,\psi+1^4\,L^3\,mh\,\psi^2+\frac{1}{3}\,1^4\,L^3\,mp\,\psi^2+2\,1^4\,L^3\,mh\,\lambda^2\,\psi^2+\frac{2}{3}\,1^4\,L^3\,mp\,\lambda^2\,\psi^2+1^4\,L^3\,mh\,\lambda^4\,\psi^2+\right.$$
$$\left.\frac{1}{3}\,1^4\,L^3\,mp\,\lambda^4\,\psi^2\right)\Big/\left(-1^4\,L^4\,mh\,\Theta^2-\frac{1}{3}\,1^4\,L^4\,mp\,\Theta^2+2\,1^4\,L^4\,mh\,\Theta\,\lambda+\frac{2}{3}\,1^4\,L^4\,mp\,\Theta\,\lambda-1^4\,L^4\,mh\,\lambda^2-\frac{1}{3}\,1^4\,L^4\,mp\,\lambda^2-1^4\,L^4\,mh\,\phi^2-\frac{1}{3}\,1^4\,L^4\,mp\,\phi^2-2\,1^4\,L^4\,mh\,\Theta\,\lambda\,\phi^2-\frac{2}{3}\,1^4\,L^4\,mp\,\Theta\,\lambda\,\phi^2-1^4\,L^4\,mh\,\Theta^2\,\lambda^2\,\phi^2-\frac{1}{3}\,1^4\,L^4\,mp\,\Theta^2\,\lambda^2\,\phi^2+\right.$$
$$\left.\frac{2}{3}\,1^4\,L^4\,mp\,\phi\,\psi+2\,1^4\,L^4\,mh\,\Theta\,\lambda\,\phi\,\psi+\frac{2}{3}\,1^4\,L^4\,mp\,\Theta\,\lambda\,\phi\,\psi+2\,1^4\,L^4\,mh\,\lambda^2\,\phi\,\psi+\frac{2}{3}\,1^4\,L^4\,mp\,\lambda^2\,\phi\,\psi+2\,1^4\,L^4\,mh\,\Theta\,\lambda^3\,\phi\,\psi+\frac{2}{3}\,1^4\,L^4\,mp\,\Theta\,\lambda^3\,\phi\,\psi-1^4\,L^4\,mh\,\psi^2-\frac{1}{3}\,1^4\,L^4\,mp\,\psi^2-2\,1^4\,L^4\,mh\,\lambda^2\,\psi^2-\frac{2}{3}\,1^4\,L^4\,mp\,\lambda^2\,\psi^2-1^4\,L^4\,mh\,\lambda^4\,\psi^2-\frac{1}{3}\,1^4\,L^4\,mp\,\lambda^4\,\psi^2\right),$$
$$\left(-1\left(1\,\lambda\left(\frac{1}{3}\,L^3\,(3\,mh+mp)\,\Theta\,(-1\,L\,\Theta+1\,L\,\lambda)+\frac{1}{3}\,L^3\,(3\,mh+mp)\,\phi\,(-1\,L\,\phi-1\,L\,\Theta\,\lambda\,\phi)\right)\psi-1\left(-\frac{1}{3}\,L^3\,(3\,mh+mp)\,(-1\,L\,\Theta+1\,L\,\lambda)+\frac{1}{3}\,L^3\,(3\,mh+mp)\,\Theta\,\phi\,(-1\,L\,\phi-1\,L\,\Theta\,\lambda\,\phi)\right)\psi\right)-\right.$$

$$
\begin{aligned}
&L\left(-\frac{1}{3}\,l\,L^3\,(3\,mh+mp)\,\theta\,\phi\,\psi\left(l^2\,\psi+l^2\,\lambda^2\,\psi\right)+\frac{1}{3}\,l\,L^3\,(3\,mh+mp)\,\lambda\,\phi\,\psi\left(l^2\,\psi+l^2\,\lambda^2\,\psi\right)\right)\Big/\\
&\left(-l^4\,L^4\,mh\,\theta^2-\frac{1}{3}\,l^4\,L^4\,mp\,\theta^2+2\,l^4\,L^4\,mh\,\theta\,\lambda+\frac{2}{3}\,l^4\,L^4\,mp\,\theta\,\lambda-l^4\,L^4\,mh\,\lambda^2-\frac{1}{3}\,l^4\,L^4\,mp\,\lambda^2-l^4\,L^4\,mh\,\phi^2-\frac{1}{3}\,l^4\,L^4\,mp\,\phi^2-2\,l^4\,L^4\,mh\,\theta\,\lambda\,\phi^2-\frac{2}{3}\,l^4\,L^4\,mp\,\theta\,\lambda\,\phi^2-l^4\,L^4\,mh\,\theta^2\,\lambda^2\,\phi^2-\frac{1}{3}\,l^4\,L^4\,mp\,\theta^2\,\lambda^2\,\phi^2+2\,l^4\,L^4\,mh\,\phi\,\psi+\right.\\
&\left.\frac{2}{3}\,l^4\,L^4\,mp\,\phi\,\psi+2\,l^4\,L^4\,mh\,\theta\,\lambda\,\phi\,\psi+\frac{2}{3}\,l^4\,L^4\,mp\,\theta\,\lambda\,\phi\,\psi+2\,l^4\,L^4\,mh\,\lambda^2\,\phi\,\psi+\frac{2}{3}\,l^4\,L^4\,mp\,\lambda^2\,\phi\,\psi+2\,l^4\,L^4\,mh\,\theta\,\lambda^3\,\phi\,\psi+\frac{2}{3}\,l^4\,L^4\,mp\,\theta\,\lambda^3\,\phi\,\psi-l^4\,L^4\,mh\,\psi^2-\frac{1}{3}\,l^4\,L^4\,mp\,\psi^2-2\,l^4\,L^4\,mh\,\lambda^2\,\psi^2-\frac{2}{3}\,l^4\,L^4\,mp\,\lambda^2\,\psi^2-l^4\,L^4\,mh\,\lambda^4\,\psi^2-\frac{1}{3}\,l^4\,L^4\,mp\,\lambda^4\,\psi^2\right),\\
&\left(l\left(-l\left(\frac{1}{3}\,L^3\,(3\,mh+mp)\,\theta\,(-l\,L\,\theta+l\,L\,\lambda)+\frac{1}{3}\,L^3\,(3\,mh+mp)\,\phi\,(-l\,L\,\phi-l\,L\,\theta\,\lambda\,\phi)\right)-l\,\lambda\left(-\frac{1}{3}\,L^3\,(3\,mh+mp)\,(-l\,L\,\theta+l\,L\,\lambda)+\frac{1}{3}\,L^3\,(3\,mh+mp)\,\theta\,\phi\,(-l\,L\,\phi-l\,L\,\theta\,\lambda\,\phi)\right)\right)+\right.\\
&\left.L\left(-\frac{1}{3}\,l\,L^3\,(3\,mh+mp)\,\phi\left(l^2\,\psi+l^2\,\lambda^2\,\psi\right)-\frac{1}{3}\,l\,L^3\,(3\,mh+mp)\,\theta\,\lambda\,\phi\left(l^2\,\psi+l^2\,\lambda^2\,\psi\right)\right)\right)\Big/\left(-l^4\,L^4\,mh\,\theta^2-\frac{1}{3}\,l^4\,L^4\,mp\,\theta^2+2\,l^4\,L^4\,mh\,\theta\,\lambda+\frac{2}{3}\,l^4\,L^4\,mp\,\theta\,\lambda-l^4\,L^4\,mh\,\lambda^2-\frac{1}{3}\,l^4\,L^4\,mp\,\lambda^2-l^4\,L^4\,mh\,\phi^2-\right.\\
&\left.\frac{1}{3}\,l^4\,L^4\,mp\,\phi^2-2\,l^4\,L^4\,mh\,\theta\,\lambda\,\phi^2-\frac{2}{3}\,l^4\,L^4\,mp\,\theta\,\lambda\,\phi^2-l^4\,L^4\,mh\,\theta^2\,\lambda^2\,\phi^2-\frac{1}{3}\,l^4\,L^4\,mp\,\theta^2\,\lambda^2\,\phi^2+2\,l^4\,L^4\,mh\,\phi\,\psi+\frac{2}{3}\,l^4\,L^4\,mp\,\phi\,\psi+2\,l^4\,L^4\,mh\,\theta\,\lambda\,\phi\,\psi+\frac{2}{3}\,l^4\,L^4\,mp\,\theta\,\lambda\,\phi\,\psi+2\,l^4\,L^4\,mh\,\lambda^2\,\phi\,\psi+\right.\\
&\left.\frac{2}{3}\,l^4\,L^4\,mp\,\lambda^2\,\phi\,\psi+2\,l^4\,L^4\,mh\,\theta\,\lambda^3\,\phi\,\psi+\frac{2}{3}\,l^4\,L^4\,mp\,\theta\,\lambda^3\,\phi\,\psi-l^4\,L^4\,mh\,\psi^2-\frac{1}{3}\,l^4\,L^4\,mp\,\psi^2-2\,l^4\,L^4\,mh\,\lambda^2\,\psi^2-\frac{2}{3}\,l^4\,L^4\,mp\,\lambda^2\,\psi^2-l^4\,L^4\,mh\,\lambda^4\,\psi^2-\frac{1}{3}\,l^4\,L^4\,mp\,\lambda^4\,\psi^2\right),\left(l^2\,L^4\,(3\,mh+mp)^2\left(l^2\,\psi+l^2\,\lambda^2\,\psi\right)\right)\Big/\\
&\left(9\left(-l^4\,L^4\,mh\,\theta^2-\frac{1}{3}\,l^4\,L^4\,mp\,\theta^2+2\,l^4\,L^4\,mh\,\theta\,\lambda+\frac{2}{3}\,l^4\,L^4\,mp\,\theta\,\lambda-l^4\,L^4\,mh\,\lambda^2-\frac{1}{3}\,l^4\,L^4\,mp\,\lambda^2-l^4\,L^4\,mh\,\phi^2-\frac{1}{3}\,l^4\,L^4\,mp\,\phi^2-2\,l^4\,L^4\,mh\,\theta\,\lambda\,\phi^2-\frac{2}{3}\,l^4\,L^4\,mp\,\theta\,\lambda\,\phi^2-l^4\,L^4\,mh\,\theta^2\,\lambda^2\,\phi^2-\frac{1}{3}\,l^4\,L^4\,mp\,\theta^2\,\lambda^2\,\phi^2+2\,l^4\,L^4\,mh\,\phi\,\psi+\frac{2}{3}\,l^4\,L^4\,mp\,\phi\,\psi+\right.\right.\\
&\left.\left.2\,l^4\,L^4\,mh\,\theta\,\lambda\,\phi\,\psi+\frac{2}{3}\,l^4\,L^4\,mp\,\theta\,\lambda\,\phi\,\psi+2\,l^4\,L^4\,mh\,\lambda^2\,\phi\,\psi+\frac{2}{3}\,l^4\,L^4\,mp\,\lambda^2\,\phi\,\psi+2\,l^4\,L^4\,mh\,\theta\,\lambda^3\,\phi\,\psi+\frac{2}{3}\,l^4\,L^4\,mp\,\theta\,\lambda^3\,\phi\,\psi-l^4\,L^4\,mh\,\psi^2-\frac{1}{3}\,l^4\,L^4\,mp\,\psi^2-2\,l^4\,L^4\,mh\,\lambda^2\,\psi^2-\frac{2}{3}\,l^4\,L^4\,mp\,\lambda^2\,\psi^2-l^4\,L^4\,mh\,\lambda^4\,\psi^2-\frac{1}{3}\,l^4\,L^4\,mp\,\lambda^4\,\psi^2\right)\right),\\
&\left(\frac{1}{9}\,l^2\,L^4\,(3\,mh+mp)^2\,\psi\left(l^2\,\psi+l^2\,\lambda^2\,\psi\right)+\frac{1}{9}\,l^2\,L^4\,(3\,mh+mp)^2\,\lambda^2\,\psi\left(l^2\,\psi+l^2\,\lambda^2\,\psi\right)\right)\Big/\left(-l^4\,L^4\,mh\,\theta^2-\frac{1}{3}\,l^4\,L^4\,mp\,\theta^2+2\,l^4\,L^4\,mh\,\theta\,\lambda+\frac{2}{3}\,l^4\,L^4\,mp\,\theta\,\lambda-l^4\,L^4\,mh\,\lambda^2-\frac{1}{3}\,l^4\,L^4\,mp\,\lambda^2-l^4\,L^4\,mh\,\phi^2-\frac{1}{3}\,l^4\,L^4\,mp\,\phi^2-\right.\\
&\left.2\,l^4\,L^4\,mh\,\theta\,\lambda\,\phi^2-\frac{2}{3}\,l^4\,L^4\,mp\,\theta\,\lambda\,\phi^2-l^4\,L^4\,mh\,\theta^2\,\lambda^2\,\phi^2-\frac{1}{3}\,l^4\,L^4\,mp\,\theta^2\,\lambda^2\,\phi^2+2\,l^4\,L^4\,mh\,\phi\,\psi+\frac{2}{3}\,l^4\,L^4\,mp\,\phi\,\psi+2\,l^4\,L^4\,mh\,\theta\,\lambda\,\phi\,\psi+\frac{2}{3}\,l^4\,L^4\,mp\,\theta\,\lambda\,\phi\,\psi+2\,l^4\,L^4\,mh\,\lambda^2\,\phi\,\psi+\frac{2}{3}\,l^4\,L^4\,mp\,\lambda^2\,\phi\,\psi+\right.\\
&\left.2\,l^4\,L^4\,mh\,\theta\,\lambda^3\,\phi\,\psi+\frac{2}{3}\,l^4\,L^4\,mp\,\theta\,\lambda^3\,\phi\,\psi-l^4\,L^4\,mh\,\psi^2-\frac{1}{3}\,l^4\,L^4\,mp\,\psi^2-2\,l^4\,L^4\,mh\,\lambda^2\,\psi^2-\frac{2}{3}\,l^4\,L^4\,mp\,\lambda^2\,\psi^2-l^4\,L^4\,mh\,\lambda^4\,\psi^2-\frac{1}{3}\,l^4\,L^4\,mp\,\lambda^4\,\psi^2\right),\left(l^2\,L^4\,(3\,mh+mp)^2\,\lambda\left(l^2\,\psi+l^2\,\lambda^2\,\psi\right)\right)\Big/\\
&\left(9\left(-l^4\,L^4\,mh\,\theta^2-\frac{1}{3}\,l^4\,L^4\,mp\,\theta^2+2\,l^4\,L^4\,mh\,\theta\,\lambda+\frac{2}{3}\,l^4\,L^4\,mp\,\theta\,\lambda-l^4\,L^4\,mh\,\lambda^2-\frac{1}{3}\,l^4\,L^4\,mp\,\lambda^2-l^4\,L^4\,mh\,\phi^2-\frac{1}{3}\,l^4\,L^4\,mp\,\phi^2-2\,l^4\,L^4\,mh\,\theta\,\lambda\,\phi^2-\frac{2}{3}\,l^4\,L^4\,mp\,\theta\,\lambda\,\phi^2-l^4\,L^4\,mh\,\theta^2\,\lambda^2\,\phi^2-\frac{1}{3}\,l^4\,L^4\,mp\,\theta^2\,\lambda^2\,\phi^2+2\,l^4\,L^4\,mh\,\phi\,\psi+\frac{2}{3}\,l^4\,L^4\,mp\,\phi\,\psi+\right.\right.\\
&\left.\left.2\,l^4\,L^4\,mh\,\theta\,\lambda\,\phi\,\psi+\frac{2}{3}\,l^4\,L^4\,mp\,\theta\,\lambda\,\phi\,\psi+2\,l^4\,L^4\,mh\,\lambda^2\,\phi\,\psi+\frac{2}{3}\,l^4\,L^4\,mp\,\lambda^2\,\phi\,\psi+2\,l^4\,L^4\,mh\,\theta\,\lambda^3\,\phi\,\psi+\frac{2}{3}\,l^4\,L^4\,mp\,\theta\,\lambda^3\,\phi\,\psi-l^4\,L^4\,mh\,\psi^2-\frac{1}{3}\,l^4\,L^4\,mp\,\psi^2-2\,l^4\,L^4\,mh\,\lambda^2\,\psi^2-\frac{2}{3}\,l^4\,L^4\,mp\,\lambda^2\,\psi^2-l^4\,L^4\,mh\,\lambda^4\,\psi^2-\frac{1}{3}\,l^4\,L^4\,mp\,\lambda^4\,\psi^2\right)\right)\right\},\\
&\left\{\left(l^2\,L^2\,(3\,mh+mp)\,\lambda\left(-l^2\,L\,\theta+l^2\,L\,\lambda\right)\right)\Big/\left(3\left(-l^4\,L^4\,mh\,\theta^2-\frac{1}{3}\,l^4\,L^4\,mp\,\theta^2+2\,l^4\,L^4\,mh\,\theta\,\lambda+\frac{2}{3}\,l^4\,L^4\,mp\,\theta\,\lambda-l^4\,L^4\,mh\,\lambda^2-\frac{1}{3}\,l^4\,L^4\,mp\,\lambda^2-l^4\,L^4\,mh\,\phi^2-\frac{1}{3}\,l^4\,L^4\,mp\,\phi^2-2\,l^4\,L^4\,mh\,\theta\,\lambda\,\phi^2-\frac{2}{3}\,l^4\,L^4\,mp\,\theta\,\lambda\,\phi^2-\right.\right.\right.\\
&\left.\left.\left.l^4\,L^4\,mh\,\theta^2\,\lambda^2\,\phi^2-\frac{1}{3}\,l^4\,L^4\,mp\,\theta^2\,\lambda^2\,\phi^2+2\,l^4\,L^4\,mh\,\phi\,\psi+\frac{2}{3}\,l^4\,L^4\,mp\,\phi\,\psi+2\,l^4\,L^4\,mh\,\theta\,\lambda\,\phi\,\psi+\frac{2}{3}\,l^4\,L^4\,mp\,\theta\,\lambda\,\phi\,\psi+2\,l^4\,L^4\,mh\,\lambda^2\,\phi\,\psi+\frac{2}{3}\,l^4\,L^4\,mp\,\lambda^2\,\phi\,\psi+2\,l^4\,L^4\,mh\,\theta\,\lambda^3\,\phi\,\psi+\right.\right.\right.\\
&\left.\left.\left.\frac{2}{3}\,l^4\,L^4\,mp\,\theta\,\lambda^3\,\phi\,\psi-l^4\,L^4\,mh\,\psi^2-\frac{1}{3}\,l^4\,L^4\,mp\,\psi^2-2\,l^4\,L^4\,mh\,\lambda^2\,\psi^2-\frac{2}{3}\,l^4\,L^4\,mp\,\lambda^2\,\psi^2-l^4\,L^4\,mh\,\lambda^4\,\psi^2-\frac{1}{3}\,l^4\,L^4\,mp\,\lambda^4\,\psi^2\right)\right),\left(l^2\,L^2\,(3\,mh+mp)\,\lambda\left(-l^2\,L\,\phi-l^2\,L\,\theta\,\lambda\,\phi+l^2\,L\,\psi+l^2\,L\,\lambda^2\,\psi\right)\right)\Big/\\
&\left(3\left(-l^4\,L^4\,mh\,\theta^2-\frac{1}{3}\,l^4\,L^4\,mp\,\theta^2+2\,l^4\,L^4\,mh\,\theta\,\lambda+\frac{2}{3}\,l^4\,L^4\,mp\,\theta\,\lambda-l^4\,L^4\,mh\,\lambda^2-\frac{1}{3}\,l^4\,L^4\,mp\,\lambda^2-l^4\,L^4\,mh\,\phi^2-\frac{1}{3}\,l^4\,L^4\,mp\,\phi^2-2\,l^4\,L^4\,mh\,\theta\,\lambda\,\phi^2-\frac{2}{3}\,l^4\,L^4\,mp\,\theta\,\lambda\,\phi^2-l^4\,L^4\,mh\,\theta^2\,\lambda^2\,\phi^2-\frac{1}{3}\,l^4\,L^4\,mp\,\theta^2\,\lambda^2\,\phi^2+2\,l^4\,L^4\,mh\,\phi\,\psi+\frac{2}{3}\,l^4\,L^4\,mp\,\phi\,\psi+\right.\right.\\
&\left.\left.2\,l^4\,L^4\,mh\,\theta\,\lambda\,\phi\,\psi+\frac{2}{3}\,l^4\,L^4\,mp\,\theta\,\lambda\,\phi\,\psi+2\,l^4\,L^4\,mh\,\lambda^2\,\phi\,\psi+\frac{2}{3}\,l^4\,L^4\,mp\,\lambda^2\,\phi\,\psi+2\,l^4\,L^4\,mh\,\theta\,\lambda^3\,\phi\,\psi+\frac{2}{3}\,l^4\,L^4\,mp\,\theta\,\lambda^3\,\phi\,\psi-l^4\,L^4\,mh\,\psi^2-\frac{1}{3}\,l^4\,L^4\,mp\,\psi^2-2\,l^4\,L^4\,mh\,\lambda^2\,\psi^2-\frac{2}{3}\,l^4\,L^4\,mp\,\lambda^2\,\psi^2-l^4\,L^4\,mh\,\lambda^4\,\psi^2-\frac{1}{3}\,l^4\,L^4\,mp\,\lambda^4\,\psi^2\right)\right),\\
&\left(\frac{1}{3}\,l\,L^3\,(3\,mh+mp)\,\psi\left(-l^2\,L\,\phi-l^2\,L\,\theta\,\lambda\,\phi+l^2\,L\,\psi+l^2\,L\,\lambda^2\,\psi\right)+1\left(-\frac{1}{3}\,L^3\,(3\,mh+mp)\,\theta\left(-l^2\,L\,\theta+l^2\,L\,\lambda\right)-\frac{1}{3}\,L^3\,(3\,mh+mp)\,\phi\left(-l^2\,L\,\phi-l^2\,L\,\theta\,\lambda\,\phi+l^2\,L\,\psi+l^2\,L\,\lambda^2\,\psi\right)\right)\right)\Big/\\
&\left(-l^4\,L^4\,mh\,\theta^2-\frac{1}{3}\,l^4\,L^4\,mp\,\theta^2+2\,l^4\,L^4\,mh\,\theta\,\lambda+\frac{2}{3}\,l^4\,L^4\,mp\,\theta\,\lambda-l^4\,L^4\,mh\,\lambda^2-\frac{1}{3}\,l^4\,L^4\,mp\,\lambda^2-l^4\,L^4\,mh\,\phi^2-\frac{1}{3}\,l^4\,L^4\,mp\,\phi^2-2\,l^4\,L^4\,mh\,\theta\,\lambda\,\phi^2-\frac{2}{3}\,l^4\,L^4\,mp\,\theta\,\lambda\,\phi^2-l^4\,L^4\,mh\,\theta^2\,\lambda^2\,\phi^2-\frac{1}{3}\,l^4\,L^4\,mp\,\theta^2\,\lambda^2\,\phi^2+2\,l^4\,L^4\,mh\,\phi\,\psi+\frac{2}{3}\,l^4\,L^4\,mp\,\phi\,\psi+\right.\\
&\left.2\,l^4\,L^4\,mh\,\theta\,\lambda\,\phi\,\psi+\frac{2}{3}\,l^4\,L^4\,mp\,\theta\,\lambda\,\phi\,\psi+2\,l^4\,L^4\,mh\,\lambda^2\,\phi\,\psi+\frac{2}{3}\,l^4\,L^4\,mp\,\lambda^2\,\phi\,\psi+2\,l^4\,L^4\,mh\,\theta\,\lambda^3\,\phi\,\psi+\frac{2}{3}\,l^4\,L^4\,mp\,\theta\,\lambda^3\,\phi\,\psi-l^4\,L^4\,mh\,\psi^2-\frac{1}{3}\,l^4\,L^4\,mp\,\psi^2-2\,l^4\,L^4\,mh\,\lambda^2\,\psi^2-\frac{2}{3}\,l^4\,L^4\,mp\,\lambda^2\,\psi^2-l^4\,L^4\,mh\,\lambda^4\,\psi^2-\frac{1}{3}\,l^4\,L^4\,mp\,\lambda^4\,\psi^2\right),
\end{aligned}
$$

$$-\left(\left(1\,l^3\,(3\,mh+mp)\,\lambda\left(-1^2\,l\,\phi-1^2\,l\,\theta\,\lambda\,\phi+1^2\,l\,\psi+1^2\,l\,\lambda^2\,\psi\right)\right)\Big/\left(3\left(-1^4\,l^4\,mh\,\theta^2-\frac{1}{3}\,1^4\,l^4\,mp\,\theta^2+2\,1^4\,l^4\,mh\,\theta\,\lambda+\frac{2}{3}\,1^4\,l^4\,mp\,\theta\,\lambda-1^4\,l^4\,mh\,\lambda^2-\frac{1}{3}\,1^4\,l^4\,mp\,\lambda^2-1^4\,l^4\,mh\,\phi^2-\frac{1}{3}\,1^4\,l^4\,mp\,\phi^2-\right.\right.\right.$$
$$2\,1^4\,l^4\,mh\,\theta\,\lambda\,\phi^2-\frac{2}{3}\,1^4\,l^4\,mp\,\theta\,\lambda\,\phi^2-1^4\,l^4\,mh\,\theta^2\,\lambda^2\,\phi^2-\frac{1}{3}\,1^4\,l^4\,mp\,\theta^2\,\lambda^2\,\phi^2+2\,1^4\,l^4\,mh\,\phi\,\psi+\frac{2}{3}\,1^4\,l^4\,mp\,\phi\,\psi+2\,1^4\,l^4\,mh\,\theta\,\lambda\,\phi\,\psi+\frac{2}{3}\,1^4\,l^4\,mp\,\theta\,\lambda\,\phi\,\psi+2\,1^4\,l^4\,mh\,\lambda^2\,\phi\,\psi+\frac{2}{3}\,1^4\,l^4\,mp\,\lambda^2\,\phi\,\psi+$$
$$\left.\left.\left.2\,1^4\,l^4\,mh\,\theta\,\lambda^3\,\phi\,\psi+\frac{2}{3}\,1^4\,l^4\,mp\,\theta\,\lambda^3\,\phi\,\psi-1^4\,l^4\,mh\,\psi^2-\frac{1}{3}\,1^4\,l^4\,mp\,\psi^2-2\,1^4\,l^4\,mh\,\lambda^2\,\psi^2-\frac{2}{3}\,1^4\,l^4\,mp\,\lambda^2\,\psi^2-1^4\,l^4\,mh\,\lambda^4\,\psi^2-\frac{1}{3}\,1^4\,l^4\,mp\,\lambda^4\,\psi^2\right)\right)\right),\ \left(1^4\,l^4\,(3\,mh+mp)^2\,\lambda\right)\Big/$$
$$\left(9\left(-1^4\,l^4\,mh\,\theta^2-\frac{1}{3}\,1^4\,l^4\,mp\,\theta^2+2\,1^4\,l^4\,mh\,\theta\,\lambda+\frac{2}{3}\,1^4\,l^4\,mp\,\theta\,\lambda-1^4\,l^4\,mh\,\lambda^2-\frac{1}{3}\,1^4\,l^4\,mp\,\lambda^2-1^4\,l^4\,mh\,\phi^2-\frac{1}{3}\,1^4\,l^4\,mp\,\phi^2-2\,1^4\,l^4\,mh\,\theta\,\lambda\,\phi^2-\frac{2}{3}\,1^4\,l^4\,mp\,\theta\,\lambda\,\phi^2-1^4\,l^4\,mh\,\theta^2\,\lambda^2\,\phi^2-\frac{1}{3}\,1^4\,l^4\,mp\,\theta^2\,\lambda^2\,\phi^2+2\,1^4\,l^4\,mh\,\phi\,\psi+\frac{2}{3}\,1^4\,l^4\,mp\,\phi\,\psi+\right.\right.$$
$$2\,1^4\,l^4\,mh\,\theta\,\lambda\,\phi\,\psi+\frac{2}{3}\,1^4\,l^4\,mp\,\theta\,\lambda\,\phi\,\psi+2\,1^4\,l^4\,mh\,\lambda^2\,\phi\,\psi+\frac{2}{3}\,1^4\,l^4\,mp\,\lambda^2\,\phi\,\psi+2\,1^4\,l^4\,mh\,\theta\,\lambda^3\,\phi\,\psi+\frac{2}{3}\,1^4\,l^4\,mp\,\theta\,\lambda^3\,\phi\,\psi-1^4\,l^4\,mh\,\psi^2-\frac{1}{3}\,1^4\,l^4\,mp\,\psi^2-2\,1^4\,l^4\,mh\,\lambda^2\,\psi^2-\frac{2}{3}\,1^4\,l^4\,mp\,\lambda^2\,\psi^2-1^4\,l^4\,mh\,\lambda^4\,\psi^2-\frac{1}{3}\,1^4\,l^4\,mp\,\lambda^4\,\psi^2\left.\right)\Big),$$
$$\left(1^2\,l^4\,(3\,mh+mp)^2\,\lambda\left(1^2\,\psi+1^2\,\lambda^2\,\psi\right)\right)\Big/\left(9\left(-1^4\,l^4\,mh\,\theta^2-\frac{1}{3}\,1^4\,l^4\,mp\,\theta^2+2\,1^4\,l^4\,mh\,\theta\,\lambda+\frac{2}{3}\,1^4\,l^4\,mp\,\theta\,\lambda-1^4\,l^4\,mh\,\lambda^2-\frac{1}{3}\,1^4\,l^4\,mp\,\lambda^2-1^4\,l^4\,mh\,\phi^2-\frac{1}{3}\,1^4\,l^4\,mp\,\phi^2-2\,1^4\,l^4\,mh\,\theta\,\lambda\,\phi^2-\right.\right.$$
$$\frac{2}{3}\,1^4\,l^4\,mp\,\theta\,\lambda\,\phi^2-1^4\,l^4\,mh\,\theta^2\,\lambda^2\,\phi^2-\frac{1}{3}\,1^4\,l^4\,mp\,\theta^2\,\lambda^2\,\phi^2+2\,1^4\,l^4\,mh\,\phi\,\psi+\frac{2}{3}\,1^4\,l^4\,mp\,\phi\,\psi+2\,1^4\,l^4\,mh\,\theta\,\lambda\,\phi\,\psi+\frac{2}{3}\,1^4\,l^4\,mp\,\theta\,\lambda\,\phi\,\psi+2\,1^4\,l^4\,mh\,\lambda^2\,\phi\,\psi+\frac{2}{3}\,1^4\,l^4\,mp\,\lambda^2\,\phi\,\psi+$$
$$\left.\left.2\,1^4\,l^4\,mh\,\theta\,\lambda^3\,\phi\,\psi+\frac{2}{3}\,1^4\,l^4\,mp\,\theta\,\lambda^3\,\phi\,\psi-1^4\,l^4\,mh\,\psi^2-\frac{1}{3}\,1^4\,l^4\,mp\,\psi^2-2\,1^4\,l^4\,mh\,\lambda^2\,\psi^2-\frac{2}{3}\,1^4\,l^4\,mp\,\lambda^2\,\psi^2-1^4\,l^4\,mh\,\lambda^4\,\psi^2-\frac{1}{3}\,1^4\,l^4\,mp\,\lambda^4\,\psi^2\right)\right),\ \left(1^4\,l^4\,(3\,mh+mp)^2\,\lambda^2\right)\Big/$$
$$\left(9\left(-1^4\,l^4\,mh\,\theta^2-\frac{1}{3}\,1^4\,l^4\,mp\,\theta^2+2\,1^4\,l^4\,mh\,\theta\,\lambda+\frac{2}{3}\,1^4\,l^4\,mp\,\theta\,\lambda-1^4\,l^4\,mh\,\lambda^2-\frac{1}{3}\,1^4\,l^4\,mp\,\lambda^2-1^4\,l^4\,mh\,\phi^2-\frac{1}{3}\,1^4\,l^4\,mp\,\phi^2-2\,1^4\,l^4\,mh\,\theta\,\lambda\,\phi^2-\frac{2}{3}\,1^4\,l^4\,mp\,\theta\,\lambda\,\phi^2-1^4\,l^4\,mh\,\theta^2\,\lambda^2\,\phi^2-\frac{1}{3}\,1^4\,l^4\,mp\,\theta^2\,\lambda^2\,\phi^2+2\,1^4\,l^4\,mh\,\phi\,\psi+\frac{2}{3}\,1^4\,l^4\,mp\,\phi\,\psi+\right.\right.$$
$$\left.\left.\left.2\,1^4\,l^4\,mh\,\theta\,\lambda\,\phi\,\psi+\frac{2}{3}\,1^4\,l^4\,mp\,\theta\,\lambda\,\phi\,\psi+2\,1^4\,l^4\,mh\,\lambda^2\,\phi\,\psi+\frac{2}{3}\,1^4\,l^4\,mp\,\lambda^2\,\phi\,\psi+2\,1^4\,l^4\,mh\,\theta\,\lambda^3\,\phi\,\psi+\frac{2}{3}\,1^4\,l^4\,mp\,\theta\,\lambda^3\,\phi\,\psi-1^4\,l^4\,mh\,\psi^2-\frac{1}{3}\,1^4\,l^4\,mp\,\psi^2-2\,1^4\,l^4\,mh\,\lambda^2\,\psi^2-\frac{2}{3}\,1^4\,l^4\,mp\,\lambda^2\,\psi^2-1^4\,l^4\,mh\,\lambda^4\,\psi^2-\frac{1}{3}\,1^4\,l^4\,mp\,\lambda^4\,\psi^2\right)\right)\right\}\right\}$$

APPENDIX B

SIMPLIFIED SIDE-SWING MODEL DERIVATION

```
hz = L * Cos[ϕ] Sin[θ]
```

$$L \cos[\phi] \sin[\theta]$$

```
hy = L * Cos[ϕ] Cos[θ]
```

$$L \cos[\theta] \cos[\phi]$$

```
hx = L * Sin[ϕ]
```

$$L \sin[\phi]$$

```
CONS = (H - hz) ^2 + (ty - hy) ^2 + (tx - hx) ^2 - l^2 // FullSimplify
```

$$H^2 - l^2 + tx^2 + ty^2 + L\,(L - 2\cos[\phi]\,(ty\cos[\theta] + H\sin[\theta]) - 2\,tx\sin[\phi])$$

```
DCONS = Dt[CONS] /. {Dt[H] → 0, Dt[l] → 0, Dt[L] → 0} // FullSimplify // Expand
```

$$2\,tx\,Dt[tx] + 2\,ty\,Dt[ty] - 2\,L\cos[\theta]\cos[\phi]\,Dt[ty] - 2\,H\,L\cos[\theta]\cos[\phi]\,Dt[\theta] - 2\,L\,tx\cos[\phi]\,Dt[\phi] + 2\,L\,ty\cos[\phi]\,Dt[\theta]\sin[\theta] - 2\,L\,Dt[tx]\sin[\phi] + 2\,L\,ty\cos[\theta]\,Dt[\phi]\sin[\phi] + 2\,H\,L\,Dt[\phi]\sin[\theta]\sin[\phi]$$

```
a = {D[DCONS, Dt[θ]], D[DCONS, Dt[ϕ]]} /. {Dt[H] → 0, Dt[l] → 0, Dt[L] → 0, ∂ϕDt[ϕ] → 0, ∂θDt[θ] -> 0}
```

$$\{-2\,H\,L\cos[\theta]\cos[\phi] + 2\,L\,ty\cos[\phi]\sin[\theta],\ -2\,L\,tx\cos[\phi] + 2\,L\,ty\cos[\theta]\sin[\phi] + 2\,H\,L\sin[\theta]\sin[\phi]\}$$

```
b = {DCONS - D[DCONS, Dt[θ]] * Dt[θ] - D[DCONS, Dt[ϕ]] * Dt[ϕ]} /. {Dt[H] → 0, Dt[l] → 0, Dt[L] → 0, ∂ϕDt[ϕ] → 0, ∂θDt[θ] -> 0}
```

$$\{2\,tx\,Dt[tx] + 2\,ty\,Dt[ty] - 2\,L\cos[\theta]\cos[\phi]\,Dt[ty] - 2\,H\,L\cos[\theta]\cos[\phi]\,Dt[\theta] - 2\,L\,tx\cos[\phi]\,Dt[\phi] + 2\,L\,ty\cos[\phi]\,Dt[\theta]\sin[\theta] - Dt[\theta]\,(-2\,H\,L\cos[\theta]\cos[\phi] + 2\,L\,ty\cos[\phi]\sin[\theta]) - 2\,L\,Dt[tx]\sin[\phi] + 2\,L\,ty\cos[\theta]\,Dt[\phi]\sin[\phi] + 2\,H\,L\,Dt[\phi]\sin[\theta]\sin[\phi] - Dt[\phi]\,(-2\,L\,tx\cos[\phi] + 2\,L\,ty\cos[\theta]\sin[\phi] + 2\,H\,L\sin[\theta]\sin[\phi])\}$$

```
ad = Dt[a] /. {Dt[H] → 0, Dt[l] → 0, Dt[L] → 0} // FullSimplify
```

$$\{2\,L\,(\cos[\phi]\,Dt[ty]\sin[\theta] + \cos[\phi]\,Dt[\theta]\,(ty\cos[\theta] + H\sin[\theta]) + Dt[\phi]\,(H\cos[\theta] - ty\sin[\theta])\sin[\phi]),\ 2\,L\,(-\cos[\phi]\,Dt[tx] + \cos[\phi]\,Dt[\phi]\,(ty\cos[\theta] + H\sin[\theta]) + (\cos[\theta]\,(Dt[ty] + H\,Dt[\theta]) + tx\,Dt[\phi] - ty\,Dt[\theta]\sin[\theta])\sin[\phi])\}$$

```
bd = Dt[b] /. {Dt[H] → 0, Dt[l] → 0, Dt[L] → 0, ∂ϕDt[ϕ] → 0, ∂θDt[θ] -> 0} // FullSimplify
```

$$\left\{2\left(\text{Dt}[\text{tx}]^2+\text{Dt}[\text{ty}]^2-\text{L}\,\text{Cos}[\phi]\,\text{Dt}[\text{tx}]\,\text{Dt}[\phi]+(\text{ty}-\text{L}\,\text{Cos}[\theta]\,\text{Cos}[\phi])\,\text{Dt}[\text{Dt}[\text{ty}]]+\text{Dt}[\text{Dt}[\text{tx}]]\,(\text{tx}-\text{L}\,\text{Sin}[\phi])+\text{L}\,\text{Dt}[\text{ty}]\,(\text{Cos}[\phi]\,\text{Dt}[\theta]\,\text{Sin}[\theta]+\text{Cos}[\theta]\,\text{Dt}[\phi]\,\text{Sin}[\phi])\right)\right\}$$

```
T = 1 / 2 (mh (L Cos[θ]) ^2) (Dt[ϕ] Cos[θ]) ^2  + 1 / 2 (1 / 3 mp (L Cos[θ]) ^2) (Dt[ϕ] Cos[θ]) ^2 + 1 / 2 (mh L^2) Dt[θ] ^2 + 1 / 2 × 1 / 3 mp L^2 Dt[θ] ^2
```

$$\frac{1}{2}\text{L}^2\,\text{mh}\,\text{Dt}[\theta]^2+\frac{1}{6}\text{L}^2\,\text{mp}\,\text{Dt}[\theta]^2+\frac{1}{2}\text{L}^2\,\text{mh}\,\text{Cos}[\theta]^4\,\text{Dt}[\phi]^2+\frac{1}{6}\text{L}^2\,\text{mp}\,\text{Cos}[\theta]^4\,\text{Dt}[\phi]^2$$

```
V = (mh + 1 / 2 mp) L g Cos[ϕ] Sin[θ]
```

$$\text{g}\,\text{L}\left(\text{mh}+\frac{\text{mp}}{2}\right)\text{Cos}[\phi]\,\text{Sin}[\theta]$$

```
g L (mh + mp/2) Cos[ϕ] Sin[θ]
```

$$\text{g}\,\text{L}\left(\text{mh}+\frac{\text{mp}}{2}\right)\text{Cos}[\phi]\,\text{Sin}[\theta]$$

```
La = T - V // FullSimplify
```

$$\frac{1}{6}\text{L}\left(\text{L}\,(3\,\text{mh}+\text{mp})\left(\text{Dt}[\theta]^2+\text{Cos}[\theta]^4\,\text{Dt}[\phi]^2\right)-3\,\text{g}\,(2\,\text{mh}+\text{mp})\,\text{Cos}[\phi]\,\text{Sin}[\theta]\right)$$

```
D[La, θ] /. {D[Dt[θ]] → 0}
```

$$\frac{1}{6}\text{L}\left(-3\,\text{g}\,(2\,\text{mh}+\text{mp})\,\text{Cos}[\theta]\,\text{Cos}[\phi]-4\,\text{L}\,(3\,\text{mh}+\text{mp})\,\text{Cos}[\theta]^3\,\text{Dt}[\phi]^2\,\text{Sin}[\theta]\right)$$

```
Dt[D[La, Dt[θ]]] /. {Dt[L] → 0, Dt[l] → 0, Dt[mp] → 0, Dt[mh] → 0} // FullSimplify
```

$$\frac{1}{3}\text{L}^2\,(3\,\text{mh}+\text{mp})\,\text{Dt}[\text{Dt}[\theta]]$$

```
La1 = 1/3 L^2 (3 mh + mp) Dt[Dt[θ]] - 1/6 L (-3 g (2 mh + mp) Cos[θ] Cos[ϕ] - 4 L (3 mh + mp) Cos[θ]^3 Dt[ϕ]^2 Sin[θ]) // FullSimplify
```

$$\frac{1}{6}\text{L}\left(3\,\text{g}\,(2\,\text{mh}+\text{mp})\,\text{Cos}[\theta]\,\text{Cos}[\phi]+2\,\text{L}\,(3\,\text{mh}+\text{mp})\left(\text{Dt}[\text{Dt}[\theta]]+2\,\text{Cos}[\theta]^3\,\text{Dt}[\phi]^2\,\text{Sin}[\theta]\right)\right)$$

```
D[La, ϕ] /. {D[Dt[ϕ]] → 0}
```

$$\frac{1}{2} g L (2 mh + mp) \text{Sin}[\theta] \text{Sin}[\phi]$$

```
Dt[D[La, Dt[ϕ]]] /. {Dt[L] → 0, Dt[l] → 0, Dt[mp] → 0, Dt[mh] → 0, Dt[k] → 0} // FullSimplify
```

$$\frac{1}{3} L^2 (3 mh + mp) \text{Cos}[\theta]^3 (\text{Cos}[\theta] \text{Dt}[\text{Dt}[\phi]] - 4 \text{Dt}[\theta] \text{Dt}[\phi] \text{Sin}[\theta])$$

```
La2 = 1/3 L^2 (3 mh + mp) Cos[θ]^3 (Cos[θ] Dt[Dt[ϕ]] - 4 Dt[θ] Dt[ϕ] Sin[θ]) - 1/2 g L (2 mh + mp) Sin[θ] Sin[ϕ] + c * Dt[ϕ] // FullSimplify
```

$$c \text{Dt}[\phi] + \frac{1}{3} L^2 (3 mh + mp) \text{Cos}[\theta]^3 (\text{Cos}[\theta] \text{Dt}[\text{Dt}[\phi]] - 4 \text{Dt}[\theta] \text{Dt}[\phi] \text{Sin}[\theta]) - \frac{1}{2} g L (2 mh + mp) \text{Sin}[\theta] \text{Sin}[\phi]$$

```
M = {{D[La1, Dt[Dt[θ]]], D[La1, Dt[Dt[ϕ]]]}, {D[La2, Dt[Dt[θ]]], D[La2, Dt[Dt[ϕ]]]}} // FullSimplify
```

$$\left\{\left\{\frac{1}{3} L^2 (3 mh + mp), 0\right\}, \left\{0, \frac{1}{3} L^2 (3 mh + mp) \text{Cos}[\theta]^4\right\}\right\}$$

```
F = {{-(La1 - (1/3 L^2 (3 mh + mp)) * Dt[Dt[θ]])}, {-(La2 - (1/3 L^2 (3 mh + mp) Cos[θ]^4) * Dt[Dt[ϕ]])}} // FullSimplify
```

$$\left\{\left\{-\frac{1}{6} L \text{Cos}[\theta] \left(3 g (2 mh + mp) \text{Cos}[\phi] + 4 L (3 mh + mp) \text{Cos}[\theta]^2 \text{Dt}[\phi]^2 \text{Sin}[\theta]\right)\right\}, \left\{\frac{1}{3} \text{Dt}[\phi] \left(-3 c + 4 L^2 (3 mh + mp) \text{Cos}[\theta]^3 \text{Dt}[\theta] \text{Sin}[\theta]\right) + \frac{1}{2} g L (2 mh + mp) \text{Sin}[\theta] \text{Sin}[\phi]\right\}\right\}$$

```
qd = {{Dt[θ]}, {Dt[ϕ]}}
```

$$\{\{\text{Dt}[\theta]\}, \{\text{Dt}[\phi]\}\}$$

```
Rightside = Join[F, ad.qd + bd] // MatrixForm
```

$$\begin{pmatrix} \left\{\frac{1}{3} \text{Dt}[\\ 2 L \text{Dt}[\theta] (\text{Cos}[\phi] \text{Dt}[ty] \text{Sin}[\theta] + \text{Cos}[\phi] \text{Dt}[\theta] (ty \text{Cos}[\theta] + H \text{Sin}[\theta]) + \text{Dt}[\phi] (H \text{Cos}[\theta] - ty \text{Sin}[\theta]) \text{Sin}[\phi]) + 2 L \text{Dt}[\phi] (-\text{Cos}[\phi] \text{Dt}[tx] + \text{Cos}[\phi] \text{Dt}[\phi] (ty \text{Cos}[\theta] + H S \end{pmatrix}$$

```
a
```

$$\{-2\,H\,L\,\text{Cos}[\theta]\,\text{Cos}[\phi]+2\,L\,ty\,\text{Cos}[\phi]\,\text{Sin}[\theta],\,-2\,L\,tx\,\text{Cos}[\phi]+2\,L\,ty\,\text{Cos}[\theta]\,\text{Sin}[\phi]+2\,H\,L\,\text{Sin}[\theta]\,\text{Sin}[\phi]\}$$

```
aa = {-2 H L Cos[θ] Cos[ϕ] + 2 L ty Cos[ϕ] Sin[θ], -2 L tx Cos[ϕ] + 2 L ty Cos[θ] Sin[ϕ] + 2 H L Sin[θ] Sin[ϕ], 0}
```

$$\{-2\,H\,L\,\text{Cos}[\theta]\,\text{Cos}[\phi]+2\,L\,ty\,\text{Cos}[\phi]\,\text{Sin}[\theta],\,-2\,L\,tx\,\text{Cos}[\phi]+2\,L\,ty\,\text{Cos}[\theta]\,\text{Sin}[\phi]+2\,H\,L\,\text{Sin}[\theta]\,\text{Sin}[\phi],\,0\}$$

```
Leftside = Join[Transpose[Join[M, -{a}]], {-aa}] // MatrixForm
```

$$\begin{pmatrix} \frac{1}{3}L^2\,(3\,mh+mp) & 0 & 2\,H\,L\,\text{Cos}[\theta]\,\text{Cos}[\phi]-2\,L\,ty\,\text{Cos}[\phi]\,\text{Sin}[\theta] \\ 0 & \frac{1}{3}L^2\,(3\,mh+mp)\,\text{Cos}[\theta]^4 & 2\,L\,tx\,\text{Cos}[\phi]-2\,L\,ty\,\text{Cos}[\theta]\,\text{Sin}[\phi]-2\,H\,L\,\text{Sin}[\theta]\,\text{Sin}[\phi] \\ 2\,H\,L\,\text{Cos}[\theta]\,\text{Cos}[\phi]-2\,L\,ty\,\text{Cos}[\phi]\,\text{Sin}[\theta] & 2\,L\,tx\,\text{Cos}[\phi]-2\,L\,ty\,\text{Cos}[\theta]\,\text{Sin}[\phi]-2\,H\,L\,\text{Sin}[\theta]\,\text{Sin}[\phi] & 0 \end{pmatrix}$$

APPENDIX C

DOUBLE PENDULUM FREE-HANGING MODEL DERIVATION

```
yh = yt + l Sin[ϕ]
```

$$yt + l \sin[\phi]$$

```
zh = -l Cos[ϕ]
```

$$-l \cos[\phi]$$

```
yp = yt + l Sin[ϕ] + 1 / 2 L Sin[θ]
```

$$yt + \frac{1}{2} L \sin[\theta] + l \sin[\phi]$$

```
zp = -l Cos[ϕ] - 1 / 2 L Cos[θ]
```

$$-\frac{1}{2} L \cos[\theta] - l \cos[\phi]$$

```
T = 1 / 2 mh (Dt[yh]) ^2 + 1 / 2 mh (Dt[zh]) ^2 + 1 / 2 mp (Dt[yp]) ^2 + 1 / 2 mp (Dt[zp]) ^2 + 1 / 2 (1 / 12 mp L ^2) Dt[θ] ^2 /. {Dt[l] → 0, Dt[L] → 0} // FullSimplify
```

$$\frac{1}{6}\left(3\,(mh+mp)\,Dt[yt]^2 + L^2\,mp\,Dt[\theta]^2 + 3\,l\,L\,mp\,\cos[\theta-\phi]\,Dt[\theta]\,Dt[\phi] + 3\,l^2\,(mh+mp)\,Dt[\phi]^2 + 3\,Dt[yt]\,(L\,mp\,\cos[\theta]\,Dt[\theta] + 2\,l\,(mh+mp)\,\cos[\phi]\,Dt[\phi])\right)$$

```
V = mp g zp + mh g zh
```

$$-g\,l\,mh\,\cos[\phi] + g\,mp\left(-\frac{1}{2} L \cos[\theta] - l \cos[\phi]\right)$$

```
La = T - V
```

$$g\,l\,mh\,\cos[\phi] - g\,mp\left(-\frac{1}{2} L \cos[\theta] - l \cos[\phi]\right) +$$
$$\frac{1}{6}\left(3\,(mh+mp)\,Dt[yt]^2 + L^2\,mp\,Dt[\theta]^2 + 3\,l\,L\,mp\,\cos[\theta-\phi]\,Dt[\theta]\,Dt[\phi] + 3\,l^2\,(mh+mp)\,Dt[\phi]^2 + 3\,Dt[yt]\,(L\,mp\,\cos[\theta]\,Dt[\theta] + 2\,l\,(mh+mp)\,\cos[\phi]\,Dt[\phi])\right)$$

```
La1b = D[La, θ] /. {D[Dt[θ]] → 0}
```

$$-\frac{1}{2} g\,L\,mp\,\sin[\theta]$$

```
La1a = Dt[D[La, Dt[θ]]] /. {Dt[L] → 0, Dt[l] → 0, Dt[mp] → 0, Dt[mh] → 0}
```

$$\frac{1}{6}\left(3\,L\,mp\,\text{Cos}[\theta]\,Dt[Dt[yt]] + 2\,L^2\,mp\,Dt[Dt[\theta]] + 3\,l\,L\,mp\,\text{Cos}[\theta-\phi]\,Dt[Dt[\phi]] - 3\,L\,mp\,Dt[yt]\,Dt[\theta]\,\text{Sin}[\theta] - 3\,l\,L\,mp\,(Dt[\theta]-Dt[\phi])\,Dt[\phi]\,\text{Sin}[\theta-\phi]\right)$$

```
La1 = La1a - La1b + c * Dt[θ]
```

$$c\,Dt[\theta] + \frac{1}{2}\,g\,L\,mp\,\text{Sin}[\theta] + \frac{1}{6}\left(3\,L\,mp\,\text{Cos}[\theta]\,Dt[Dt[yt]] + 2\,L^2\,mp\,Dt[Dt[\theta]] + 3\,l\,L\,mp\,\text{Cos}[\theta-\phi]\,Dt[Dt[\phi]] - 3\,L\,mp\,Dt[yt]\,Dt[\theta]\,\text{Sin}[\theta] - 3\,l\,L\,mp\,(Dt[\theta]-Dt[\phi])\,Dt[\phi]\,\text{Sin}[\theta-\phi]\right)$$

```
La2b = D[La, ϕ] /. {D[Dt[ϕ]] → 0}
```

$$-g\,l\,(mh+mp)\,\text{Sin}[\phi]$$

```
La2a = Dt[D[La, Dt[ϕ]]] /. {Dt[L] → 0, Dt[l] → 0, Dt[mp] → 0, Dt[mh] → 0}
```

$$\frac{1}{6}\left(6\,l\,(mh+mp)\,\text{Cos}[\phi]\,Dt[Dt[yt]] + 3\,l\,L\,mp\,\text{Cos}[\theta-\phi]\,Dt[Dt[\theta]] + 6\,l^2\,(mh+mp)\,Dt[Dt[\phi]] - 3\,l\,L\,mp\,Dt[\theta]\,(Dt[\theta]-Dt[\phi])\,\text{Sin}[\theta-\phi] - 6\,l\,(mh+mp)\,Dt[yt]\,Dt[\phi]\,\text{Sin}[\phi]\right)$$

```
La2 = La2a - La2b + c * Dt[ϕ]
```

$$c\,Dt[\phi] + g\,l\,(mh+mp)\,\text{Sin}[\phi] + \frac{1}{6}\left(6\,l\,(mh+mp)\,\text{Cos}[\phi]\,Dt[Dt[yt]] + 3\,l\,L\,mp\,\text{Cos}[\theta-\phi]\,Dt[Dt[\theta]] + 6\,l^2\,(mh+mp)\,Dt[Dt[\phi]] - 3\,l\,L\,mp\,Dt[\theta]\,(Dt[\theta]-Dt[\phi])\,\text{Sin}[\theta-\phi] - 6\,l\,(mh+mp)\,Dt[yt]\,Dt[\phi]\,\text{Sin}[\phi]\right)$$

```
Solve[{La1 == 0, La2 == 0}, {Dt[Dt[θ]], Dt[Dt[ϕ]]}] // FullSimplify
```

$$\left\{\left\{Dt[Dt[\theta]] \to -\left(\left(6\left(-l\,(mh+mp)\,(2\,c\,Dt[\theta] + L\,mp\,\text{Cos}[\theta]\,Dt[Dt[yt]] + g\,L\,mp\,\text{Sin}[\theta] - L\,mp\,Dt[yt]\,Dt[\theta]\,\text{Sin}[\theta] + l\,L\,mp\,Dt[\phi]\,(-Dt[\theta]+Dt[\phi])\,\text{Sin}[\theta-\phi]\right) + L\,mp\,\text{Cos}[\theta-\phi]\left(c\,Dt[\phi] + l\,(mh+mp)\,\text{Cos}[\phi]\,Dt[Dt[yt]] + \frac{1}{2}\,l\,L\,mp\,Dt[\theta]\,(-Dt[\theta]+Dt[\phi])\,\text{Sin}[\theta-\phi] + g\,l\,(mh+mp)\,\text{Sin}[\phi] - l\,(mh+mp)\,Dt[yt]\,Dt[\phi]\,\text{Sin}[\phi]\right)\right)\right)\Big/\left(l\,L^2\,mp\left(-4\,(mh+mp) + 3\,mp\,\text{Cos}[\theta-\phi]^2\right)\right)\right),\right.$$

$$\left.Dt[Dt[\phi]] \to \left(\text{Sec}[\theta-\phi]^2\left(4\,l\,L^2\,mp\,Dt[\theta]^2\,\text{Sin}[\theta-\phi] - l\,Dt[\theta]\right.\right.\right.$$

$$\left.\left.\left.(6\,\text{Cos}[\theta-\phi]\,(-2\,c + L\,mp\,Dt[yt]\,\text{Sin}[\theta]) + 2\,L\,mp\,(2\,L + 3\,l\,\text{Cos}[\theta-\phi])\,Dt[\phi]\,\text{Sin}[\theta-\phi]) + L\left(-8\,c\,Dt[\phi] + l\,(3\,mp\,\text{Cos}[2\,\theta-\phi] - (8\,mh+5\,mp)\,\text{Cos}[\phi])\,Dt[Dt[yt]] +\right.\right.\right.$$

$$3\,l^2\,mp\,Dt[\phi]^2\,Sin[2\,(\theta-\phi)]+3\,g\,l\,mp\,Sin[2\,\theta-\phi]+l\,(-g\,(8\,mh+5\,mp)+8\,(mh+mp)\,Dt[yt]\,Dt[\phi])\,Sin[\phi]\Big)\Big)\Big)\Big/\Big(2\,l^2\,L\,\Big(-3\,mp+4\,(mh+mp)\,Sec[\theta-\phi]^2\Big)\Big)\Big\}\Big\}$$

thetadd =

$$-\Big(\Big(6\,\Big(-l\,(mh+mp)\,(2\,c\,Dt[\theta]+L\,mp\,Cos[\theta]\,Dt[Dt[yt]]+g\,L\,mp\,Sin[\theta]-L\,mp\,Dt[yt]\,Dt[\theta]\,Sin[\theta]+l\,L\,mp\,Dt[\phi]\,(-Dt[\theta]+Dt[\phi])\,Sin[\theta-\phi])+$$
$$L\,mp\,Cos[\theta-\phi]\,\Big(c\,Dt[\phi]+l\,(mh+mp)\,Cos[\phi]\,Dt[Dt[yt]]+\frac{1}{2}\,l\,L\,mp\,Dt[\theta]\,(-Dt[\theta]+Dt[\phi])\,Sin[\theta-\phi]+g\,l\,(mh+mp)\,Sin[\phi]-l\,(mh+mp)\,Dt[yt]\,Dt[\phi]\,Sin[\phi]\Big)\Big)\Big)\Big/$$
$$\Big(l\,L^2\,mp\,\Big(-4\,(mh+mp)+3\,mp\,Cos[\theta-\phi]^2\Big)\Big)\Big)$$

$$-\Big(\Big(6\,\Big(-l\,(mh+mp)\,(2\,c\,Dt[\theta]+L\,mp\,Cos[\theta]\,Dt[Dt[yt]]+g\,L\,mp\,Sin[\theta]-L\,mp\,Dt[yt]\,Dt[\theta]\,Sin[\theta]+l\,L\,mp\,Dt[\phi]\,(-Dt[\theta]+Dt[\phi])\,Sin[\theta-\phi])+$$
$$L\,mp\,Cos[\theta-\phi]\,\Big(c\,Dt[\phi]+l\,(mh+mp)\,Cos[\phi]\,Dt[Dt[yt]]+\frac{1}{2}\,l\,L\,mp\,Dt[\theta]\,(-Dt[\theta]+Dt[\phi])\,Sin[\theta-\phi]+$$
$$g\,l\,(mh+mp)\,Sin[\phi]-l\,(mh+mp)\,Dt[yt]\,Dt[\phi]\,Sin[\phi]\Big)\Big)\Big)\Big/\Big(l\,L^2\,mp\,\Big(-4\,(mh+mp)+3\,mp\,Cos[\theta-\phi]^2\Big)\Big)\Big)$$

phidd =

$$\Big(Sec[\theta-\phi]^2\,\Big(4\,l\,L^2\,mp\,Dt[\theta]^2\,Sin[\theta-\phi]-l\,Dt[\theta]\,(6\,Cos[\theta-\phi]\,(-2\,c+L\,mp\,Dt[yt]\,Sin[\theta])+2\,L\,mp\,(2\,L+3\,l\,Cos[\theta-\phi])\,Dt[\phi]\,Sin[\theta-\phi])+$$
$$L\,\Big(-8\,c\,Dt[\phi]+l\,(3\,mp\,Cos[2\,\theta-\phi]-(8\,mh+5\,mp)\,Cos[\phi])\,Dt[Dt[yt]]+3\,l^2\,mp\,Dt[\phi]^2\,Sin[2\,(\theta-\phi)]+3\,g\,l\,mp\,Sin[2\,\theta-\phi]+$$
$$l\,(-g\,(8\,mh+5\,mp)+8\,(mh+mp)\,Dt[yt]\,Dt[\phi])\,Sin[\phi]\Big)\Big)\Big)\Big/\Big(2\,l^2\,L\,\Big(-3\,mp+4\,(mh+mp)\,Sec[\theta-\phi]^2\Big)\Big)$$

$$\Big(Sec[\theta-\phi]^2\,\Big(4\,l\,L^2\,mp\,Dt[\theta]^2\,Sin[\theta-\phi]-l\,Dt[\theta]\,(6\,Cos[\theta-\phi]\,(-2\,c+L\,mp\,Dt[yt]\,Sin[\theta])+2\,L\,mp\,(2\,L+3\,l\,Cos[\theta-\phi])\,Dt[\phi]\,Sin[\theta-\phi])+$$
$$L\,\Big(-8\,c\,Dt[\phi]+l\,(3\,mp\,Cos[2\,\theta-\phi]-(8\,mh+5\,mp)\,Cos[\phi])\,Dt[Dt[yt]]+3\,l^2\,mp\,Dt[\phi]^2\,Sin[2\,(\theta-\phi)]+$$
$$3\,g\,l\,mp\,Sin[2\,\theta-\phi]+l\,(-g\,(8\,mh+5\,mp)+8\,(mh+mp)\,Dt[yt]\,Dt[\phi])\,Sin[\phi]\Big)\Big)\Big)\Big/\Big(2\,l^2\,L\,\Big(-3\,mp+4\,(mh+mp)\,Sec[\theta-\phi]^2\Big)\Big)$$

thetadds =

```
thetadd /. {Sin[ϕ] → ϕ, Sin[θ] → θ, Cos[ϕ] → 0, Cos[θ] → 0, Cos[2 (θ - ϕ)] → 0, Sin[2 (θ - ϕ)] → 2 (θ - ϕ), Sin[θ - ϕ] → (θ - ϕ), Cos[θ - ϕ] → 0,
   Sec[θ - ϕ]^2 → 1, Sec[θ - ϕ] → 1, Tan[θ - ϕ] → (θ - ϕ), Dt[ϕ]^2 → 0, Dt[θ]^2 → 0} // FullSimplify
```

$$-\frac{3\,(g\,L\,mp\,\theta+2\,c\,Dt[\theta]-L\,mp\,\theta\,Dt[yt]\,Dt[\theta]+l\,L\,mp\,(\theta-\phi)\,Dt[\phi]\,(-Dt[\theta]+Dt[\phi]))}{2\,L^2\,mp}$$

```
phidds =
 phidd /. {Sin[ϕ] → ϕ, Sin[θ] → θ, Cos[ϕ] → 0, Cos[θ] → 0, Cos[2 (θ - ϕ)] → 0, Sin[2 (θ - ϕ)] → 2 (θ - ϕ), Sin[θ - ϕ] → (θ - ϕ), Cos[θ - ϕ] → 0,
    Sec[θ - ϕ]^2 → 1, Sec[θ - ϕ] → 1, Tan[θ - ϕ] → (θ - ϕ), Dt[ϕ]^2 → 0, Dt[θ]^2 → 0} // FullSimplify
```

$$\frac{d\phi\,(-8c + 4lL\,\mathrm{mp}\,(\phi-\theta)\,d\theta + 8l\phi\,(\mathrm{mh}+\mathrm{mp})\,d\mathrm{yt}) - gl\phi\,(8\,\mathrm{mh}+5\,\mathrm{mp}) + 3l\,\mathrm{mp}\,(g\sin(2\theta-\phi)) + d(d\mathrm{yt})\cos(2\theta-\phi))}{2l^2\,(4\,\mathrm{mh}+\mathrm{mp})}$$

```
A =
 {{0, 1, 0, 0, 0, 0}, {D[thetadd, θ], D[thetadd, Dt[θ]], D[thetadd, ϕ], D[thetadd, Dt[ϕ]], D[thetadd, yt], D[thetadd, Dt[yt]]}, {0, 0, 0, 1, 0, 0},
   {D[phidd, θ], D[phidd, Dt[θ]], D[phidd, ϕ], D[phidd, Dt[ϕ]], D[phidd, yt], D[phidd, Dt[yt]]}, {0, 0, 0, 0, 0, 1}, {0, 0, 0, 0, 0, 0}} /.
  {D[Dt[θ]] → 0, D[Dt[ϕ]] → 0, ∂yt Dt[Dt[yt]] → 0, ∂Dt[yt] Dt[Dt[yt]] → 0} /. {θ → 0, ϕ → 0} // FullSimplify
```

$$\left\{\{0,\,1,\,0,\,0,\,0,\,0\},\ \left\{-\frac{6\,g\,(\mathrm{mh}+\mathrm{mp})}{L\,(4\,\mathrm{mh}+\mathrm{mp})},\ -\frac{12\,c\,(\mathrm{mh}+\mathrm{mp})}{L^2\,\mathrm{mp}\,(4\,\mathrm{mh}+\mathrm{mp})},\ \frac{6\,g\,(\mathrm{mh}+\mathrm{mp})}{L\,(4\,\mathrm{mh}+\mathrm{mp})},\ \frac{6\,c}{4\,l\,L\,\mathrm{mh}+l\,L\,\mathrm{mp}},\ 0,\ 0\right\},\right.$$
$$\left.\{0,\,0,\,0,\,1,\,0,\,0\},\ \left\{\frac{3\,g\,\mathrm{mp}}{4\,l\,\mathrm{mh}+l\,\mathrm{mp}},\ \frac{6\,c}{4\,l\,L\,\mathrm{mh}+l\,L\,\mathrm{mp}},\ -\frac{4\,g\,(\mathrm{mh}+\mathrm{mp})}{l\,(4\,\mathrm{mh}+\mathrm{mp})},\ -\frac{4\,c}{l^2\,(4\,\mathrm{mh}+\mathrm{mp})},\ 0,\ 0\right\},\ \{0,\,0,\,0,\,0,\,0,\,1\},\ \{0,\,0,\,0,\,0,\,0,\,0\}\right\}$$

```
B = {0, D[thetadd, Dt[Dt[yt]]], 0, D[phidd, Dt[Dt[yt]]], 0, 1} /. {θ → 0, ϕ → 0} // FullSimplify
```

$$\left\{0,\,0,\,0,\,-\frac{1}{1},\,0,\,1\right\}$$

APPENDIX D

MRC CONTROL LAW DERIVATION

$$A = \left\{\{0, 1, 0, 0\}, \left\{-\frac{2\,g\,(mh+mp)}{L\,mh}, -\frac{4\,c\,(mh+mp)}{L^2\,mh\,mp}, \frac{2\,g\,(mh+mp)}{L\,mh}, \frac{2\,c}{l\,L\,mh}\right\}, \{0, 0, 0, 1\}, \left\{\frac{g\,mp}{l\,mh}, \frac{2\,c}{l\,L\,mh}, -\frac{g\,(mh+mp)}{l\,mh}, -\frac{c}{l^2\,mh}\right\}\right\}$$

$$\left\{\{0, 1, 0, 0\}, \left\{-\frac{2\,g\,(mh+mp)}{L\,mh}, -\frac{4\,c\,(mh+mp)}{L^2\,mh\,mp}, \frac{2\,g\,(mh+mp)}{L\,mh}, \frac{2\,c}{l\,L\,mh}\right\}, \{0, 0, 0, 1\}, \left\{\frac{g\,mp}{l\,mh}, \frac{2\,c}{l\,L\,mh}, -\frac{g\,(mh+mp)}{l\,mh}, -\frac{c}{l^2\,mh}\right\}\right\}$$

$$Am = \left\{\{0, 1, 0, 0\}, \left\{-\frac{2\,g\,(mh+mp)}{L\,mh}, -\frac{4\,cm\,(mh+mp)}{L^2\,mh\,mp}, \frac{2\,g\,(mh+mp)}{L\,mh}, \frac{2\,cm}{lm\,L\,mh}\right\}, \{0, 0, 0, 1\}, \left\{\frac{g\,mp}{lm\,mh}, \frac{2\,cm}{lm\,L\,mh}, -\frac{g\,(mh+mp)}{lm\,mh}, -\frac{cm}{lm^2\,mh}\right\}\right\}$$

$$\left\{\{0, 1, 0, 0\}, \left\{-\frac{2\,g\,(mh+mp)}{L\,mh}, -\frac{4\,cm\,(mh+mp)}{L^2\,mh\,mp}, \frac{2\,g\,(mh+mp)}{L\,mh}, \frac{2\,cm}{L\,lm\,mh}\right\}, \{0, 0, 0, 1\}, \left\{\frac{g\,mp}{lm\,mh}, \frac{2\,cm}{L\,lm\,mh}, -\frac{g\,(mh+mp)}{lm\,mh}, -\frac{cm}{lm^2\,mh}\right\}\right\}$$

$$P = \{\{p11, p12, p13, p14\}, \{p12, p22, p23, p24\}, \{p13, p23, p33, p34\}, \{p14, p24, p34, p44\}\}$$

$$\{\{p11, p12, p13, p14\}, \{p12, p22, p23, p24\}, \{p13, p23, p33, p34\}, \{p14, p24, p34, p44\}\}$$

$$B = -\text{Transpose}[Am].P - P.Am$$

$$\left\{\left\{\frac{4\,g\,(mh+mp)\,p12}{L\,mh} - \frac{2\,g\,mp\,p14}{lm\,mh}, -p11 + \frac{4\,cm\,(mh+mp)\,p12}{L^2\,mh\,mp} - \frac{2\,cm\,p14}{L\,lm\,mh} + \frac{2\,g\,(mh+mp)\,p22}{L\,mh} - \frac{g\,mp\,p24}{lm\,mh},\right.$$
$$\left. -\frac{2\,g\,(mh+mp)\,p12}{L\,mh} + \frac{g\,(mh+mp)\,p14}{lm\,mh} + \frac{2\,g\,(mh+mp)\,p23}{L\,mh} - \frac{g\,mp\,p34}{lm\,mh}, -\frac{2\,cm\,p12}{L\,lm\,mh} - p13 + \frac{cm\,p14}{lm^2\,mh} + \frac{2\,g\,(mh+mp)\,p24}{L\,mh} - \frac{g\,mp\,p44}{lm\,mh}\right\},$$
$$\left\{-p11 + \frac{4\,cm\,(mh+mp)\,p12}{L^2\,mh\,mp} - \frac{2\,cm\,p14}{L\,lm\,mh} + \frac{2\,g\,(mh+mp)\,p22}{L\,mh} - \frac{g\,mp\,p24}{lm\,mh}, -2\,p12 + \frac{8\,cm\,(mh+mp)\,p22}{L^2\,mh\,mp} - \frac{4\,cm\,p24}{L\,lm\,mh},\right.$$
$$\left. -p13 - \frac{2\,g\,(mh+mp)\,p22}{L\,mh} + \frac{4\,cm\,(mh+mp)\,p23}{L^2\,mh\,mp} + \frac{g\,(mh+mp)\,p24}{lm\,mh} - \frac{2\,cm\,p34}{L\,lm\,mh}, -p14 - \frac{2\,cm\,p22}{L\,lm\,mh} - p23 + \frac{cm\,p24}{lm^2\,mh} + \frac{4\,cm\,(mh+mp)\,p24}{L^2\,mh\,mp} - \frac{2\,cm\,p44}{L\,lm\,mh}\right\},$$
$$\left\{-\frac{2\,g\,(mh+mp)\,p12}{L\,mh} + \frac{g\,(mh+mp)\,p14}{lm\,mh} + \frac{2\,g\,(mh+mp)\,p23}{L\,mh} - \frac{g\,mp\,p34}{lm\,mh}, -p13 - \frac{2\,g\,(mh+mp)\,p22}{L\,mh} + \frac{4\,cm\,(mh+mp)\,p23}{L^2\,mh\,mp} + \frac{g\,(mh+mp)\,p24}{lm\,mh} - \frac{2\,cm\,p34}{L\,lm\,mh},\right.$$
$$\left. -\frac{4\,g\,(mh+mp)\,p23}{L\,mh} + \frac{2\,g\,(mh+mp)\,p34}{lm\,mh}, -\frac{2\,cm\,p23}{L\,lm\,mh} - \frac{2\,g\,(mh+mp)\,p24}{L\,mh} - p33 + \frac{cm\,p34}{lm^2\,mh} + \frac{g\,(mh+mp)\,p44}{lm\,mh}\right\},$$
$$\left\{-\frac{2\,cm\,p12}{L\,lm\,mh} - p13 + \frac{cm\,p14}{lm^2\,mh} + \frac{2\,g\,(mh+mp)\,p24}{L\,mh} - \frac{g\,mp\,p44}{lm\,mh}, -p14 - \frac{2\,cm\,p22}{L\,lm\,mh} - p23 + \frac{cm\,p24}{lm^2\,mh} + \frac{4\,cm\,(mh+mp)\,p24}{L^2\,mh\,mp} - \frac{2\,cm\,p44}{L\,lm\,mh},\right.$$
$$\left. -\frac{2\,cm\,p23}{L\,lm\,mh} - \frac{2\,g\,(mh+mp)\,p24}{L\,mh} - p33 + \frac{cm\,p34}{lm^2\,mh} + \frac{g\,(mh+mp)\,p44}{lm\,mh}, -\frac{4\,cm\,p24}{L\,lm\,mh} - 2\,p34 + \frac{2\,cm\,p44}{lm^2\,mh}\right\}\right\}$$

```
Solve[{Part[B, 1, 1] == 10, Part[B, 1, 2] == 0, Part[B, 1, 3] == 0, Part[B, 1, 4] == 0, Part[B, 2, 2] == 1, Part[B, 2, 3] == 0, Part[B, 2, 4] == 0,
  Part[B, 3, 3] == 10, Part[B, 3, 4] == 0, Part[B, 4, 4] == 1}, {p11, p12, p13, p14, p22, p23, p24, p33, p34, p44}]
```

$$\left\{\left\{p11 \to -\frac{-40\,cm^2 - g^2\,L^2\,mp^2 - 5\,g\,L^3\,mp^2}{4\,cm\,g\,L\,mp},\ p12 \to \frac{5\,L}{2\,g},\ p13 \to \frac{5\,L\,lm\,mp}{2\,cm},\ p14 \to \frac{5\,lm}{g},\ p22 \to -\frac{-g\,L^2\,mh\,mp - 5\,L^3\,mh\,mp - g\,L^2\,mp^2 - 5\,L^3\,mp^2 - 10\,L^2\,lm\,mp^2}{8\,cm\,g\,(mh+mp)},\ p23 \to \frac{5\,L\,mp}{2\,g\,(mh+mp)},\right.\right.$$
$$p24 \to -\frac{-g\,L\,lm\,mp - 5\,L^2\,lm\,mp - 10\,L\,lm^2\,mp}{4\,cm\,g},\ p33 \to -\frac{-10\,cm^2 - g^2\,lm^2\,mh^2 - 10\,g\,lm^3\,mh^2 - 2\,g^2\,lm^2\,mh\,mp - 20\,g\,lm^3\,mh\,mp - g^2\,lm^2\,mp^2 - 10\,g\,lm^3\,mp^2}{2\,cm\,g\,lm\,(mh+mp)},$$
$$\left.\left.p34 \to \frac{5\,lm}{g},\ p44 \to -\frac{-g\,lm^2\,mh - 10\,lm^3\,mh - g\,lm^2\,mp - 5\,L\,lm^2\,mp - 10\,lm^3\,mp}{2\,cm\,g}\right\}\right\}$$

```
<< ToMatlab.m
```

```
ToMatlab[-(-g lm^2 mh - 10 lm^3 mh - g lm^2 mp - 5 L lm^2 mp - 10 lm^3 mp)/(2 cm g)]
```

```
(-1/2).*cm.^(-1).*g.^(-1).*((-1).*g.*lm.^2.*mh+(-10).*lm.^3.*mh+( ...
  -1).*g.*lm.^2.*mp+(-5).*L.*lm.^2.*mp+(-10).*lm.^3.*mp);
```

```
X = {{x1}, {x2}, {x3}, {x4}}
```

$$\{\{x1\}, \{x2\}, \{x3\}, \{x4\}\}$$

```
M = {e1, e2, e3, e4}.P.((Am - A).X + {{0}, {0}, {0}, {1 / l}} * (v - u))
```

$$\left\{(e1\,p14 + e2\,p24 + e3\,p34 + e4\,p44)\left(\frac{-u+v}{l} + \left(-\frac{g\,mp}{l\,mh} + \frac{g\,mp}{lm\,mh}\right)x1 + \left(-\frac{2\,c}{l\,L\,mh} + \frac{2\,cm}{L\,lm\,mh}\right)x2 + \left(\frac{g\,(mh+mp)}{l\,mh} - \frac{g\,(mh+mp)}{lm\,mh}\right)x3 + \left(\frac{c}{l^2\,mh} - \frac{cm}{lm^2\,mh}\right)x4\right) +\right.$$
$$\left.(e1\,p12 + e2\,p22 + e3\,p23 + e4\,p24)\left(\left(\frac{4\,c\,(mh+mp)}{L^2\,mh\,mp} - \frac{4\,cm\,(mh+mp)}{L^2\,mh\,mp}\right)x2 + \left(-\frac{2\,c}{l\,L\,mh} + \frac{2\,cm}{L\,lm\,mh}\right)x4\right)\right\}$$

```
Solve[{M == e1^2 (p14 + p12) + e2^2 (p22 + p24) + e3^2 (p34 + p23) + e4^2 (p44 + p24) }, {u}]
```

$$\left\{\left\{u \to -\frac{1}{e1\,p14 + e2\,p24 + e3\,p34 + e4\,p44}\,l\left(e1^2\,(p12+p14) + e2^2\,(p22+p24) +\right.\right.\right.$$

$$e3^2\,(p23+p34)+e4^2\,(p24+p44)-\frac{(e1\,p14+e2\,p24+e3\,p34+e4\,p44)\,v}{l}-\left(-\frac{g\,mp}{l\,mh}+\frac{g\,mp}{lm\,mh}\right)(e1\,p14+e2\,p24+e3\,p34+e4\,p44)\,x1-$$
$$\left(-\frac{2\,c}{l\,L\,mh}+\frac{2\,cm}{L\,lm\,mh}\right)(e1\,p14+e2\,p24+e3\,p34+e4\,p44)\,x2-\left(\frac{g\,(mh+mp)}{l\,mh}-\frac{g\,(mh+mp)}{lm\,mh}\right)(e1\,p14+e2\,p24+e3\,p34+e4\,p44)\,x3-$$
$$\left(\frac{c}{l^2\,mh}-\frac{cm}{lm^2\,mh}\right)(e1\,p14+e2\,p24+e3\,p34+e4\,p44)\,x4-(e1\,p12+e2\,p22+e3\,p23+e4\,p24)\left(\left(\frac{4\,c\,(mh+mp)}{L^2\,mh\,mp}-\frac{4\,cm\,(mh+mp)}{L^2\,mh\,mp}\right)x2+\left(-\frac{2\,c}{l\,L\,mh}+\frac{2\,cm}{L\,lm\,mh}\right)x4\right)\Big)\Big\}$$

```
ToMatlab[e1^2 (p14 + p12) + e2^2 (p22 + p24) + e3^2 (p34 + p23) + e4^2 (p44 + p24)]
```

```
e1.^2.*(p12+p14)+e2.^2.*(p22+p24)+e3.^2.*(p23+p34)+e4.^2.*(p24+ ...
  p44);
```

```
good =
 {e1, e2, e3, e4, e5, e6}.{{p11, p12, p13, p14, p15, p16}, {p12, p22, p23, p24, p25, p26}, {p13, p23, p33, p34, p35, p36},
    {p14, p24, p34, p44, p45, p36}, {p15, p25, p35, p45, p55, p56}, {p16, p26, p36, p46, p56, p66}} .
   ({{0, 0, 0, 0, 0, 0}, {0, -(12 (cm - c) (mh + mp))/(L^2 mp (4 mh + mp)), 0, (6 (cm - c))/(4 l L mh + l L mp), 0, 0}, {0, 0, 0, 0, 0, 0}, {0, (6 (cm - c))/(4 l L mh + l L mp), 0, -(4 (cm - c) (mh + mp))/(l^2 mp (4 mh + mp)), 0, 0}, 97
    {0, 0, 0, 0, 0, 0}, {0, 0, 0, 0, 0, 0}}.{{x1}, {x2}, {x3}, {x4}, {x5}, {x6}} + {{0}, {0}, {0}, {-1 / l}, {0}, {0}} (v - u)) +
  (e1^2 + e2^2 + e3^2 + e4^2 + e5^2 + e6^2)
```

$$\left\{e1^2+e2^2+e3^2+e4^2+e5^2+e6^2+(e1\,p14+e2\,p24+e3\,p34+e4\,p44+e5\,p45+e6\,p46)\left(-\frac{-u+v}{l}+\frac{6\,(-c+cm)\,x2}{4\,l\,L\,mh+l\,L\,mp}-\frac{4\,(-c+cm)\,(mh+mp)\,x4}{l^2\,mp\,(4\,mh+mp)}\right)+\right.$$
$$\left.(e1\,p12+e2\,p22+e3\,p23+e4\,p24+e5\,p25+e6\,p26)\left(-\frac{12\,(-c+cm)\,(mh+mp)\,x2}{L^2\,mp\,(4\,mh+mp)}+\frac{6\,(-c+cm)\,x4}{4\,l\,L\,mh+l\,L\,mp}\right)\right\}$$

```
Solve[good == 0, {u}] // FullSimplify
```

$$\left\{\left\{u\to\left(l\left(-e1^2-e2^2-e3^2-e4^2-e5^2-e6^2+\frac{(e1\,p14+e2\,p24+e3\,p34+e4\,p44+e5\,p45+e6\,p46)\,v}{l}-\right.\right.\right.$$
$$\left.\left.\frac{6\,(-c+cm)\,(e1\,p14+e2\,p24+e3\,p34+e4\,p44+e5\,p45+e6\,p46)\,x2}{4\,l\,L\,mh+l\,L\,mp}+\frac{4\,(-c+cm)\,(mh+mp)\,(e1\,p14+e2\,p24+e3\,p34+e4\,p44+e5\,p45+e6\,p46)\,x4}{l^2\,mp\,(4\,mh+mp)}-\right.\right.$$

APPENDIX E

MRC CONTROL LAW DERIVATION

$$A = \left\{\{0, 1, 0, 0\}, \left\{-\frac{2\,g\,(mh+mp)}{L\,mh}, -\frac{4\,c\,(mh+mp)}{L^2\,mh\,mp}, \frac{2\,g\,(mh+mp)}{L\,mh}, \frac{2\,c}{l\,L\,mh}\right\}, \{0, 0, 0, 1\}, \left\{\frac{g\,mp}{l\,mh}, \frac{2\,c}{l\,L\,mh}, -\frac{g\,(mh+mp)}{l\,mh}, -\frac{c}{l^2\,mh}\right\}\right\}$$

$$\left\{\{0, 1, 0, 0\}, \left\{-\frac{2\,g\,(mh+mp)}{L\,mh}, -\frac{4\,c\,(mh+mp)}{L^2\,mh\,mp}, \frac{2\,g\,(mh+mp)}{L\,mh}, \frac{2\,c}{l\,L\,mh}\right\}, \{0, 0, 0, 1\}, \left\{\frac{g\,mp}{l\,mh}, \frac{2\,c}{l\,L\,mh}, -\frac{g\,(mh+mp)}{l\,mh}, -\frac{c}{l^2\,mh}\right\}\right\}$$

$$Am = \left\{\{0, 1, 0, 0\}, \left\{-\frac{2\,g\,(mh+mp)}{L\,mh}, -\frac{4\,cm\,(mh+mp)}{L^2\,mh\,mp}, \frac{2\,g\,(mh+mp)}{L\,mh}, \frac{2\,cm}{lm\,L\,mh}\right\}, \{0, 0, 0, 1\}, \left\{\frac{g\,mp}{lm\,mh}, \frac{2\,cm}{lm\,L\,mh}, -\frac{g\,(mh+mp)}{lm\,mh}, -\frac{cm}{lm^2\,mh}\right\}\right\}$$

$$\left\{\{0, 1, 0, 0\}, \left\{-\frac{2\,g\,(mh+mp)}{L\,mh}, -\frac{4\,cm\,(mh+mp)}{L^2\,mh\,mp}, \frac{2\,g\,(mh+mp)}{L\,mh}, \frac{2\,cm}{L\,lm\,mh}\right\}, \{0, 0, 0, 1\}, \left\{\frac{g\,mp}{lm\,mh}, \frac{2\,cm}{L\,lm\,mh}, -\frac{g\,(mh+mp)}{lm\,mh}, -\frac{cm}{lm^2\,mh}\right\}\right\}$$

$$P = \{\{p11, p12, p13, p14\}, \{p12, p22, p23, p24\}, \{p13, p23, p33, p34\}, \{p14, p24, p34, p44\}\}$$

$$\{\{p11, p12, p13, p14\}, \{p12, p22, p23, p24\}, \{p13, p23, p33, p34\}, \{p14, p24, p34, p44\}\}$$

$$B = -\text{Transpose}[Am].P - P.Am$$

$$\left\{\left\{\frac{4\,g\,(mh+mp)\,p12}{L\,mh} - \frac{2\,g\,mp\,p14}{lm\,mh}, -p11 + \frac{4\,cm\,(mh+mp)\,p12}{L^2\,mh\,mp} - \frac{2\,cm\,p14}{L\,lm\,mh} + \frac{2\,g\,(mh+mp)\,p22}{L\,mh} - \frac{g\,mp\,p24}{lm\,mh},\right.$$
$$\left. -\frac{2\,g\,(mh+mp)\,p12}{L\,mh} + \frac{g\,(mh+mp)\,p14}{lm\,mh} + \frac{2\,g\,(mh+mp)\,p23}{L\,mh} - \frac{g\,mp\,p34}{lm\,mh}, -\frac{2\,cm\,p12}{L\,lm\,mh} - p13 + \frac{cm\,p14}{lm^2\,mh} + \frac{2\,g\,(mh+mp)\,p24}{L\,mh} - \frac{g\,mp\,p44}{lm\,mh}\right\},$$
$$\left\{-p11 + \frac{4\,cm\,(mh+mp)\,p12}{L^2\,mh\,mp} - \frac{2\,cm\,p14}{L\,lm\,mh} + \frac{2\,g\,(mh+mp)\,p22}{L\,mh} - \frac{g\,mp\,p24}{lm\,mh}, -2\,p12 + \frac{8\,cm\,(mh+mp)\,p22}{L^2\,mh\,mp} - \frac{4\,cm\,p24}{L\,lm\,mh},\right.$$
$$\left. -p13 - \frac{2\,g\,(mh+mp)\,p22}{L\,mh} + \frac{4\,cm\,(mh+mp)\,p23}{L^2\,mh\,mp} + \frac{g\,(mh+mp)\,p24}{lm\,mh} - \frac{2\,cm\,p34}{L\,lm\,mh}, -p14 - \frac{2\,cm\,p22}{L\,lm\,mh} - p23 + \frac{cm\,p24}{lm^2\,mh} + \frac{4\,cm\,(mh+mp)\,p24}{L^2\,mh\,mp} - \frac{2\,cm\,p44}{L\,lm\,mh}\right\},$$
$$\left\{-\frac{2\,g\,(mh+mp)\,p12}{L\,mh} + \frac{g\,(mh+mp)\,p14}{lm\,mh} + \frac{2\,g\,(mh+mp)\,p23}{L\,mh} - \frac{g\,mp\,p34}{lm\,mh}, -p13 - \frac{2\,g\,(mh+mp)\,p22}{L\,mh} + \frac{4\,cm\,(mh+mp)\,p23}{L^2\,mh\,mp} + \frac{g\,(mh+mp)\,p24}{lm\,mh} - \frac{2\,cm\,p34}{L\,lm\,mh},\right.$$
$$\left. -\frac{4\,g\,(mh+mp)\,p23}{L\,mh} + \frac{2\,g\,(mh+mp)\,p34}{lm\,mh}, -\frac{2\,cm\,p23}{L\,lm\,mh} - \frac{2\,g\,(mh+mp)\,p24}{L\,mh} - p33 + \frac{cm\,p34}{lm^2\,mh} + \frac{g\,(mh+mp)\,p44}{lm\,mh}\right\},$$
$$\left\{-\frac{2\,cm\,p12}{L\,lm\,mh} - p13 + \frac{cm\,p14}{lm^2\,mh} + \frac{2\,g\,(mh+mp)\,p24}{L\,mh} - \frac{g\,mp\,p44}{lm\,mh}, -p14 - \frac{2\,cm\,p22}{L\,lm\,mh} - p23 + \frac{cm\,p24}{lm^2\,mh} + \frac{4\,cm\,(mh+mp)\,p24}{L^2\,mh\,mp} - \frac{2\,cm\,p44}{L\,lm\,mh},\right.$$
$$\left. -\frac{2\,cm\,p23}{L\,lm\,mh} - \frac{2\,g\,(mh+mp)\,p24}{L\,mh} - p33 + \frac{cm\,p34}{lm^2\,mh} + \frac{g\,(mh+mp)\,p44}{lm\,mh}, -\frac{4\,cm\,p24}{L\,lm\,mh} - 2\,p34 + \frac{2\,cm\,p44}{lm^2\,mh}\right\}\right\}$$

```
Solve[{Part[B, 1, 1] == 10, Part[B, 1, 2] == 0, Part[B, 1, 3] == 0, Part[B, 1, 4] == 0, Part[B, 2, 2] == 1, Part[B, 2, 3] == 0, Part[B, 2, 4] == 0,
  Part[B, 3, 3] == 10, Part[B, 3, 4] == 0, Part[B, 4, 4] == 1}, {p11, p12, p13, p14, p22, p23, p24, p33, p34, p44}]
```

$$\left\{\left\{p11 \to -\frac{-40\,cm^2 - g^2\,L^2\,mp^2 - 5\,g\,L^3\,mp^2}{4\,cm\,g\,L\,mp},\ p12 \to \frac{5\,L}{2\,g},\ p13 \to \frac{5\,L\,lm\,mp}{2\,cm},\ p14 \to \frac{5\,lm}{g},\ p22 \to -\frac{-g\,L^2\,mh\,mp - 5\,L^3\,mh\,mp - g\,L^2\,mp^2 - 5\,L^3\,mp^2 - 10\,L^2\,lm\,mp^2}{8\,cm\,g\,(mh+mp)},\ p23 \to \frac{5\,L\,mp}{2\,g\,(mh+mp)},\right.\right.$$
$$p24 \to -\frac{-g\,L\,lm\,mp - 5\,L^2\,lm\,mp - 10\,L\,lm^2\,mp}{4\,cm\,g},\ p33 \to -\frac{-10\,cm^2 - g^2\,lm^2\,mh^2 - 10\,g\,lm^3\,mh^2 - 2\,g^2\,lm^2\,mh\,mp - 20\,g\,lm^3\,mh\,mp - g^2\,lm^2\,mp^2 - 10\,g\,lm^3\,mp^2}{2\,cm\,g\,lm\,(mh+mp)},$$
$$\left.\left.p34 \to \frac{5\,lm}{g},\ p44 \to -\frac{-g\,lm^2\,mh - 10\,lm^3\,mh - g\,lm^2\,mp - 5\,L\,lm^2\,mp - 10\,lm^3\,mp}{2\,cm\,g}\right\}\right\}$$

```
<< ToMatlab.m
```

```
ToMatlab[-(-g lm^2 mh - 10 lm^3 mh - g lm^2 mp - 5 L lm^2 mp - 10 lm^3 mp)/(2 cm g)]
```

```
(-1/2).*cm.^(-1).*g.^(-1).*((-1).*g.*lm.^2.*mh+(-10).*lm.^3.*mh+( ...
  -1).*g.*lm.^2.*mp+(-5).*L.*lm.^2.*mp+(-10).*lm.^3.*mp);
```



```
X = {{x1}, {x2}, {x3}, {x4}}
```

```
{{x1}, {x2}, {x3}, {x4}}
```

```
M = {e1, e2, e3, e4}.P.((Am - A).X + {{0}, {0}, {0}, {1 / l}} * (v - u))
```

$$\left\{(e1\,p14 + e2\,p24 + e3\,p34 + e4\,p44)\left(\frac{-u+v}{l} + \left(-\frac{g\,mp}{l\,mh} + \frac{g\,mp}{lm\,mh}\right)x1 + \left(-\frac{2\,c}{l\,L\,mh} + \frac{2\,cm}{L\,lm\,mh}\right)x2 + \left(\frac{g\,(mh+mp)}{l\,mh} - \frac{g\,(mh+mp)}{lm\,mh}\right)x3 + \left(\frac{c}{l^2\,mh} - \frac{cm}{lm^2\,mh}\right)x4\right) +\right.$$
$$\left.(e1\,p12 + e2\,p22 + e3\,p23 + e4\,p24)\left(\left(\frac{4\,c\,(mh+mp)}{L^2\,mh\,mp} - \frac{4\,cm\,(mh+mp)}{L^2\,mh\,mp}\right)x2 + \left(-\frac{2\,c}{l\,L\,mh} + \frac{2\,cm}{L\,lm\,mh}\right)x4\right)\right\}$$

```
Solve[{M == e1^2 (p14 + p12) + e2^2 (p22 + p24) + e3^2 (p34 + p23) + e4^2 (p44 + p24) }, {u}]
```

$$\left\{\left\{u \to -\frac{1}{e1\,p14 + e2\,p24 + e3\,p34 + e4\,p44}\,l\left(e1^2\,(p12 + p14) + e2^2\,(p22 + p24) +\right.\right.\right.$$

$$e3^2\,(p23+p34)+e4^2\,(p24+p44)-\frac{(e1\,p14+e2\,p24+e3\,p34+e4\,p44)\,v}{l}-\left(-\frac{g\,mp}{l\,mh}+\frac{g\,mp}{lm\,mh}\right)(e1\,p14+e2\,p24+e3\,p34+e4\,p44)\,x1-$$
$$\left(-\frac{2\,c}{l\,L\,mh}+\frac{2\,cm}{L\,lm\,mh}\right)(e1\,p14+e2\,p24+e3\,p34+e4\,p44)\,x2-\left(\frac{g\,(mh+mp)}{l\,mh}-\frac{g\,(mh+mp)}{lm\,mh}\right)(e1\,p14+e2\,p24+e3\,p34+e4\,p44)\,x3-$$
$$\left(\frac{c}{l^2\,mh}-\frac{cm}{lm^2\,mh}\right)(e1\,p14+e2\,p24+e3\,p34+e4\,p44)\,x4-(e1\,p12+e2\,p22+e3\,p23+e4\,p24)\left(\left(\frac{4\,c\,(mh+mp)}{L^2\,mh\,mp}-\frac{4\,cm\,(mh+mp)}{L^2\,mh\,mp}\right)x2+\left(-\frac{2\,c}{l\,L\,mh}+\frac{2\,cm}{L\,lm\,mh}\right)x4\right)\Big)\Big\}$$

```
ToMatlab[e1^2 (p14 + p12) + e2^2 (p22 + p24) + e3^2 (p34 + p23) + e4^2 (p44 + p24)]
```

```
e1.^2.*(p12+p14)+e2.^2.*(p22+p24)+e3.^2.*(p23+p34)+e4.^2.*(p24+ ...
  p44);
```

```
good =
 {e1, e2, e3, e4, e5, e6}.{{p11, p12, p13, p14, p15, p16}, {p12, p22, p23, p24, p25, p26}, {p13, p23, p33, p34, p35, p36},
    {p14, p24, p34, p44, p45, p36}, {p15, p25, p35, p45, p55, p56}, {p16, p26, p36, p46, p56, p66}} .
   ({{0, 0, 0, 0, 0, 0}, {0, -12 (cm - c) (mh + mp)/(L^2 mp (4 mh + mp)), 0, 6 (cm - c)/(4 l L mh + l L mp), 0, 0}, {0, 0, 0, 0, 0, 0}, {0, 6 (cm - c)/(4 l L mh + l L mp), 0, -4 (cm - c) (mh + mp)/(l^2 mp (4 mh + mp)), 0, 0}, 101
     {0, 0, 0, 0, 0, 0}, {0, 0, 0, 0, 0, 0}}.{{x1}, {x2}, {x3}, {x4}, {x5}, {x6}} + {{0}, {0}, {0}, {-1 / l}, {0}, {0}} (v - u)) +
  (e1^2 + e2^2 + e3^2 + e4^2 + e5^2 + e6^2)
```

$$\left\{e1^2+e2^2+e3^2+e4^2+e5^2+e6^2+(e1\,p14+e2\,p24+e3\,p34+e4\,p44+e5\,p45+e6\,p46)\left(-\frac{-u+v}{l}+\frac{6\,(-c+cm)\,x2}{4\,l\,L\,mh+l\,L\,mp}-\frac{4\,(-c+cm)\,(mh+mp)\,x4}{l^2\,mp\,(4\,mh+mp)}\right)+\right.$$
$$\left.(e1\,p12+e2\,p22+e3\,p23+e4\,p24+e5\,p25+e6\,p26)\left(-\frac{12\,(-c+cm)\,(mh+mp)\,x2}{L^2\,mp\,(4\,mh+mp)}+\frac{6\,(-c+cm)\,x4}{4\,l\,L\,mh+l\,L\,mp}\right)\right\}$$

```
Solve[good == 0, {u}] // FullSimplify
```

$$\left\{\left\{u\to\left(l\left(-e1^2-e2^2-e3^2-e4^2-e5^2-e6^2+\frac{(e1\,p14+e2\,p24+e3\,p34+e4\,p44+e5\,p45+e6\,p46)\,v}{l}-\right.\right.\right.$$
$$\left.\left.\frac{6\,(-c+cm)\,(e1\,p14+e2\,p24+e3\,p34+e4\,p44+e5\,p45+e6\,p46)\,x2}{4\,l\,L\,mh+l\,L\,mp}+\frac{4\,(-c+cm)\,(mh+mp)\,(e1\,p14+e2\,p24+e3\,p34+e4\,p44+e5\,p45+e6\,p46)\,x4}{l^2\,mp\,(4\,mh+mp)}-\right.\right.$$

APPENDIX F

PAYLOAD ALIGNMENT SIMULATION

Natural Frequency of Side Swing

```
clear

clc
%% Inital Condition
%Input constants
g = 9.807;
c = 0.0068;
L = 0.61;
m_h = 0.66;
m_p = 3.13;
H = 1.82;
t_x = 0;
t_y = 0.65;
% Input variable initial values
theta_i = 2/180*pi;
phi_i = 2/180*pi;
l = sqrt((H-L*sind(theta_i)*cosd(phi_i))^2+(t_x-L*sind(phi_i))^2+(t_y-
L*cosd(theta_i)*cosd(phi_i))^2); %calculated cable length in tension
h_i = H-l;
%% Run Simulation
sim('sideswingt')
%% Process Data
[pk, loc] = findpeaks(simout1.data/pi*180);
tim = simout1.time(loc);
period = tim(3) - tim(2);
w = 2*pi/period
```

Natural Frequency of Side Swing with Varying Payload

```
clc
%% Inital Condition
%Input constants
g = 9.807;
c = 0.0068;
L = 0.61;
m_h = 0.66;
m_p = 3.13;
H = 1.85;
t_x = 0;
% Input variable initial values
theta_i = 2/180*pi;
phi_i = 15/180*pi;
wn = zeros(1,length((0.61-0.15):0.001:(0.61+0.15)));
for i = (0.61-0.15):0.001:(0.61+0.15)
t_y = i;
%% Run Simulation
sim('sideswingt')
[pk, loc] = findpeaks(simout1.data/pi*180);
tim = simout1.time(loc);
period = tim(3) - tim(2);
wn(round((i-(0.61-0.15))/0.001 + 1)) = 2*pi/period;
end
%% Process Data
```

```
wn1 = zeros(1,length((0.61-0.15):0.001:(0.61+0.15)));
ll = [];
sig = [];
for i = (0.61-0.15):0.001:(0.61+0.15)
l = sqrt((i-L)^2+H^2);
sigma = atan((L-i)/H);
sig = [sig sigma];
wn1(round((i-(0.61-0.15))/0.001 + 1)) =
sqrt(g*(m_h+0.5*m_p)*cos(sigma)/(l*(m_h+1/3*m_p)));
end

plot((0.61-0.15):0.001:(0.61+0.15),wn,(0.61-0.15):0.001:(0.61+0.15),wn1,'b')

error = [];
for i = 1:length((0.61-0.15):0.001:(0.61+0.15))
   error = [error, abs((wn(i)-wn1(i))/wn(i))];
end

plot((0.61-0.15):0.001:(0.61+0.15),error)
```

Natural Frequency of Side Swing with Varying Trolley Position

```
clc
clear
%% Inital Condition
%Input constants
g = 9.807;
c = 0.0068;
L = 0.61;
m_h = 0.66;
m_p = 3.13;
H = 1.82;
t_x = 0;
t_y = 0.57;
% Input variable initial values
theta_step = 0.2;
phi_step = 0.5;
wn = zeros(length(1:phi_step:15),length(1:theta_step:5));
[X,Y] = meshgrid(1:theta_step:5,1:phi_step:15);
for i = 1:theta_step:5
for j = 1:phi_step:15
theta_i = i/180*pi;
phi_i = j/180*pi;
%% Run Simulation
sim('sideswingt')
%% Process Data
[pk, loc] = findpeaks(simout1.data/pi*180);
if length(pk) >=2
tim = simout1.time(loc);
period = tim(3) - tim(2);
wn(round((j-1)/phi_step+1),round((i-1)/theta_step+1)) = 2*pi/period;
end
end
end
figure
```

```
surf(X,Y,wn)
```

Natural Frequency of Side Swing with Input Shaping

```
%% Inital Condition
%Input constants
g = 9.807;
c = 0.0068;
L = 0.61;
m_p = 3.13;
m_h = 0.66;
H = 1.82;
t_x = 0;
t_y = 0.58;
d_d = 10/180*pi;
d_e = 0;
% Input variable initial values
theta_i = 2/180*pi;
phi_i = 15/180*pi;
d_i = phi_i*cos(theta_i);
l = H - L*sin(theta_i);
ty_ii = L*cos(phi_i)*cos(theta_i);
tx_ii = sin(phi_i)*L;
t_i = 1;
wn = 2.67;
wd = wn*sqrt(1-c^2);
dt = pi/wd;
K = exp(-c*pi/sqrt(1-c^2));

pk = [];
freq = [];
mm = [];
for i = -0.2:0.01:0.4
ty_i = ty_ii + i*sin(phi_i*cos(theta_i));
tx_i = tx_ii + i*cos(phi_i*cos(theta_i));

mm = [mm i];
% a1 = 1/(1+K);
% a2 = K/(1+K);
% a3 = 0;

% a1 = 1/(K^2+1+2*K);
% a2 = 2*K/(K^2+1+2*K);
% a3 = K^2/(K^2+1+2*K);

% a1 = 1;
% a2 = 0;
% a3 = 0;


%% Run Simulation
sim('sideswingis')
%% Process Data
[pp loc] = findpeaks(-simout1.data);
```

```
pk = [pk abs(pp(1))/0.1181];
freq = [freq 2*pi/(simout1.time(loc(3))-simout1.time(loc(2)))];
freq1 = ((freq - wn))/wn;
end
plot(freq1,pk)
```

Force Calculation in Input-Shaped Side Swing

```
clear
clc
%% Inital Condition
%Input constants
g = 9.807;
c = 0.0068;
L = 0.61;
m_p = 3.13;
m_h = 0.66;
H = 1.82;
t_x = 0;
t_y = 0.61;

d_e = 0;
% Input variable initial values
theta_i = 2/180*pi;
phi_i = 15/180*pi;
d_i = phi_i*cos(theta_i);
l = H - L*sin(theta_i);
ty_ii = L*cos(phi_i)*cos(theta_i);
tx_ii = sin(phi_i)*L;
t_i = 0;
wn = 2.67;
wd = wn*sqrt(1-c^2);
dt = pi/wd;
K = exp(-c*pi/sqrt(1-c^2));
II = 1/3*m_p*L^2;
Ii = m_h*L^2;

ty_i = ty_ii + 0*sin(phi_i*cos(theta_i));
tx_i = tx_ii + 0*cos(phi_i*cos(theta_i));

a1 = 1;
a2 = 0;
a3 = 0;
head = [];
final = cell(length(0.1:0.1:0.5),1);
for u = 0.1:0.1:0.5;

for i = 1: 0.5:40
d_d = i/180*pi;
time = (d_i - d_e)/d_d+t_i;

%% Run Simulation
sim('sideswingis')
%% Process Data
```

```
ln = length(phi.data);
mu = u;
f = [];
tt = [];
ttz = [];
for e = 1:ln
   pd = phi_d.data(e);
   p = phi.data(e);
   td = theta_d.data(e);
   t = theta.data(e);
   tcx = txd.data(e);
   tcy = tyd.data(e);
   hcx = L*sin(p);
   hcy = L*cos(p)*cos(t);
   hcz = L*cos(p)*sin(t);
   tx =  (II+Ii)*pd/L;
   tz = ((II+Ii)*td + (0.5*m_p+m_h)*g*L*cos(t))/L/cos(cos(t));
   f = [f,mu*((m_p + m_h)*g-tz)];
   a = tcy-hcy;
   b = tcx-hcx;
   tt = [tt, tx/cos(atan(a/b))];

end
tt = smooth(tt,151,'moving');
tt = -tt';
f = -f;
[pk lk] = findpeaks(tt);
head = [head, tt(lk(1))-f(lk(1))];
end
head = smooth(head,21,'moving');
final{round(u/0.1)} = head;
head = [];
end
xa = 1: 0.5:40;
plot(xa,final{1}',xa,final{2}',xa,final{3}',xa,final{4}',xa,final{5}')
```

Simulation of Side Swing

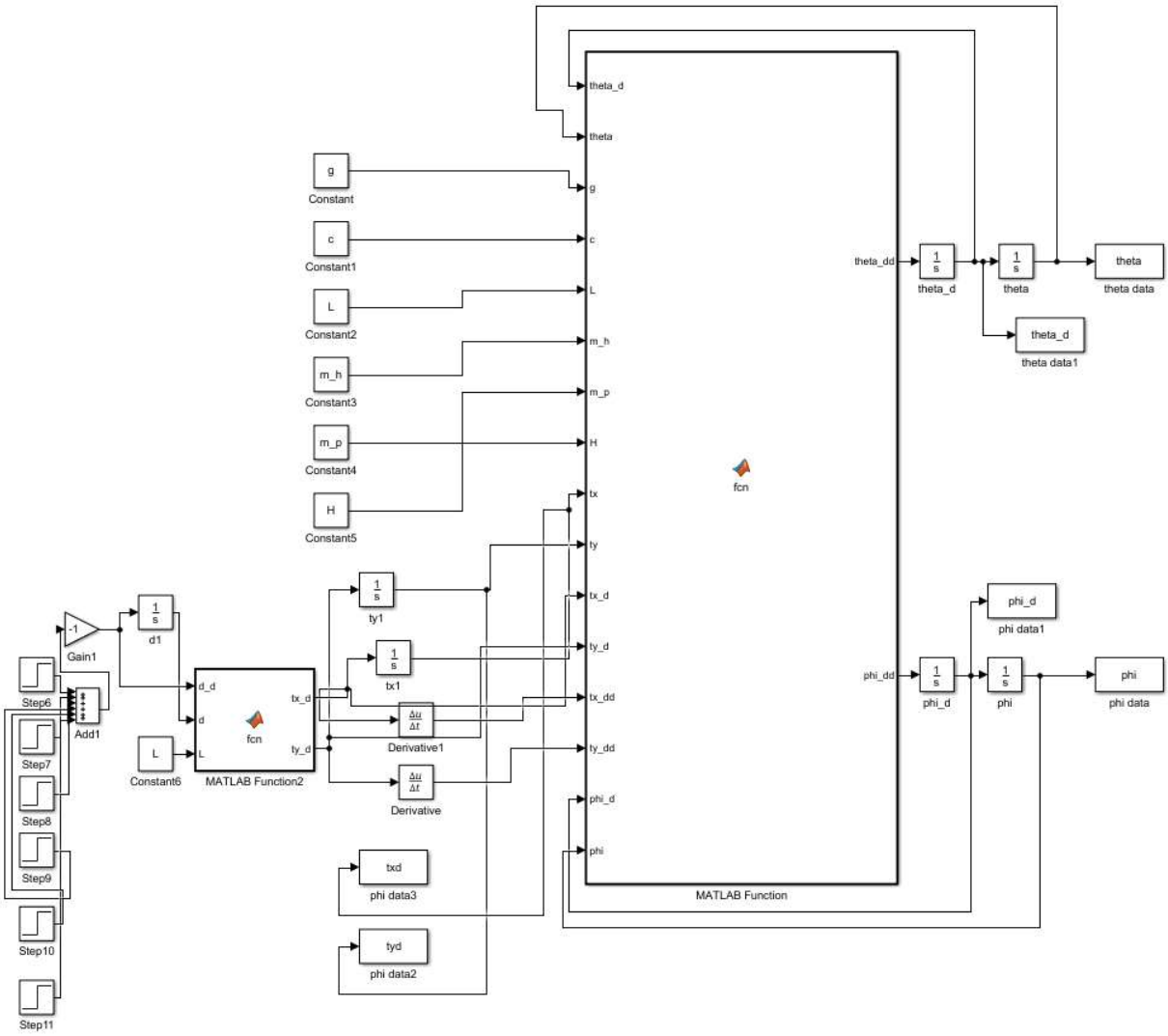

APPENDIX G

LIFT-UP TRAJECTORY GENERATION

Liftup Trajectory Static Boundary Calculation

```
clear
clc
g = 9.807;
L = 0.61;
m_h = 0.66;
m_p = 3.13;
H = 1.82;
p = 3.1415926;
t0 = [];
n0 = [];
eq = [];
f0 = [];
mu = 0.1;
nn = [];
ff = [];
for i = 0:0.01:90
  n = [];
  f = [];
   for e = 90:180
f = [f, -((0.5*m_p+m_h)*g*cosd(i)*cosd(e)/sind(e-
i))/((m_p*g*(sind(e)*cosd(i)-2*cosd(e)*sind(i))/2/sind(e-i) +
m_h*g*(sind(e)*cosd(i)-2*cosd(e)*sind(i))/sind(e-i))) - mu  ];
   end
 index = 90:180;
 n = abs(n);
 f = abs(f);
 [mim, low] = min(n);
 nn = [nn, index(low)];
 [mim, low] = min(f);
 ff = [ff, index(low)];
end
```

Liftup Trajectory Dynamic Boundary Calculation

```
clear
clc
g = 9.807;
L = 0.61;
m_h = 0.66;
m_p = 3.13;
H = 1.82;
p = 3.1415926;
t0 = [];
n0 = [];
eq = [];
f0 = [];
mu = 0.5;
ld = -0.2;
final = zeros(length(0:90),length(0:180));
index = 0.01:0.005:0.5;
I = (1/3*m_p+m_h)*L^2;
```

```
for i = 0:90
   for e = 0:180
      ff = [];

     for u = 0:0.005:0.2
         yd = -u;
         l = (H-L*sind(i))/sind(e);
thd = -(ld+yd*cosd(e))/(L*sind(e-i));
phd = (ld*cosd(e-i)-yd*cosd(i))/(l*sind(e-i));
thdd = (cotd(e-i)*(ld-cosd(i)-yd)*(phd-thd)-yd*sind(i)*thd)/(L^2*sind(e-i));
T = ((0.5*m_p+m_h)*g*cosd(i)+I*thdd)/sind(e-i);
N = (m_p+m_h)*g  - ((0.5*m_p+m_h)*g*cosd(i)+I*thdd)/sind(e-i)*sind(e)  +
0.5*L*(m_p+2*m_h)/(m_p+m_h)*(thdd*cosd(i)-thd^2*sind(i));
f =  -  ((0.5*m_p+m_h)*g*cosd(i)+I*thdd)/sind(e-i)*cosd(e)  -
0.5*L*(m_p+2*m_h)/(m_p+m_h)*(thdd*cosd(i)-thd^2*sind(i));
  if T > 0 && N > 0
ff = [ff, -abs(f)+mu*N];
  else
ff = [ff, 0];
  end
     end

      ff = ff(ff~=0);
      if isempty(ff)
          final(round(i)+1,round(e)+1) = 0;
      else
      if ff(end)>ff(1)
          ff = ff(end:-1:1);
      end
          [mim loc] = min(abs(ff));
    final(round(i)+1,round(e)+1) = index(loc);
      end

   end
end
[xx,yy] = meshgrid(0:90,0:180);
xx = xx';
yy = yy';
z = surf(xx,yy,final);

daspect([1 1 0.001])
set(z,'edgecolor','none')
ylabel('Phi (degree)','FontName','Times New Roman','FontSize',26)
xlabel('Theta (degree)','FontName','Times New Roman','FontSize',26)
axis([0 90 0 180 0 1])
view(2)
```

Liftup Trajectory Speed Calculation

```
clear
clc
x = 2:0.5:88;
y = [90:10/154:100  , 100:-10/19:90];
y(155:156) = [];

g = 9.807;
L = 0.61;
m_h = 0.66;
m_p = 3.13;
H = 1.82;
p = 3.1415926;
mu = 0.5;
index = 0.0:0.005:0.2;
I = (1/3*m_p+m_h)*L^2;
final = zeros(2,173);

for z = 1:length(x)
i = x(z);
e = y(z);
l  = (H-L*sind(i))/sind(e);
ff = [];
ld1 = [];
yd1 = [];
theta1 = [];
ld2 = [];
yd2 = [];
theta2 = [];
for v = 0:0.001:0.2
  yd = -v;
       if z <=155 && z>= 1
          C = 10/78;
         ld =  yd*(cosd(i)*L+C*cosd(e))/(cosd(e-i)*L+C*l);
      else
          C = -10/8;
          ld = yd*(cosd(i)*L+C*cosd(e))/(cosd(e-i)*L+C*l);
       end
  if abs(ld) < 0.2
thd = (-ld+yd*cosd(e))/(L*sind(e-i));
phd = (ld*cosd(e-i)-yd*cosd(i))/(l*sind(e-i));
thdd = (cotd(e-i)*(ld-cosd(i)-yd)*(phd-thd)-yd*sind(i)*thd)/(L^2*sind(e-i));
T = ((0.5*m_p+m_h)*g*cosd(i)+I*thdd)/sind(e-i);
N = (m_p+m_h)*g  - ((0.5*m_p+m_h)*g*cosd(i)+I*thdd)/sind(e-i)*sind(e)  +
0.5*L*(m_p+2*m_h)/(m_p+m_h)*(thdd*cosd(i)-thd^2*sind(i));
f =  -  ((0.5*m_p+m_h)*g*cosd(i)+I*thdd)/sind(e-i)*cosd(e)  -
0.5*L*(m_p+2*m_h)/(m_p+m_h)*(thdd*cosd(i)-thd^2*sind(i));
  if T > 0 && N > 0 && mu - abs(f/N) > 0
      ld1 = [ld1,ld];
      yd1 = [yd1,yd];
      theta1 = [theta1,thd];
  end
  end
```

```
end
  for v = 0:0.001:0.2
   ld = -v;
       if z <=155 && z>= 1
          C = 10/78;
         yd = ld*(cosd(e-i)*L+C*l)/(cosd(i)*L+C*cosd(e));

      else
          C = -10/8;
          yd = ld*(cosd(e-i)*L+C*l)/(cosd(i)*L+C*cosd(e));

       end
  if abs(yd) < 0.2
thd = (-ld+yd*cosd(e))/(L*sind(e-i));
phd = (ld*cosd(e-i)-yd*cosd(i))/(l*sind(e-i));
thdd = (cotd(e-i)*(ld-cosd(i)-yd)*(phd-thd)-yd*sind(i)*thd)/(L^2*sind(e-i));
T = ((0.5*m_p+m_h)*g*cosd(i)+I*thdd)/sind(e-i);
N = (m_p+m_h)*g  - ((0.5*m_p+m_h)*g*cosd(i)+I*thdd)/sind(e-i)*sind(e)  +
0.5*L*(m_p+2*m_h)/(m_p+m_h)*(thdd*cosd(i)-thd^2*sind(i));
f =  -  ((0.5*m_p+m_h)*g*cosd(i)+I*thdd)/sind(e-i)*cosd(e)  -
0.5*L*(m_p+2*m_h)/(m_p+m_h)*(thdd*cosd(i)-thd^2*sind(i));
  if T > 0 && N > 0 && mu - abs(f/N) > 0
      ld1 = [ld1,ld];
      yd1 = [yd1,yd];
      theta1 = [theta1,thd];
  end

  end
  end
[max1, loc1] = max(abs(theta1));
final(1,z) = ld1(loc1);
final(2,z) = yd1(loc1);
end
subplot(1,2,1)
plot(-final(1,:))
axis([0 180 0 0.2])
subplot(1,2,2)
plot(-final(2,:))
axis([0 180 0 0.2])
```

APPENDIX H

MRC + OBSERVER RESIDUAL VIBRATION REDUCTION

Free Hanging Double Pendulum Simulation

```
clear
clc
%% Inital Condition
%Input constants
g = 9.807;
L = 0.61;
m_h = 0.66;
m_p = 3.13;
l = 1.5;
c = 0.002;
yt_d = 0;
yt_dd = 0;

% Input variable initial values
theta_i = -20/180*pi;
phi_i = 5/180*pi;

%% Run Simulation
sim('offground')
subplot(2,2,1)
plot(simout1)
subplot(2,2,2)
plot(simout)
sim('offgroundlin')
subplot(2,2,3)
plot(simout1)
subplot(2,2,4)
plot(simout)
%Nonlinear
function [theta_dd,phi_dd] =
fcn(theta_d,theta,g,c,L,l,m_h,m_p,yt_d,yt_dd,phi_d,phi)
theta_dd = l.^(-1).*L.^(-2).*m_p.^(-1).*((-2).*m_h+(-
1).*m_p+m_p.*cos(2.*(theta+(-1).*phi))).^(-
1).*(l.*theta_d.*(8.*c.*(m_h+m_p)+(-
4).*L.*m_p.*(m_h+m_p).*yt_d.*sin(theta)+(-
2).*L.*m_p.*(2.*l.*(m_h+m_p)+L.*m_p.*cos(theta+(-
1).*phi)).*phi_d.*sin(theta+(-
1).*phi))+l.*L.^2.*m_p.^2.*theta_d.^2.*sin(2.*(theta+(-
1).*phi))+4.*L.*m_p.*(l.^2.*(m_h+m_p).*phi_d.^2.*sin(theta+(-
1).*phi)+cos(theta+(-1).*phi).*phi_d.*((-
1).*c+l.*(m_h+m_p).*yt_d.*sin(phi))+l.*(m_h+m_p).*sin(theta+(-
1).*phi).*(g.*cos(phi)+(-1).*yt_dd.*sin(phi))));

phi_dd = (1/2).*l.^(-2).*L.^(-1).*sec(theta+(-1).*phi).*((-
1).*m_p+(m_h+m_p).*sec(theta+(-1).*phi).^2).^(-1).*(2.*(l.*theta_d.*(2.*c+(-
1).*L.*m_p.*yt_d.*sin(theta))+L.*sec(theta+(-1).*phi).*((-
1).*l.*m_h.*(cos(phi).*yt_dd+g.*sin(phi))+phi_d.*((-
1).*c+l.*(m_h+m_p).*yt_d.*sin(phi))))+(-1).*l.*L.*m_p.*((-
2).*g.*cos(theta)+(-1).*(theta_d+(-1).*phi_d).*(L.*theta_d+(-
2).*l.*cos(theta+(-1).*phi).*phi_d)+2.*yt_dd.*sin(theta)).*tan(theta+(-
1).*phi));
end
```

```
%Linear
function [theta_dd,phi_dd] =
fcn(theta_d,theta,g,c,L,l,m_h,m_p,yt_d,yt_dd,phi_d,phi)
theta_dd = (-2).*g.*L.^(-1).*m_h.^(-1).*(m_h+m_p)*theta + (-4).*c.*L.^(-
2).*m_h.^(-1).*m_p.^(-1).*(m_h+m_p)*theta_d + 2.*g.*L.^(-1).*m_h.^(-
1).*(m_h+m_p)*phi +2.*c.*l.^(-1).*L.^(-1).*m_h.^(-1)*phi_d;

phi_dd =g.*l.^(-1).*m_h.^(-1).*m_p*theta + 2.*c.*l.^(-1).*L.^(-1).*m_h.^(-
1)*theta_d + (-1).*g.*l.^(-1).*m_h.^(-1).*(m_h+m_p)*phi + (-1).*c.*l.^(-
2).*m_h.^(-1)*phi_d -1/l*yt_dd;
end
```

Free Hanging Double Pendulum Simulation with Observer

```
clear
clc
%% Inital Condition
%Input constants
g = 9.807;
L = 0.61;
m_h = 0.66;
m_p = 3.13;
l = 1.3;
c = 0.01;
yt_d = 0;
yt_dd = 0;

%% State Space4
A = [0,1,0,0,0,0;  (-2).*g.*L.^(-1).*m_h.^(-1).*(m_h+m_p), (-4).*c.*L.^(-
2).*m_h.^(-1).*m_p.^(-1).*(m_h+m_p), 2.*g.*L.^(-1).*m_h.^(-1).*(m_h+m_p),
2.*c.*l.^(-1).*L.^(-1).*m_h.^(-1),0,0; 0, 0, 0, 1,0,0; g.*l.^(-1).*m_h.^(-
1).*m_p,  2.*c.*l.^(-1).*L.^(-1).*m_h.^(-1), (-1).*g.*l.^(-1).*m_h.^(-
1).*(m_h+m_p), (-1).*c.*l.^(-2).*m_h.^(-1),0,0; 0,0,0,0,0,1;0,0,0,0,0,0];

%A = [0,1,0,0,0,0;  (-2).*g.*L.^(-1).*m_h.^(-1).*(m_h+m_p), (-4).*c.*L.^(-
2).*m_h.^(-1).*m_p.^(-1).*(m_h+m_p), 2.*g.*L.^(-1).*m_h.^(-1).*(m_h+m_p),
2.*c.*l.^(-1).*L.^(-1).*m_h.^(-1),0,0; 0, 0, 0, 1,0,0; g.*l.^(-1).*m_h.^(-
1).*m_p,  2.*c.*l.^(-1).*L.^(-1).*m_h.^(-1), (-1).*g.*l.^(-1).*m_h.^(-
1).*(m_h+m_p), (-1).*c.*l.^(-2).*m_h.^(-1),0,0; 0,0,0,0,0,1;0,0,0,0,0,0];
B = [0,0,0,-1/l,0,1]';
C = [0,0,1,0,0,0;0,0,0,0,1,0;0,0,0,0,0,1];

ga = 1;
P = eig(A)*ga;
LL = place(A',C',[-5 -10  -15 -20 -25 -30]*ga)';

% Input variable initial values
theta_i = 10/180*pi;
phi_i =  10/180*pi;

%% Run Simulation
sim('offgroundob')

time = simout.time;
theta_real = simout.data/pi*180*0.5;
```

```
phi_real = simout1.data/pi*180;
theta_predict = simout4.data(:,1)/pi*180*0.5;
phi_predict = simout4.data(:,3)/pi*180;

simout.data = simout.data/pi*180*0.5;
simout1.data = simout1.data/pi*180;
simout4.data(:,1) = simout4.data(:,1)/pi*180*0.5;
simout4.data(:,3) = simout4.data(:,3)/pi*180;

subplot(2,1,1)
plot(time,theta_real,time,theta_predict)
axis([0,25,-20,20])
subplot(2,1,2)
plot(time,phi_real,time,phi_predict)
axis([0,25,-20,20])
```

Free Hanging Double Pendulum Simulation with Observer+MRC

```
clear
clc
%% Inital Condition
%Input constants
g = 9.807;
L = 0.61;
m_h = 0.66;
mh = m_h;
m_p = 3.13;
mp = m_p;
l = 1;
c = 0.01;
cm = 5;
yt_dd = 0;
up = 1;
low = -1;
lm = 1.5;

p11 = (-1/4).*cm.^(-1).*g.^(-1).*L.^(-1).*mp.^(-1).*((-40).*cm.^2+(-1).* ...
  g.^2.*L.^2.*mp.^2+(-5).*g.*L.^3.*mp.^2);
p12 = 5*L/2/g;
p13 = 5*lm*L*mp/2/cm;
p14 = 5*lm/g;
p22 = (-1/8).*cm.^(-1).*g.^(-1).*(mh+mp).^(-1).*((-1).*g.*L.^2.*mh.*mp+( ...
  -5).*L.^3.*mh.*mp+(-1).*g.*L.^2.*mp.^2+(-5).*L.^3.*mp.^2+(-10).* ...
  L.^2.*lm.*mp.^2);
p23 = (5/2).*g.^(-1).*L.*mp.*(mh+mp).^(-1);
p24 = (-1/4).*cm.^(-1).*g.^(-1).*((-1).*g.*L.*lm.*mp+(-5).*L.^2.*lm.*mp+ ...
  (-10).*L.*lm.^2.*mp);
p33 = (-1/2).*cm.^(-1).*g.^(-1).*lm.^(-1).*(mh+mp).^(-1).*((-10).*cm.^2+ ...
  (-1).*g.^2.*lm.^2.*mh.^2+(-10).*g.*lm.^3.*mh.^2+(-2).*g.^2.* ...
  lm.^2.*mh.*mp+(-20).*g.*lm.^3.*mh.*mp+(-1).*g.^2.*lm.^2.*mp.^2+( ...
  -10).*g.*lm.^3.*mp.^2);
p34 = 5*lm/g;
p44 = (-1/2).*cm.^(-1).*g.^(-1).*((-1).*g.*lm.^2.*mh+(-10).*lm.^3.*mh+( ...
```

```
-1).*g.*lm.^2.*mp+(-5).*L.*lm.^2.*mp+(-10).*lm.^3.*mp);


c1 = g.*l.^(-1).*mh.^(-1).*mp+(-1).*g.*lm.^(-1).*mh.^(-1).*mp;
c2 = 2.*c.*l.^(-1).*L.^(-1).*mh.^(-1)+(-2).*cm.*L.^(-1).*lm.^(-1).* ...
  mh.^(-1);
c3 = (-1).*g.*l.^(-1).*mh.^(-1).*(mh+mp)+g.*lm.^(-1).*mh.^(-1).*(mh+mp);
c4 = (-1).*c.*l.^(-2).*mh.^(-1)+cm.*lm.^(-2).*mh.^(-1);
c5 = (-4).*c.*L.^(-2).*mh.^(-1).*mp.^(-1).*(mh+mp)+4.*cm.*L.^(-2).* ...
  mh.^(-1).*mp.^(-1).*(mh+mp);
c6 = 2.*c.*l.^(-1).*L.^(-1).*mh.^(-1)+(-2).*cm.*L.^(-1).*lm.^(-1).* ...
  mh.^(-1);

%% State Space
A = [0,1,0,0,0,0;  (-2).*g.*L.^(-1).*m_h.^(-1).*(m_h+m_p), (-4).*c.*L.^(-
2).*m_h.^(-1).*m_p.^(-1).*(m_h+m_p), 2.*g.*L.^(-1).*m_h.^(-1).*(m_h+m_p),
2.*c.*l.^(-1).*L.^(-1).*m_h.^(-1),0,0; 0, 0, 0, 1,0,0; g.*l.^(-1).*m_h.^(-
1).*m_p,  2.*c.*l.^(-1).*L.^(-1).*m_h.^(-1), (-1).*g.*l.^(-1).*m_h.^(-
1).*(m_h+m_p), (-1).*c.*l.^(-2).*m_h.^(-1),0,0; 0,0,0,0,0,1;0,0,0,0,0,0];
B = [0,0,0,-1/l,0,1]';
C = [0,0,1,0,0,0;0,0,0,0,1,0;0,0,0,0,0,1];

Am = [0,1,0,0;  (-2).*g.*L.^(-1).*m_h.^(-1).*(m_h+m_p), (-4).*cm.*L.^(-
2).*m_h.^(-1).*m_p.^(-1).*(m_h+m_p), 2.*g.*L.^(-1).*m_h.^(-1).*(m_h+m_p),
2.*cm.*l.^(-1).*L.^(-1).*m_h.^(-1); 0, 0, 0, 1; g.*l.^(-1).*m_h.^(-1).*m_p,
2.*cm.*l.^(-1).*L.^(-1).*m_h.^(-1), (-1).*g.*l.^(-1).*m_h.^(-1).*(m_h+m_p),
(-1).*cm.*l.^(-2).*m_h.^(-1)];
Bm = B(1:4);
Cm = eye(4,4);

ga = 1;
ga1 = 1;
P = eig(A)*ga;
pp = [-5 -10  -15 -20 -25 -30];
LL = place(A',C',pp*ga)'*ga1;

% Input variable initial values
theta_i = -20/180*pi;
phi_i = 5/180*pi;

%% Run Simulation
sim('offgroundmrc')
%sim('test')

time = simout.time;
theta_real = simout.data/pi*180*0.5;
phi_real = simout1.data/pi*180;
theta_predict = simout4.data(:,1)/pi*180*0.5;
phi_predict = simout4.data(:,3)/pi*180;
subplot(2,1,1)
plot(time,theta_real,time,theta_predict)
axis([0,25,-30,30])
subplot(2,1,2)
plot(time,phi_real,time,phi_predict)
axis([0,25,-20,20])
```

REFERENCES

[1] Singer, N. C. and S., W. P., "Preshaping command inputs to reduce system vibration," *Journal of Dynamic Systems, Measurement, and Control*, 1990.

[2] Starr, G. P., "Swing-free transport of suspended objects with a path controlled robot manipulator," *Journal of Dynamic Systems, Measurement, and Control*, May 1985.

[3] Smith, J. Y., Kozak, K., and S., W. E., "Input shaping for a simple nonlinear system," *IEEE American Control Conference*, 2002.

[4] Singer, N., S., W., and Krikku, E., "An input shaping controller enabling cranes to move without sway," *American Nuclear Society 7th Topical Meeting on Robotics and Remote Systems*, 1997.

[5] Singhose, W., S., W., and Singer, N., "Shaping inputs to reduce vibration: A vector diagram approach," *IEEE International Conference on Robotics and Automation*, 1990.

[6] Singhose, W. E and Singer, N. C., "Effects of input shaping on two dimensional trajectory following," *IEEE Transactions on Robotics and Automa- tion*, 1996.

[7] Han, J., Zhu, Z., and Q., Y. H., "A novel input shaping method based on system output," *Journal of Vibration and Sound*, 2014.

[8] Chen, K.-S., Yang, T.-S., and Y., J., "Residual vibration suppression for duffing nonlinear systems with electromagnetical actuation using nonlinear command shaping techniques," *Journal of Vibration and Acoustics*, 2006.

[9] Chien, C. J. and Fu, L. C., "A new approach to model reference control for a class of arbitrarily fast time-varying unknown plants," *Automatica*, 1992.

[10] Huang, P. Y. and Chen, B. S., "Robust model-reference control of linear mimo time-varying systems," *Control Theory and Advanced Technology*, 1993.

[11] Abdullah, A. and Zribi, M., "Model reference control of lpv systems," *Journal of the Franklin Institute - Engineering and Applied Mathematics*, 2009.

[12] Lal, M. and Mehrotra, R., "Design of model reference adaptive control systems for non-linear plants," *International Journal of Control*, 1972.

[13] Nijmeijer, H. and Savaresi, S. M., "On approximate model-reference control of siso discrete-time nonlinear systems," *Automatica*, 1998.

[14] Jun, V. N., Kim, Y., Kelly, S. D., and Bentsman, J., "Partial difference equation based model reference control of a multiagent network of underactuated aquatic vehicles with strongly nonlinear dynamics," *Nonlinear Analysis: Hybrid Systems*, 2010.

[15] Chen, F. C. and Liu, C. C., "Adaptively controlling nonlinear continuoustim systems using neural networks," *IEEE Transactions on Automatic Control*, 1994.

[16] Sastry, S. and Isidori, A., "Adaptive control of linearizable systems," *IEEE Transactions on Automatic Control*, 1989.

[17] Chen, Z. J. and Cook, P. A., "Robustness of model-reference adaptive control systems with unmodelled dynamics," *International Journal of Control*, 1984.

[18] Datta, A. and Ioannou, P. A., "Performance analysis and improvement in model reference adaptive control," *IEEE Transactions on Automatic Control*, 1994.

[19] Duan, G. R., Liu, W. Q., and Liu, G. P., "Robust model reference control for multivariable linear systems subject to parameter uncertainties," *Journal of Systems and Control Engineering*, 2001.

[20] Sun, J., Olbrot, A. W., and Polis, M. P., "Robust stabilization and robust performance using model reference control and modeling error compensation," *IEEE Transactions on Automatic Control*, 1994.

[21] Patino, H. D. and Liu, D. R., "Neural network-based model reference adaptive control system," *IEEE Transactions on Systems Man and Cybernetics Part B-Cybernetics*, 2000.

[22] Pedret, C., Vilanova, R., Moreno, R., and Ser, I., "A new architecture for robust model reference control," *IEEE Conference on Decision Control, Seville, Spain*, 2005.